Vascular and Cellular Responses to Traumatic Brain Injury

Jennifer R. Hay, BSc (Hons), MSc

A thesis submitted to the University of Glasgow in fulfilment of the requirements for the degree of Doctor of Philosophy.

Department of Neuropathology, Queen Elizabeth University Hospital, Glasgow, UK.

Graduate School of the College of Medical, Veterinary and Life Sciences, the University of Glasgow.

Abstract

There is growing evidence that suggests Traumatic brain injury (TBI) may initiate long-term neurodegenerative processes. Exposure to a single moderate or severe TBI, or to repetitive TBI, reveals a complex of pathologies including abnormalities of tau, amyloid-β and TDP-43; neuronal loss; neuroinflammation; and white matter degradation. The mechanisms driving these late post-TBI neurodegenerative pathologies remain elusive.

Firstly, a potential association between blood-brain barrier (BBB) disruption and TBI was investigated. Results showed that increased and widespread BBB disruption was observed in material from patients dying in the acute phase following a single, moderate to severe TBI and persisted in a high proportion of patients surviving years following injury. Furthermore, there was preferential distribution to the deep layers of the cortex and to the crests of the gyri rather than the depths of the sulci. This post-TBI BBB disruption was investigated further within a paediatric TBI cohort. BBB disruption was noted in both paediatric and adult TBI in a similar pattern and distribution, however, interestingly, in sharp contrast to adult TBI cases, BBB disruption in paediatric cases appears preferentially distributed to capillary sized vessels. This vulnerability of the small vessels was rarely observed in adult material.

In addition to the post-TBI vascular change observed, the cellular response was investigated, which interestingly, demonstrated regional differences. Specifically, in the grey matter, reactive astrogliosis was observed subpially, around cortical vessels, at the grey and white matter boundaries and subependymally. This astrogliosis was evident in a proportion of acute and continued into the late phase following TBI. In contrast, microglial activation was observed as a delayed response and localised to the white matter tracts. In addition, this delayed microglial response expressed an M2-like phenotype. Furthermore, there was an increased population of inactivated perivascular microglia beyond the perivascular space in the grey matter regions, observed in the acute phase and persisted in a proportion of patients surviving years following injury. Collectively these findings are interesting and indicate TBI induces both a vascular and cellular responses which may contribute to the long-term post-TBI neurodegenerative processes.

Table of Contents

List of Tables

List of Figures

Publications arising from this thesis

Reviews:

Hay J, Johnson VE, Smith DH, Stewart W. Chronic Traumatic Encephalopathy: The Neuropathological Legacy of Traumatic Brain Injury. Annual review of pathology. 2016;11:21-45. doi:10.1146/annurev-pathol-012615-044116.

Manuscripts:

Hay JR, Johnson VE, Young AM, Smith DH, Stewart W. Blood-Brain Barrier Disruption Is an Early Event That May Persist for Many Years After Traumatic Brain Injury in Humans. J Neuropathol Exp Neurol. 2015 Dec;74(12):1147-57. doi: 10.1097/NEN.0000000000000261.

Pischiutta F, Micotti E, **Hay JR**, Marongiu I, Sammali E, Tolomeo D, Vegliante G, Stocchetti N, Forloni G, De Simoni MG, Stewart W, Zanier ER. Single severe traumatic brain injury produces progressive pathology with ongoing contralateral white matter damage one year after injury. Exp Neurol. 2018 Feb;300:167-178. doi: 10.1016/j.expneurol.2017.11.003. Epub 2017 Nov 7.

McMillan TM, McSkimming P, Wainman-Lefley J, Maclean LM, **Hay J**, McConnachie A, Stewart W. Long-term health outcomes after exposure to repeated concussion in elite level: rugby union players. J Neurol Neurosurg Psychiatry. 2017 Jun;88(6):505-511. doi: 10.1136/jnnp-2016-314279. Epub 2016 Oct 7.

Abstracts and Posters:

Hay J, Johnson V, Young A, Smith DH, Stewart W. Blood-brain barrier disruption persists for years after a single traumatic brain injury in humans. International Neurotrauma Society, Budapest, March 2014.

Hay J, Johnson V, Young A, Smith DH, Stewart W. Blood-brain barrier disruption persists for years after a single traumatic brain injury in humans. British Neuropathological Society, London, 2014.

Hay J, Johnson V, Young A, Smith DH, Stewart W. Blood-brain barrier disruption persists for years after a single traumatic brain injury in humans. Sackler Institute Conference, Glasgow, November 2015.

Hay J, Bryant-Craig C, Johnson V, Smith DH, Stewart W. Trauma associated blood-brain barrier disruption is a capillary level pathology in the young. National Neurotrauma Society, Santa Fe, July 2015.

Hay J, Fullerton J, Johnson V, Smith DH, Stewart W. Neuroinflammation following traumatic brain injury is a white matter pathology. Sacker Institute Conference, Edinburgh, October 2016.

Hay J, Fullerton J, Johnson V, Smith DH, Stewart W. Neuroinflammation following traumatic brain injury is a white matter pathology. QEUH Laboratory Medicine Poster day, Queen Elizabeth University Hospital, Glasgow, June 2017.

Hay J, Fullerton, Johnson V, Smith DH, Stewart W. The astrocytic response following traumatic brain injury is a grey matter pathology. Sacker Institute Conference, Edinburgh, October 2016.

Hay J, Fullerton J, Johnson V, Smith DH, Stewart W. Neuroinflammation following traumatic brain injury is a white matter pathology. QEUH Laboratory Medicine Poster day, Queen Elizabeth University Hospital, Glasgow, June 2017.

List of Accompanying Material

Appendix 1: Ethical approval documentation.

Appendix 2: Table of full cohort and demographics

Appendix 3: Table of all antibodies used.

Appendix 4: Copies of Publication printed and accepted

HAY, J. R., JOHNSON, V. E., YOUNG, A. M., SMITH, D. H. & STEWART, W. 2015. Blood-Brain Barrier Disruption Is an Early Event That May Persist for Many Years After Traumatic Brain Injury in Humans. J Neuropathol Exp Neurol, 74, 1147-57.

HAY, J., JOHNSON, V. E., SMITH, D. H. & STEWART, W. 2016. Chronic Traumatic Encephalopathy: The Neuropathological Legacy of Traumatic Brain Injury. Ann Rev Pathol, 11, 21-45.

PISCHIUTTA F, MICOTTI E, HAY JR, MARONGIU I, SAMMALI E, TOLOMEO D, VEGLIANTE G, STOCCHETTI N, FORLONI G, DE SIMONI MG, STEWART W, ZANIER ER. Single severe traumatic brain injury produces progressive pathology with ongoing contralateral white matter damage one year after injury. Exp Neurol. 2018 Feb;300:167-178. doi: 10.1016/j.expneurol.2017.11.003. Epub 2017 Nov 7

MCMILLAN TM, MCSKIMMING P, WAINMAN-LEFLEY J, MACLEAN LM, HAY J, MCCONNACHIE A, STEWART W. Long-term health outcomes after exposure to repeated concussion in elite level: rugby union players. J Neurol Neurosurg Psychiatry. 2017 Jun;88(6):505-511. doi: 10.1136/jnnp-2016-314279. Epub 2016 Oct 7.

Appendix 5: Permissions

Journal of Neuropathology and Experimental Neurology

Annual Reviews

Experimental Neurology

Permission from the British Medical Journal

Acknowledgements

The thesis has been made possible through the support and encouragement of many individuals, of whom I would like to thank.

Firstly, I owe gratitude to my primary supervisor, Dr William Stewart of the Department of Neuropathology, Queen Elizabeth University Hospital, Glasgow. His constant motivational pushes and training helped me focus when I felt I could not. Prof. Johnathan Cavanagh, my second supervisor was great with words of encouragement and the research meeting he led made me feel part of something when I often felt isolated. I also want to thank Vicky Johnson and Prof. Doug Smith of the Department of Neurosurgery at The University of Pennsylvania for the expertise and guidance they shared with me over the years.

I would like to thank my husband Fergus for standing by me throughout the whole journey, running me endless baths when times were difficult. I also owe so much to my parents, for helping me get to where I am today, through the countless degrees. I promise it is the last! Josie Fullerton, Hannah Morgan and Tess Atkinson for all their support, advice and shoulders to cry on. My Inverness girls, for distracting my mind with fun weekends, nights out and endlessly long phone calls! I would like to thank all my friends in Glasgow for supporting me and de-stressing me with lovely nights filled with food, wine and laughter. Lastly, but not least, my dog Baxter, who always makes me smile.

Author's Declaration

I declare that, except where explicit reference is made to the contribution of others, that this dissertation is the result of my own work and has not been submitted for any other degree at the University of Glasgow or any other institution.

Signed: _____Date: _____

Abbreviations

AASBP	age-associated systolic blood pressure
AB	amyloid beta
AD	Alzheimer's disease
ADC	apparent diffusion coefficient
ALS	amyotrophic lateral sclerosis
ApoE	apolipoprotein E
APP	amyloid precursor protein
ARDS	acute respiratory distress syndrome
ARTAG	aging-related tau astrogliopathy
ATP	adenosine triphosphate
BBB	blood brain barrier
CAA	cerebral amyloid angiopathy
CBF	cerebral blood flow
CBV	cerebral blood volume
CC	corpus callosum
CG	cingulate gyrus
CT	computed tomography
CCI	controlled cortical impact
CNS	central nervous system
CSF	cerebrospinal fluid
CSP	cavum septum pellucidum
CTE	chronic traumatic encephalopathy
DAB	3,3'-diaminobenzidine
DAI	diffuse axonal injury
DBS	diffuse brain syndrome
DMRB	microscope
DNA	deoxyribonucleic acid
DP	dementia pugilistica
DTI	diffuse tensor imaging
EDH	epidural haematoma
EDTA	ethylenediaminetetraacetic acid
FBG	fibrinogen
FTLD	frontotemporal lobar degeneration
GIT	gastrointestinal tract
IHC	immunohistochemistry
ICH	intracerebral haemorrhage
ICP	intracranial pressure
IgG	immunoglobulin G
H202	hydrogen peroxide
HIV	Human Immunodeficiency Virus
HIVE	Human Immunodeficiency Virus Encephalopathy
LFB	luxol fast blue
LRP1	low-density lipoprotein receptor-related protein
MAPT	Microtubule associated protein Tau
MIRAGE	Multi-Institutional Research in Alzheimer Genetic Epidemiology
MMP	matrix metalloproteinase
MRC CFAS	Medical Research Council Cognitive Function and Ageing Study
MRI	magnetic resonance imaging
MS	multiple sclerosis
MVC	motor vehicle collision

mTBI	mild traumatic brain injury
NEP	neprilysin
NFTs	neurofibrillary tangles
NOX2	nicotinamide adenine dinucleotide phosphate-oxidase
NS	not significant
PBS	phosphate buffered saline
PET	positron emission tomography
PNS	peripheral nervous system
PM	post mortem
PTE	post traumatic epilepsy
PTSD	post-traumatic stress disorder
PSP	progressive Supranuclear Palsy
RAGE	receptor for advanced glycation end products
RECA-1	rat endothelial cell antigen-1
RTA	road traffic accident
rTBI	repetitive mild traumatic brain injury
SAH	subarachnoid haemorrhage
SEZ	subependymal astrocytic zone
SDH	subdural haematoma
SEM	standard error of the mean
SFG	superior frontal gyrus
SGL	superficial glial limitans
SIS	second impact syndrome
sTBI	Single moderate or severe Traumatic Brain Injury
SUDEP	sudden unexpected death due to epilepsy
SIV	simian immunodeficiency virus
TBI	traumatic brain injury
TDP-43	transactive response DNA-binding protein 43
TGF	tumour growth factor
TLR	toll-like receptors
Tris	tris(hydroxymethyl)aminomethane
TSPO	translocator protein
vCJD	Variant Creutzfeldt-Jakob disease
VEGF	vascular endothelial growth factor
WMI	white matter interface

Chapter 1 **Introduction**

Traumatic brain injury (TBI) is a leading cause of mortality and morbidity worldwide. In the UK alone, approximately 1.3 million people are living with TBI-related disabilities, with 160,000 hospital admissions annually (Parsonage, 2016). In the US this number is significantly increased with nearly 300,000 patients requiring hospitalisation and a further 5 million individuals living with chronic disabilities following a TBI (Coronado VG, 2012, Faul M, 2010, CDC, 1999). There is growing acknowledgment of the association between a history of TBI and late neurodegenerative disorders; however, the pathologies driving these late outcomes remain poorly described. Historically, clinical studies in TBI have described increased risk of Alzheimer's disease in a proportion of survivors (Molgaard et al., 1990, Mortimer et al., 1985, Mortimer et al., 1991, Graves et al., 1990, O'Meara et al., 1997, Salib and Hillier, 1997, Guo et al., 2000, Schofield et al., 1997, Plassman et al., 2000, Fleminger et al., 2003), although others have demonstrated conflicting data (Chandra et al., 1987, Amaducci et al., 1986, Broe et al., 1990, Ferini-Strambi et al., 1990, van Duijn et al., 1992, Katzman et al., 1989, Launer et al., 1999, Williams et al., 1991, Mehta et al., 1999). However, common to all studies, thus far, is a striking lack of autopsy confirmation of pathology in late TBI series, with resultant absence of adequate clinicopathological correlation.

The first report describing potential late consequences of TBI followed the careful observations of Dr Harrison S Martland in 1928, who described a variety of neuropsychiatric and motor symptoms in a limited case series of boxers exposed to repetitive traumatic brain injury (rTBI); referred to as punch-drunk syndrome (Martland, 1928). Subsequent studies in the years following Martland's original observations provided early accounts of a distinct neurodegenerative pathology in former boxers, further supporting the link between rTBI and a neurodegenerative disease, termed dementia pugilistica (DP) (J, 1937, Critchley, 1957, Mawdsley and Ferguson, 1963, Spillane, 1962). More recently, there has been growing recognition that this pathology is not limited to boxers but also observed in brains of individuals exposed to rTBI from other sports and circumstances (Omalu et al., 2011a, Omalu et al., 2011b, Omalu et al., 2005, Omalu et al., 2006a, Omalu et al., 2010a, Omalu et al., 2010b, McKee et al., 2009, McKee et al., 2010, McKee et al., 2013, Goldstein et al., 2012) and in survivors of a single, moderate to severe TBI (sTBI) (Johnson et al., 2012, Smith et al., 2013, Johnson et al., 2013a, Roberts et al., 1991, Roberts et al., 1994). Therefore suggesting it is exposure to TBI that is associated with the risk of development of late neurodegenerative disease rather participation in a particular sport or activity. Thus, the term

chronic traumatic encephalopathy (CTE) replaces DP in current literature, reflecting the wider exposures beyond boxing. While 90 years have passed since the first recognition of a clinical syndrome in former boxers, there remains remarkably little understanding of the complex pathologies of CTE. Limited case series have been described with only autopsy assessments to base the criteria of diagnosis on.

1.1 Traumatic brain injury and dementia

TBI is widely recognised as the strongest environmental risk factor for dementia (Molgaard et al., 1990, Mortimer et al., 1985, Mortimer et al., 1991, Graves et al., 1990, O'Meara et al., 1997, Salib and Hillier, 1997, Guo et al., 2000, Schofield et al., 1997, Plassman et al., 2000, Fleminger et al., 2003), with a direct dose-response relationship proposed between injury severity and subsequent risk of dementia (Guo et al., 2000, Plassman et al., 2000). In support of this relationship, meta-analyses of case-control studies, head injury which resulted in loss of consciousness had approximately a 50% increased risk in developing dementia (Mortimer et al., 1991). Further, the Multi-Institutional Research in Alzheimer Genetic Epidemiology study (MIRAGE) collected head injury information on a total of 2,233 Alzheimer's disease (AD) patients, and from 14,668 of their first-degree family members, by interviews and review of medical records. It was ascertained that a head injury with loss of consciousness and, to a lesser extent, head injury without loss of consciousness increased the risk of AD (Guo et al., 2000). If there was a loss of consciousness following the TBI, the risk of developing AD was double that of a head injury that did not have such an impact. However, a common concern with a majority of studies to date is their retrospective nature, with inevitable concerns on recall bias. Only one prospective study used level-1 evidence where head injured US veterans and non-head injured US veterans were interviewed and clinical assessments were carried out 50 years after the injury (Plassman et al., 2000). Those who sustained a severe TBI (loss of consciousness or post-traumatic amnesia longer than 24 hours) were 4 times as likely to have dementia compared with uninjured controls, while those who sustained a moderate TBI (loss of consciousness or post-traumatic amnesia between 30 minutes and 24 hours) were twice as likely to have dementia. Based on all studies to date, there is undoubtedly sufficient evidence to link moderate and severe TBI and an increased risk of dementia (Health, 2009, Li et al., 2017, Plassman and Grafman, 2015).

It has been estimated that between 5% and 15% of current dementia cases are TBI related (Shively et al., 2012). While there are currently approximately 850,000 dementia patients in the UK alone, this represents between 42,500 and 127,500 dementia patients attributed to

TBI. The Dementia UK report estimated that in 2014 dementia care cost £26 billion, therefore, the costs of TBI-attributed dementia are upwards of £1.3 billion a year, but as our understanding of this link develops these numbers will undoubtedly alter (Prince, 2007).

To date, cases of TBI-associated dementia have been considered as distinct entities dependent on whether exposure to TBI has been through either sTBI or rTBI; the former considered AD, the latter CTE. However, the presumption that CTE is restricted to patients who sustain rTBI, the majority being sportsmen and women, and development of AD is limited to patients who sustain a sTBI is arguably flawed.

Multiple studies have expanded on Martland's original observations of chronic neuropsychiatric sequelae in former boxers (Martland, 1928, Roberts, 1969, Corsellis et al., 1973); Roberts *et al* (Roberts, 1969) reported that out of 224 randomly selected professional boxers 17% demonstrated emotional liability, personality change, memory impairment and dementia. Corsellis (Corsellis et al., 1973) carried out case reports of 15 ex-boxers and noticed neuropsychiatric symptoms, such as speech and motor problems and dementia. More recent descriptions of former non-boxer athletes (including from American football, ice hockey, and rugby) and military personnel have reported similar neuropsychiatric and behavioural problems, while expanding the descriptions to include aggression, poor judgment, depression, suicidal ideation, and, in some instances, suicide (McKee et al., 2009, McKee et al., 2013, Stewart et al., 2016, McKee et al., 2014).

Although the dementia that develops following a moderate to severe sTBI is typically described as AD in type (Mortimer et al., 1985, Mortimer et al., 1991, Graves et al., 1990, O'Meara et al., 1997, Salib and Hillier, 1997, Schofield et al., 1997, Guo et al., 2000, Plassman et al., 2000, Fleminger et al., 2003), these studies include no neuropathological confirmation that the pathology that follows sTBI conforms to AD. Certainly, there have been no suitably designed, robust studies in the current era of understanding of the neuropathology of CTE to confirm the dementia occurring in late survivors of a sTBI is AD. However, dementia attributed to a sTBI has been reported to demonstrate prominent motor and neuropsychiatric symptoms, including depression and suicide (Dams-O'Connor et al., 2013, Sayed et al., 2013). As such, in cases where it has been critically assessed, the clinical syndrome of neurodegeneration following a sTBI appears distinct from AD and echoes that of rTBI. Therefore, the current view permeating the literature that a sTBI is specifically associated with the development of AD (DeKosky et al., 2013, DeKosky et al., 2010) should be regarded as speculative, and without confirmatory neuropathology.

1.2 Chronic traumatic encephalopathy

Following Martland's original clinical description in 1928, the first neuropathological assessment of neurodegeneration in boxers was not performed until 1954 (Brandenburg and Hallervorden, 1954), with multiple further case series reported in the following decades (Mawdsley and Ferguson, 1963, Payne, 1968, Neubuerger et al., 1959, Constantinidis and Tissot, 1967, Ferguson FR, 1965, Grahmann and Ule, 1957). Of these, perhaps the most informative was that of Corsellis in 1973 (Corsellis et al., 1973) describing the neurological features in the brains of 15 ex-boxers including fenestrated cavum cerebellar scarring, enlarged ventricles, thinning of corpus callosum, degeneration of substantia nigra and diffuse neurofibrillary tangles. Since these early studies, the picture that has emerged in subsequent descriptions is that of a complex of pathologies arising following exposure to TBI, single or repetitive, best described as a polypathology.

1.3 Macroscopic neuropathology

Often reported in early studies on the brains of boxers was atrophy of the cerebral hemispheres (Mawdsley and Ferguson, 1963, McKee et al., 2009, Brandenburg and Hallervorden, 1954, Payne, 1968, Neubuerger et al., 1959, Constantinidis and Tissot, 1967, Grahmann and Ule, 1957, Corsellis et al., 1973, Roberts et al., 1990a, Jordan et al., 1995, Schmidt et al., 2001, Saing et al., 2012, Nowak et al., 2009), demonstrating preferential involvement of the temporal (Drachman and Newell 1999, Areza-Fegyveres et al., 2007) and frontal lobes (Mawdsley and Ferguson, 1963, Neubuerger et al., 1959, Ferguson FR, 1965, Nowak et al., 2009, Areza-Fegyveres et al., 2007) and the cerebellum (Grahmann and Ule, 1957, Williams and Tannenberg, 1996). However, more recently, reports on non-boxer athletes observe a mild global atrophy and inconsistent reports of a reduction in brain weight (Omalu et al., 2011a, Omalu et al., 2006b, Omalu et al., 2006a, Omalu et al., 2010a, Omalu et al., 2010b, McKee et al., 2009, McKee et al., 2013). Despite this contrast, there is a pattern emerging of macroscopic features in rTBI which includes atrophy of the mammillary bodies, a mild degree of ventricular enlargement (perhaps preferentially of the third ventricle), pallor of the substantia nigra, and thinning of the corpus callosum (Brandenburg and Hallervorden, 1954, Payne, 1968, Neubuerger et al., 1959, Constantinidis and Tissot, 1967, Grahmann and Ule, 1957, Corsellis et al., 1973, Roberts et al., 1990a, Saing et al., 2012, Nowak et al., 2009, Drachman and Newell 1999). Widespread brain atrophy has been recognised following sTBI in both autopsy and imaging studies (Farbota et al., 2012, Ross et al., 2012, Ross, 2011, Tomaiuolo et al., 2004, Warner et al., 2010) with the latter suggesting this atrophy continues

beyond the acute phase and into longer-term survival. As with rTBI, reports have demonstrated a thinning of the corpus callosum in a proportion of sTBI patients with over 1-year survival (Johnson et al., 2013a).

Abnormalities of the septum pellucidum are a common feature described in material from those exposed to rTBI, in particular cavum septum pellucidum (CSP) or septal fenestration, with occasional reports of complete loss of the septum (Mawdsley and Ferguson, 1963, Omalu et al., 2011a, Omalu et al., 2006a, Omalu et al., 2005, Omalu et al., 2010b, McKee et al., 2009, Brandenburg and Hallervorden, 1954, Payne, 1968, Neubuerger et al., 1959, Constantinidis and Tissot, 1967, Ferguson FR, 1965, Grahmann and Ule, 1957, Roberts et al., 1990a, Jordan et al., 1995, Schmidt et al., 2001, Saing et al., 2012, Nowak et al., 2009, Williams and Tannenberg, 1996, Drachman and Newell 1999, Allsop et al., 1990, Geddes et al., 1999, Hof et al., 1992, Hof et al., 1991). Although CSP has been reported as a normal finding in up to one third of participants in population studies (Corsellis et al., 1973, Bogdanoff and Natter, 1989, Bodensteiner and Schaefer, 1997, Macpherson and Teasdale, 1988, JT, 1952) evidence supports CSP is of higher prevalence and to a greater extent in those exposed to rTBI (Gardner et al., 2014, Gardner et al., 2016, Corsellis et al., 1973). Further, imaging studies confirm CSP in rTBI and provide evidence it is an evolving pathology in longitudinal studies (Mawdsley and Ferguson, 1963, Ferguson FR, 1965, Casson et al., 1984, Jordan et al., 1992). Thus far, CSP has not been reported as a feature in pathology studies of sTBI yet this could be largely a consequence of an absence of studies rather than absence of pathology (Smith et al., 2013).

1.4 Microscopic neuropathology

While to date over 200 cases have been reported describing the neuropathology of rTBI exposure in a range of sports, including boxing (Smith et al., 2013, Brandenburg and Hallervorden, 1954, Corsellis et al., 1973), American football, ice hockey, wrestling, soccer, rugby union, in former military personnel (Omalu et al., 2011a, Omalu et al., 2006a, Omalu et al., 2006b, Omalu et al., 2010a, Omalu et al., 2010b, McKee et al., 2009, McKee et al., 2010, Goldstein et al., 2012, McKee et al., 2013, Omalu et al., 2011b, Stewart et al., 2016, McKee et al., 2014, Shively et al., Lindsley, 2017, Mez et al., 2017) and in cases of domestic abuse (Williams and Tannenberg, 1996, Hof et al., 1991, Roberts et al., 1990b), only approximately 40 cases have been described reporting the pathology of survival after a sTBI (Johnson et al., 2012, Johnson et al., 2013a, Johnson et al., 2011). From these limited case series, the pathology of late survival from TBI is recognised as a complex polypathology

featuring abnormalities in tau, amyloid β (Aβ), and TDP-43; neuroinflammation; axonal degeneration; degradation of white matter; and neuronal loss.

1.1.1 Tau

Axons encounter high strain rates during TBI in which mechanical breaking of the microtubules occurs and axoplasmic transport is disrupted (Tang-Schomer et al., 2010, Tang-Schomer et al., 2012, Ahmadzadeh et al., 2014). This diffuse axonal injury (DAI) (Sirko et al.) arises due to the viscoelastic nature of axons, in turn thought to derive from the biophysical properties of the microtubule-associated protein tau (Ahmadzadeh et al., 2014). Whilst abnormal accumulation of hyperphosphorylated tau is reported in cases of CTE (Smith et al., 2013) and in patients dying 1 year or more after a sTBI (Johnson et al., 2012) there has been no evidence of immediate tau pathology in patients dying in the acute phase after a sTBI (up to 4 weeks) (Smith et al., 2003a). In late TBI, whether following rTBI or sTBI, tau pathology is characterised by the accumulation of abnormal, hyperphosphorylated tau in both neurons and glia, around vessels and with preferential involvement of the depths of the sulci in the neocortical grey matter (Omalu et al., 2011a, McKee et al., 2009, McKee et al., 2010, Goldstein et al., 2012, McKee et al., 2013, Stewart et al., 2016, Geddes et al., 1999, Johnson et al., 2012) (Figure 1-1). First described in tau pathology of boxers, there is an irregular, patchy involvement both within and between the affected cortical areas (McKee et al., 2009, McKee et al., 2013, Stewart et al., 2016, Geddes et al., 1996, Geddes et al., 1999).

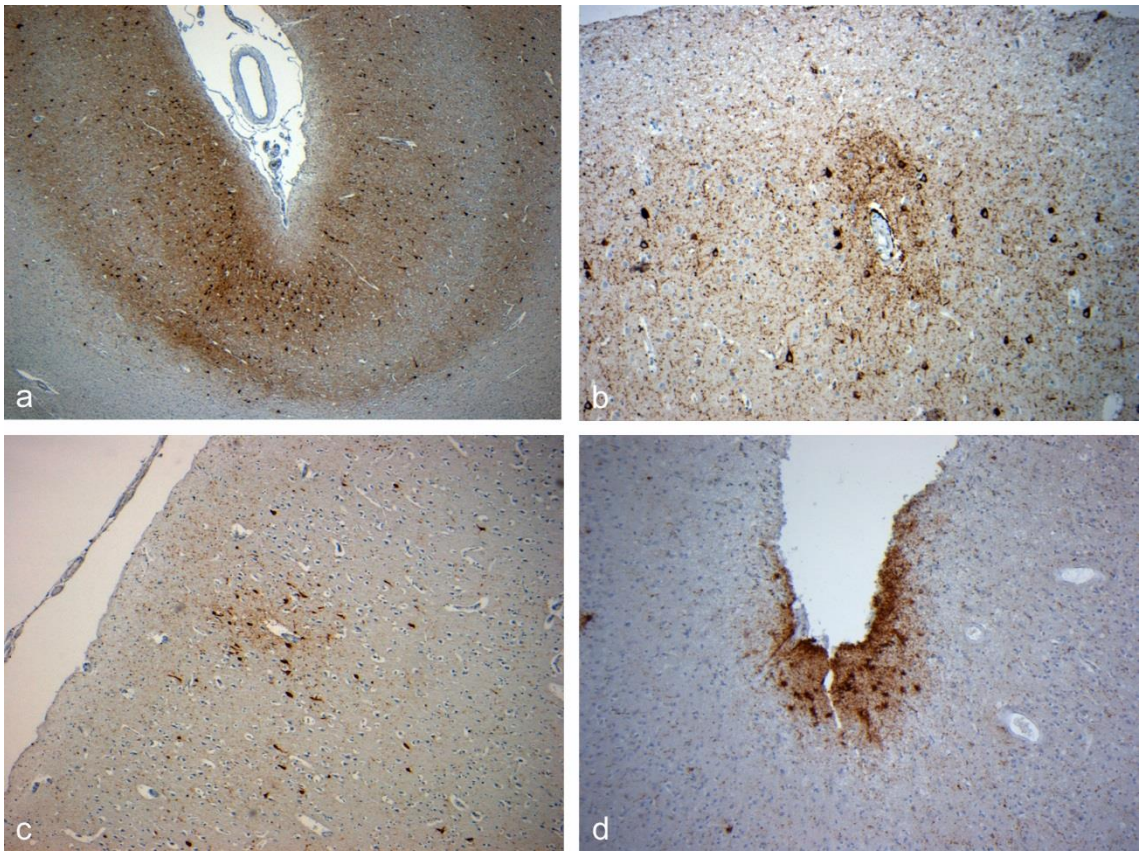

Figure 1-1 Neocortical tau pathology in CTE Tau immunoreactive profiles are distributed throughout the neocortex, though typically show preferential distribution towards the superficial neocortical layers and depths of sulci (a: 49M 12 months following single severe TBI), with a distinctive and characteristic perivascular accentuation of immunoreactive neurons and glia whether exposed to repetitive mild TBI (b: 56M former rugby player) or single moderate to severe TBI (c: 48M 3 years following single severe TBI). Accumulations of subpial thorn-shaped astrocytes may also be observed (d: 59M former soccer player). All sections stained for phosphorylated tau using antibody CP13 (courtesy Dr P Davies)

Using antibodies to hyperphosphorylated tau (AT8, CP13, PHF-1) the neuronal tau pathologies present as typical neurofibrillary tangles (NFT) and pretangles which, as noted, show preferential involvement towards depths of sulci and perivascular accentuation, and often demonstrate a distribution to superficial cortical layers (layers II and III) (McKee et al., 2013). This contrasts with AD where tau involvement is preferentially in the deeper layers of the cortex (Braak and Braak, 1991, Braak et al., 1993). In the hippocampus, CTE is noted for the preferential involvement of sector CA2 by NFTs and extracellular tangles (Figure 1-2), with NFTs and astroglial tau pathology also a feature in the hypothalamic region, in particular the mammillary bodies (McKee et al., 2013). Other regions involved may include deep grey nuclei and brainstem in the nucleus basalis of Meynert, substantia nigra (Figure 1-2), locus coeruleus, raphe nuclei, and tectum, while the dorsal striatum (the caudate and putamen) and cerebellar dentate nuclei are relatively spared. Further, tau-immunoreactive axonal profiles are often observed in the subcortical and midline white matter tracts (Figure 1-2) and tau-immunoreactive thorn-shaped astrocytes are demonstrated

in subpial and perivascular locations in the neocortex and subependymally (McKee et al., 2013). Biochemical characterisation of tau in CTE has only been performed in two former boxers (Schmidt et al., 2001) and in both cases the tau deposits were indistinguishable from those observed in AD.

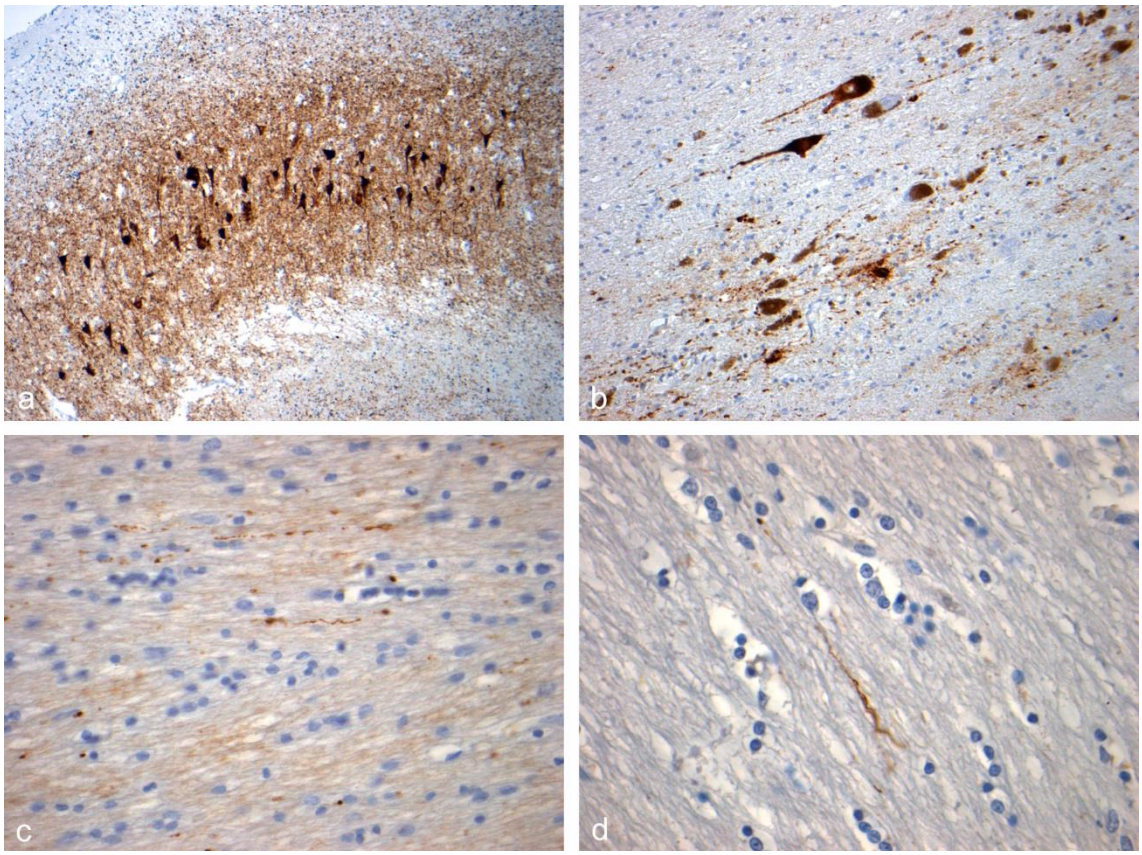

Figure 1-2 Tau pathology in CTE In addition to neocortical tau pathology, tau-immunoreactive profiles are common in the hippocampus in CTE, with preferential involvement of sector CA2 by NFTs and extracellular tangles and astroglial tau pathology (a: 59M former soccer player). Elsewhere, tau pathologies are described in the deep grey nuclei and brainstem, where tau-immunoreactive substantia nigra neurons and neurites may be present, together with a degree of pigment incontinence (b: same case as in (a)). Scattered tau-immunoreactive axonal profiles are also common in subcortical and midline white matter (c: same case as (a); d: 60M former boxer). All sections stained for phosphorylated tau using antibody CP13 (courtesy Dr P Davies).

While these tau pathologies have been reported in virtually all rTBI cases, there has been an unavoidable case-selection bias and a virtual absence of control material from uninjured cases in reports of CTE, rendering interpretations of the incidence of this pathology meaningless in the context of exposure to rTBI (Mez et al., 2017). In the single study examining sTBI, tau pathology was demonstrated in up to 30% of cases which was, in turn, in greater density and wider distribution than uninjured, age-matched controls (Johnson et al., 2012). However, as a retrospective, archive-based study, no information was provided on the clinical status of these post-TBI tau-positive patients. Hence, the clinical significance of the pathology identified at autopsy remains uncertain. Some attempts of staging of tau pathologies in CTE have been suggested by authors reviewing rTBI cases, from a restricted, focal, cortical pathology (stage I) to more extensive, widespread, cortical, hippocampal, and brainstem involvement of tau (stage IV) (McKee et al., 2013). However, this proposed staging has yet to be validated.

1.4.1 Amyloid β

Diffuse axonal injury is an early and consistent event in TBI which results in cytoskeleton disruption and interruption of axonal transport (Farbota et al., 2012, Johnson et al., 2013b, Adams et al., 1982, Adams et al., 1989a). DAI and transport interruption is demonstrated via immunocytochemical staining using β-amyloid precursor protein (APP) which visualises abnormal accumulation in injured axons (Johnson et al., 2013b, Gentleman et al., 1993, Sherriff et al., 1994). Normally transported by fast axonal transport, following TBI, APP may be observed in damaged axons within hours of injury. At the sites of axonal injury, colocalisation of APP with enzymes presenilin-1 and β-site-APP-cleaving enzyme, enables APP to cleave into Aβ (Smith et al., 2003b, Smith et al., 2003c, Smith et al., 1999, Chen et al., 2004, Chen et al., 2009, Johnson et al., 2010). Therefore, DAI creates an environment promoting the production of localised, high concentrations of Aβ protein (Johnson et al., 2010).

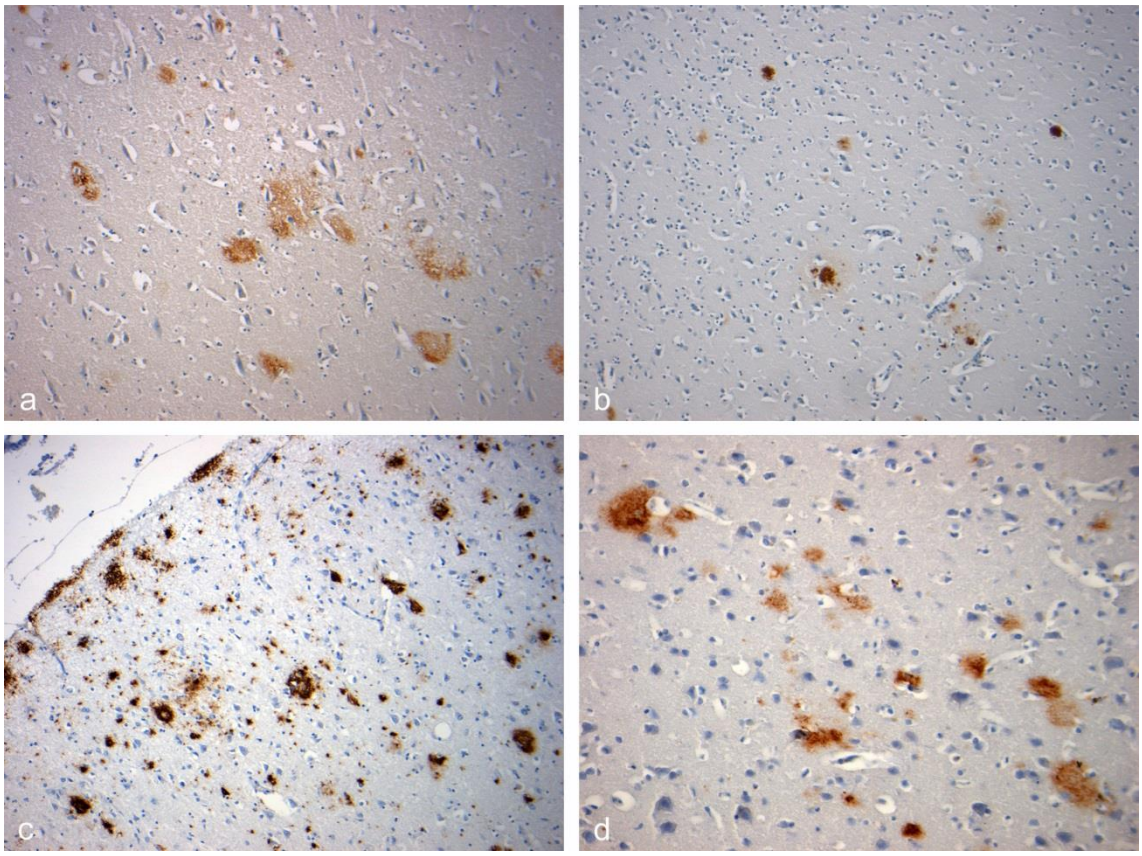

Figure 1-3 Aβ plaque pathologies following TBI Diffuse Aβ plaques can be identified in autopsy and surgical material from approximately 30% of TBI patients in the acute phase post-injury (a: 51M 24hours following severe TBI). In the following weeks to months, these diffuse plaques resolve, only to re-emerge in around 30% of survivors a year or more from single moderate to severe TBI, as both neuritic and diffuse Aβ plaques (b: 55F 47 years survival from single severe TBI). Aβ plaques are also present in a majority of cases of CTE following exposure to repetitive mild TBI, typically, though not exclusively, diffuse in subtype (c: 60M former boxer; d: 59M former soccer player). All sections stained using antibody 6F3D, specific for the N-terminal epitope of Aβ (Dako).

Aβ plaques are a hallmark of AD, but are also identified in autopsy material from up to 30% of patients dying acutely following a single moderate to severe TBI, and at higher density than observed in equivalent material from uninjured age-matched controls (Figure 1-3) (Roberts et al., 1991, Roberts et al., 1994, Johnson et al., 2012). Aβ plaques have also been demonstrated in pericontusional, surgically excised tissue from sTBI survivors immediately after injury (Ikonomovic et al., 2004). These acute plaques are diffuse in nature and similar to those of early-stage AD. However, where plaques in AD are thought to develop slowly and occur predominantly in the elderly, TBI-associated plaques are detectable within hours of injury and across a range of ages, including in young adults.

Evidence suggests that, over time, these acute TBI plaques clear and normal amyloid cycling is restored (Chen et al., 2009). However, in autopsy material from patients who survived 1 year or more after a sTBI Aβ plaques were observed in considerably greater density and in wider distribution than in material from age-matched, uninjured controls (Johnson et al.,

2012). In addition, these long-term TBI amyloid plaques are more typically neuritic in type, much like the plaques established in AD (Johnson et al., 2012) (Figure 1-3).

When reviewing the Corsellis Archive material acquired at autopsy from a cohort of 20 retired amateur and professional boxers, Roberts and colleagues observed often-abundant, diffuse Aβ plaques in all but one case; a 22-year-old former professional boxer 3-year career and only 3 professional fights. All NFT-positive cases in this cohort contained plaque pathology. In current reviews of CTE in former athletes, reports of Aβ plaques are less consistent (McKee et al., 2013). However, where documented, this pathology is present in a majority of cases, the proportion of cases with plaque pathology increasing with age (Stein et al., 2015). In studies of material from patients with exposure to rTBI, these Aβ plaques are almost invariably described as diffuse in nature (Figure 1-3), in contrast to the neuritic plaque more often observed in long-term survivors of a sTBI. However, although much research attention is focused on tau pathology in CTE, comparatively little attention is directed toward amyloid pathologies.

1.4.2 Transactive response DNA-binding protein

The 43 kDa transactive response DNA-binding protein 43 (TDP-43) is a nuclear protein widely expressed throughout the body. TDP-43 can, however, translocate from the nucleus into the cytoplasm under certain conditions forming polyubiquitinated and hyperphosphorylated inclusion bodies. This abnormal TDP-43 is recognised as a major disease-associated protein in a number of neurodegenerative conditions, including frontotemporal lobar dementia and amyotrophic lateral sclerosis (Neumann et al., 2006), and as a minor component of a variety of other conditions, including AD, Parkinson's disease, and a small proportion of normal-aged individuals (Chen-Plotkin et al., 2010, Geser et al., 2010, Neumann et al., 2007). Some animal models of TBI have suggested that the translocation is caused by upregulation of TDP-43 which is, in turn, caused by axonal injury (Sato et al., 2009, Moisse et al., 2009a, Moisse et al., 2009b). This translocation has been suggested as part of the acute-phase response as, upon recovery, TDP-43 moves back to the nucleus (Sato et al., 2009, Moisse et al., 2009a). Therefore, there is the potential that TBI-induced axonal injury might influence neuronal TDP-43 processing.

Following exposure to rTBI in both boxers and non-boxer athletes', neuronal cytoplasmic TDP-43 inclusions and distinctive grain-like profiles in the surrounding neuropil have been documented in the hippocampus, temporal neocortex, and amygdala in a majority of CTE

cases (McKee et al., 2010, McKee et al., 2013, Johnson et al., 2011, King et al., 2010). This abnormal TDP-43 observed coincides with a clinical diagnosis of amyotrophic lateral sclerosis in a small proportion of these cases, with the autopsy examination revealing features consistent with CTE (McKee et al., 2010). Based on these limited observations a diagnosis of CTE has been suggested (McKee et al., 2010) although many more cases are required to validate this proposition.

Where similarities in tau and Aβ pathologies in survivors of rTBI and sTBI are apparent, there is a notable difference in TDP-43 pathology. Following late survival of sTBI abnormally phosphorylated TDP- 43 cytoplasmic inclusions have not been reported in any greater extent than in material from uninjured controls. However, increased cytoplasmic immunoreactivity to physiological, non-phosphorylated TDP-43 has been observed in acute and late survivors (Johnson et al., 2011). This intriguing apparent difference in pathologies between survivors of rTBI and sTBI might suggest a physiological role for TDP-43 in the response to injury, which is somehow modified after exposure to repetitive brain injury, and thus precipitates cytoplasmic translocation and accumulation of hyperphosphorylated TDP-43.

1.4.3 Neuroinflammation

Neuroinflammation is increasingly regarded as a key feature of the pathology of a range of neurodegenerative disorders (Perry et al., 2010, Brettschneider et al., 2012b, Brettschneider et al., 2012a), depression (Miller and Raison, 2016) and as an early event in AD pathogenesis (Town et al., 2008, Wright et al., 2013, Yamamoto et al., 2007, Yoshiyama et al., 2007); studies examining serum or cerebrospinal fluid from patients surviving a sTBI, have also shown evidence of elevated proinflammatory cytokine levels that correlated with poor neuropsychiatric outcome, including suicidal ideation (Juengst et al., 2014, Lindqvist et al., 2014, Kumar et al., 2015).

Immediately following injury, TBI induces a complex neuroinflammatory response in both humans and animal models, associated with an acute-phase inflammatory cell reaction featuring polymorphonuclear leukocytes, T lymphocytes, macrophages, and natural killer cells, together with activation of resident microglia (Johnson et al., 2013a, Loane and Byrnes, 2010). It could be expected that this acute-phase inflammation resolves itself under normal circumstances; however, in a proportion of survivors there is increasing evidence that this post-TBI neuroinflammation persists long-term. In autopsy material from patients

surviving a TBI there is evidence of an ongoing neuroinflammatory response years after survival following a single injury (Figure 1-4) (Johnson et al., 2013a). Interestingly, where these observations demonstrate distinct activated microglia in the corpus callosum, in vivo positron emission tomography studies in surviving patients after a sTBI, using the ligand [11C]PK-11195, have reported no significant differences in binding in this region, although they have reported a difference in binding in the thalamic region compared with control patients (Ramlackhansingh et al., 2011a). However, [11C]PK-1195 is a translocator protein (TSPO) ligand which is non-specific for microglia and is expressed on other cells such as astrocytes and endothelial cells (Chechneva and Deng, 2016b). Therefore, the possibility that imaging studies might underestimate or misrepresent neuroinflammation following TBI could be considered.

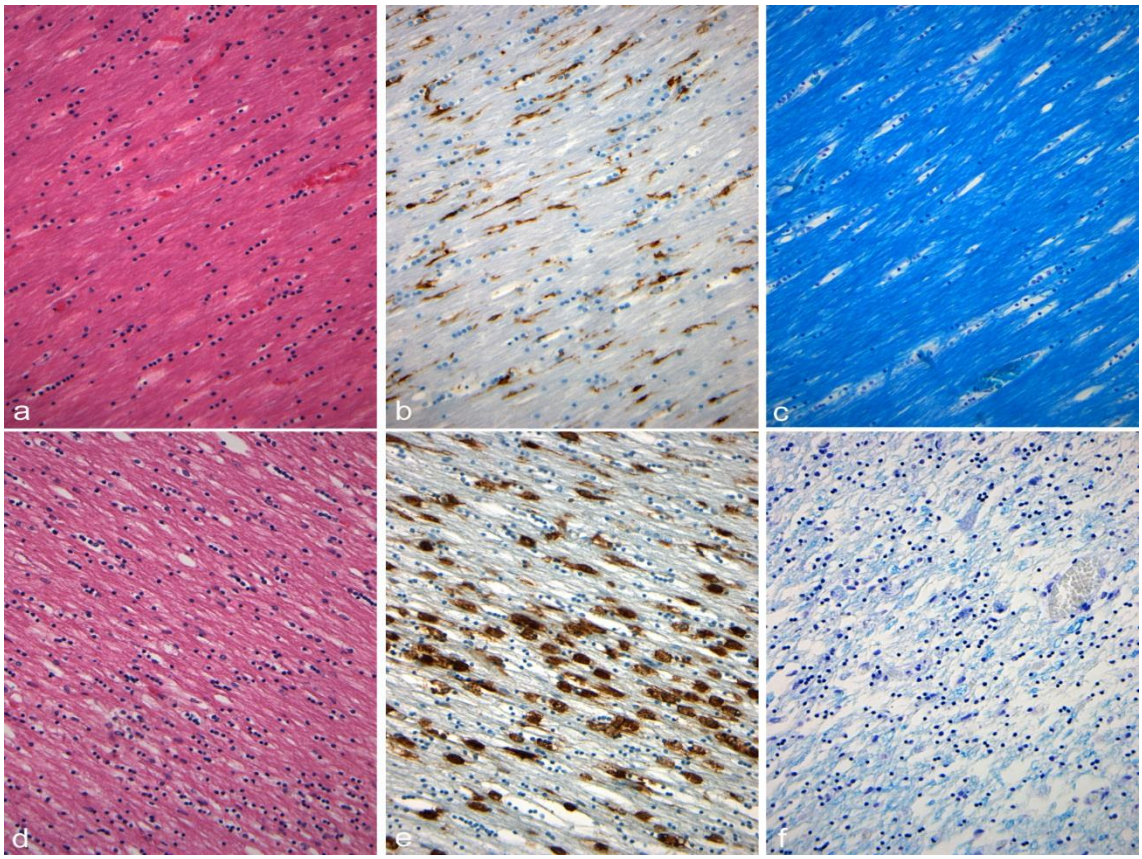

Figure 1-4 Neuroinflammation and white matter degradation in the corpus callosum with survival following TBI Approximately 30% of survivors a year or more from single moderate to severe TBI show evidence of white matter degradation as rarefaction in staining to Haematoxylin and eosin (d) when compared to uninjured control material (a). Accompanying this is evidence of ongoing neuroinflammation in the form of numerous amoeboid, activated microglia (e) in contrast to quiescent, ramified microglia in uninjured controls (b). Staining from myelin with Luxol fast blue/ Cresyl violet demonstrates an associated loss of myelin with evidence of continued myelin degradation (f). (a)(b)(c) sections from the corpus callosum of a 38M non-TBI control, cause of death sudden unexpected death in epilepsy. (d)(e)(f) sections from the corpus callosum of a 56M with a 3-year survival from single severe TBI. (b) and (e) stained for HLA-DP, DQ, DR using antibody CR3/43 (Dako) to reveal activated microglia.

There has been very little characterisation of the extent and distribution of the neuroinflammatory response following rTBI in boxers or non-boxer athletes, although it has been mentioned in several publications (Payne, 1968, Corsellis et al., 1973, Saing et al., 2012, Adams and Bruton, 1989). However, there have been numerous experimental models of rTBI which have demonstrated persistent microglial activation with an association with degenerative pathology and cognitive deficit (Mouzon et al., 2014, Petraglia et al., 2014a).

It is still unclear if this neuroinflammatory process that is acquired following TBI is a primary response (abnormal inflammation driving late TBI pathology) or a secondary response (abnormal inflammation reacting to other ongoing TBI pathologies occurring in parallel). Some animal models have suggested that the immediate microglial inflammatory response following TBI is both reparative (M2a microglial phenotype) and neurotoxic (M1 microglial phenotype) which possibly switches to M1 predominant phenotype during the late phase (Loane and Byrnes, 2010, Kumar et al., 2013, Loane et al., 2014). The key functional effects of the M1 activation state are killing of intracellular pathogens and antigen presenting. These produce inflammatory cytokines, reactive oxygen species and reactive nitrogen species, which generate a neurotoxic environment (MacMicking et al., 1997); while the M2 activation state involves an anti-inflammatory phenotype which promotes tissue repair and debris clearance, aiding the healing process (Cherry et al., 2014). Whether the microglial responses in human TBI, in particular the phenotypic profiles in early-versus-late survivors, mirror observations from animal studies has yet to be confirmed.

1.4.4 Astrocytic response

Animal models of TBI have demonstrated that as a consequence of injury astrocytes can exhibit membrane instability and cytoskeleton disassembly (Cullen et al., 2011). In response to this, a number of events are initiated in astrocytes including rapid influx of extracellular calcium, sodium release of matrix metalloproteinase-9, secretion of vasoactive molecules and adenosine triphosphate release (Hekmatpanah and Hekmatpanah, Hoffman et al., 2000, Ostrow et al., 2011, Ahmed et al., 2000). Astrocytes have been recognised as important early responders following TBI, preceding the microglial response (Kim and Dustin, 2006), with ATP released from injured astrocytic networks guide the microglial population to site of focal injury (Kim and Dustin, 2006, Davalos et al., 2005, Rouach et al., 2002, Stout et al., 2002, Verderio and Matteoli, 2001). Similar to the heterogeneity in M1 and M2 microglia, reactive astrogliosis has been attributed to both neuroprotective and detrimental effects in the central nervous system (CNS) (Laird et al., 2008, Sirko et al., 2015, Bardehle et al., 2013,

Myer et al., 2006). The characterisation of reactive astrogliosis following a sTBI has yet to be defined and developed. One limited post-mortem case series, investigating blast-related injuries, recorded prominent astroglial scarring and reactive astrogliosis in grey–white matter boundaries and at the subpial glial plate in all chronic blast exposure cases (up to 9 years survival) and did not find similar such patterns in sTBI; however, numbers were small (Shively et al., 2016).

Following rTBI in transgenic mice, astrocytes display an acute presence of reactive astrogliosis (Petraglia et al., 2014a, Ojo et al., 2013). A key focus on astrocytes following rTBI, however, remains the tau-immunoreactive astrocytes observed in CTE (McKee et al., 2009, Stein et al., 2014). This astrocytic p-tau pathology in CTE is proposed to be topographically distinct from aging-related tau astrogliopathy (ARTAG) which presents itself as four-repeat tau immunoreactive thorn-shaped astrocytes (Lopez-Gonzalez et al., 2013, Lace et al., 2012) and may go on to form astrocytic tangles. Limited animal work suggests a reactive astrocytic response following TBI which may have heterogenic attributes and, to date, the late response still requires to be established and expanded.

1.4.5 Neuronal loss

In autopsy studies, material from patients who sustained a sTBI demonstrate a degree of neuronal loss in the acute-phase (Shaw et al., 2001, Maxwell et al., 2003). Given the multiple acute pathologies of TBI, including diffuse axonal injury and the acute-phase neuroinflammatory response, this neuronal loss is to be anticipated. However, this neuronal loss may continue into the late phase in a proportion of patients, with active degeneration of neurons via programmed cell death being observed in material from patients up to 1 year following a single, severe TBI (Maxwell et al., 2003, Williams et al., 2001b, Maxwell et al., 2006).

With regards to rTBI, neuronal loss in the neocortex, substantia nigra, locus coeruleus, and cerebellum has been described in the majority of CTE cases (both boxers and non-boxer athletes) (Omalu et al., 2011b, Omalu et al., 2005, Omalu et al., 2006a, Omalu et al., 2010a, Omalu et al., 2010b, Brandenburg and Hallervorden, 1954, Neubuerger et al., 1959, Constantinidis and Tissot, 1967, Grahmann and Ule, 1957, Schmidt et al., 2001, Nowak et al., 2009, Williams and Tannenberg, 1996, Hof et al., 1992, Corsellis et al., 1973, Mann et al., 1983). The cell loss has been described as varying from patchy and selective alterations through to widespread and diffuse loss. Although there have been reports of neuronal loss

from the substantia nigra, synuclein-associated pathologies, including Lewy bodies, have not been reported, which, given the evidence of motor symptoms in CTE (Parkinsonian symptoms) is unique (Omalu et al., 2006a, Omalu et al., 2005, Brandenburg and Hallervorden, 1954, Constantinidis and Tissot, 1967, Corsellis et al., 1973, Drachman and Newell 1999). This vulnerability of the substantia nigra is unknown in patients surviving a sTBI.

1.4.6 White matter degradation and continued axonal degeneration

In all severities of TBI, DAI is a constant pathology in varying degrees. It is associated with interruption of axonal transport via cytoskeletal disruption which creates an environment for rapid Aβ genesis in the acute phase post TBI (Johnson et al., 2013c, Adams et al., 1982, Adams et al., 1989a, Smith et al., 2003b, Smith et al., 1999, Chen et al., 2004, Johnson et al., 2010). In one of the earliest pathologies determined in sTBI, Strich (Strich, 1956) demonstrated evidence of ongoing myelin degeneration at autopsy up to 15 months after survival from a single, severe TBI using the Marchi technique. Using a swine model of axopathy, continual axonal degeneration has been demonstrated months after injury (Chen et al., 2004). This observation has also been recognised in patients surviving a single moderate-to-severe TBI where there is ongoing axonal pathology in a proportion of survivors; decades after injury (Chen et al., 2009, Johnson et al., 2013a). Performing immunohistochemistry on brain sections, this continual axonal degeneration is characterised as morphologically abnormal APP-immunoreactive swollen axonal profiles throughout the white matter regions (Figure 1-5). These swollen bulbs of amyloid precursor protein (APP) are found in isolation and in small clusters in the white matter, indicative of disconnected axon terminals and providing evidence of ongoing axonal disruption in long-term survival in humans. In addition to the axonal degeneration, there is marked thinning of the white matter in the corpus callosum and reduced myelin staining which coincided with amoeboid microglia that contained myelin breakdown products, in keeping with ongoing myelin phagocytosis (Johnson et al., 2013a).

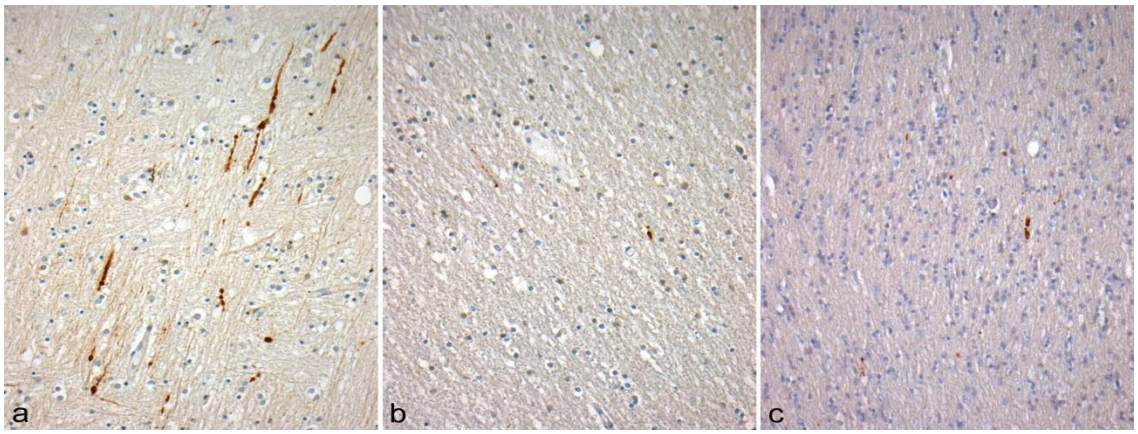

Figure 1-5 Axonal pathology in the corpus callosum with varying survival from TBI Diffuse axonal injury (DAI) is observed in all severities of TBI with associated axonal transport interruption. DAI is revealed in sections stained for APP and is detectable within hours of injury as immunoreactive axonal profiles with abnormal morphologies (a) 18M 11hours survival from severe TBI. Beyond this acute phase axonal injury, evidence of ongoing axonal transport interruption marked by scattered, morphologically abnormal axons staining for APP remains present in survivors a year or more from single moderate to severe TBI (b) 24M 8years survival from single severe TBI (c) and in material from individuals exposed to repetitive mild TBI,59M former soccer player. All sections stained for an antibody to the N-terminal amino acids 66-81 of APP (Millipore).

Where there is a concordance of reports of white matter pathology following a sTBI, there is limited evidence of this pathology following rTBI. Later publications in rTBI have described abnormal axonal profiles which accumulates transport proteins such as phosphorylated tau (Goldstein et al., 2012, McKee et al., 2013) where earlier publications did not seek evidence of such pathology. Some reports have described mixed observations; from foci of degeneration (Omalu et al., 2011b, Payne, 1968, Saing et al., 2012, Corsellis et al., 1973) with reduced myelin staining (McKee et al., 2009, Payne, 1968, Neubuerger et al., 1959, Corsellis et al., 1973) to no evidence of demyelination at all (Constantinidis and Tissot, 1967). Thus said, the formal characterisation of this axonal pathology following rTBI still remains to be completed.

1.4.7 Blood-brain barrier

The breakdown in blood-brain barrier (BBB) integrity is becoming increasingly recognised in a range of disorders such as ischemia (Sandoval and Witt, 2008), multiple sclerosis (Kirk et al., 2003) and neurodegeneration (Zlokovic, 2011, Bell and Zlokovic, 2009a). Both imaging (Starr et al., 2009) and animal models (Zlokovic, 2011, Ujiie et al., 2003) of AD have proposed that disruption of the BBB occurs early in the disease process and it may contribute to its pathogenesis due to impaired amyloid-β clearance or associated neuroinflammation (Zlokovic, 2011, Grammas, 2011, Shibata et al., 2000b, Zlokovic et al., 2010, Deane et al., 2004a, Jaeger et al., 2009). Additionally, neuropathology studies have described multifaceted vascular changes connected to BBB disruption in AD patients (Zipser

et al., 2007a, Brown and Thore, 2011a, Buee et al., 1994) with a correlation between evidence of BBB leakage and AD-type pathologies in "normal" aging (Viggars et al., 2011).

BBB disruption following sTBI has been described in the acute phase in several animal TBI models; however, the data is inconsistent on the time course of this disruption. While some studies have reported that BBB disruption occurs early, within hours of injury, and quickly resolves (Barzo et al., 1996, Habgood et al., 2007, Baldwin et al., 1996, Shapira et al., 1993, Rinder and Olsson, 1968, Shreiber et al., 1999, Smith et al., 1995, Cortez et al., 1989, Ommaya et al., 1964, Hekmatpanah and Hekmatpanah, 1985, Hicks et al., 1993, Povlishock et al., 1978), others have described a more dynamic, biphasic course following TBI with an early-phase BBB disruption occurring 3 to 6 hours after injury followed by a further BBB injury at 1 to 3 days post-injury (Baldwin et al., 1996, Baskaya et al., 1997). BBB disruption has also been observed in mice 3 months post-TBI with focal immunoglobulin G (IgG) deposition around callosal blood vessels ipsilateral to controlled cortical impact site (Glushakova et al., 2014). In support of these observations in animal TBI models, evidence of acute BBB disruption has been described following severe TBI in humans through reports of elevated serum albumin in cerebrospinal fluid and elevated S100β in serum (Saw et al., 2014, Stahel et al., 2001, Ho et al., 2014a, Blyth et al., 2009, Di Battista et al., 2015, Csuka et al., 1999, Kossmann et al., 1995). This acute BBB disruption following sTBI may predict a poor long-term outcome in a population of patients (Ho et al., 2014a). Neuroimaging studies have also demonstrated evidence of BBB disruption after TBI in humans, with this disruption persisting at sites of focal contusions for up to 11 years post injury and with greater frequency in TBI patients with post-traumatic epilepsy (Tomkins et al., 2011).

Following rTBI, there is imaging evidence of BBB disruption in American football participants, independent of clinical evidence of TBI, possibly as a result of exposure to "subconcussive" head impacts (Weissberg et al., 2014). Other studies using blood biomarkers have also demonstrated elevated serum S100β in American football players suggesting transient BBB damage in players with the greatest number of sub-concussive hits (Marchi et al., 2013). However, some animal models of rTBI failed to demonstrated BBB disruption (Kane et al., 2012) as did studies on boxers and military personnel (chronic blast exposure) suggesting the BBB remains undamaged (Blennow et al., 2011, Zetterberg et al., 2006, Zetterberg et al., 2013b). Longitudinal studies of biomarker levels in patients with mild TBI are scarce. In the absence of such studies, it is difficult to determine BBB disruption following mild TBI and, therefore, clear biomarkers that could diagnose mild TBI and predict clinical outcomes

1.5 Genetics

1.5.1 APOE and traumatic brain injury

Several studies have examined the relationship between the apolipoprotein ε4 (*APOE* ε4) allele and dementia after TBI. APOE regulates lipid homeostasis by mediating lipid transport from one tissue or cell to another (Mahley and Rall, 2000). Specifically in the CNS, ApoE is produced by astrocytes and transports cholesterol to neurons via lipoprotein (LDLR) receptors (Bu, 2009). The ε4 allele of the *APOE* gene is associated with hyperlipidaemia and hypercholesterolaemia, which lead to atherosclerosis, coronary heart disease and stroke (Mahley and Rall, 2000, Lahoz et al., 2001).

It has been well documented that possession of the ε4 allele of the *APOE* gene is also associated with an increased risk of AD (Corder et al., 1993, Saunders et al., 1993); specifically this allele is related to an increased incidence of Aβ pathologies in AD and to age-related Aβ deposition in healthy individuals (Jack et al., 2015). Regarding TBI, there is increasing evidence of an association between the ε4 allele (ApoE4) and prognosis following a sTBI, with worse immediate and 6-month outcomes in carriers of the ε4 allele than in non-carriers (Teasdale et al., 1997, Sorbi S, 1995, Friedman et al., 1999, Liberman et al., 2002, Sundstrom A, 2004, Lichtman et al., 2000, Liaquat et al., 2002, Smith et al., 2006, Diaz-Arrastia et al., 2003, Teasdale et al., 2005). Long-term survivors of sTBI who are carriers of ApoE4 also have a higher risk of dementia following injury than non-carriers (O'Meara et al., 1997, Guo et al., 2000, Plassman et al., 2000, Mayeux et al., 1995, Katzman et al., 1989, Mauri et al., 2006). Regarding influence on pathology after injury, following sTBI, individuals who have the ε4 allele demonstrate more severe contusional injury and more notable diffuse hypoxic brain injury than sTBI patients who do not carry the ε4 allele (Smith et al., 2006). There is also evidence of increased amyloid plaque pathology in patients dying during the acute-phase after a sTBI compared with those who do not carry the ε4 allele (Nicoll et al., 1995). However, the long-term implications of *APOE* genotype on late pathology after exposure to TBI are yet to be described.

There is much less documented evidence of an association between the ε4 allele and cognitive impairment in rTBI (Kristman et al., 2008, Tierney et al., 2010). In the longer-term outcomes after rTBI some studies have described an association between the ε4 allele and increased cognitive impairment in boxers (high exposure only, those with more than 12 professional bouts) (Jordan et al., 1997) and in older professional American footballers

(Kutner et al., 2000); however, as discussed previously, the numbers of participants in these studies was small. Studies of the association between the *APOE* genotype and late pathology after exposure to rTBI have been informative. Although original reports described a lack of an association between *APOE* genotype and CTE pathology as defined by characteristic tau deposition (Omalu et al., 2011a, McKee et al., 2013), when an appraisal of neuropathologically confirmed CTE cases was carried out, specifically those with Aβ pathologies, a clear association was discovered between the ε4 allele, Aβ pathologies and an acceleration of CTE disease progression (Stein et al., 2015).

Interestingly, where the majority of the literature on CTE has focused on pathognomonic lesion being tau, the limited clinical reports of outcomes after rTBI and of dementia following a sTBI indicate an association between the possession of the *APOE* ε4 allele and a worse prognosis. In addition, the ε4 allele has been described as being associated mainly with Aβ pathologies rather than with tau pathologies. This information suggests that clinically relevant CTE might extend beyond the description of a tauopathy, with other pathologies such as Aβ deposition being as (if not more) important in the disease progression.

1.5.2 Neprilysin and traumatic brain injury

Neprilysin is the main Aβ-degrading enzyme, with microsatellite GT repeat polymorphism in the promoter region of the neprilysin gene (*NEP*) linked to amyloid pathologies, including AD and cerebral amyloid angiopathy (CAA) (Iwata et al., 2000, Turner et al., 2001, Yasojima et al., 2001). Following a sTBI, this polymorphism has been associated with Aβ plaque pathology (Johnson et al., 2009) where individuals carrying a longer repeat (greater than 41 GT repeats) were at higher risk of Aβ pathology than those carrying the shorter repeats. This suggests *NEP* has a key role in the breakdown of Aβ and plaque formation. Although an increase in intra-axonal neprilysin immunoreactivity and an association with Aβ accumulation has been described in patients surviving up to 3 years following a sTBI (Chen et al., 2009), the longer-term relationship between *NEP* and neurodegenerative pathologies are yet to be described. In terms of the role of *NEP* in the predictor of outcome in rTBI and relationship of neuropathologies, this is yet to be examined.

The pathology of late survival from TBI is recognised as a complex polypathology featuring abnormalities in tau, amyloid β (Aβ), and TDP-43; neuroinflammation; axonal degeneration; degradation of white matter; and neuronal loss; however, the literature is limited in parts.

Thus far, it is acknowledged that tauopathy is a key feature of CTE following rTBI and is observed in late survivors of sTBI. Amyloid-β has been revealed in tissue acutely following a sTBI and can be found in higher density and in younger cases in the late response following a sTBI, yet evidence following rTBI is limited. In addition, TDP-43 has been demonstrated translocated into the cytoplasm following rTBI, however, to date, there appears to be an absence of evidence following sTBI and axonal degeneration has been observed in both sTBI and rTBI (again there is limited evidence in rTBI).

1.5.3 MAPT

The gene *MAPT* (microtubule-associated protein Tau) encodes for the protein tau. *MAPT* resides within a 900kb inversion polymorphism that results in two haplotypes, H1 and H2 (Stefansson et al., 2005). Mutations in this gene have demonstrated that tau dysfunction alone was sufficient to initiate neurodegeneration (Gasparini et al., 2007), specifically tauopathies. Rare missense and exon 10 splicing mutations which result in increased levels of tau isoforms (4-repeat) lead to familial frontotemporal dementia with parkinsonism (Hutton et al., 1998, Spillantini and Goedert, 1998), whereas H1 haplotype is associated with increased risk of progressive supranuclear palsy (PSP) (Pittman et al., 2004). The association between these haplotypes and TBI is unknown although one study noted an increase in H1 haplotype in CTE however this was not significant (Bieniek et al., 2015).

Where most pathologies have a certain degree of understanding, the complexity of the BBB following TBI has yet to be explored. Disruption of the BBB has been demonstrated in a limited capacity in animal studies in the acute phase, however the pathology and temporal course in humans is unknown. Neuroinflammation following TBI has been observed in several studies, however this could be expanded into microglial phenotypes and regional locations of inflammation. As could the astrocytic response which has been observed is some animal studies and one (very limited) case series. Common to all sTBI and rTBI studies to date, is a striking lack of autopsy confirmation of pathology in late TBI series, with resultant absence of adequate clinicopathological correlation and, therefore, much more work is required to confirm such pathologies.

1.6 Hypotheses and aims

Table 1 Hypotheses and aims

Hypotheses	Background summary	Aims
sTBI results in disruption of BBB function acutely and in long-term survivors.	BBB disruption following sTBI has been described in the acute phase in several animal TBI models; however, the data is inconsistent on the time course of this disruption. Some imaging studies have reported BBB disruption up to 11 years post-injury.	To characterise the pattern, distribution and temporal evolution of BBB disruption at varying survivals from sTBI.
sTBI results in a mixed astroglial and microglial neuroinflammatory response that is geographically and temporally distinct.	The characterisation of reactive astrogliosis following sTBI has yet to be defined and developed; one limited post-mortem case series with blast-related injuries reported reactive astrogliosis in grey–white matter junctions and subpial glial plate. Autopsy studies report activated microglia in corpus callosum of patients surviving years following a sTBI; however, imaging studies report binding of PK-1195 in thalamic regions.	To characterise the extent, distribution and temporal evolution of the astroglial and microglial response to sTBI.
The microglial response to sTBI is defined by phenotypically distinct microglial population.	Animal models of TBI report an immediate microglial inflammatory response following TBI of both reparative (M2a microglial phenotype) and neurotoxic (M1 microglial phenotype) which possibly switches to M1 predominant phenotype during the late phase. The response in humans following TBI is unclear.	To determine the microglial phenotypes associated with survival from sTBI.

2 General Material and Methods

2.1 Ethical approval for use and source of human tissue

All human brain tissue used it the following studies were selected from the Glasgow TBI Archive of the department of Neuropathology, Glasgow, UK. The Glasgow TBI archive contains 1474 TBI cases collected from 1963 to 2006, together with a quantity of uninjured controls. Within the TBI archive 1133 cases are males (77%) and 341 cases are females (23%). All cases have corresponding post-mortem reports available and, where necessary, supplemented by forensic and clinical records. As such, the Archive database includes information on demographics, clinical data, and detail on neuropathology findings at the original autopsy. All procedures were performed in accordance with approval granted by the South Glasgow and Clyde Research Ethics Committee (REC Nos 10/S0704/60) and the Greater Glasgow and Clyde Bio-repository Governance Committee (**Appendix 1**).

2.2 Studies using post-mortem brain tissue

All tissue was acquired at routine diagnostic post-mortem and was available for use as formalin-fixed, paraffin embedded blocks. Whole brains were immersed in 10% formol saline for a minimum of 3 weeks, then dissected using a standardised block selection protocol. Tissue was then processed to paraffin using standardized techniques. All cases were anonymised with no patient-identifiers available to the researcher.

All cases had a confirmed diagnosis of moderate to severe TBI based on clinical and pathological assessments. Cases included various survival times and ages. Acute cases (survival < 14 days) were included (n = 74) with ages ranging from 4 - 60 years old. Intermediate cases were selected (n = 11) with survival intervals ranging from 14 days to 1 year and long-term TBI cases (n = 32) with ages ranging from 19 – 60 years old and survival intervals ranging from 1 year to 47 years. Mean PM delay, sex, cause of injury and cause of death can be found in **Appendix 2**. Age-matched, uninjured controls were included (n = 30), with ages ranging from 7 years to 60 years old at time of death and with no known history of neurological disease or of TBI. Varying causes of death are reported with SUDEP and heart disease predominant. All TBI cases and controls were aged 60 years old or younger at time of death to minimise influence of ageing-associated pathologies on observations.

2.3 Tissue preparation for immunohistochemistry

Sections were cut at 8µm using a rotary microtome (Leica Microsystems, Wetzlar, Germany) and mounted onto Superfrost Plus microscope slides (Cellpath, Powys, UK). The slides were placed into an oven at 37ºC for minimum of 72 hours for the tissue to adhere to the slides. Sections were then deparaffinised in xylene (3 x 5 minutes) followed by immersion in 100% methanol (3 x 5 minutes), 95% methanol (2 x 5 minutes) then rehydrate to distilled water (dH_20). Sections were then immersed in 3% hydrogen peroxide solution (H_20_2) for 15 minutes to reduce endogenous peroxidase activity. After washing in water, antigen retrieval was performed as required for each specific antibody. Heat/pressure antigen retrieval was performed by immersing slides in preheated Tris EDTA buffer (pH8.0) or Citrate buffer (pH6.0) and placing them in a microwave pressure cooker for 8 minutes on high power. The pin on the pressure cooker should have popped after 3 minutes to guarantee the sections are immersed in boiling solution for exactly 5 minutes. To ensure consistent heat dispersion, the same number of slides were places in the pressure cooker each run.

The lid of the pressure cooker was then removed, carefully, and sections left for 10 minutes to cool on the bench, followed by slow introduction to cold water to bring up to temperature. Once cooled, sections were then blocked for 30 minutes using 50µl horse serum blocking agent (Vector Labs, Burlingame, CA, USA) per 5 ml Optimax buffer (Biogenex, San Ramon, CA, USA). The primary antibody was diluted in optimax buffer (for specific antibody dilutions see **appendix 3**) and applied to the sections for 20 hours at 4oC. Once incubated with the primary antibody, the sections went through 3 separate washes in PBS/Tween for 10 minutes each on a belly dancer (Stovall, Life Science Inc, Greensboro, US). Following these washes, a biotinylated secondary antibody (10µl horse serum and 10µl secondary antibody per 5ml Optimax buffer) was applied for 30 minutes RT (Universal Elite Kit, Vector Labs, Burlingame, CA, USA), followed again by 3, 10 minute washes in PBS/Tween. The avidin/biotin horse-radish peroxidase (HRP) complex (10µl Avidin DH solution and 10µl biotinylated enzyme per 5ml Optimax buffer) was then applied for 30 minutes RT followed by another washing step in PBS/Tween (3 x 10 minutes). Visualisation was achieved using the DAB peroxidase substrate kit (Vector Labs, Burlingame, CA, USA) which was applied as per manufacturer's instructions. The sections were then rinsed in dH_20 and counterstained by immersion in Mayer's haematoxylin for 1 minute. Slides were rinsed again in dH_20 and then immersed in Scott's Tap Water Substitute for 1 minute to 'blue' the sections. The slides were then dehydrated through 95% and 100% methanol (3 x 5 minutes each), immersed in xylene to clear sections (3 x 5 minutes) and then coverslipped.

Negative controls were used in each experiment to demonstrate the absence of non-specific binding. The primary antibody was omitted from these sections, optimax buffer was used only. Positive sections were used in each experiment to demonstrate correct staining of the specific antibody.

All sections were viewed using a Leica DMRB light microscope (Leica Microsystems). In addition, sections were scanned and analysed using a 20x optic on a Hamamatsu Nanozoomer 2.0-HT slide scanner which has a 0.75NA and scans images at a digital resolution of 0.46µm per pixel. Furthermore, where appropriate sections were scanned using a 40x optic which scans images at a digital resolution of 0.23µm per pixel. The images viewed via the SlidePath Digital Image Hub application (Leica Microsystems). Observations were made blind to all clinical and demographic data of all cases.

2.4 Statistical analysis

Statistical analyses were performed using SPSS (version 22, IBM.com). The exact details of particular tests used are given in each chapter. Semi quantitative data of BBB disruption (Chapter 3 and 4) and microglia activation (Chapters 6 and 7) were analysed using the $\chi 2$ test to assess differences in scoring between and within cohorts. Cramer's V was calculated to determine the effect size. A Cramer's V value of 0.1 suggested a low practical significance, a value of 0.3 suggested a moderate practical significance and a value of 0.5 suggested a high practical significance. Where quantitative data were collected (Chapters 5, 6 and 7) values were, where possible, expressed as mean ± standard error of the mean. The Student's *t*-test was used to compare data sets between and within cohorts. Cohen's *d* was calculated to determine the effect size and to indicate the standardised difference between two means. A Cohen's *d* value of 0.2 suggested a low practical significance, a value of 0.5 suggested a moderate practical significance and a value of 0.8 suggested a high practical significance. All effects were considered statistically significant when $p \leq 0.05$.

.

3 Blood-brain barrier disruption is an early event that may persist for many years after traumatic brain injury

3.1 Introduction

Traumatic brain injury (TBI) is acknowledged as the strongest environmental risk factor for the development of neurodegenerative disease, historically reported as Alzheimer's disease (AD) (Molgaard et al., 1990, Mortimer et al., 1985, Mortimer et al., 1991, Graves et al., 1990, O'Meara et al., 1997, Salib and Hillier, 1997, Guo et al., 2000, Schofield et al., 1997, Plassman et al., 2000, Fleminger et al., 2003, Lye and Shores, 2000, Johnson et al., 2010, Plassman and Grafman, 2015), although more recently regarded as chronic traumatic encephalopathy (CTE) (Corsellis et al., 1973, Smith et al., 2013, McKee et al., 2013, McKee and Daneshvar, 2015, Hay et al., 2016). In the UK alone, there are approximately 160,000 hospital admissions annually, this number is significantly higher in the US with 300,000 TBI patients requiring hospitalisation (Coronado VG, 2012, Faul M, 2010, CDC, 1999). Potentially, this TBI population could significantly impact the financial burden allocated to dementia care globally. Exposure to a single moderate or severe, or to repetitive TBI, reveals a complex of pathologies including abnormalities of tau, amyloid-β and TDP-43; neuronal loss; neuroinflammation; and white matter degradation (Johnson et al., 2010, Smith et al., 2013, McKee et al., 2013, McKee and Daneshvar, 2015, Johnson et al., 2012, Johnson et al., 2013a, Ramlackhansingh et al., 2011a, Johnson et al., 2013d). The mechanisms driving these late post-TBI neurodegenerative pathologies remain elusive.

3.1.1 Blood-brain barrier disruption in disease

Disruption of the blood-brain barrier (BBB) is increasingly recognised in a variety of disorders such as ischemia (Sandoval and Witt, 2008), multiple sclerosis (Kirk et al., 2003) and neurodegeneration (Zlokovic, 2011, Bell and Zlokovic, 2009b). Various studies suggest that disruption of the BBB integrity is an early event in the progression of AD and may contribute to its pathogenesis, perhaps as a result of impaired amyloid-β clearance or associated neuroinflammation (Zlokovic, 2011, Grammas, 2011, Shibata et al., 2000b, Zlokovic et al., 2010, Deane et al., 2004a, Jaeger et al., 2009). Specifically, a case-control magnetic resonance imaging (MRI) study investigated BBB permeability in both AD patients and healthy, older controls. A noted increase in BBB permeability was present at an early stage in AD although the extent of the leakage was similar to the controls of a similar

age (mean age of AD patients was 73.7 years and mean age of controls 72.7 years). In a systematic review of the literature, increasing age in healthy subjects was a risk factor of BBB disruption, which increased further in vascular dementia and AD (Farrall and Wardlaw, 2009). Animal models of AD have also suggested that BBB permeability is an early event in AD (Ujiie et al., 2003). Using an AD model Tg2576 mice, Ujiie et al assessed the uptake of Evans blue dye and albumin into the brain of transgenic mice. Increased BBB permeability was found in the cortex of 10-month-old Tg2576 mice, preceding AD presentation. Furthermore, younger (4-month-old) Tg2576 mice exhibited BBB disruption compared to their non-transgenic counterparts (Ujiie et al., 2003).

Neuropathology studies also suggest complex vascular changes associated with increased BBB permeability in AD patients (Zipser et al., 2007b, Brown et al., 2001, Buee et al., 1994), where an association between histologic evidence of BBB leakage and AD-type pathologies in "normal" aging has also been demonstrated (Viggars et al., 2011). Utilising the brain donations from the Medical Research Council Cognitive Function and Ageing Study (MRC CFAS), Viggars et al investigated BBB disruption in the temporal cortex of 92 participants in the study. By staining sections with BBB permeability markers albumin and fibrinogen, along with tight-junction protein markers claudin-5, ZO-1 and occludin they demonstrated that BBB disruption increased with the progression of AD-type pathology, such as neurofibrillary tangles, and this increase in disruption was accompanied with an increase in vascular density (Viggars et al., 2011).

3.1.2 Blood-brain barrier disruption after TBI

Blood-brain barrier disruption has been demonstrated in the acute phase following TBI using several animal models, but the temporal course of this disruption is unclear. Some studies suggest a short-lived opening of the BBB following injury which is resolved within hours (Barzo et al., 1996, Habgood et al., 2007, Baldwin et al., 1996, Shapira et al., 1993, Rinder and Olsson, 1968, Shreiber et al., 1999, Smith et al., 1995, Cortez et al., 1989, Ommaya et al., 1964, Hekmatpanah and Hekmatpanah, 1985, Hicks et al., 1993, Povlishock et al., 1978). However, other models of TBI suggest a more dynamic biphasic course of BBB disruption where an early-phase BBB opening occurs at 3–6 hours post-injury followed by a later BBB opening at 1–3 days post-injury (Baldwin et al., 1996, Baskaya et al., 1997). Of note, several of the studies that suggest a short-lived opening of the BBB also suggest some continual leakage for up to 4 days post-injury (Shapira et al., 1993, Habgood et al., 2007), while others only monitored the rodents for a short time-period following the injury (Barzo et al., 1996,

Shreiber et al., 1999). Deposits of focal immunoglobulin-G (IgG) around callosal blood vessels ipsilateral to controlled cortical impact in mice have been demonstrated 3 months following injury, which supports this later BBB disruption (Glushakova et al., 2014).

Where evidence of acute-phase BBB disruption following injury has been demonstrated in various animal models of TBI, several clinical studies report elevated levels of serum albumin and S100β in the cerebrospinal fluid (CSF) following a severe TBI (Saw et al., 2014, Stahel et al., 2001, Ho et al., 2014a, Blyth et al., 2009). Ho et al performed a retrospective cohort study on 97 TBI patients in which they observed BBB disruption in 43 of the 97 patients. Furthermore, this disruption is associated with more severe TBI and may predict an unfavourable long-term outcome (Ho et al., 2014a). In addition, neuroimaging studies have reported evidence of prolonged BBB disruption in patients following TBI, even mild to moderate injury in some cases, which can present in greater frequency in patients with post-traumatic epilepsy (PTE) (Tomkins et al., 2011). Using MRI, Tomkins et al investigated BBB breakdown in 37 TBI patients, 19 of which suffered from PTE. Disruption was observed in 53% of TBI patients, lasting up to 11 years post-injury, with PTE patients more likely to have BBB disruption than non-epileptic patients (82.4% versus 25%) (Tomkins et al., 2011). Furthermore, BBB disruption has been observed following mild TBI in American football participants using imaging techniques, independent of clinical evidence of TBI (Weissberg et al., 2014). Weissberg et al recruited 16 football players and 13 track and field athletes where, following at least 2 months of training and competing, they underwent MRI to assess BBB integrity. The results revealed that BBB disruption was evident in 40% of the football players and 8.3% of the control athletes. Furthermore, elevated S100β serum levels have been reported in football players, in the absence of recorded concussions, indicating that this BBB disruption may be a result of 'subconcussive' events (Marchi et al., 2013).

There is, therefore, evidence from both animal models and limited clinical studies of BBB disruption following a TBI; however, the extent and temporal course of this BBB dysfunction in humans has not been researched fully. Specifically, evidence of late phase BBB disruption has not been explored. In this study, material from the Glasgow TBI Archive will be used to characterise the extent, distribution and temporal dynamics of BBB disruption following a moderate or severe single TBI in comparison with age-matched controls.

Hypothesis: BBB disruption is present following TBI observed by increased deposits of fibrinogen and IgG throughout the brain compared to uninjured controls.

3.2 Specific methods

3.2.1 Case selection and brain tissue preparation

Ethical approval for this study was granted by the Greater Glasgow and Clyde Bio-repository Governance Committee. From the Glasgow TBI Archive, cases aged 60 years or younger at the time of death with a history of a single moderate or severe TBI were selected. They represented a range of survival times from injury to include acute cases with survival times of 10 hours to less than 14 days (n = 27); intermediate cases with survival times of 14 days to less than 1 year (n = 11); and long-term cases with survival times from 1 year to 47 years (n = 32). Detailed reports from the original diagnostic autopsy were available for all cases; where necessary these were supplemented by forensic and clinical records, and a history of moderate or severe TBI at presentation was confirmed, as defined by Glasgow Coma Scale. Age-matched uninjured controls aged 60 years or younger at the time of death and with no known history of neurologic disease or history of TBI (n = 21) were selected for comparison. Post-mortem delays were comparable across the cohorts ($p > 0.05$ in all comparisons across cohorts; Student's *t*-test). Demographics, clinical data, and detail on neuropathology findings at the original autopsy for each cohort are presented in Table 2.

Table 2 Demographic and clinical information of all groups

		TBI: Acute survival (n = 27)	TBI: Intermediate survival (n = 11)	TBI: Long-term survival (n = 32)	Controls (n = 21)
Mean age (range)		44.4 years (9-60)	32 years (17-56)	46.3 years (19-60)	39.9 years (14-60)
Males		17 (63%)	11 (100%)	31 (96.9%)	13 (62%)
Mean PM delay (range)		56.1 hours (3-240)	74.7 hours (26-192)	65.5 hours (9-184.5)	71.6 hours (12-144)
Mean survival interval (range)		69.3 hours (6-216)	72.8 days (14-279)	7.8 years (1-47)	Not applicable
Cause of TBI	Fall	15 (55.5%)	2 (18%)	15 (46.9%)	Not applicable (No history of TBI)
	RTA	7 (25.9%)	5 (45.5%)	5 (15.60%)	
	Assault	4 (14.8%)	3 (27%)	8 (25%)	
	Unknown	1 (3.7%)	1 (9.1%)	4 (12.5%)	
Cause of death	Head injury	25(92.6%)	4(36.4%)	0	0
	Bronchopneumonia	2(7.4%)	4(36.4%)	7(21.9%)	1(4.8%)
	ARDS	0	2(18.1%)	1(3.125%)	0
	Pulmonary thromboembolism	0	1(9.1%)	0	0
	Heart disease	0	0	6(18.8%)	5(23.8%)
	Alcohol related	0	0	2(6.25%)	0
	Pyelonephritis	0	0	1(3.125%)	0
	Multi-organ failure	0	0	1(3.125%)	0
	GIT haemorrhage	0	0	1(3.125%)	0
	Polytrauma	0	0	1(3.125%)	0
	Drug overdose	0	0	0	3(14.3%)
	SUDEP	0	0	7(21.9%)	8(38.1%)
	Pulmonary oedema	0	0	1(3.125%)	0
	Septicaemia	0	0	0	2(8.3%)
	Inhalation of gastric contents	0	0	0	2(8.3%)
	Unknown	0	0	4(12.5%)	0

Key: *TBI = traumatic brain injury; SUDEP = sudden unexpected death in epilepsy; GIT = gastrointestinal tract; ARDS = acute respiratory distress syndrome; RTA = road traffic accident*

3.2.2 Routine histology

Haematoxylin and eosin staining was performed on sections from all tissue blocks. Slides were deparaffinised in xylene and rehydrated to water followed by immersion for 10 minutes in haematoxylin (Mayer; Leica Microsystems, Wetzlar, Germany). After rinsing and immersion in Scott's tap water substitute (Leica Microsystems) to “blue” the sections, slides were differentiated in 1% acid alcohol and rinsed. The sections were then immersed in 25% aqueous eosin Y solution (TCS Biosciences, Buckingham, United Kingdom) for 5 minutes, rinsed, dehydrated, cleared, and coverslipped.

3.2.3 Immunohistochemistry

After deparaffinisation and rehydration, sections were immersed in 3% aqueous H2O2 for 15 minutes to quench endogenous peroxidase activity. Antigen retrieval was performed via microwave pressure cooker for 8 minutes in preheated 0.1 mol/L Tris EDTA buffer (pH8). Subsequent blocking was achieved by applying 50 μL of normal horse serum (Vector Labs, Burlingame, CA) per 5 mL of Optimax buffer (BioGenex, San Ramon, CA) for 30 minutes. Incubation with the primary antibody was then performed for 20 hours at 4°C. Polyclonal rabbit anti-human antibodies for fibrinogen (FBG) and IgG (Dako, Carpinteria, CA) were used at dilutions of 1: 17,500 and 1: 10,000, respectively. A biotinylated secondary antibody was then applied for 30 minutes, followed by avidin-biotin complex as per the manufacturer's instructions (Vectastain Universal Elite kit, Vector Labs). Finally, visualisation was achieved using the DAB peroxidase substrate kit (Vector Labs) followed by counterstaining with haematoxylin. Known positive tissue sections were run in parallel with test sections in all antibody runs, in addition to sections with primary antibody omitted as standard controls for antibody specificity.

3.2.4 Image analysis

All sections were viewed using a Leica DMRB light microscope (Leica Microsystems). In addition, sections were scanned at 20x using a Hamamatsu Nanozoomer 2.0-HT slide scanner, with the images viewed via the SlidePath Digital Image Hub application (Leica Microsystems). Furthermore, where appropriate sections were scanned using a 40x optic which scans images at a digital resolution of 0.23μm per pixel. The images in this chapter have been digitally captured at 4x (2.3μm per pixel), 20x (0.46μm per pixel) and 40x (0.23μm per pixel).

All observations were conducted blind to demographic and clinical data. Anatomically distinct regions were defined for assessment to include the neocortical grey matter of the cingulate gyrus, cingulate sulcus, superior frontal gyrus, parahippocampal gyrus, collateral sulcus, fusiform gyrus, and insular cortex. A sub-analysis of neocortical grey matter was performed by dividing the cortex into superficial (layers 1 and 2), mid (layers 3 and 4), and deep layers (layers 5 and 6) (Figure 3-1). In addition, the white matter of the midline and lateral extent of the corpus callosum and internal capsule, hippocampal sectors CA1 to CA4, and the thalamus (subdivided into medial, intermediate, and lateral regions) were assessed. Each anatomic region was reviewed, and, in a semi-quantitative assessment, the frequency and intensity of immunoreactivity were determined as absent (score 0), sparse (score 1), moderate (score 2), or extensive (score 3). Representative examples of immunohistochemical findings and the corresponding semi-quantitative scores are shown in Figure 3-2.

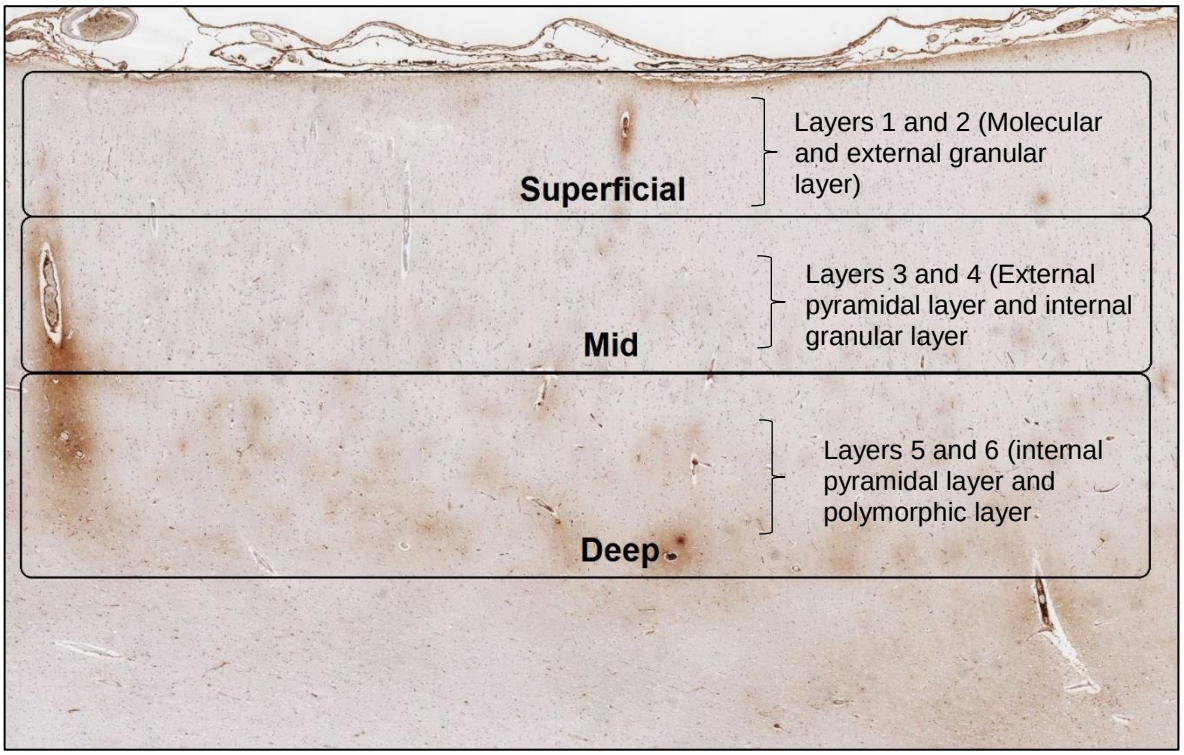

Figure 3-1 Separation of Cortical lamination The sub-analysis of neocortical grey matter was performed by dividing the cortex into 3 distinct layers based on the cortical distribution of neurons

3.2.5 Statistical analysis

All data were analysed using SPSS (version 22; IBM, Inc). The $\chi 2$ test was used to assess differences in data between and within cohorts, where appropriate. Cramer's V was used to determine the effect size. A Cramer's V value of 0.1 suggested a low practical significance, a value of 0.3 suggested a moderate practical significance and a value of 0.5 suggested a

high practical significance. All effects were considered statistically significant when $p \leq 0.05$.

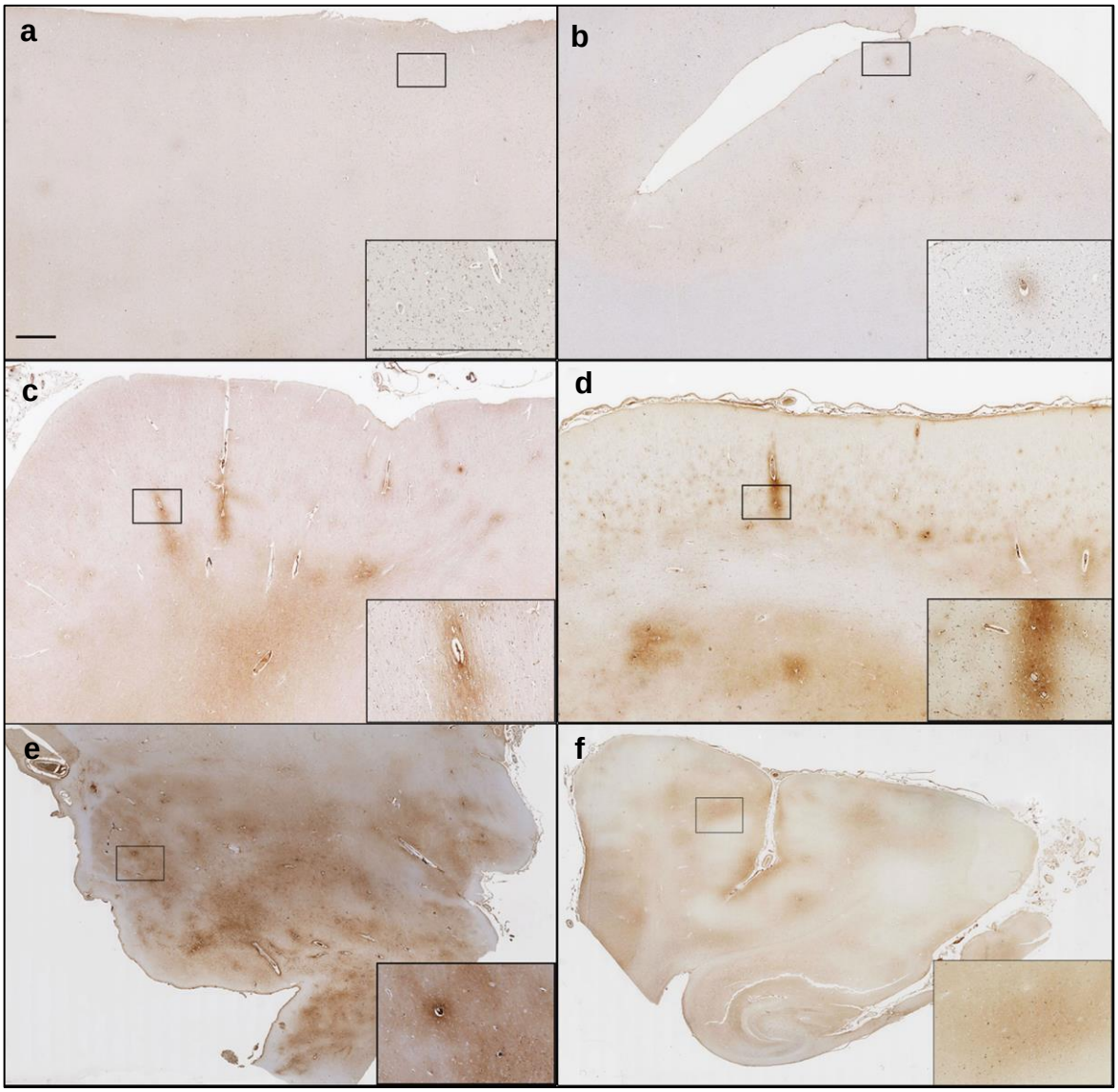

Figure 3-2 Representative images of semi-quantitative scoring Representative examples of the patterns of fibrinogen (FBG) immunoreactivity. (a) The superior frontal gyrus of a 47-year-old male traumatic brain injury (TBI) patient who died 1 year after a fall. No abnormal FBG immunoreactivity is present (score of 0). (b) Limited sparse perivascular FBG immunoreactivity (score of 1) in a 60-year-old male TBI patient who died 16 years after a road traffic accident. (c) More widespread moderate perivascular FBG immunoreactivity (score of 2) in the superior frontal gyrus of a 60-year-old male TBI patient who survived 10 hours after a fall. (d) Extensive perivascular and adjacent parenchymal FBG immunoreactivity (score of 3) in a 50-year-old male TBI patient who survived 1 year after an assault. (e) Extensive perivascular FBG immunoreactivity (score of 3) in the thalamic region of a 60-year-old male TBI patient who survived 8 days after a fall. (f) Sparse perivascular FBG immunoreactivity (score of 1) in the parahippocampal region of a 56-year-old female TBI patient who survived 24 hours after a road traffic accident. Scale bar = 1mm (low magnification), scale bar = 100μm (high magnification).

3.3 Results

3.3.1 FBG immunoreactivity in control group

In uninjured controls, where present, FBG immunoreactivity was observed in a predominantly perivascular distribution highlighting small vessels throughout the neuropil. In addition, occasional sparse immunoreactive neurons and glia were observed. In an overwhelming majority of controls (17 of 21), FBG immunoreactivity was limited (score 0 or 1) (Figure 3-3a) and localised (Figure 3-4). In the remaining 4 controls, localised foci of moderate (score 2) levels of FBG immunoreactivity were observed in single tissue blocks; in 2 cases localised to the thalamus, one to the fusiform gyrus and the last to the superior frontal gyrus (Figure 3-5). Causes of death in these controls with localised moderate FBG immunoreactivity were mixed; there was 1 case each of sudden death in epilepsy, sudden death of cardiac origin, sepsis with multi-organ failure, and pneumonia.

3.3.2 FBG immunoreactivity in acute TBI survival

In material from patients dying acutely after TBI (10 hours to less than 14 days survival), in addition to perivascular FBG immunoreactivity, regions of more confluent diffuse immunostaining were also present (Figure 3-3b). In contrast to the typically limited abnormal FBG immunoreactivity observed in controls, in this acute TBI survival cohort, 88% of cases showed at least 1 anatomic region with moderate (score 2) or extensive (score 3) FBG immunoreactivity ($p < 0.001$; $\chi 2$; Cramer's $V = 0.703$). Furthermore, in contrast to the localised pathology in controls, FBG immunoreactivity after TBI often appeared multifocal, that is, involving 2 or more regions in 11 of 27 (40%) acute survival cases (Figure 3-4). Of the regions examined, moderate or extensive FBG immunoreactivity was detected most frequently in material from the cingulate and superior frontal gyri (16 cases), followed by the thalamus (12 cases), medial temporal lobe (11 cases) and insular cortex (6 cases) (Figure 3-5). Within the neocortical regions (cingulate, superior frontal, fusiform and parahippocampal gyri), there was evidence of preferential anatomic distribution, with moderate or extensive FBG immunoreactivity more evident in the crests of gyri than in the depths of the adjacent sulci in both cingulate and medial temporal lobe cortical regions (Figure 3-6). Furthermore, within the crests of gyri, FBG immunoreactivity was greater in the mid and deeper layers than the superficial layers of the cortex. In the superior frontal gyrus, 60% of cases showed moderate or extensive FBG immunostaining in the deeper layers versus 15% of cases in the superficial layers ($p = 0.0079$; $\chi 2$; Cramer's $V = 0.46$) (Figure 3-6). There was no notable FBG immunoreactivity in the corpus callosum.

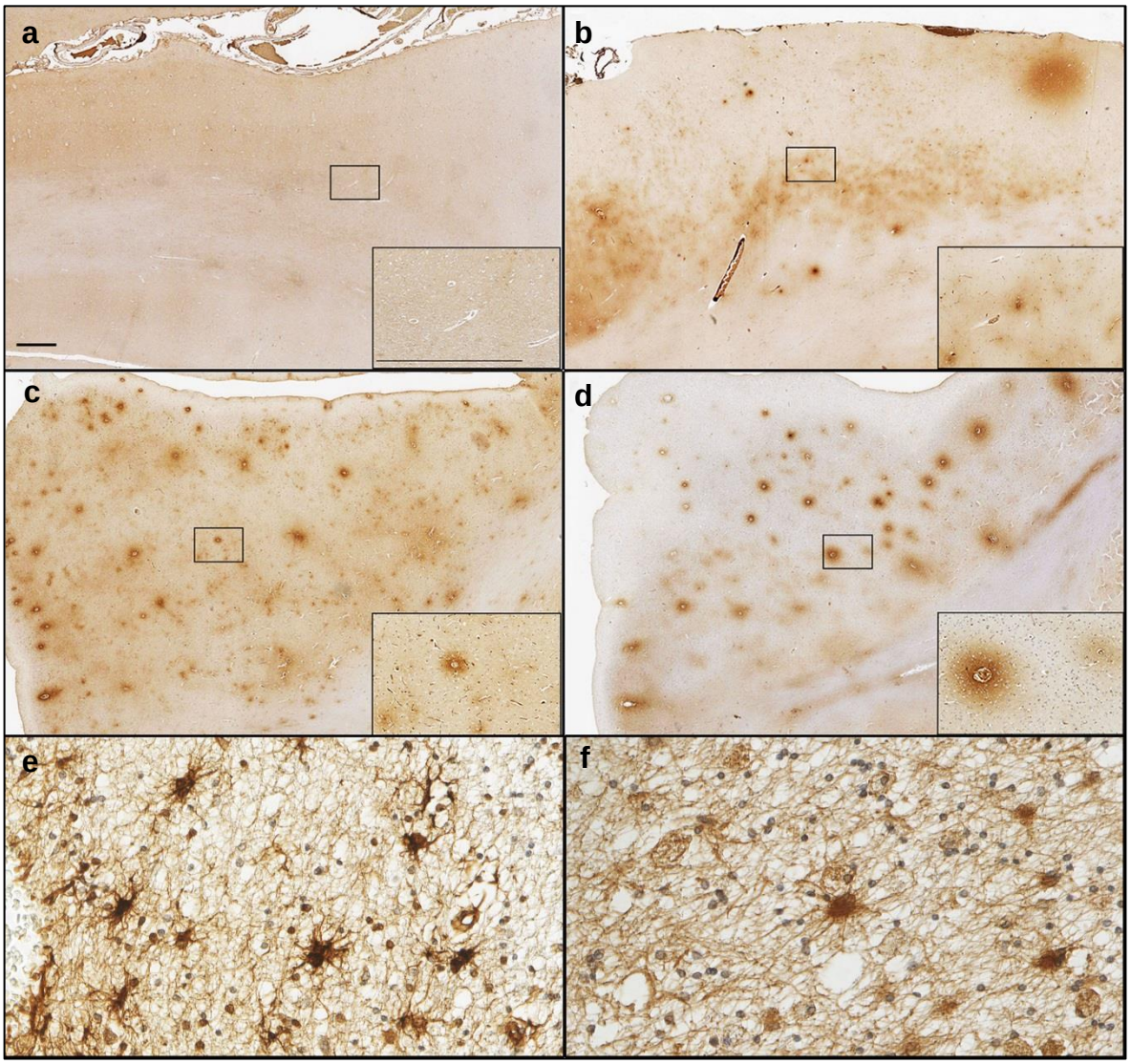

Figure 3-3 Representative images of fibrinogen (FBG) and immunoglobulin G (IgG) immunoreactivity after traumatic brain injury (TBI) and controls (a) Absence of FBG immunoreactivity in the superior frontal gyrus (Score of 0) of a 46-year-old man with no history of TBI. (b) Extensive FBG immunoreactivity in the superior frontal gyrus (Score of 3), with preferential distribution of staining to the mid and deep cortical layers in a 20-year-old male TBI patient who survived 2 days after an assault. (c, d) Extensive FBG (c) and IgG (d) immunoreactivity in adjacent sections from the superior frontal gyrus (Score of 3) of a 60-year-old male TBI patient who survived 18 years after a fall (e) FBG immunoreactivity and (f) IgG immunoreactivity in astrocytes in a 37-year-old male TBI patient who survived 4 years after a fall. Scale bar = 1mm (low magnification), scale bar = 100µm (high magnification), scale bar = 10µm (higher magnification in e and f).

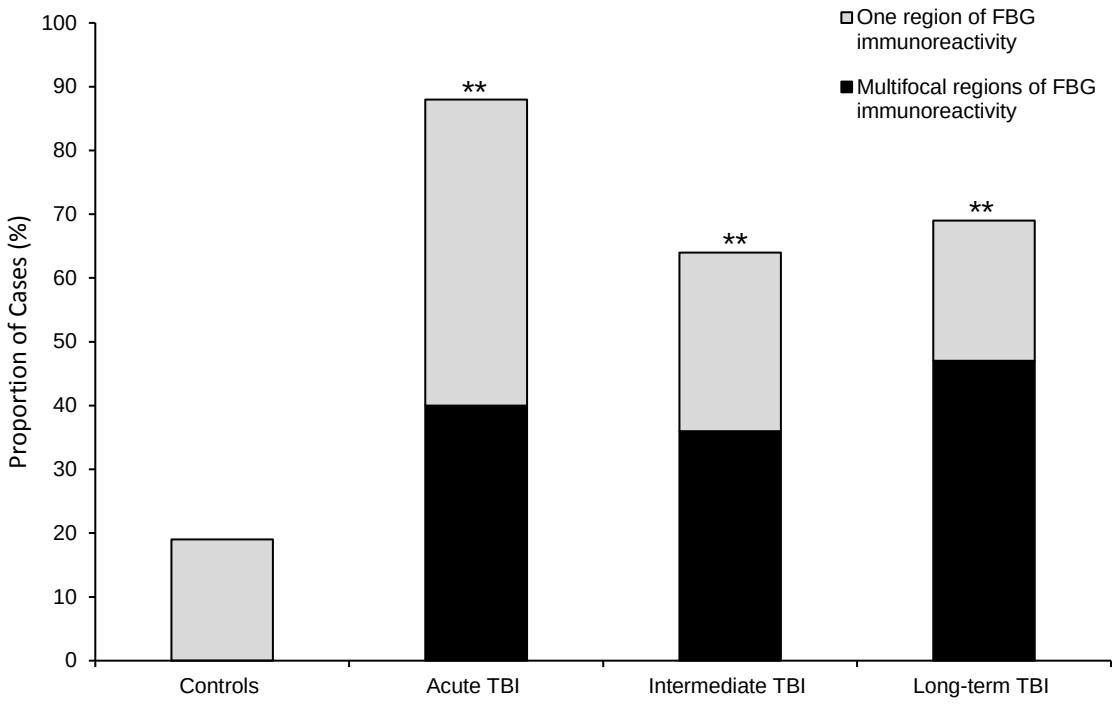

Figure 3-4 Extent of abnormal FBG immunoreactivity after TBI at varying survivals versus controls Moderate or extensive FBG immunoreactivity was an uncommon observation in controls, occurring in just 4 of 21 cases (19%), but it was a frequent observation after TBI at all survival time points assessed, being present in 88%, 64%, and 69% of acute, intermediate, and long-term survival cases, respectively. Furthermore, abnormal FBG immunostaining in controls was restricted to single anatomic region in contrast to the often multifocal pathology in patients after TBI (** $p < 0.001$; $\chi 2$ TBI cohort vs control FBG positivity).

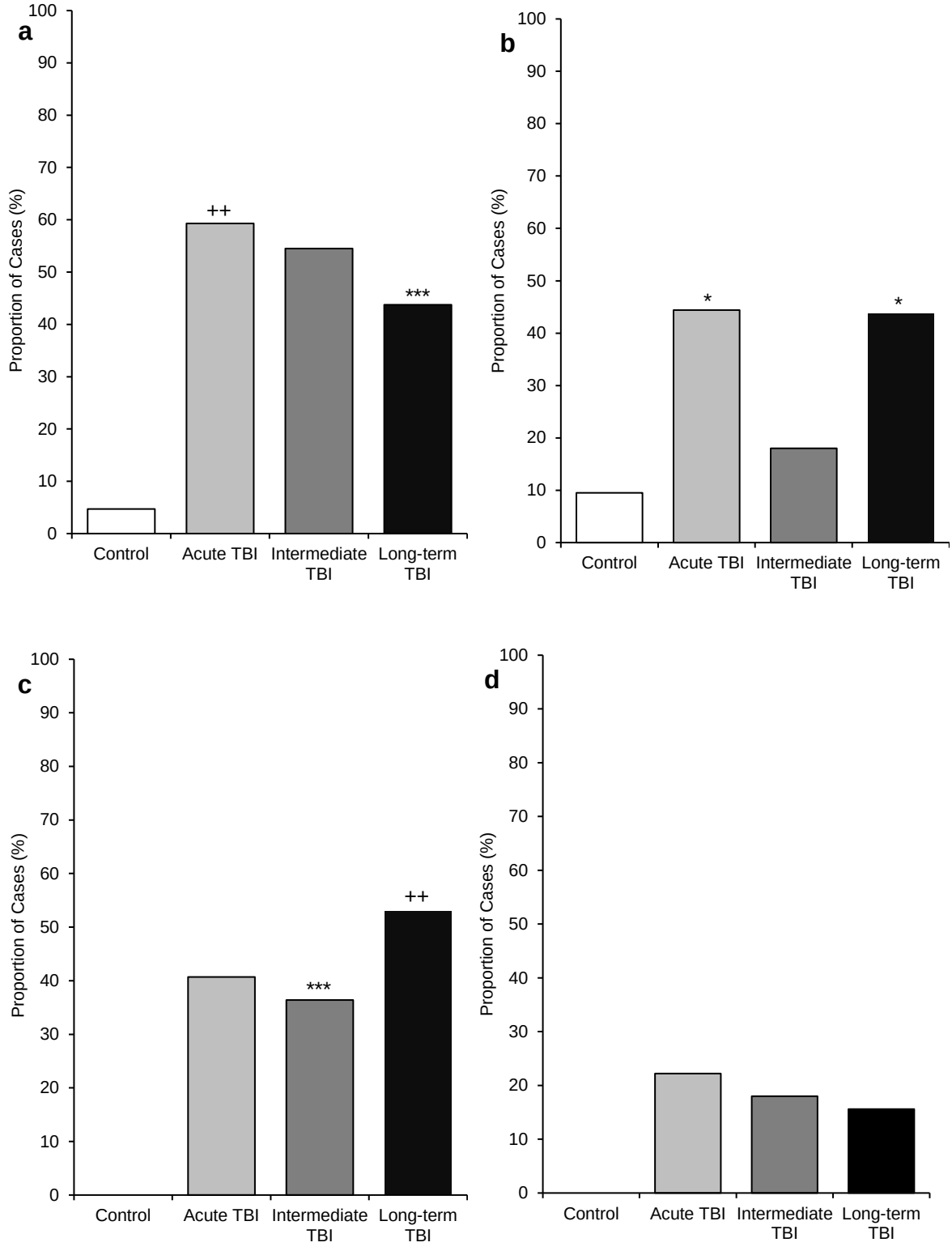

Figure 3-5 Regional distribution of FBG immunoreactivity following TBI versus controls At all survival intervals and in each region analysed there was evidence of BBB disruption following TBI, evidenced by moderate/extensive FBG immunoreactivity, in a higher proportion of TBI survivors than matched, uninjured controls in material from the (a) cingulate/superior frontal gyri, (b) thalamus, (c) hippocampus, and (d) insular cortex. (*p<0.05; **p<0.01; ***p<0.005; +p<0.0005; ++p<0.0001; X2 TBI cohort v control).

3.3.3 FBG immunoreactivity in intermediate TBI survival

Similar to material from patients dying acutely after TBI, regions of moderate or extensive FBG immunoreactivity were present in a greater number of intermediate (>2 weeks to 1 year after TBI) survival patients versus controls, with 7 of 11 (64%) ($p = 0.004$; $\chi 2$; Cramer's $V = 0.446$) demonstrating at least 1 anatomic sub-region with moderate or extensive FBG immunoreactivity; 4 of these cases showed multifocality (Figure 3-4). Again, the cingulate and superior frontal gyri most frequently showed increased staining (6 cases), followed by medial temporal lobe (4 cases), thalamus (2 cases), and insular cortex (2 cases) (Figure 3-5). As in the acute survival cases, there was a predilection for gyral crests over sulcal depths in the cingulate gyrus and medial temporal lobe. Although the small number of cases precludes formal statistical assessment, there was a trend toward preferential staining in mid to deep rather than superficial neocortical layers in all cortical regions (Figure 3-6). As with the acute TBI survival, there was no notable FBG immunoreactivity in the corpus callosum.

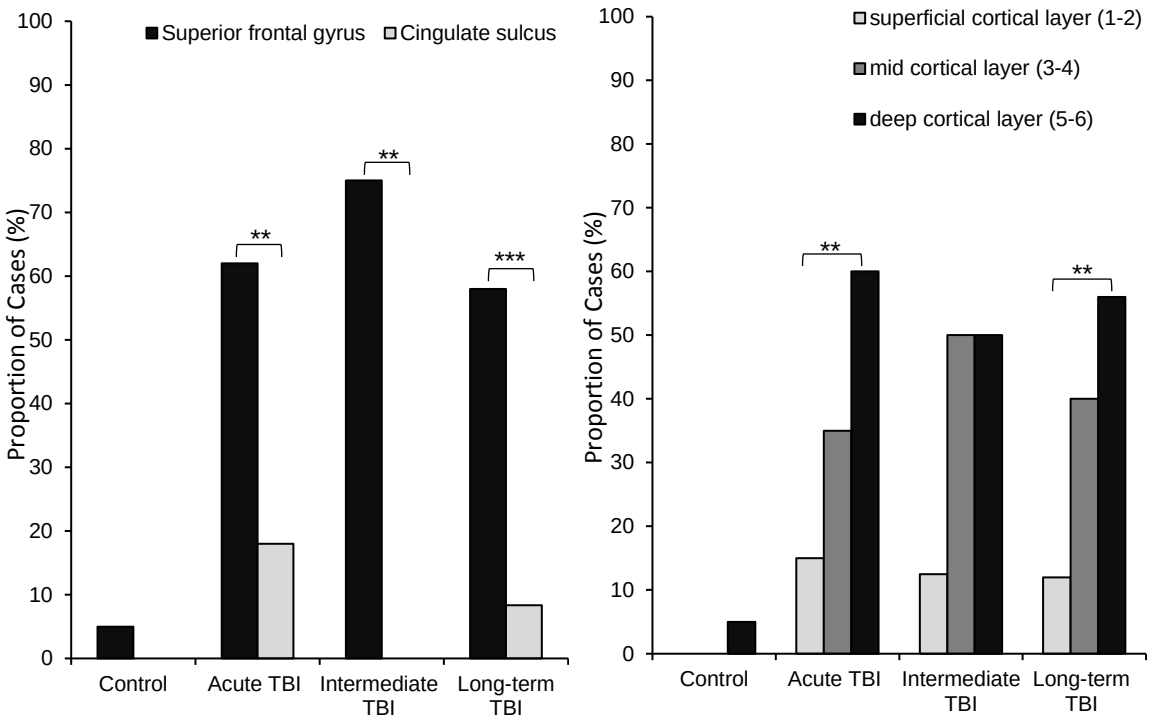

Figure 3-6 Neocortical distribution of FBG immunoreactivity after TBI (a) There was a clear preferential distribution of abnormal FBG immunoreactivity to the crests of gyri when compared to the depths of sulci across all survival points, as illustrated here for the superior frontal gyrus versus the adjacent cingulate sulcus (*$p<0.01$; **$p<0.001$; $\chi 2$ sulcus versus gyrus). (b) Further, within the neocortical grey matter region of the cingulate gyrus there was preferential distribution of abnormal staining to the mid (layers 3 and 4) and deep (layers 5 and 6) cortical layers when compared to superficial layers (layers 1 and 2). (*$p<0.01$; **$p<0.001$; $\chi 2$ deep versus superficial cortical layers).

3.3.4 FBG immunoreactivity in long-term TBI survival

A higher proportion of long-term survival cases showed evidence of increased FBG immunoreactivity versus matched uninjured controls (Figure 3-3c); at least 1 anatomic region showed moderate or extensive FBG immunoreactivity in 22 of 32 (69%) cases ($p < 0.001$; $\chi 2$; Cramer's $V = 0.486$). Multifocality was again common, present in 15 of the long-term survival cases (47%) (Figure 3-4). This increased staining was most frequent in material from the medial temporal lobe (17 cases), followed by cingulate and superior frontal gyri and thalamus (14 cases each) and insular cortex (5 cases) (Figure 3-5). As in acute and intermediate cases, there was a preferential distribution to the crests of gyri over depths of sulci (Figure 3-6). Furthermore, within the crests of gyri, FBG immunoreactivity was greater in the mid and deeper layers than the superficial layers of the cortex. Thus, in the superior frontal gyrus, 56% showed moderate or extensive FBG immunostaining in the deeper layers versus 12% in the superficial layers ($p = 0.0023$; $\chi 2$; Cramer's $V = 0.461$) (Figure 3-6). This pattern was reflected in all cortical regions assessed. In the medial temporal lobe, 40% showed extensive FBG immunostaining in the deep layers compared with 14% in the superficial layers ($p = 0.0683$; $\chi 2$; Cramer's $V = 0.278$). In contrast to earlier survival time points and controls, 53% of cases in this long-term survival cohort showed hippocampal FBG immunoreactivity greater than sparse (score 1) in at least 1 hippocampal sector ($p = 0.0001$; $\chi 2$; Cramer's $V = 0.124$). There was no clear preferential distribution to any particular sector; however, in keeping with this widespread increased FBG immunoreactivity in these long-term survival cases, 44% showed increased thalamic staining versus 10% of controls ($p = 0.0015$; $\chi 2$; Cramer's $V = 0.461$). Again, there was no increase in FBG immunoreactivity detected in material from the corpus callosum.

3.3.5 IgG immunoreactivity in all groups

Observations in the anti-IgG-stained material paralleled the observations in material immunostained for FBG (Figure 3-3d). Thus, at all post-TBI survival points and in controls, the extent and distribution of IgG immunoreactivity were comparable to those of FBG immunoreactivity, that is, there was greater perivascular and confluent diffuse staining IgG immunoreactivity in a proportion of TBI cases at all survivals versus controls. Specifically, IgG immunoreactivity in the control cohort was limited, with only 4 (19%) of 21 cases displaying moderate IgG immunoreactivity (score of 2): in 2 cases, this was localised to the superior frontal gyrus; 1 case localised to the thalamus; and 1 to the fusiform gyrus. Again,

no multifocality was observed. Causes of death in the controls included sudden death in epilepsy (n = 2), drug overdose (n = 1), and pneumonia (n = 1).

The acute TBI survival cohort demonstrated moderate or extensive IgG immunoreactivity in at least 1 anatomic sub-region in 63% of cases ($p < 0.005$; $\chi 2$; Cramer's $V = 0.439$), with multifocality present in 10 of 27 (37%). Of the regions examined, moderate or extensive IgG immunoreactivity was detected most frequently in material from the medial temporal lobe (10 cases), followed by the cingulate/superior frontal gyri and the thalamus (8 cases), and lastly the insular cortex (2 cases). As with FBG immunoreactivity, there was evidence of preferential anatomic distribution, with moderate or extensive IgG immunoreactivity more evident in the crests of gyri than in the depths of the adjacent sulci and in the mid to cortical deep layers when compared with the superficial cortical layers.

Following intermediate survival from TBI, regions of moderate or widespread IgG immunoreactivity were present in a greater number than in controls, with 6 of 11 (55%) demonstrating at least 1 anatomic sub-region with moderate/extensive IgG immunoreactivity ($p = 0.05$; $\chi 2$; Cramer's $V = 0.183$), multifocality was present in 45%. The long-term survival TBI cohort demonstrated 71% (23 of 32 cases) of moderate/extensive IgG immunoreactivity in at least 1 anatomic sub-region ($p = 0.0002$; $\chi 2$; Cramer's $V = 0.517$). Multifocality again was common, with 14 of 32 (43%) long-term TBI cases showing immunoreactivity in 2 or more sub-regions. Increased IgG staining was most frequent in the medial temporal lobe (13 cases each), followed by cingulate/superior frontal gyri and thalamus (12 cases), and insular cortex (3 cases). The pattern and distribution of IgG immunoreactivity also paralleled the results in anti-FBG-immunostained material, with preferential distribution to the crests of gyri over the depths of sulci in both cingulate gyri and hippocampal gyri, and greater IgG immunoreactivity observed in the mid and deeper layers versus the superficial neocortical layers.

3.3.6 Association of BBB disruption with TBI-associated pathologies

Reviewing haematoxylin and eosin–stained sections from the multiple tissue blocks examined for immunohistochemical evidence of BBB disruption confirmed the anticipated BBB disruption in association with acute focal haemorrhagic pathologies, in addition to more widespread and diffuse BBB disruption independent of focal pathology. Specifically, in material from acute TBI survivors, 21 TBI-associated focal haemorrhagic lesions or

contusions were observed across 13 of the 27 cases; virtually all (12 of 13 cases) displayed some degree of extravascular FBG immunoreactivity in the surrounding parenchyma. However, in the majority of these cases (9 of 13; 69%), BBB disruption was not confined to the region of focal pathology, with evidence of widespread diffuse BBB injury present in the remaining tissue blocks. Notably, in the 14 acute survival TBI cases without focal haemorrhage or contusion, 12 (86%) also displayed extensive FBG immunoreactivity in at least 1 region examined. In material from patients surviving beyond the acute phase of injury, there was evidence of healed haemorrhages or contusions, with histologic features consistent with their having dated from the time of the original TBI in 2 of 11 intermediate survival (comprising 6 individual lesions) and 8 of 32 long-term survival cases (12 distinct lesions).

Although not as extensive as observed in relation to focal haemorrhages or contusions in acute survivors, some evidence of BBB disruption was observed in the immediate locality of all 6 lesions in material from intermediate survivors. In contrast, evidence of focal BBB disruption in association with healed haemorrhages or contusions was less frequently observed in material from long-term survivors, with just 6 of 12 lesions associated with abnormal FBG or IgG immunoreactivity. Of note, both the intermediate survival cases and all 8 of the long-term survival cases with BBB disruption in association with focal pathologies also displayed more widespread diffuse BBB disruption remote from focal pathology. Six of 9 intermediate and 15 of 24 long-term survival cases showed no evidence of focal haemorrhagic or contusion pathology, and the material examined displayed evidence of extensive FBG immunoreactivity in at least 1 region. In addition to these focal haemorrhagic and contusional pathologies, there was evidence of diffuse hypoxic/ischemic injury, microgliosis, and/or astrogliosis in varying stages of evolution identified in a proportion of TBI cases across all survivals. No correlation between these TBI-related pathologies and evidence of BBB disruption were identified.

3.4 Discussion

This study demonstrates histologic evidence of widespread, diffuse BBB disruption in the acute phase, which persists into the late phase of survivors of a single moderate or severe TBI when compared with uninjured controls. Increased and widespread immunoreactivity for FBG and IgG was observed in material from patients dying in the acute phase following a TBI and this increase is demonstrated in a high proportion of patients surviving years following injury. Thus, this study raises the possibility that a single moderate or severe TBI is responsible for immediate and long-lasting alterations in BBB function after injury, which might contribute to post-TBI neurodegeneration.

Fibrinogen (340kDa) and IgG (150kDa) are plasma proteins which, under normal conditions, do not cross the BBB. This study, however, has demonstrated widespread, multifocal, perivascular, and parenchymal FBG and IgG deposition in nearly half of acute phase patients dying within the first 2 weeks following a single moderate or severe TBI, indicating that the BBB has been compromised. Similar post-TBI BBB disruption has been demonstrated in a variety of animal models where the presence of disruption is identified through extravasated serum proteins or by intravascularly injected labels in the brain parenchyma (Barzo et al., 1996, Habgood et al., 2007, Baldwin et al., 1996, Shapira et al., 1993, Rinder and Olsson, 1968, Shreiber et al., 1999, Smith et al., 1995, Cortez et al., 1989, Ommaya et al., 1964, Hicks et al., 1993, Povlishock et al., 1980, Wei et al., 1980). This acute phase BBB disruption can be detected in the absence of haemorrhage, which is consistent with the observations in this study of human autopsy tissue.

Possible structural alterations to account for this acute BBB disruption have been explored by ultrastructural studies in animal models of TBI which have identified a variety of alterations in the vascular endothelia in the acute phase after injury, including the formation of vacuoles, craters, and microvilli (Baskaya et al., 1997, Wei et al., 1980, Maxwell et al., 1988, Vaz et al., 1998). Some of these changes have been demonstrated in human TBI (Rodriguez-Baeza et al., 2003, Vaz et al., 1997). These rapid alterations in vascular structure have been associated with various mechanisms such as direct perturbation of the vessels by mechanical forces, including the immediate disruption of vascular endothelial cells. Secondary insults following injury may also indirectly contribute to these changes thus damaging the normal endothelial cell integrity and function by increases in arterial pressure and intravascular thrombus formation (Hekmatpanah and Hekmatpanah, 1985, Povlishock et al., 1980, Wei et al., 1980). Furthermore, active physiological changes such as increased

transendothelial vesicular transport via normally intact tight junctions (Povlishock et al., 1978, Vaz et al., 1998, Vaz et al., 1997, Maxwell et al., 1992) and alterations to other components of the BBB, such as early astrocyte disruption and swelling, have been described in both animals and humans after TBI (Hekmatpanah and Hekmatpanah, 1985, Maxwell et al., 1988).

Studies suggest that acute BBB disruption may predict a worse long-term outcome after TBI clinically (Ho et al., 2014b), although the relative role of these pathologic alterations is unknown. However, BBB disruption following TBI may just present itself in severe cases; therefore showing poorer outcomes than in those with a better prognosis. Nonetheless, specific deleterious mechanisms of BBB disruption after TBI may include influx of fluid together with chemical and protein mediators promoting vasogenic oedema, disruption in the normal pathways to clear toxic metabolites, and a failure to deliver normal metabolites vital for function. In turn, the temporal course and relative contribution of these various consequences of BBB disruption may differ with the severity of injury.

Although some animal studies show evidence of a two-staged BBB opening (Baldwin et al., 1996, Baskaya et al., 1997), this current study using human autopsy material showed no clear evidence of this, in particular, in the acute phase. However, this biphasic approach to BBB disruption following injury cannot be excluded due to the diverse and heterogeneous nature of post-mortem TBI cases with varying intercurrent illnesses, survival times, and causes of injury that conceivably could mask such an observation. Further studies directly investigating the temporal course of this BBB disruption following TBI may reveal important potential therapeutic targets with defined windows of opportunity. A degree of acute BBB disruption was anticipated, based on current literature; however, the proportion of long-term survival cases with extensive BBB disruption was surprising and intriguing, specifically that extensive, multifocal, extravascular FBG and IgG deposition was observed in approximately half of cases surviving a year or longer following TBI. Notably, clearance of large soluble proteins from the brain parenchyma, such as IgG or FBG, occurs via convective bulk flow of interstitial fluid over hours to days, or more rapidly via reverse transcytosis (Zhang and Pardridge, 2001). Thus, the presence of these soluble plasma proteins in the brain parenchyma of patients exposed to TBI more than a year before death is consistent with ongoing BBB disruption, rather than evidence of protein deposition at the time of injury that is not cleared in the intervening period.

Observations were made in the study that the pattern and distribution of chronic BBB disruption after TBI was more frequently localised to the grey matter of the neocortical ribbon and deep grey nuclei, with a preferential distribution in the former to mid and deeper cortical layers over superficial layers, and the crests of gyri over depths of sulci. This pattern indicates specific areas of BBB vulnerability within a more global and diffuse process, rather than a heterogeneous multifocal pathology. This intriguing observation challenges the current descriptions of aspects of the neuropathology of post-TBI neurodegeneration and CTE, in which localisation of tau pathologies to the depths of sulci is reported. However, at present, the neuropathological criteria for CTE diagnosis remain provisional; therefore, more research is required to determine how these pathologies interact.

With regard to other TBI-associated pathologies, this study did not demonstrate any evidence of an association between widespread, diffuse BBB disruption and focal TBI pathologies, such as contusions or haemorrhages. Furthermore, there was no correlation between diffuse and widespread BBB disruption and diffuse ischemic pathology. The number of cases and necessary heterogeneity in pathologies within the examined cohorts were limited. Therefore, it was difficult to determine such an association and whether specific diffuse primary or secondary pathologies in the acute phase can account for later patterns of BBB disruption. This, however, opens opportunities to explore much larger cohorts and animal models.

There has been increasing evidence reported of the clinical and neuropathologic sequelae of TBI and, in particular, the association of TBI survival and the increased risk of neurodegenerative disorders, specifically CTE (Corsellis et al., 1973, Smith et al., 2013, McKee et al., 2013). Neuropathologic examination of autopsy material from patients with survival greater than a year from a single moderate or severe TBI reveals an increased frequency of neurodegeneration-associated pathologies when compared with material from matched controls, including amyloid-β plaques, neurofibrillary tangles, inflammation, and white matter degradation (Johnson et al., 2010, Johnson et al., 2012, Johnson et al., 2013a, Johnson et al., 2013c). The role of the BBB in the pathological process of neurodegeneration is becoming increasingly interesting with evidence indicating that alterations in the brain's microvasculature contribute to this decline (Zlokovic, 2011). Changes in the microvascular such as a decrease in vessel structure and density (Brown and Thore, 2011a), BBB disruption and subsequent leakage (Zipser et al., 2007a, Viggars et al., 2011), and secretion of potentially neurotoxic factors from the vascular endothelium (Grammas et al., 1999), have been reported in AD pathology.

Although the extravasation of serum proteins such as FBG have been demonstrated to correlate with the presence of AD-type pathology (Viggars et al., 2011), the association between the changes observed in the brain's microvasculature and key neurodegenerative pathologies is not known. However, there is increasing clinical and experimental evidence that suggests some of these vascular changes occur early in the disease process and may contribute to states of hypoperfusion promoting neuronal injury (Zlokovic, 2011, Brown and Thore, 2011a, Hirao et al., 2005, Johnson et al., 2005). Future studies to investigate this relationship between BBB breakdown and other neurodegenerative pathologies will be crucial in understanding the disease progression.

Fibrinogen alone has been widely attributed to the progression of AD with individuals with high serum FBG shown to be at greater risk of the disease (van Oijen et al., 2005, Xu et al., 2008). Fibrinogen was also shown to accelerate inflammation and neurovascular damage in a mouse model of AD (Paul et al., 2007, Petersen et al., 2018). Perhaps the most widely studied aspect of BBB regarding AD is its role in the clearance and sequestration of amyloid-β to the peripheral circulation (Shibata et al., 2000b, Mawuenyega et al., 2010, Sutcliffe et al., 2011, Eisele et al., 2010). Influx of amyloid-β is mediated by receptor for advanced glycation end products (RAGE) which is located in the BBB and it has been reported that the increase of amyloid-β in the CNS perpetuates increased RAGE expression (Yan et al., 1996, Yan et al., 2010). Clearance of amyloid-β is also diminished in AD and one of the key receptors in this role, the low-density lipoprotein receptor-related protein 1 (LRP1), is also located in the BBB. There are indications that reduced LRP1 levels in microvessels (Bell et al., 2009, Deane et al., 2004b, Shibata et al., 2000a, Donahue et al., 2006) and blockage by the ε4 allele of ApoE (Deane et al., 2008) may contribute to poor clearance and subsequent pathological accumulation of amyloid-β. Although the number of cases described in the present study precludes analysis of multiple covariants, the interplay and temporal relationship between BBB disruption and subsequent progressive neurodegenerative pathologies will be an important direction for future investigation.

3.4.1 Conclusion

This study presents the first preliminary data indicating that, after just a single moderate or severe TBI, there is neuropathologic evidence of widespread, diffuse, multifocal BBB disruption in a proportion of TBI patients, even after many years of survival from injury. Given that vascular dysfunction may be an important contributor to neurodegenerative disorders, acute and chronic BBB alterations after TBI will be important to examine in this context along with associations with known TBI pathologies.

4 Blood-brain barrier disruption is a distinct, capillary level pathology following paediatric traumatic brain injury

4.1 Introduction

Traumatic brain injury (TBI) is a leading cause of death and disability amongst children and adolescents. In common with all age groups, the majority of TBI in children and adolescents is classified as mild (Glasgow Coma Scale 13 or greater), often arising from sports or recreational exposure. However, in contrast to adult TBI, injuries in the paediatric age group are associated with unique risks of poor, occasionally catastrophic outcome. In particular, paediatric TBI patients show increased propensity for diffuse brain swelling (DBS). Occurring anywhere from minutes to hours after all severities of injury, even mild TBI, DBS is associated with a deteriorating conscious level in the absence of significant intracranial haemorrhage.

4.1.1 Second impact syndrome

Though a phenomenon first acknowledged in the 1950's (Pickles, 1950), it was not until some decades later that the propensity for DBS in the paediatric population, in particular adolescents, came to prominence through short cases series highlighting its occurrence in mild TBI (Cantu, 1998, Fekete, 1968, Bruce et al., 1981, Bruce, 1984). Of note, in 1984, an index case report describing a patient with fatal DBS arising on a background of a previous but recent mild TBI (concussion) introduced the term second impact syndrome (SIS), which has since largely supplanted DBS in much of the literature (Saunders and Harbaugh, 1984).

Despite the catastrophic outcomes associated with DBS/SIS in paediatric TBI, the pathophysiology of SIS is relatively unknown; however, alterations in cerebral blood flow and damage to the cerebrovasculature are increasingly recognised as contributors. A case report studied CT scans of children between the first and second TBI and an additional MRI after the second; they confirmed profound rapid blood flow dysautoregulation, vascular engorgement and increased intracranial pressure following TBI (Weinstein et al., 2013). Along with this absence of autoregulation, which renders the brain incapable of responding to increases in blood pressure, there is a rush of catecholamines (stress response to injury) which, when occurring simultaneously after injury might produce uncontrolled brain swelling (Wetjen et al., 2010).

Though only a few cases of SIS have been described, careful autopsy review of cases in the Glasgow TBI Archive confirmed a high incidence of DBS in material from paediatric patients succumbing in the acute phase following a single moderate or severe TBI when compared to adults (Graham et al., 1989). Subsequent review in clinical studies confirms incidence of DBS, associated with poorer outcome, is 2 to 5 times greater in the paediatric population than in adults (Kazan et al., 1997). Further, in contrast to adult TBI, DBS in the paediatric population more often arises in isolation, that is, without evidence of other intracranial TBI pathologies. The suggestion from the literature is that an unusually high predisposition to disturbed autoregulation or hyperaemia in the immature brain might underlie this pathology (Adelson et al., 2011).

4.1.2 Cerebral blood flow alterations in TBI

Dysfunction of the cerebral blood flow and autoregulation is a prominent pathology in paediatric TBI cases. Some imaging studies report that low cerebral blood flow (CBF) is related to poorer outcome and a higher mortality after TBI in children (Pigula et al., 1993, Kokoska et al., 1998, Adams et al., 1989b). Another study further confirmed these findings and extended them by investigating the relationship with age-associated systolic blood pressure (AASBP) and worse neurological outcomes (Vavilala et al., 2003). A higher AASBP was associated with a favourable outcome and an AASBP < 90mmHg was associated with a poorer neurological outcome. Of note, it is reported that there is a wide CBF range varying between 6 months old and 9–10 years old therefore comparisons of data between normal and TBI patients could only be valid when small, well-defined age ranges are selected (Suzuki et al., 1990, Zwienenberg and Muizelaar, 1999). Studies in alterations of cerebral autoregulation following paediatric TBI demonstrate a correlation in impaired cerebral autoregulation and severity of brain injury (Muizelaar et al., 1989, Sharples et al., 1995, Vavilala et al., 2004, Vavilala et al., 2006). One study found that one third of the children examined displayed increasing dysautoregulation during the 9 days following the TBI (Tontisirin et al., 2007). However, these numbers are small and experiments investigating paediatric TBI are poorly replicated in animal models. This does indicate evolving and transient changes following TBI in children.

4.1.3 Diffuse brain swelling

Low CBF can result in poorer outcome following paediatric TBI and is associated with cerebral dysautoregulation and diffuse cerebral brain swelling (Bruce et al., 1981, Muizelaar

et al., 1989, Cold and Jensen, 1980). It has been proposed that two types of brain swelling exist: vasogenic oedema caused by blood-brain barrier (BBB) disruption resulting in extracellular water accumulation; and cytotoxic oedema caused by sustained intracellular water collection (Unterberg et al., 2004, Huh and Raghupathi, 2009). Vasogenic oedema was originally considered to be the dominant form following TBI yet, in contrast, imaging studies suggest the cytotoxic form is prevalent (Unterberg et al., 2004, Marmarou et al., 2006a, Marmarou et al., 2006b). Marmarou *et al* used MRI to study oedema types in 45 brain-injured patients. By applying and calculating the apparent diffusion coefficient (ADC) they found it was significantly reduced in TBI patients, supporting cytotoxic oedema (Marmarou et al., 2006a).

It has been suggested that the developing brain may have greater susceptibility to TBI than an adult brain due to structural differences, such as BBB integrity (Saunders et al., 2012, Anderson et al., 2000, Stiles and Jernigan, 2010); however, difficulties in age-adjusting animal models results in limited evidence available on the effects of paediatric TBI (Semple et al., 2013). The BBB is a key component of cerebral autoregulation and CBF, disruption of which may lead to raised intracranial pressure. Previous studies have described evidence of widespread BBB disturbance in autopsy-derived material from a high proportion of adults dying in the acute phase following a single moderate or severe TBI, manifesting as multifocal, abnormal, perivascular fibrinogen (FBG) and immunoglobulin G (IgG) immunoreactivity (Hay et al., 2015). Such widespread disruption in vascular integrity might serve as a substrate for cerebral oedema and, as such, might contribute to DBS in the paediatric TBI population. This study examines autopsy brain sections from paediatric and adult acute TBI patients for histological evidence of BBB disruption and, if present, the characteristics of involved vessels.

Hypothesis: BBB disruption is present in paediatric TBI patients as with adult TBI, however, an association between DBS and BBB disruption is suggested in the paediatric TBI cohort.

4.2 Material and methods

4.2.1 Case selection and brain tissue preparation

Ethical approval for this study was granted by the Greater Glasgow and Clyde Bio-repository Governance Committee. From the unique Glasgow TBI Archive, both adult and paediatric TBI cases were selected with a history of a single moderate or severe TBI based on information in the detailed autopsy reports and clinical records, as defined by Glasgow Coma Scale, and dying in the acute phase post injury (defined as survival less than 14 days from injury). For the paediatric TBI, cohort cases were selected as aged 18 or under (mean 13 years; range 4–18 years; n = 52) at the time of death, with cases aged 19 years or over (mean 50 years; range 20–60; n = 22) selected as the adult TBI cohort. Control, uninjured paediatric patients with no history of TBI or neurological disease were selected for comparison (mean 14 years; range 7–18; n = 9). Clinical variables, including cause of death, survival time and post mortem intervals, were comparable between TBI cohorts. However, the cause of injury differed between cohorts. The predominant cause of TBI in the paediatric cohort was road traffic accident (RTAs) with 79% of paediatric TBI cases compared with 18% in the adult TBI cohort ($p = 0.0001$; $\chi 2$). In the adult TBI cohort the predominant cause of injury was falls with 68% of cases compared with 12% in the paediatric TBI cohort ($p = 0.0001$; $\chi 2$). Full demographic and clinical data for each cohort are presented in Table 3**.**

Table 3 Demographic and clinical information of all groups

		Paediatric uninjured control (n = 9)	**Paediatric TBI (n = 52)**	**Adult TBI (n = 22)**
Mean age (range)		14 years (7–18)	13 years (4–18)	50 years (20–60)
Males		6 (67%)	36 (69%)	15 (68%)
Mean PM delay (range)		85 hours (15–264 hours)	40 hours (6–120 hours)	56 hours (5–240 hours)
Mean survival interval (range)		n/a	68 hours (0–186 hours)	72 hours (6–216 hours)
Cause of TBI	**Fall*** **	**n/a**	**6 (12%)**	**15 (68%)**
	RTA* **	**n/a**	**41 (79%)**	**4 (18%)**
	Assault	n/a	5 (10%)	2 (9%)
	Unknown	n/a	0	1 (5%)
Cause of death	Head injury	0	50 (96%)	20 (91%)
	Bronchopneumonia	0	0	2 (9%)
	Cardiac arrest	0	2 (4%)	0
	SUDEP	2 (22%)	0	0
	Drug overdose	2 (22%)	0	0
	Cardiomyopathy	1 (11)	0	0
	Aspiration pneumonia	1 (11%)	0	0
	Inhalation of gastric contents	1 (11%)	0	0
	Leukaemia	1 (11%)	0	0
	Unascertained	1 (11%)	0	0

Key: *TBI = traumatic brain injury; SUDEP = sudden unexpected death in epilepsy; GIT = gastrointestinal tract; ARDS = acute respiratory distress syndrome; RTA = road traffic accident*

4.2.2 Haematoxylin and eosin staining

Slides were deparaffinised in xylene and rehydrated to water by graded alcohol. They were then immersed in haematoxylin (Mayer's, Leica Microsystems, Wetzlar, Germany) for 10 minutes. After rinsing in water and immersing in Scott's tap water substitute (Leica Microsystems, Wetzlar, Germany) the slides were differentiated in 1% acid alcohol and rinsed again. The slides were then immersed in 25% aqueous eosin Y solution (TCS biosciences, Buckingham, UK) for 5 minutes, rinsed, dehydrated by graded alcohol, cleared in xylene and then coverslipped.

4.2.3 Immunohistochemistry

Tissue sections were deparaffinised, rehydrated and immersed in 3% aqueous H_20_2 to quench endogenous peroxidase activity, following which heat induced antigen retrieval was

performed using a microwave pressure cooker for 8 minutes in preheated 0.1M Tris EDTA buffer. Subsequent blocking was achieved by applying 50µL of normal horse serum (Vector Labs, Burlingame, CA, USA) per 5 mL of Optimax buffer (BioGenex, San Ramon, CA, USA) for 30 minutes. Sections were then incubated for 20 hours at 4°C with polyclonal rabbit anti-human antibodies for fibrinogen (FBG; 1:17,500; Dako, Carpinteria, CA, USA) or IgG (1: 10,000; Dako, Carpinteria, CA, USA) or monoclonal mouse anti-human antibody for CD34 (1:100; Leica Biosystems, Milton Keynes, UK). A biotinylated secondary antibody was applied for 30 minutes followed by avidin-biotin complex as per the manufacturer's instructions (Vectastain Universal Elite kit, Vector Labs, Burlingame, CA, USA). Visualisation was achieved using the DAB peroxidase substrate kit (Vector Laboratories, Burlingame, CA, USA) followed by counterstaining with haematoxylin. All sections were viewed using a Leica DMRB light microscope (Leica Microsystems, Wetzlar, Germany). All sections were viewed using a Leica DMRB light microscope (Leica Microsystems). In addition, sections were scanned at 20x using a Hamamatsu Nanozoomer 2.0-HT slide scanner, with the images viewed via the SlidePath Digital Image Hub application (Leica Microsystems). Furthermore, where appropriate sections were scanned using a 40x optic which scans images at a digital resolution of 0.23µm per pixel. The images in this chapter have been digitally captured at 4x (2.3µm per pixel), 20x (0.46µm per pixel) and 40x (0.23µm per pixel).

4.2.4 Analysis of immunohistochemical findings

4.2.4.1 Fibrinogen and Immunoglobulin G quantification

All observations were conducted blind to demographic and clinical data by two independent observers (JH, WS). Extent and distribution of FBG and IgG immunoreactivity were assessed using established semi-quantitative techniques (Hay et al., 2015). Briefly, the neocortical grey matter of the cingulate gyrus, cingulate sulcus, superior frontal gyrus, parahippocampal gyrus, collateral sulcus, fusiform gyrus and insular cortex were divided into superficial (layers 1–2), mid (layers 3–4) and deep layers (5–6). In addition, the thalamus was divided into medial, intermediate and lateral regions. Each of these cortical divisions and thalamic regions were then semi-quantitatively assessed for the frequency and intensity of immunoreactivity determined as absent (0), sparse (1), moderate (2) or extensive (3).

4.2.4.2 Assessment of vessel diameters

In all cases where FBG immunoreactivity was scored moderate to extensive (score of 2 or 3) in any layer of the cingulate gyrus, assessment of the diameters of cortical vessels and of vessels showing BBB disruption was performed. In scanned images of either FBG or CD34 stained sections a 3 x 3 mm grid comprising of 10 x 10 300µm smaller squares was placed over the cortical region of the cingulate gyrus (Figure 4-1). The grid diameter was selected to maximise the number of vessels measured in order to obtain robust results. If any larger, the grid would be too big for the gyral area. Within the 3 x 3 mm grid, a sample of vessels showing abnormal staining in FBG stained sections and a sample of all immunoreactive vessels in CD34 stained sections were measured. Vessels were measured at the smallest diameter (Figure 4-2). Vessels that transected all gridlines, internal and external, through all 100 individual 300µm squares were measured. Those vessels that landed in the middle of each square, not transected by a gridline, were not measured. This was to reduce sampling bias.

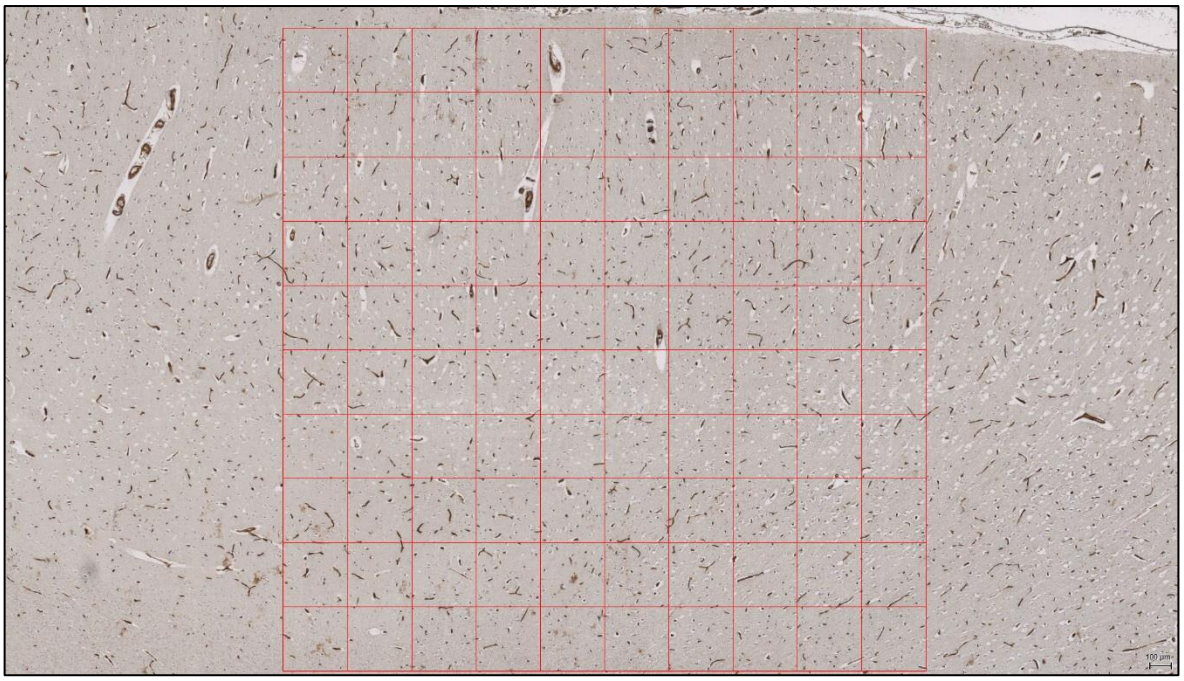

Figure 4-1 Example of grid placement A 3 x 3 mm grid comprising of 10 x 10 300µm smaller squares was placed over the cortical region of the cingulate gyrus.

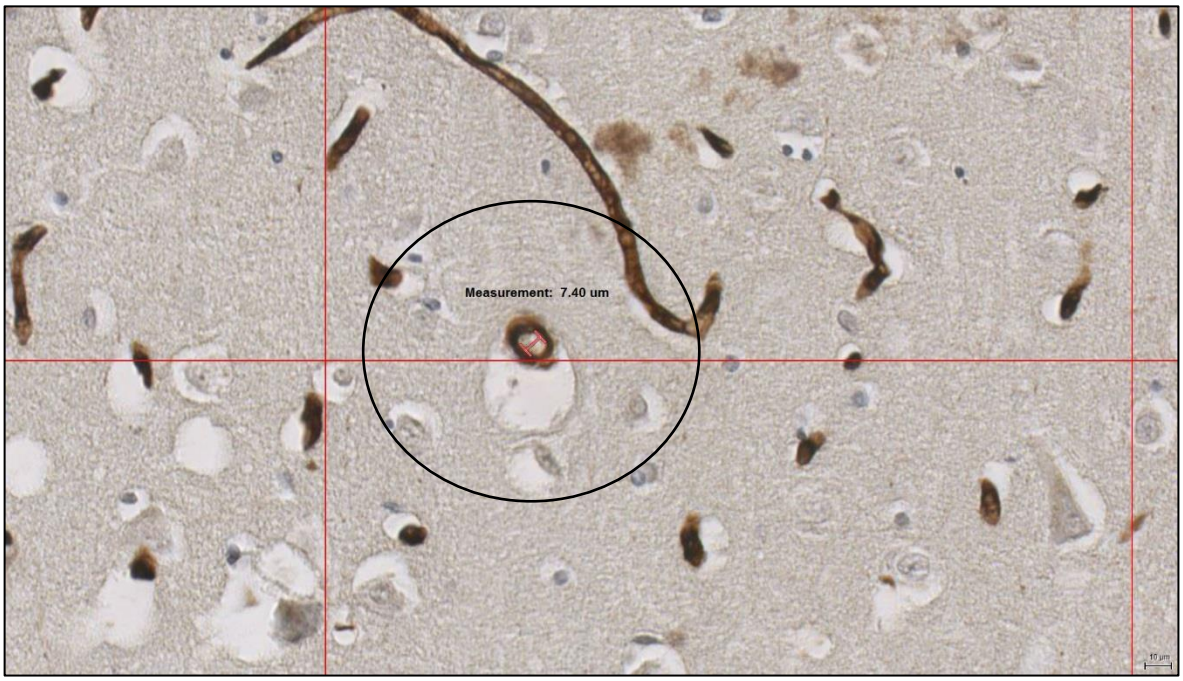

Figure 4-2 Example of capillary measurement Example of capillary measurement of those vessels that transect the grid using the SlidePath measuring tool.

4.2.5 Statistical analysis

All data were analysed using SPSS (version 22; IBM, Inc). The $\chi 2$ test was used to assess differences in data between and within cohorts, where appropriate. Cramer's V was used to determine the effect size. A Cramer's V value of 0.1 suggested a low practical significance, a value of 0.3 suggested a moderate practical significance and a value of 0.5 suggested a high practical significance. All effects were considered statistically significant when $p \leq 0.05$.

4.3 Results

4.3.1 Evidence of BBB disruption in paediatric TBI compared with controls

Where 79% of the paediatric TBI cohort demonstrated moderate or extensive FBG immunoreactivity score of 2 or 3, 44% of uninjured paediatric patients also demonstrated moderate or extensive FBG immunoreactivity in at least one region. Although not significant, an overall lowered FBG immunoreactivity is observed in the control group (Figure 4-3). Within those uninjured control cases with diffuse FBG immunoreactivity, the reported cause of death was SUDEP, cardiomyopathy, leukaemia and one was unascertained.

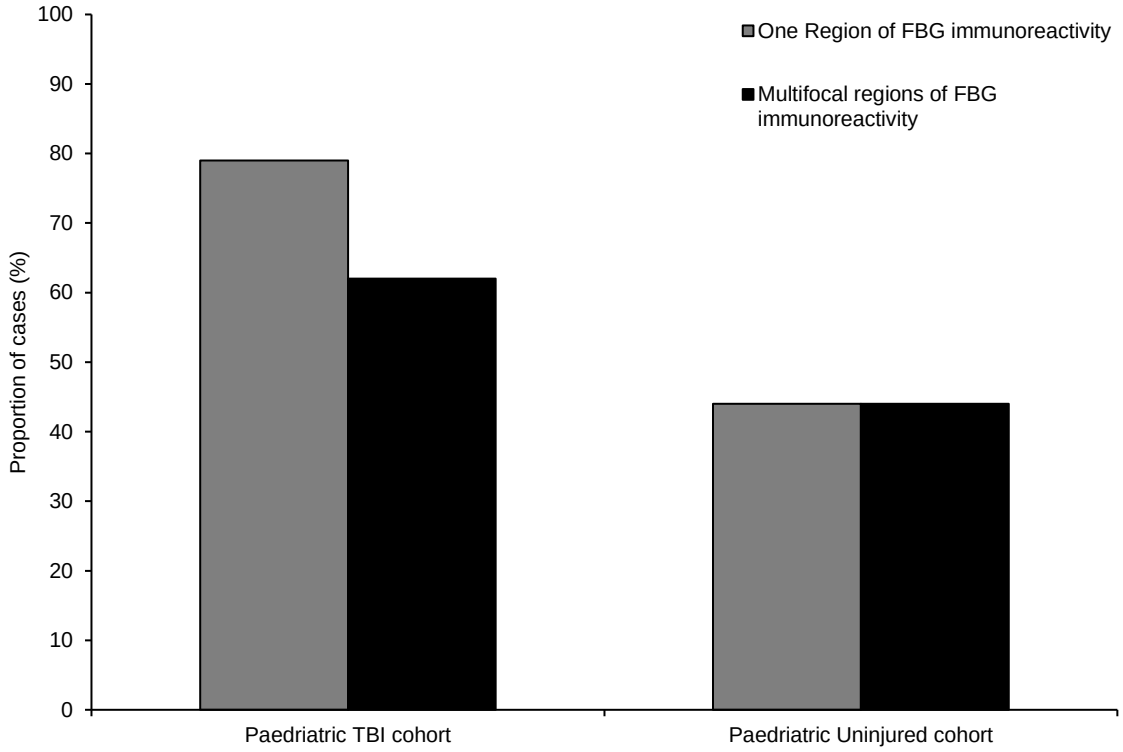

Figure 4-3 Extent of abnormal FBG immunoreactivity in the Paediatric TBI cohort versus Paediatric Uninjured controls Moderate or extensive FBG immunoreactivity was a frequent observation in both Paediatric TBI and in the Paediatric Uninjured controls, where it was present in 79% of the Paediatric TBI and in 44% of the Paediatric Uninjured controls (NS). Furthermore, abnormal FBG immunoreactivity was a common multifocal pathology in both cohorts (NS).

Where FBG immunoreactivity was present, the pattern and distribution of FBG immunoreactivity between the paediatric TBI group and the control group was similar. In both groups FBG immunoreactivity was largely confined to the grey matter; however, in the control group evidence of BBB disruption was higher in the white matter of the corpus callosum (NS) (Figure 4-4). Finally, preferential distribution to the crests of gyri and deeper cortical layers (layers 3–6) over depths of sulci and superficial cortical layers was common to both paediatric TBI and the control group showing moderate or extensive abnormal FBG or IgG immunostaining (Figure 4-5).

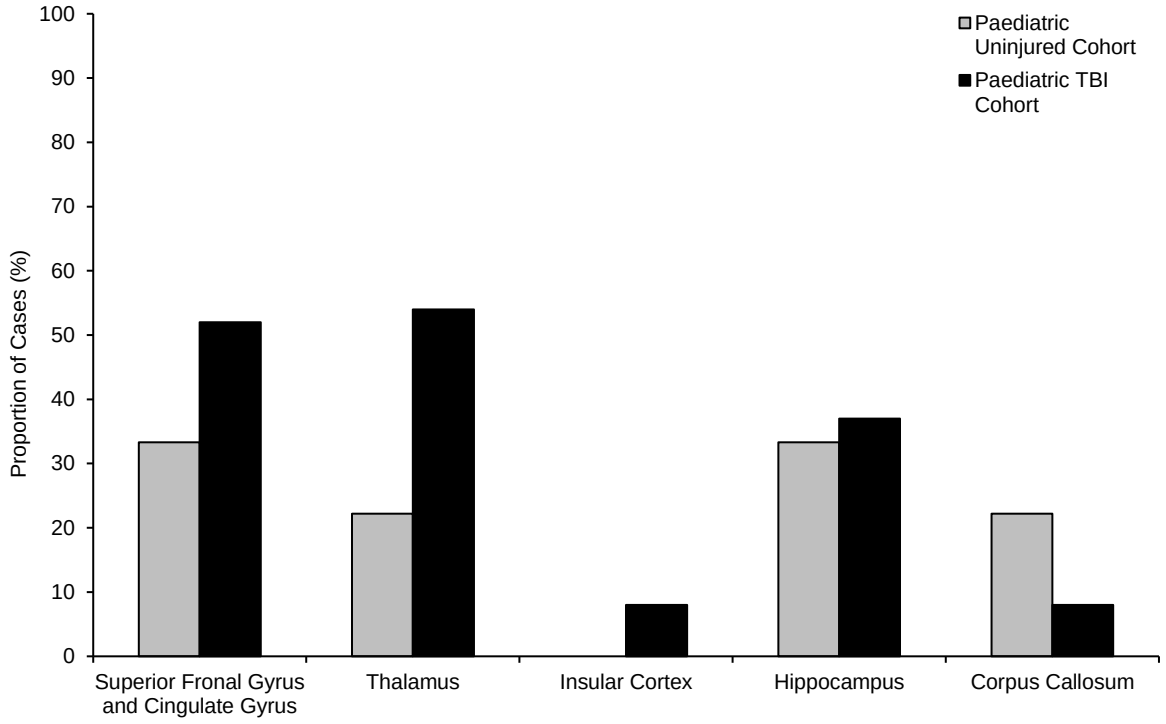

Figure 4-4 Regional Distribution of FBG immunoreactivity in Paediatric TBI cohort versus Uninjured Paediatric controls In all regions analysed in the Paediatric TBI cohort there was evidence of FBG immunoreactivity in a higher proportion of Paediatric TBI survivors than uninjured Paediatric cohort, however in the white matter of the corpus callosum 22.2% of the Uninjured Paediatric cohort demonstrated moderate or extensive fibrinogen compared with only 8% in the paediatric TBI cohort (NS).

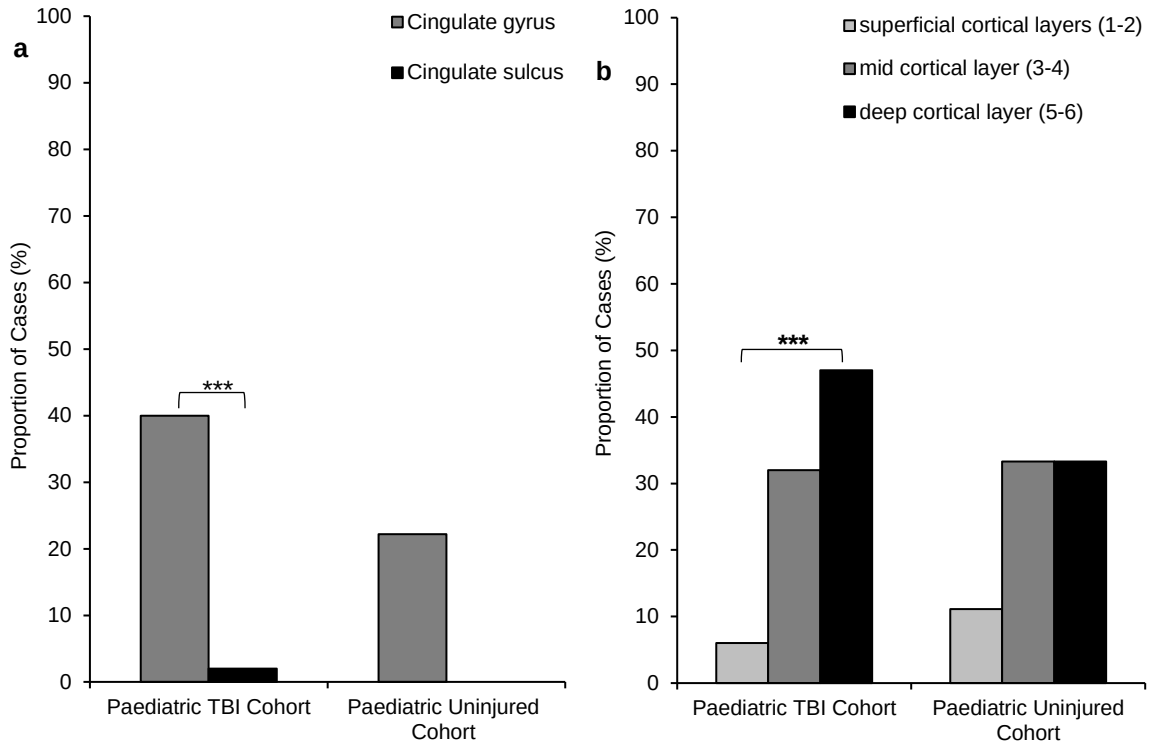

Figure 4-5 Neocortical distribution of FBG immunoreactivity in Paediatric TBI cohort versus Paediatric Uninjured cohort (a) Similar to the Adult TBI there was a clear preferential distribution of abnormal FBG immunoreactivity to the crests of the gyri when compared to the depths of the sulci in the Paediatric TBI cohort as illustrated here for the cingulate gyrus versus the adjacent cingulate sulcus (***$p<0.0001$; $\chi 2$ sulcus versus gyrus) (b) Further, within the neocortical grey matter region of the cingulate gyrus there was preferential distribution of abnormal staining to the mid (layers 3 and 4) and deep (layers 5 and 6) cortical layers when compared to superficial layers (layers 1 and 2) in the Paediatric TBI cohort. (***$p<0.0001$; $\chi 2$ deep versus superficial cortical layers).

4.3.2 Evidence of BBB disruption in paediatric TBI compared with adult TBI

Moderate or extensive abnormal perivascular FBG and IgG immunostaining representing evidence of BBB disruption was confirmed in a similar proportion of both adult and paediatric TBI patients dying in the acute phase (Figure 4-6). Specifically, 86% (19 out of 22) of adult and 79% (41 out of 52) of paediatric acute TBI cases demonstrated moderate or extensive FBG immunoreactivity, whilst 68% (15 out of 22) of adult and 64% (33 out of 52) of paediatric acute TBI cases demonstrated moderate or extensive IgG immunoreactivity in at least one anatomical region. Further, evidence of multifocal BBB disruption, defined as abnormal moderate or extensive FBG immunoreactivity in 2 or more anatomical regions, was identified in a similar proportion of cases in both cohorts, being present in 60% of adult and 62% of paediatric cases stained for FBG (Figure 4-6) and 50% of adult and 44% of paediatric cases stained for IgG.

Pattern and distribution of FBG immunoreactivity between the paediatric TBI group and the adult TBI group was similar. In both paediatric and adult acute TBI, BBB disruption was largely confined to grey matter, with only occasional cases showing evidence of BBB disruption in the white matter of the corpus callosum (Figure 4-7). Finally, there was preferential distribution to the crests of gyri rather than the depths of the sulci in both groups ($p = 0.0001$; $\chi 2$; Cramer's $V = 0.471$, *paediatric TBI gyrus versus sulcus*; $p = 0.0324$; $\chi 2$; Cramer's $V = 0.42$, *adult TBI cingulate gyrus versus cingulate sulcus*). Furthermore, preferential distribution to the deeper cortical layers rather than the superficial cortical layers was common to both paediatric and adult TBI cases ($p = 0.0001$; $\chi 2$; Cramer's $V = 0.461$, *paediatric TBI deep layers versus superficial layers*; $p = 0.0134$; $\chi 2$; Cramer's $V = 0.462$, *adult TBI deep layers versus superficial layers*) showing moderate or extensive abnormal FBG or IgG immunostaining (Figure 4-8).

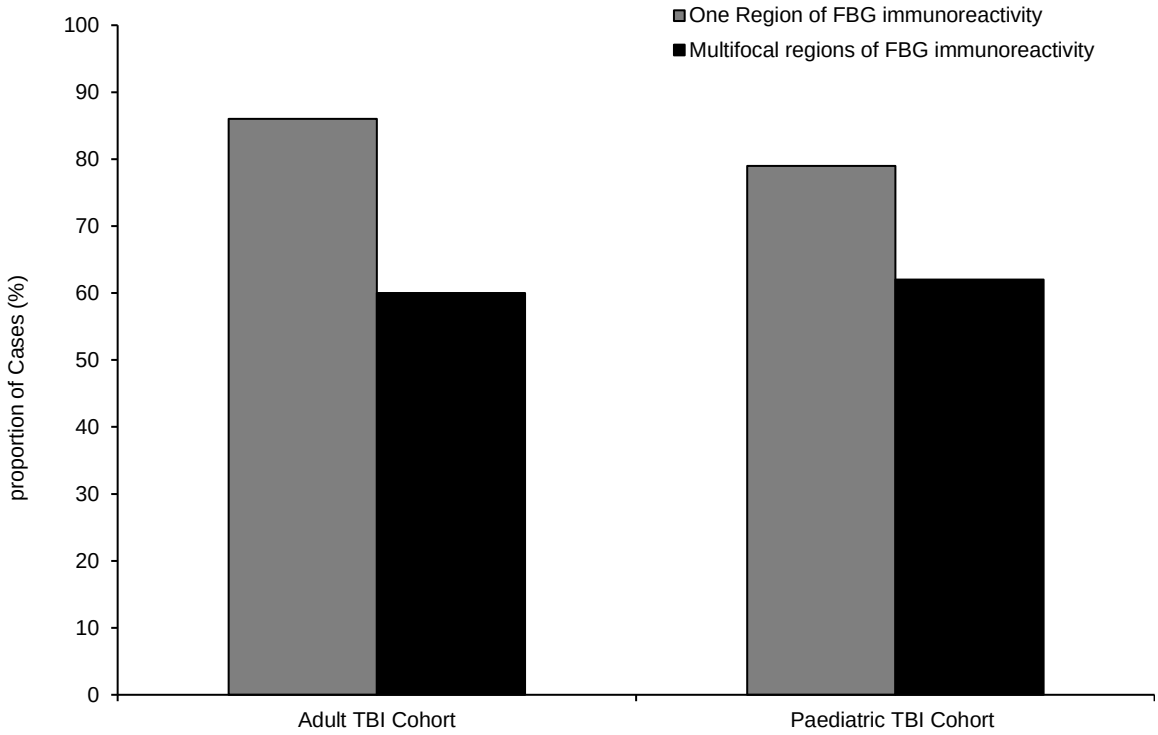

Figure 4-6 Extent of abnormal FBG immunoreactivity following TBI in Adult versus Paediatric cohorts in acute survival Moderate or extensive FBG immunoreactivity was a frequent observation in both Paediatric and Adult TBI groups where it was present in 79% or the Paediatric TBI cohort and in 86% of the Adult TBI cohort (NS). Following TBI, the Paediatric cohort expressed multifocal FBG immunoreactivity in 62% of cases where the adult TBI cohort expressed multifocality in 64% of cases (NS).

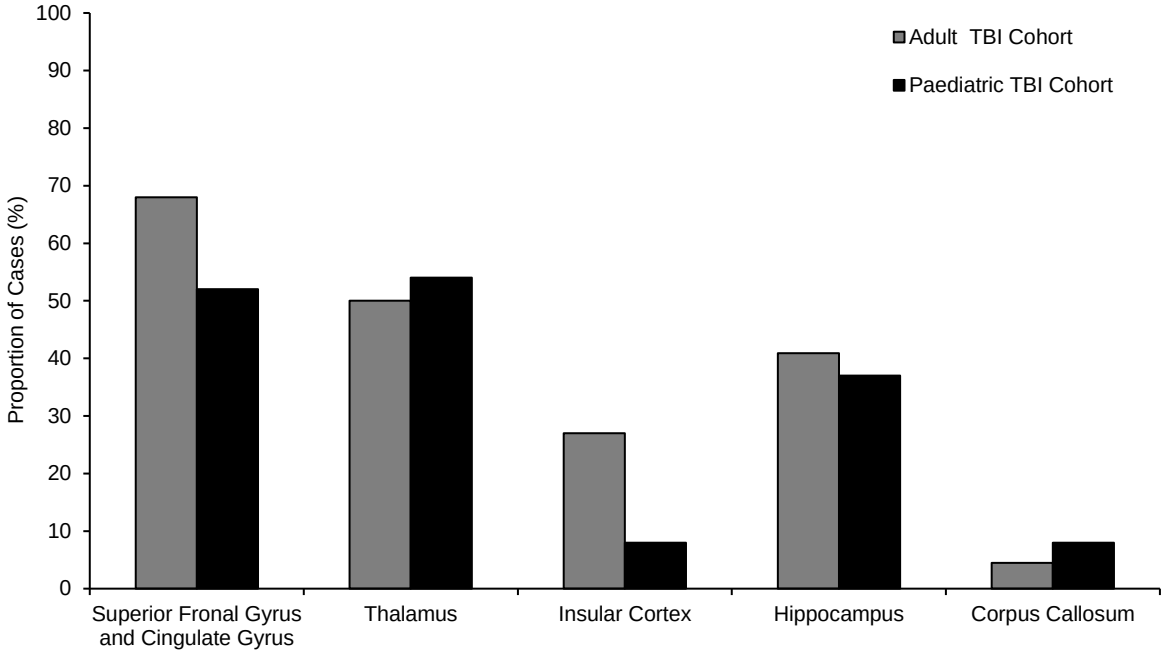

Figure 4-7 Regional Distribution of FBG immunoreactivity following TBI in both Adult and Paediatric cohorts In all regions analysed there was evidence BBB disruption following TBI, evidenced by moderate/extensive FBG immunoreactivity with a similar pattern of FBG immunoreactivity observed in both Adult TBI and Paediatric TBI.

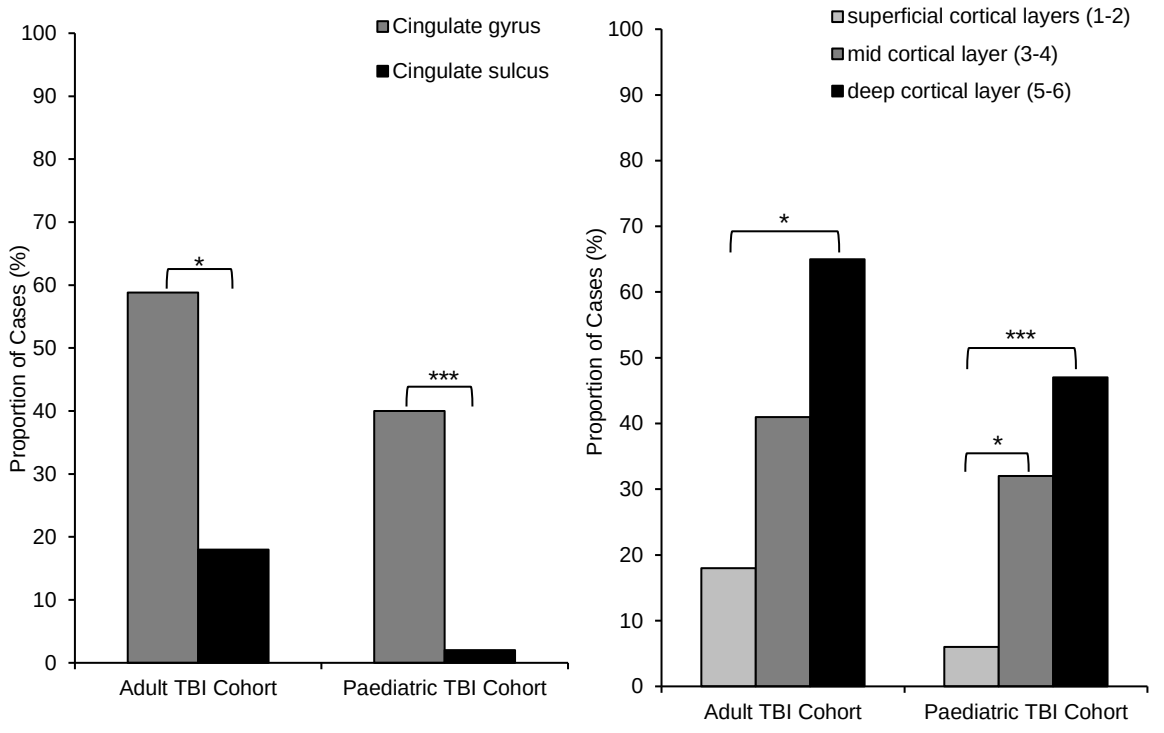

Figure 4-8 Neocortical distribution of FBG immunoreactivity after TBI A similar pattern of BBB disruption was observed between the Adult TBI and Paediatric TBI where there was preferential distribution of abnormal FBG immunoreactivity to the crests of the gyri when compared to the depths of the sulci in both TBI cohorts (*p<0.01' **<0.001; ***p<0.0001; $\chi 2$ sulcus versus gyrus). (b) In addition, within the neocortical grey matter region there was preferential distribution of abnormal FBG to the mid layers (layers 3 and 4) and deep (layers 5 and 6) cortical layers when compared to superficial layers (layers 1 and 2) in both TBI cohorts (*p<0.01' **<0.001; ***p<0.0001; $\chi 2$ deep versus superficial cortical layers).

4.3.3 BBB disruption is a capillary-level pathology in paediatric acute TBI

Although incidence and distribution of FBG immunoreactivity in acute TBI was similar in adult and paediatric TBI patients, the pattern of vascular involvement appeared qualitatively different between the two cohorts. Specifically, in paediatric material abnormal FBG or IgG immunoreactivity was marked by numerous punctate, perivascular foci of staining in cortical sections (Figure 4-9a-d). In contrast, in adult acute TBI patients immunoreactivity for these markers was typified by fewer and larger foci of staining (Figure 4-9e-f), suggesting BBB disruption was localised to larger diameter vessels in adults than in paediatric patients.

Examination of sections from the cingulate gyrus stained for the endothelial protein CD34 revealed the overwhelming majority of cortical vessels in both adult and paediatric material to be less than 10µm in diameter, in keeping with capillary-sized small vessels (Figure 4-10). Thus, vessels measured at less than 10µm in diameter comprised 92% and 95% of all cortical vessels in adult and paediatric TBI cohorts respectively. In contrast, however, where a proportion of capillary-sized vessels was similar in adult and paediatric material, BBB disruption was preferentially distributed to capillary-level vessels in paediatric cases when compared to adults. In material from the paediatric TBI cohort 82% of vessels showed abnormal FBG immunoreactivity less than 10µm in diameter, compared to just 41% of vessels in adults ($p = 0.0001$; $\chi 2$; Cramer's $V = 0.394$) (Figure 4-11).

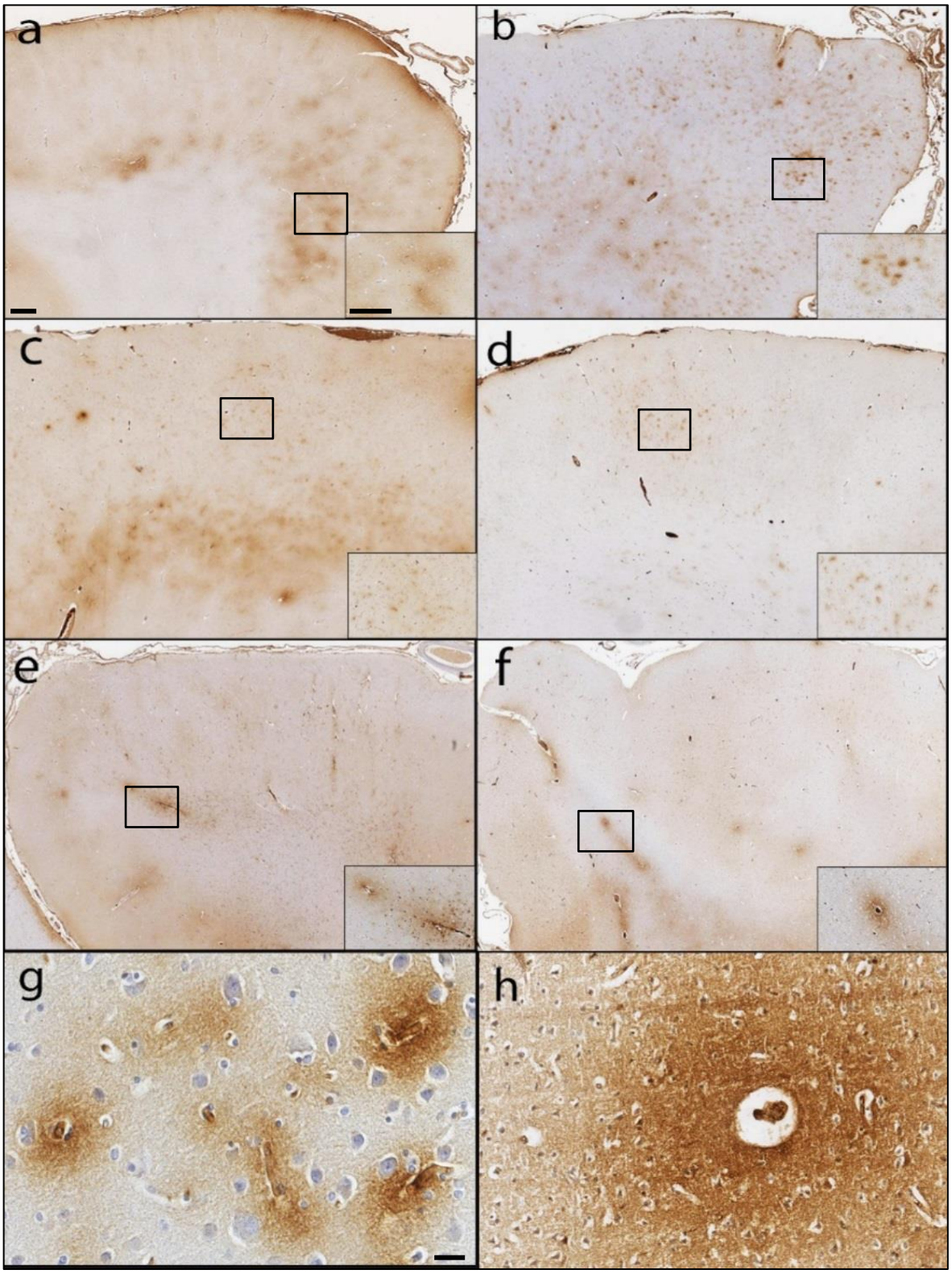

Figure 4-9 Representative images of FBG immunoreactivity in adult and paediatric TBI (a) Perivascular FBG immunoreactivity in small vessels of the cingulate gyrus in a 13-year-old male TBI patient who died 3 hours after an RTA (b) Similar pattern of FBG immunoreactivity around small vessels observed in the cingulate gyrus of an 18-year-old male TBI patient who died 72 hours after an assault. (c) FBG immunoreactivity around small vessels observed in a 20-year-old male who died 24 hours after an assault (d) The same case as (c) but using IgG immunoreactivity (e) FBG immunoreactivity apparent surrounding larger vessels in the cingulate gyrus of a 60-year-old male TBI patient who survived 8 days after a fall (e) Similar FBG immunoreactivity pattern around the larger vessels of the cingulate gyrus of a 51-year-old male who died 96 hours after an assault (g) 40x image of FBG immunoreactivity around the capillaries of a 18-year-old male TBI patient who survived 3 days following an assault and (h) diffuse FBG immunoreactivity surrounding a large vessel in a 37-year old TBI patient who survived 4 years following a fall. Scale bars = 1mm, scale bar = 100µm (high magnification) and scale bar = 10µm in 40x image (g and h).

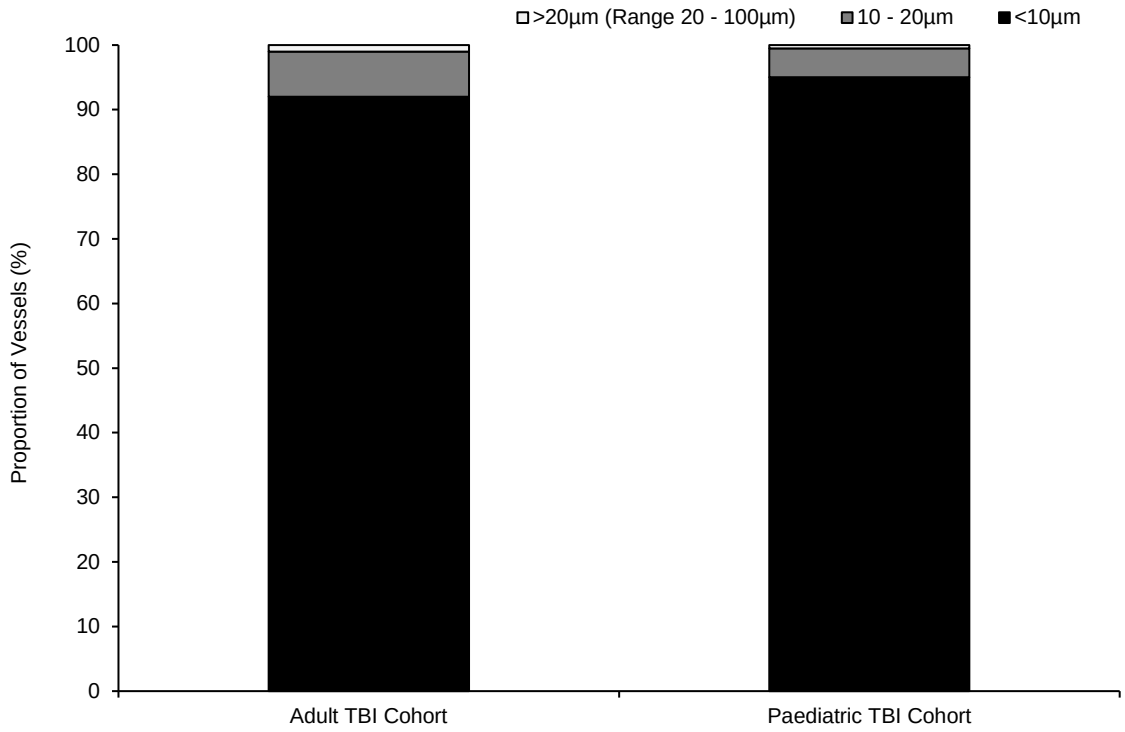

Figure 4-10 Distribution of vessel size following TBI in all vessels in cingulate gyrus in Adult TBI versus Paediatric TBI. Similar patterns of distribution of vessels were observed in both age groups. In the adult TBI cohort 92% of vessels were less than 10µm in diameter. In the paediatric TBI cohort this was 95% (NS). In the adult TBI cohort vessels 10-20µm in diameter made up 7% and the remainder were distributed between 20-100µm. In the paediatric cohort vessels 10-20µm in diameter made up 4.5% and the remainder were distributed between 20-100µm.

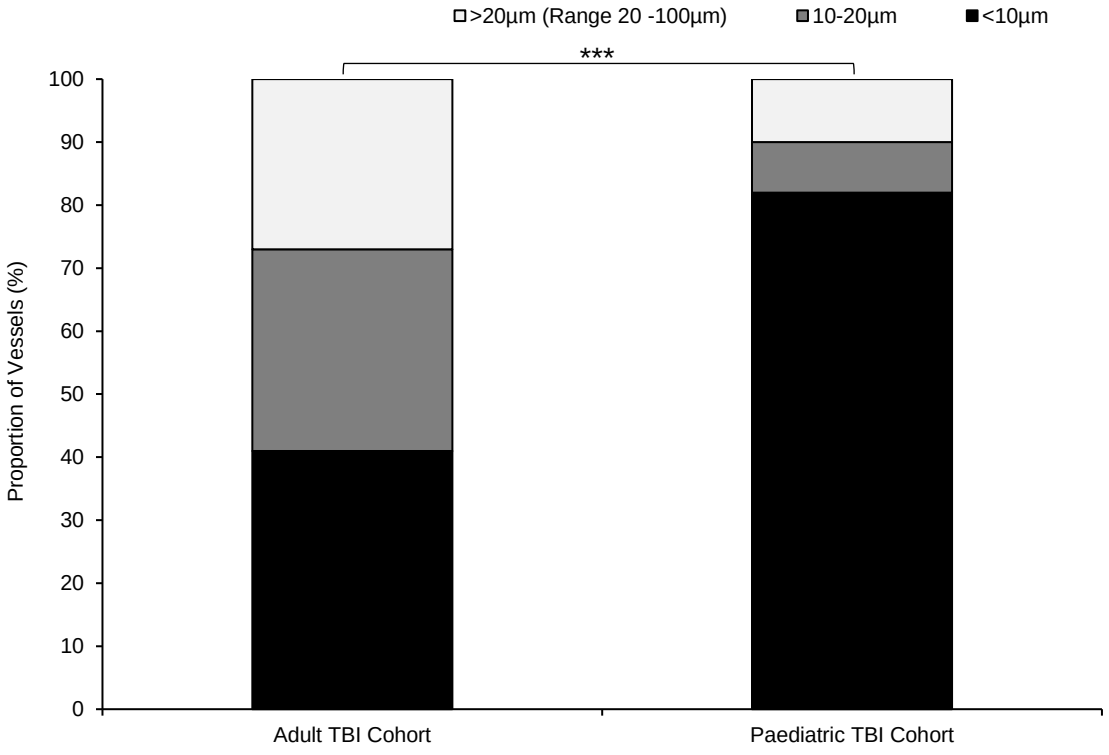

Figure 4-11 Distribution of BBB disrupted vessel size in cingulate gyrus in Adult TBI versus Paediatric TBI. Of all disrupted vessels in the adult TBI cohort small vessels (less than 10µm) accounted for 41%; in the paediatric cohort, this was 82% ($p = 0.0001$; $\chi 2$). Disrupted vessels 10-20µm accounted for 32% in the adult TBI cohort and 8% in the paediatric TBI cohort ($p = 0.0001$; $\chi 2$). Disrupted vessels over 20µm in size accounted for 27% in the adult TBI cohort and only 10% in the paediatric TBI cohort ($p = 0.0242$; $\chi 2$).

Of the cases in the uninjured paediatric cohort, which demonstrated widespread moderate or extensive FBG immunoreactivity, only 2 cases displayed BBB disruption in the cingulate gyrus. One case demonstrated a mean vessel diameter for damaged vessels of 43μm and one case demonstrated a mean vessel diameter for damaged vessels of 5μm.

4.3.4 Association of BBB disruption with focal TBI pathologies

As anticipated, reviewing haematoxylin and eosin-stained sections demonstrated evidence of BBB disruption in association with acute focal haemorrhagic pathologies in both adult and paediatric material. In addition, more widespread and diffuse BBB disruption independent of focal pathologies was also present. In the paediatric TBI cohort, 53 TBI-associated focal haemorrhagic lesions or contusions were observed across 27 of the 52 cases (52%). Virtually all of these cases (25 out of 27) displayed extravascular FBG immunoreactivity adjacent to focal pathology. In addition, 18 cases (72%) demonstrated evidence of widespread diffuse BBB disruption remote from focal pathology. Furthermore, in the 25 remaining cases with no focal haemorrhagic or contusional pathology, 17 (68%) displayed extensive FBG immunoreactivity in at least 1 anatomical area. Similarly, whilst localised BBB was identified adjacent to the TBI-associated focal haemorrhagic or contusional pathologies in 11 of the 12 (92%) cases, where present it was not limited to these regions, with 7 of these adult cases also exhibiting widespread diffuse BBB injury. In the remaining 10 adult cases without focal haemorrhage or contusion, extensive FBG immunoreactivity in at least 1 anatomical region was displayed in all cases. There was evidence of diffuse hypoxic/ischemic injury in a similar proportion in both acute paediatric TBI (85%) and acute adult TBI (90%) cohorts. No correlation with BBB disruption and this TBI-associated pathology was identified.

4.3.5 Brain swelling and BBB disruption

Where clinical data was available, 41 of 42 (98%) of the paediatric TBI cases showed evidence of brain swelling, in contrast, 12 of 22 (55%) of adult cases showed evidence of brain swelling at autopsy ($p = 0.0001$; $\chi 2$; Cramer's $V = 0.542$). Further, where brain swelling was identified, 63% of paediatric TBI cases was bilateral swelling, compared to just 17% of adult TBI cases ($p = 0.004$; $\chi 2$; Cramer's $V = 0.416$) (Table 4).

Of the 42 paediatric TBI cases with clinical data available, 32 cases had BBB disruption (76%), of those cases, 31 cases had brain swelling (97%) and only 1 case had no swelling (3%) (Figure 4-12). Where both BBB disruption and brain swelling were present, 77% had

widespread BBB disruption and 23% had localised BBB disruption (p = 0.0001; $\chi 2$; Cramer's V = 0.563). In the paediatric TBI cases with bilateral brain swelling, 14 demonstrated widespread BBB disruption (70%). In the adult TBI cohort 10 cases had BBB disruption (45%), of which 5 cases were reported to have brain swelling (50%) and 5 cases had no swelling (50%) (p = 0.0016; $\chi 2$; Cramer's V = 0.248). (Figure 4-12). Where both BBB disruption and brain swelling were present, 60% had widespread BBB disruption and 40% had localised BBB disruption (NS). In the adult TBI cases with bilateral brain swelling (2 out of 12), no cases demonstrated widespread BBB disruption. In the uninjured paediatric cohort, 44% of cases demonstrated multifocal BBB disruption, 3 out of the 4 cases had no abnormalities in the brain at autopsy. Of note, the remainder case was reported to show vascular engorgement in the white matter where moderate/extensive FBG immunoreactivity was also demonstrated.

Table 4 Pathologies of all cohorts

Pathologies	Paediatric uninjured cohort (n = 9)	Paediatric TBI (n = 42)	Acute adult TBI (n = 22)	*p* value
Skull fracture	0	25 (60%)	15 (68%)	*p = 0.5918*
Contusions	0	38 (90%)	19 (86%)	*p = 0.6837*
DAI	0	20 (48%)	9 (40%)	*p = 0.7920*
Brain Swelling of which bilateral	0	41 (98%) 26 (63%)	12 (55%) 2 (17%)	***p = 0.0001*** ***p = 0.0082***
SDH	0	19 (45%)	15 (68%)	*p = 0.1145*
EDH	0	8 (19%)	1 (5%)	*p = 0.192*
SAH	0	16 (38%)	11 (50%)	*p = 0.649*

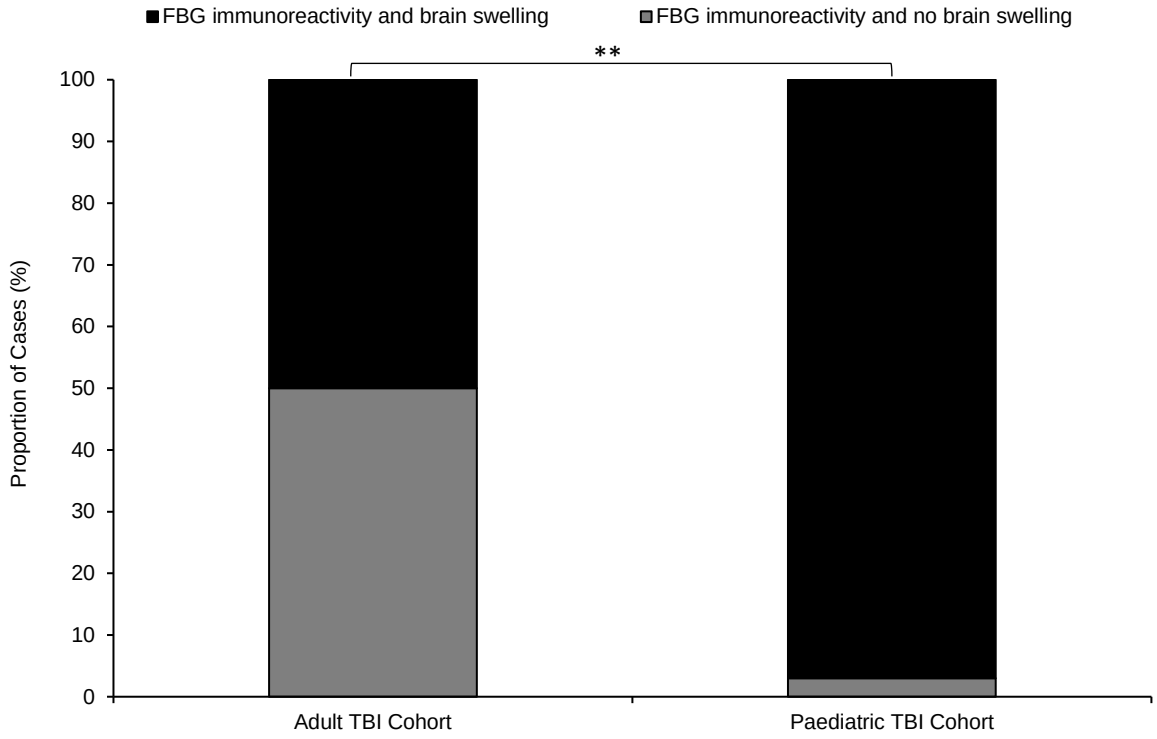

Figure 4-12 Proportion of cases with FBG immunoreactivity and presence or absence of brain swelling. There was a clear relationship between TBI cases with increased abnormal FBG immunoreactivity and TBI cases with DBS as reported in clinical data. Where 97% of Paediatric TBI cases demonstrated both abnormal FBG immunoreactivity and brain swelling (both unilateral and bilateral) only 50% of Adult TBI cases demonstrated this relationship ($p = 0.0016$; $\chi 2$).

4.4 Discussion

This study has demonstrated autopsy evidence of BBB disruption in the majority of paediatric patients dying in the acute phase following a single moderate or severe TBI. Further, for a considerable number of those patients, BBB disruption is widespread and not solely localised to regions of focal TBI pathologies, again paralleling observations in adult material. However, in sharp contrast to adult TBI cases, BBB disruption in paediatric cases appears preferentially distributed to vessels of 10μm or less in diameter, in keeping with capillary sized vessels. This vulnerability of the small vessels was rarely observed in adult material. Indeed, in only one case within the adult cohort was this preferential capillary-level vascular involvement observed, intriguingly, in a younger adult, aged 20 years.

Blood-brain barrier disruption was also demonstrated in the uninjured paediatric cohort, but to a lesser extent than in the paediatric TBI cohort. The cause of death for those uninjured control cases displaying diffuse BBB disruption were reported as epilepsy, leukaemia, cardiomyopathy and unascertained. The majority of these disorders are known to affect the BBB integrity (Michalak et al., 2017, van Vulpen et al., 2002). White matter BBB disruption, specifically in the corpus callosum, was also more prominent in the uninjured paediatric controls than the both paediatric and adult TBI cohorts. Interestingly, vascular pathology was reported in the white matter in one control case at autopsy, which may be associated with BBB disruption. Such complex cohorts generate difficulties in drawing conclusions between paediatric TBI and uninjured paediatric controls; however, since BBB disruption was demonstrated in both paediatric and adult TBI cohorts, comparisons could be made between these groups.

A particular phenomenon recognised in paediatric TBI populations is a risk of diffuse brain swelling (DBS), even after apparently mild injury when it is often referred to as second impact syndrome (SIS). With incidence of DBS in clinical series of paediatric severe TBI approximately twice that recorded in adults, DBS is also associated with high mortality (Kazan et al., 1997). In line with this, whilst autopsy studies in fatal TBI confirm similar overall patterns of brain injury in paediatric and adult TBI, a notable observation is of a considerably higher incidence of DBS in paediatric cases (Graham et al., 1989, Adams et al., 1989b) with one series reporting its presence in 70% of paediatric cases compared to just 17% of adults (Graham et al., 1989). This current data is broadly in line with this observation, demonstrating DBS in 63% of paediatric cases compared to just 17% of adult cases. Furthermore, 70% of paediatric TBI cases with DBS also demonstrated BBB disruption.

Although cases included in this current study were moderate or severe TBI, DBS after even mild TBI is recognised in the paediatric population, often in context of sports participation. In 1984, 'second impact syndrome' (SIS) was first described by Saunders *et al* (Saunders and Harbaugh, 1984) where it was observed in a 19-year-old college and is suggested to occur when an individual suffers a second head injury before the symptoms of the first injury have resolved (Saunders and Harbaugh, 1984, Cantu, 1998). A study by Thomas *et al.* aimed to define the clinical profile, epidemiology and frequency of trauma-related deaths in young US-athletes (Thomas et al., 2011). Of the 138 football players who died due to head blows, 12% had previously reported a history of concussion between a few days and 4 weeks prior to the blow; these were all 14–18 year olds (Thomas et al., 2011); consistent with SIS. However, a systematic review completed in 2016 states there is a lack of established diagnostic signs and symptoms and studies to support a standardised definition for SIS (Hebert et al., 2016).

This study demonstrates a clear neuropathological difference between paediatric and adult TBI, which could explain the increased risk of cerebral swelling observed in children after injury and suggested vascular vulnerability of DBS/SIS. The association of these unique pathologies, however, is poorly understood. Suggestions have been made that poor outcome following DBS may be due to disrupted autoregulation. Studies by Bruce *et al.* (Bruce et al., 1978, Bruce et al., 1981) discuss that DBS is due to an increase in intracerebral blood, either as an increase in cerebral blood volume or as a redistribution of intracranial blood from the pial to the intraparenchymal vessels. Vasogenic oedema which results in extracellular water accumulation, and is induced by BBB disruption, has been suggested to be predominant following TBI (Marmarou et al., 2006a, Unterberg et al., 2004, Huh and Raghupathi, 2009). In this study almost all paediatric TBI cases with BBB disruption demonstrated brain swelling which indicates a capillary vessel vulnerability possibly resulting in a propensity for brain swelling.

In an animal model of hypertensive encephalopathy, BBB disruption precedes a reduction in CBF (Tamaki et al., 1984). Rapid, transient changes to the permeability of BBB were also observed in a neonatal animal model of cerebral ischemia (Ek et al., 2015) where the areas of BBB disruption correlated to the areas of ischemic damage and reduced CBF. A similar pattern of ischemic damage was observed between adult TBI (90% of cases) and paediatric TBI (85% of cases) although no correlation with BBB disruption in the acute phase was identified. This suggest ischemia is a prominent pathology in the acute phase following TBI;

however, further studies would warrant an understanding of how this pathology is linked, directly or indirectly, to vascular changes.

In a rat model of intracerebral haemorrhage, Yang *et al* demonstrated a relationship between a decrease in CBF, an increase in BBB permeability and oedema formation (Yang et al., 1994). After an initial drop in CBF levels post haemorrhage, levels returned to normal before dropping again due to oedema development which, subsequently, was caused by BBB disruption (Yang et al., 1994). In a similar rat model of subarachnoid haemorrhage (SAH), Li *et al* (Li et al., 2015) demonstrated 2 peaks of BBB dysfunction at 3 hours and 72 hours following SAH. In this study, evidence of BBB disruption in association with acute focal haemorrhagic pathologies was identified in both adult and paediatric material. In addition, more widespread and diffuse BBB disruption independent of focal pathologies was also present in both cohorts.

Many reports state that low CBF and dysfunctional autoregulation lead to a poorer outcome after head injury (Adelson et al., 2011, Tontisirin et al., 2007, Pigula et al., 1993, Vavilala et al., 2003). Decreased CBF has been documented even in mild TBI amongst young adults (Maugans et al., 2012, Wang et al., 2015b). This is contradicted by Sharples (Sharples et al., 1995), who found normal CBF levels after severe paediatric head injury. Much of the evidence following paediatric TBI is surrounding CBF alterations and ICP with regard to DBS; however, this is the first autopsy study to address a unique vascular response in children following TBI. Where the distribution of vessels is similar between adult and paediatric TBI (92% and 95%, respectively) the BBB disruption that occurs after TBI favours capillary-sized vessels in paediatric TBI cases (82% of capillaries disrupted compared to 41% in adult TBI). This BBB disruption is observed in the majority of paediatric TBI cases with bilateral brain swelling, indicating that there may be a relationship between capillary-based BBB disruption, brain swelling, and possibly CBF alterations; however, further investigations would be required to confirm this.

4.4.1 Conclusion

This autopsy study is the first to report significant vascular differences between adult and paediatric TBI, demonstrating evidence of BBB disruption is predominantly at the level of capillary-sized vessels in paediatric TBI cases. The majority of paediatric TBI cases demonstrating bilateral brain swelling also demonstrated BBB disruption. The pathologies observed in this current study suggest a potential association between capillary-based BBB

disruption and DBS and may play a role in possible CBF changes following TBI. This could be important in understanding the pathological processes involved in the poorer outcome observed following paediatric TBI, specifically DBS/SIS. However, more work would need to be carried out to investigate these interesting and unique pathologies.

5 Cortical atrophy and vascular changes following TBI

5.1 Introduction

Traumatic Brain Injury (TBI) is widely recognised as the strongest environmental risk factor for dementia (Molgaard et al., 1990, Mortimer et al., 1985, Mortimer et al., 1991, Graves et al., 1990, O'Meara et al., 1997, Salib and Hillier, 1997, Guo et al., 2000, Schofield et al., 1997, Plassman et al., 2000, Fleminger et al., 2003), with a direct dose-response relationship proposed between injury severity and subsequent risk of dementia (Guo et al., 2000, Plassman et al., 2000). Key dementia-associated pathologies have been observed following TBI, such as, abnormal accumulation of tau, Aβ plaques, neuroinflammation and white matter degeneration. Evidence of vascular alterations in dementia have also been reported (Zlokovic, 2011, Sweeney et al., 2018, Buee et al., 1994, Kalaria, 1996, Kalaria and Pax, 1995, Farkas and Luiten, 2001) however, following TBI the evidence is less clear. Blood-brain barrier dysfunction has been demonstrated in Alzheimer's disease (AD) patients (Sweeney et al., 2018, Viggars et al., 2011) and this pathology has also been observed in TBI cases both in the acute phase and persisting into the later phase (Chapter 3) (Hay et al., 2015). However, vascular pathologies such as increased collagen deposition and decreased vascular density which have been demonstrated in dementia (Kalaria and Pax, 1995, Brown and Thore, 2011b) are yet to be investigated and characterised in TBI survivors.

5.1.1 Cortical atrophy

Cortical atrophy has been reported in AD patients where it has been suggested that it correlates with cognitive decline (Mungas et al., 2002), and might precede the onset of dementia (Im et al., 2008). By means of computational neuroanatomy, Lerch *et al.* demonstrated significant cortical thinning in temporal, orbitofrontal and parietal regions in AD; the most pronounced changes occurring in the allocortical region of the medial temporal lobes, outlining the parahippocampal gyrus and representing a loss of <1.25 mm of cortical thickness (Lerch and Evans, 2005, Lerch et al., 2005). Cortical thinning in different brain regions is suggested to correlate with various neurodegenerative disorders; in frontotemporal dementia (FTD) cortical thinning occurs in the left cingulate gyrus and the left occipitotemporal gyri; yet, in AD it occurs in the inferior parietal, occipitoparietal and the pericalcarine regions and is more pronounced in the right hemisphere (Hartikainen et al., 2012, Blanc et al., 2015, Du et al., 2007, O'Brien et al.).

Several studies have investigated cortical atrophy following mTBI, specifically in military populations and in athletes (Michael et al., 2015, Hayes et al., 2017, Savjani et al., 2017, McKee et al., 2013). In each of these studies, all cases demonstrated a decrease in cortical thickness; furthermore, Michael *et al.* (2015) suggested a correlation between cortical atrophy, posttraumatic stress disorder (PTSD), depression and post-concussive symptoms (Michael et al., 2015), while Hayes *et al.*(2017) suggested an association between an increased polygenetic risk of AD and cortical atrophy (Hayes et al., 2017). All note varying levels of cortical thickness across different regions in the brain with several studies collectively suggesting thinning of the frontal and temporal cortex was prominent following mTBI (Govindarajan et al., 2016, Michael et al., 2015, Wang et al., 2015a). Mckee *et al.* (2009) noted gross mild cerebral atrophy with dilation of the second and third ventricles in athletes that demonstrated stage III CTE with a more severe cerebral atrophy in Stage IV CTE (McKee et al., 2013). These studies suggest, similarly to AD, that the cortex undergoes atrophy following mTBI.

Imaging studies have consistently demonstrated cortical atrophy following TBI in humans, with one study observing atrophy after mild to moderate TBI and injury with a loss of consciousness associated with increased rate of thinning (Bergeson et al., 2004, MacKenzie et al., 2002, Ross, 2011). Using a predictive model of normal ageing based on MRI estimates of both grey and white matter Cole *et al*. (2015) reported that TBI brains were ‘older’ than their chronological age, suggesting that TBI accelerates the rate of brain atrophy (Cole et al., 2015). Atrophy following TBI has been reported to be greatest in white matter with higher rates of atrophy observed in the cortical sulci compared to the gyri (Cole et al., 2018). White matter atrophy has also been demonstrated and confirmed in autopsy studies with a 25% reduction in the corpus callosum thickness observed (Johnson et al., 2013a). However, cortical atrophy following TBI has not been assessed in autopsy studies using pathological techniques.

5.1.2 Vascular Density

Increasing evidence suggests changes in the vasculature might be associated with progression of dementia. Significant reductions in vessel density of the basal forebrain and hippocampal regions, together with structural alterations, such as kinking and looping of vessels have been reported in AD patients, which are absent in non-demented patients (Fischer et al., 1990). Furthermore, autopsy studies demonstrate a decrease in microvascular density in AD brains (Buee et al., 1994). Although Buee *et al.* reported changes in both

ageing and AD patients, vascular pathology in AD exceeded that of normal ageing (Buee et al., 1994). However, conflicting evidence suggests there is an increase in vascular density and angiogenesis in AD (Viggars et al., 2011, Desai et al., 2009). Viggars *et al.*, reported that the increase in vascular density was associated with the increase of AD-like pathologies, such as neurofibrillary tangles (Viggars et al., 2011).

Regarding vascular changes following TBI, limited animal evidence offers similar inconsistencies. Obenaus *et al.*, used a controlled cortical impact (CCI) rodent model of TBI and vessel painting perfusion techniques to label the vascular structure in the cortex (Obenaus et al., 2017). In the acute phase following TBI, significant global reductions in vessel junctions and vessel length were observed. Conversely, a lateral fluid-percussion animal model of TBI demonstrated an increase in vessel density in the perilesional cortex and thalamus, and no change in vessel density in the hippocampus (Hayward et al., 2010). These contradictory results in rodent models of TBI indicate vascular changes may be present following injury and warrant further investigation.

5.1.3 Collagen Deposition

Changes in the vasculature in the progression of dementia can alter brain perfusion and BBB permeability (Kalaria, 1996). Autopsy studies using AD brains demonstrate a thickened basement membrane (BM) compared to age-matched non-demented brains (Hardy et al., 1986, Mancardi et al., 1980, Vinters et al., 1994) associated with increased collagen IV deposition (Viggars et al., 2011), which may affect microvascular function (Kalaria and Pax, 1995). In the study by Viggars *et al.*, this increased collagen deposition was observed to be associated with an increase in local neurofibrillary tangle score (Viggars et al., 2011). However, to date, there has been no evidence of collagen deposition in humans following TBI and reported vascular changes are limited.

Previously in this thesis evidence of vascular pathology following TBI was described (Chapter 3) (Hay et al., 2015). Specifically, following a single, moderate or severe TBI there is neuropathological evidence of widespread, diffuse, multifocal BBB disruption in nearly half of patients – even after many years of survival from injury. However, the structural basis for this acute and persistent BBB disruption following TBI is unknown. This study will assess vascular alterations after a single, moderate to severe TBI, in particular, changes in vascular density, cortical atrophy and collagen deposition.

Hypothesis: Following TBI, vascular density is reduced and there is an increase of collagen IV deposition which is associated with BBB disruption. In addition, there will be an observed presence of cortical atrophy.

5.2 Material and Methods

5.2.1 Case selection and brain tissue preparation

From the Glasgow TBI archive cases of a single, moderate to severe TBI were collected, with acute survival times ranging from 6 hours to less than 14 days (n = 11); and long-term TBI cases ranged from a survival time of 1 year to 47 years (n = 19). Age-matched controls were selected as having no history of brain injury or neurological disease (n = 18). All ages were matched between cohorts (NS). The demographics and clinical data for all cohorts are shown in Table 5.

At the time of the original diagnostic autopsy, whole brains were immersion fixed in 10% formal saline for a minimum of 3 weeks, following which the specimens were examined, sampled using standardized techniques and processed to paraffin tissue blocks. For this study, blocks from a coronal slice of the cerebral hemispheres at mid-thalamic level were selected to include the corpus callosum, with adjacent cingulate, superior frontal gyri and sulcus. From these tissue blocks 8μm sections were prepared for immunohistochemistry procedures.

5.2.2 Luxol Fast blue

Following standard deparaffinisation and rehydration, sections with immersed in Luxol Fast blue (LFB) solution (Solvent Blue 38, Sigma) overnight at 27°C. After a rinse in 95% ethanol to remove excess stain, sections were washed in deionized water. Differentiation of the Luxol stain was carried out by immersion in 0.05% aqueous lithium carbonate for 10 seconds followed by multiple immersion in fresh 70% ethanol until grey/white matter boundaries could be clearly distinguished. Following washing in deionized water, sections were stained with Cresyl violet solution for 5 minutes at 60°C and washed again in deionised water. Sections were then differentiated in 95% ethanol (containing 100ml per 300ml glacial acetic acid) and rinsed in 95% ethanol. Sections were then dehydrated and coverslipped.

Table 5: Demographic and clinical information of all groups

		TBI: Acute Survival (n = 11)	TBI: Long-Term Survival (n = 19)	Controls (n = 18)
Mean age (Range) (years)		39.3 (16-60)	46 (19-60)	37.7 (20-60)
Males		8 (73%)	18 (95%)	10 (55.6%)
Mean PM Delay (Range)		72.6 hours (3-240)	58.4 hours (9-184.5)	72 hours (12-168)
Mean Survival Interval (Range)		44.4 hours (6-96)	8.1 years (1-47)	N/A
Cause of TBI	Fall	6 (55%)	9 (47.4%)	N/A
	RTA	1 (9%)	2 (10.5%)	
	Assault	3 (27%)	4 (21%)	
	Unknown	1(9%)	4 (21%)	
Cause of Death	Head injury	10 (91%)	0	0
	Bronchopneumonia	1 (9%)	6 (31.5%)	0
	ARDS	0	0	0
	Pulmonary thromboembolism	0	0	0
	Heart disease	0	3 (15.8%)	4 (22.2%)
	Alcohol related	0	2 (10.5%)	0
	Pyelonephritis	0	1 (5%)	0
	Multi-organ failure	0	1 (5%)	0
	GIT haemorrhage	0	0	0
	Polytrauma	0	0	0
	Drug overdose	0	0	2 (11.1%)
	SUDEP	0	3 (15.8%)	8 (44.4%)
	Pulmonary oedema	0	1 (5%)	0
	Septicaemia	0	0	2 (11.1%)
	Inhalation of gastric contents	0	0	2 (11.1%)
	Unknown	0	2 (10.5%)	0
	Key: *TBI = traumatic brain injury; SUDEP = sudden unexpected death in epilepsy; GIT = gastrointestinal tract; ARDS= acute respiratory distress syndrome; RTA = road traffic accident*			

5.2.3 Immunohistochemistry

Tissue sections were deparaffinised and rehydrated using xylene and graded alcohols. Following this step, sections were immersed in 3% aqueous H_20_2 for a minimum of 15 minutes to quench endogenous activity. Heat antigen retrieval was performed via microwave pressure cooker for 8 minutes in preheated 0.1M Tris EDTA buffer. Blocking was carried out by applying 50µL of normal horse serum (Vector Labs, Burlingame, CA, USA) per 5 mL of Optimax buffer (BioGenex, San Ramon, CA, USA) for 30 minutes. Primary antibodies were then applied and sections incubated overnight at 4°C. Polyclonal rabbit anti-human antibody for CD34 used at a dilution of 1:100 (QBEnd 10, Leica Biosystems, Milton Keynes, UK), collagen IV (CIV 22, Dako, Carpinteria, CA, USA) at a dilution of 1:25 and fibrinogen at a dilution of 1:17,500 (Dako, Carpinteria, CA). After washing in PBS, a biotinylated secondary antibody was applied (100µl in 5ml of horse serum and 100µl of secondary per 5ml Optimax buffer) and incubated for 30 minutes. The secondary antibody was then washed off with PBS. Visualization was achieved using the DAB peroxidase substrate kit (Vector Labs, Burlingame, CA, USA) followed by counterstaining with haematoxylin. All sections were viewed using a Leica DMRB light microscope (Leica Microsystems). In addition, sections were scanned at 20x using a Hamamatsu Nanozoomer 2.0-HT slide scanner, with the images viewed via the SlidePath Digital Image Hub application (Leica Microsystems). Furthermore, where appropriate sections were scanned using a 40x optic which scans images at a digital resolution of 0.23µm per pixel. The images in this chapter have been digitally captured at 4x (2.3µm per pixel), 20x (0.46µm per pixel) and 40x (0.23µm per pixel).

5.2.3.1 Cortical thickness

Once sections were scanned using the Hamamatsu Nanozoomer Slide Scanning Machine (Hamamatsu, Hertfordshire, UK), the cortex of the cingulate gyrus and cingulate sulcus were measured using the measuring tool in SlidePath Digital Image Hub application (Leica Microsystems, Wetzlar, Germany). The narrowest point in the cingulate gyrus and cingulate sulcus was chosen to avoid cortical variance within sections. For confirmation of correct cortical thickness, sections were also measured under a microscope using the graticule. Between the SlidePath tool and graticule the measurements were comparable (NS).

5.2.3.2 Vascular density and collagen deposition

To measure vessel density and collagen deposition and compare with BBB disruption, a subset of the cohort was analysed based on the fibrinogen score. Scoring of fibrinogen was previously described in Chapter 3. There were 7 acute TBI cases with survival times of 10 hours to 9 days; which were split based on amount of fibrinogen present in the cingulate gyrus region (4 increased and 3 decreased fibrinogen cases). The subset also consisted of 8 long-term cases with survival times 3 to 18 years; which were split into increased fibrinogen deposition (score of 2 or 3; n = 4) and decreased fibrinogen deposition (score of 0 or 1; n = 4). For comparison, four uninjured, non-demented controls cases were selected.

ImageJ (ImageJ, USA) software was used to quantify the vascular density and collagen IV staining. Using the SlidePath Digital Image Hub application, a 1mm x 1mm square was randomly placed over sections of the superficial, mid and deep layers of the cingulate gyrus and cingulate sulcus and isolated. A similar region was isolated from the corpus callosum. The percentage staining was then calculated using an ImageJ plugin tool. To assess the overall density of the cingulate gyrus and cingulate sulcus the mean of all layers was calculated.

5.2.3.3 Fibrinogen analysis

Extent and distribution of fibrinogen (FBG) and IgG immunoreactivity were assessed using established semi-quantitative techniques (Chapter 3). Briefly, the neocortical grey matter of the cingulate gyrus, cingulate sulcus, superior frontal gyrus, were divided into superficial (layers 1-2), mid (layers 3-4) and deep layers (5-6). Each of these cortical divisions and thalamic regions were then semi-quantitatively assessed for the frequency and intensity of immunoreactivity determined as absent (0), sparse (1), moderate (2) or extensive (3).

5.2.4 Statistical analysis

All data were analysed using SPSS (version 22; IBM, Inc). The Student's *t*-test was used to assess differences in data between and within cohorts, where appropriate. Cohen's *d* was calculated to determine the effect size and to indicate the standardised difference between two means. A Cohen's *d* value of 0.2 suggested a low practical significance, a value of 0.5 suggested a moderate practical significance and a value of 0.8 suggested a high practical significance. All effects were considered statistically significant when $p \leq 0.05$. Quantitative results are expressed as mean ± standard error of the mean.

5.3 Results

5.3.1 Cortical thickness of TBI cases compared with controls

In the cingulate gyrus there was no difference in cortical thickness between TBI and control cohorts. Cortical areas in the LFBs staining were defined as the pale blue region compared with the myelin-rich white matter regions defined as dark blue (Figure 5-1). Cingulate gyrus measurements were similar between all the groups with comparable gyral thicknesses (Figure 5-2).

The mean cortical thickness of the control group was 2.17 ± 0.075 mm, similar to the acute TBI group which had a cortical measurement of 2.30 ± 0.155 mm ($p = 0.452$; Student's *t*-test; Cohen's $d = 0.3$). In the long-term TBI group the mean cortical measurement was 2.39 ± 0.08 mm, again, similar to the uninjured control group ($p = 0.0630$; Student's *t*-test; Cohen's $d = 0.7$) (Figure 5-2). In the cingulate sulcus the mean cortical thickness of the control group in the cingulate sulcus was 1.82 ± 0.067 mm, whereas, the acute TBI group had a cortical measurement of 1.92 ± 0.05 mm ($p = 0.169$; Student's *t*-test; Cohen's $d = 0.51$). In the long-term TBI group the mean cortical measurement was 1.80 ± 0.05 mm, again, similar to the uninjured control group ($p = 0.903$; Student's *t*-test; Cohen's $d = 0.04$) (Figure 5-2).

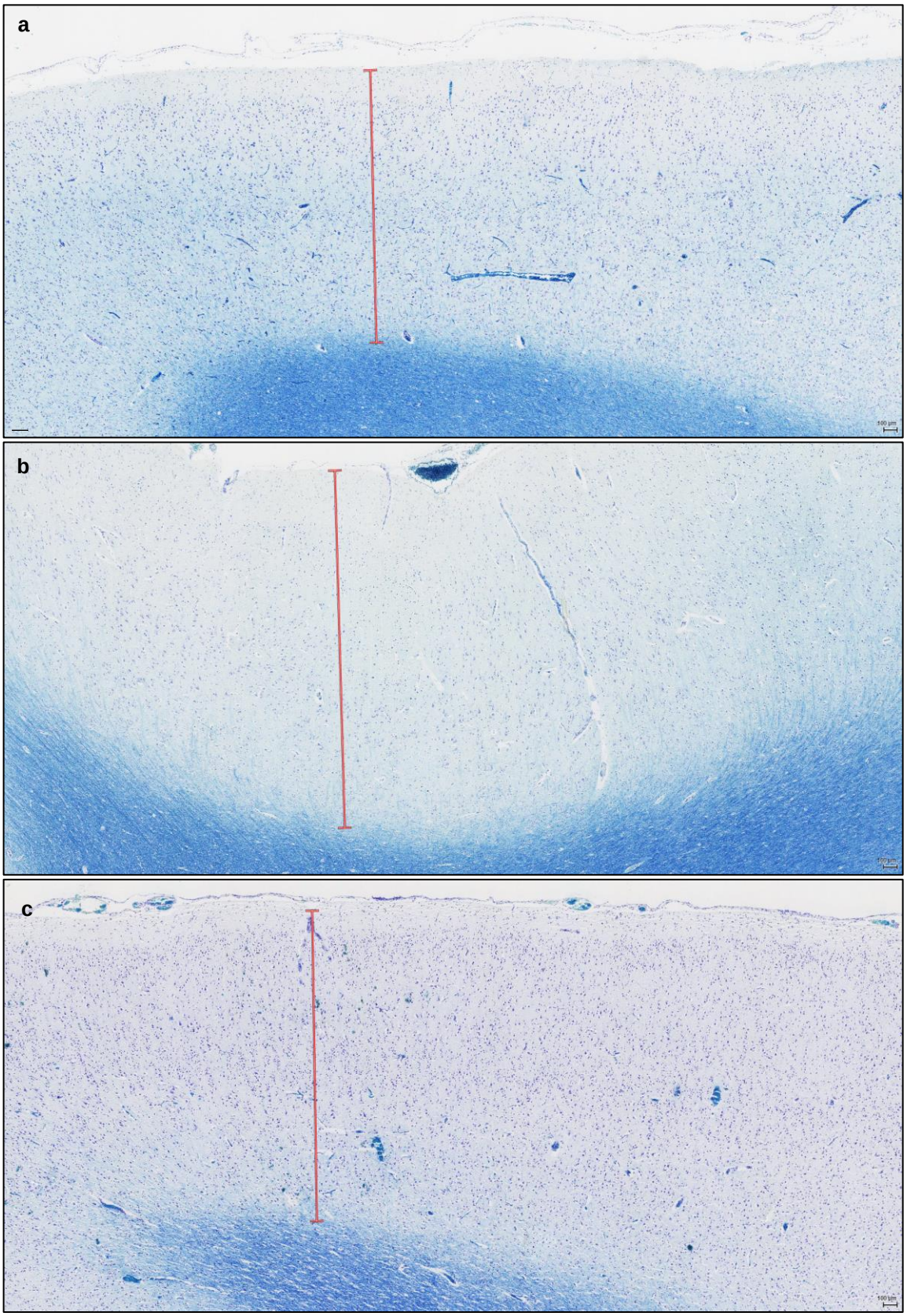

Figure 5-1 Representative images of LFB staining for measurement of cortical thickness (a) Where a clear separation of cortical regions and white matter regions as defined by the light blue staining (grey matter), in contrast to the darker blue staining of the white matter tracts in the cingulate gyrus of a 37-year-old female with no history of TBI (cortical thickness as measurement by SlidePath measuring tool (in red) 2.01mm) (b) LFB staining in the cingulate gyrus of a 20-year-old male who died 48 hours after sustaining a TBI by an assault (cortical thickness 2.48mm as seen by SlidePath measuring tool in red) (c) LFB staining in the cingulate gyrus of a 54-year-old male who died 9 years following a TBI sustained by a fall (cortical thickness 2.25mm as seen by SlidePath measuring tool in red 2.25mm) Scale bars =100µm for all images.

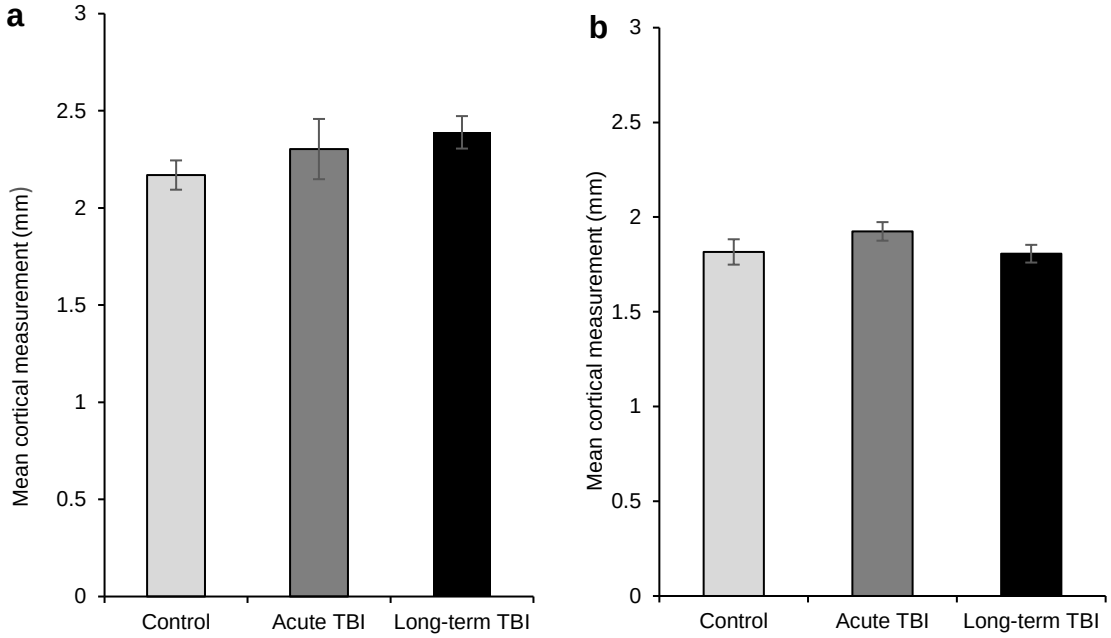

Figure 5-2 Measurement of cortical thickness in all cohorts in cingulate gyrus and cingulate sulcus (a) The mean cortical thickness in the cingulate gyrus of the long-term TBI group was 2.39 mm compared to 2.17mm in the control group (NS). (b) In the cingulate sulcus, the mean cortical thickness was 1.92 mm in the acute TBI group and 1.82 mm in the uninjured control group (NS).

5.3.2 Vascular density

There was no difference in percentage area stain of CD34 between the TBI cohorts and the control cohort in the cingulate gyrus and the cingulate sulcus, however, a trend toward a higher percentage area stain of CD34 was observed in the acute phase. The pattern and distribution of vessels was evenly spread throughout the cortical layers in both cingulate gyrus and cingulate sulcus and density of vessels in both cortical regions was greater than in the corpus callosum. CD34 staining was localised to the blood vessels and predominant in the vascular rich cortical regions compared with the white matter regions, as expected (Figure 5-3).

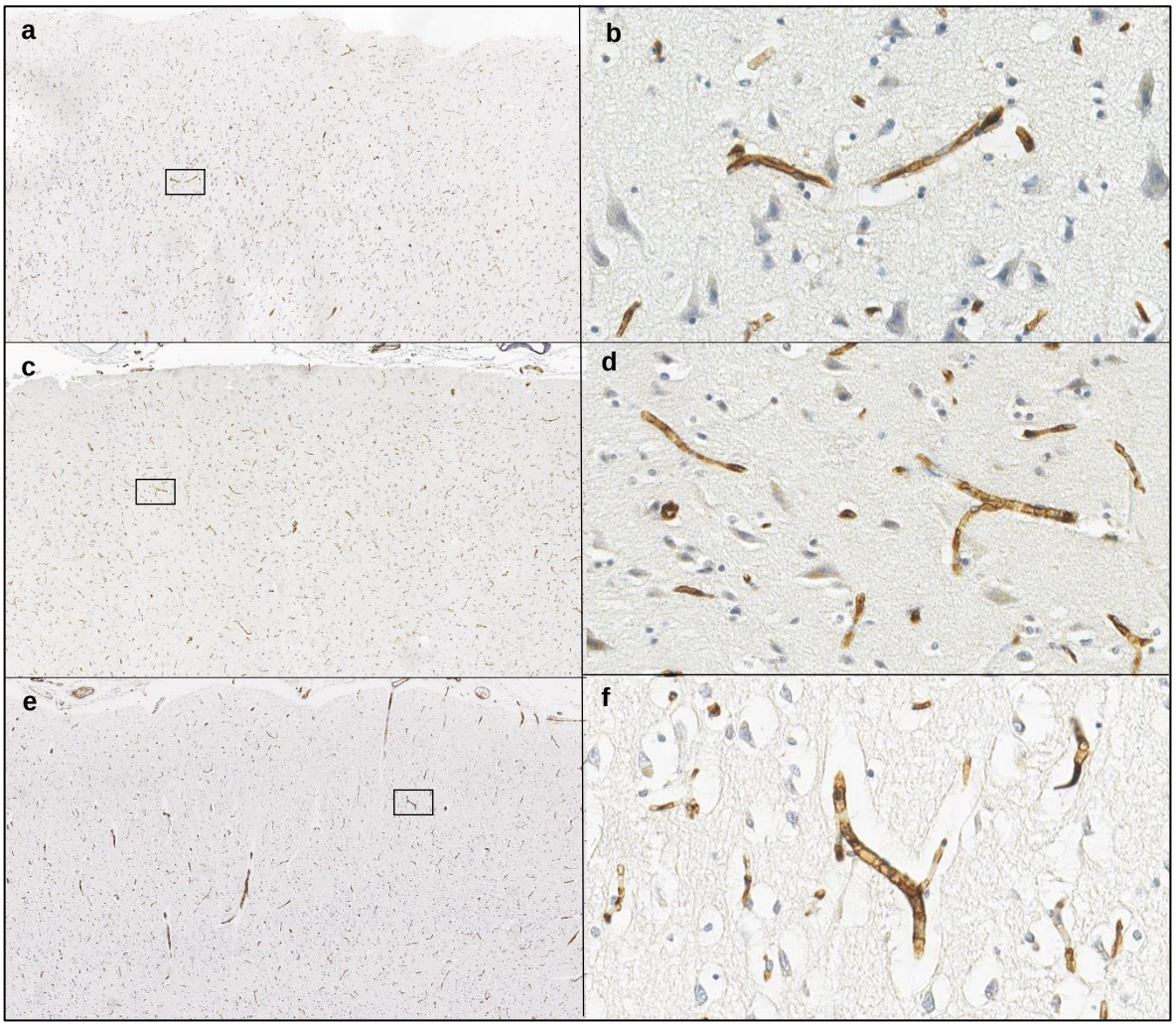

Figure 5-3 Representative images of CD34 staining in the cortical region of the cingulate gyrus in TBI and uninjured controls (a) where CD34 immunoreactivity highlights the vascular endothelial cells and visualises vessel density in the cingulate gyrus of a 55-year-old male with no history of TBI, with corresponding 40x scanned image (b) (c) CD34 immunoreactivity in the cingulate gyrus of a 51-year-old male who died 96 hours after sustaining a TBI by an assault with corresponding 40x scanned image (d) (c) CD34 immunoreactivity in the cingulate gyrus of a 56-year-old male who died 3 years following a TBI sustained by an assault with corresponding 40x scanned image (f). Scale bar = 100µm and scale bar = 10µm (higher magnification). In the cingulate gyrus the mean percentage staining of CD34 in the control group was 2.73% ± 0.13%. This was similar to all TBI groups with the acute TBI group demonstrating a percentage area stain of CD34 of 3.06% ± 0.19% (p = 0.170; Student's *t*-test; Cohen's *d* = 0.48). While the long-term TBI group demonstrating a percentage area stain of CD34 of 2.62% ± 0.16% (p = 0.502; Student's *t*-test; Cohen's *d* = 0.26) (Figure 5-4). The cingulate sulcus demonstrated a similar pattern of CD34 immunoreactivity as in the cingulate gyrus. Percentage staining of CD34 in the control group was 2.36% ± 0.23% with both the acute TBI group and Long-term TBI group comparable (*Acute TBI vs control*: p = 0.1097; Student *t*-test; Cohen's *d* = 0.78; *Long-term TBI vs control*: p = 0.0773; Student's *t*-test; Cohen's *d* = 0.79) (Figure 5-4). In the corpus callosum, in the control group, the mean percentage area stain of CD34 was 1.22% ± 0.05% and the acute TBI group had a mean percentage area stain of CD34 of 1.45% ± 0.08% (p = 0.092; Student's *t*-test; Cohen's *d* =

0.86). The long-term TBI group the area staining of CD34 was 1.75% ± 0.24% (p =0.056; Student's *t*-test; Cohen's *d* = 1.05) (Figure 5-4).

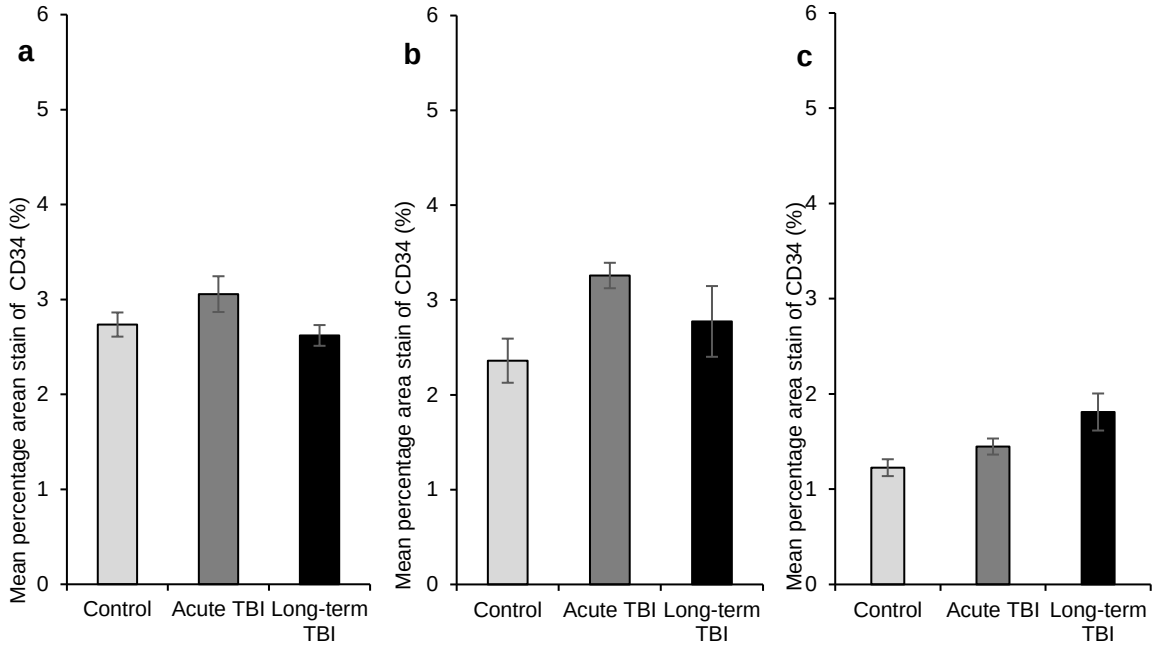

Figure 5-4 Regional distribution of CD34 immunoreactivity following TBI versus controls
Where the CD34 immunoreactivity was observed to be similar throughout the TBI groups compared with the controls in all regions assessed (a) Cingulate gyrus (b) Cingulate Sulcus and (c) Corpus callosum (all NS).

No association could be demonstrated between CD34 immunoreactivity and fibrinogen immunoreactivity. In the cingulate gyrus of the acute TBI cohort the mean percentage staining for CD34 was 2.96% ± 0.19% in cases with minimal fibrinogen immunoreactivity; this was similar in cases with high fibrinogen immunoreactivity where the percentage area stain of CD34 was 3.1% ± 0.29% (p = 0.638; Student's *t*-test; Cohen's *d* = 0.2) (Figure 5-5). A similar pattern was observed in the long-term TBI cohort where cases with minimal fibrinogen immunoreactivity had a CD34 percentage staining of 2.5% ± 0.14% this was similar in cases with high fibrinogen immunoreactivity where the percentage area stain of CD34 was 2.84% ± 0.14% (p = 0.078; Student's *t*-test; Cohen's *d* = 0.77) (Figure 5-5). The cingulate sulcus demonstrated a similar pattern and distribution as the cingulate gyrus, however the numbers were challenging as the presence of fibrinogen immunoreactivity was minimal in this region.

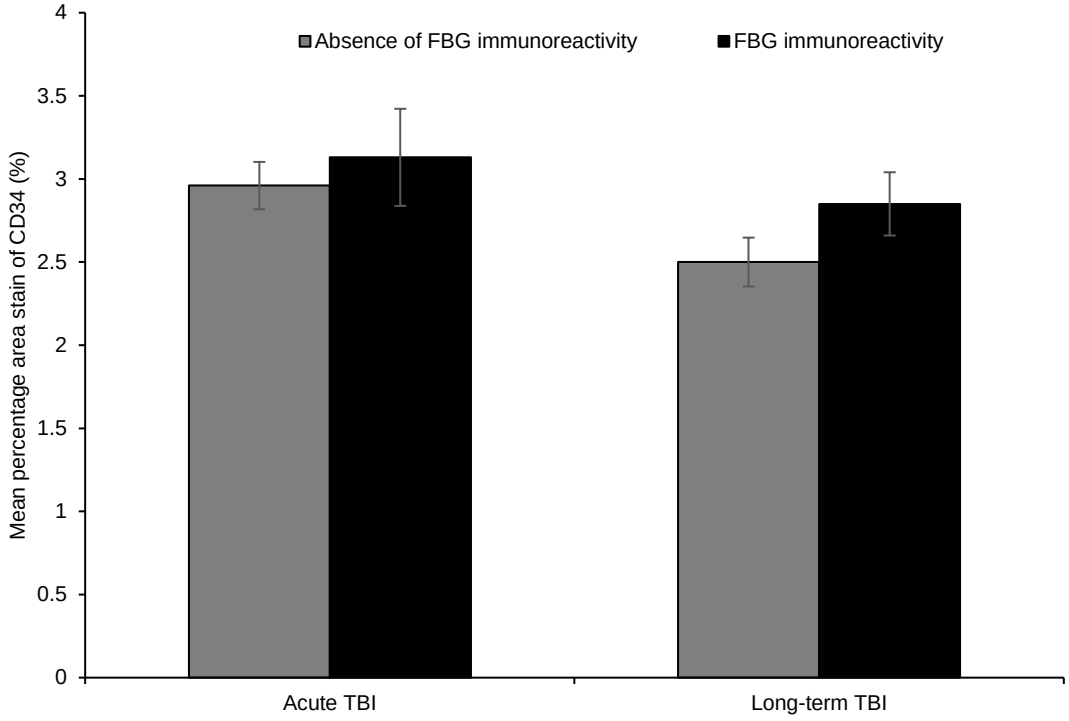

Figure 5-5 Association of CD34 immunoreactivity and abnormal FBG immunoreactivity following TBI at varying survivals. There is no association between CD34 immunoreactivity and presence or absence of abnormal FBG immunoreactivity in varying survivals following TBI (NS).

Of note, the pattern and distribution of fibrinogen immunoreactivity previously described a preferential distribution towards the deeper layers of the cortex. However, the CD34 immunoreactivity did not show such distribution. In the cingulate gyrus of acute TBI cases with minimal fibrinogen immunoreactivity the percentage staining of CD34 in the superficial, mid and deep layers of the cingulate gyrus was 3.15%, 2.98% and 2.74% respectively. Those cases with high fibrinogen immunoreactivity in the acute TBI cohort demonstrated similar percentage staining of CD34 of 2.97%, 3.27% and 3.15% for CD34 in the superficial, mid and deep layers respectively (Table 6**,** Figure 5-6). Furthermore, the long-term TBI group demonstrated no difference between layers. The mean percentage staining of CD34 in cases with minimal fibrinogen immunoreactivity was 2.15%, 2.42% and 2.32% in the superficial, mid and deep layers respectively. In cases with high fibrinogen immunoreactivity the mean percentage area staining of CD24 was 2.62%, 3.19% and 2.72% (Table 6**,** Figure 5-6). A similar pattern was observed in the cingulate sulcus with no difference between groups.

Table 6 Mean percentage stain of CD34 within cortical layers split by FBG immunoreactivity

	Acute TBI				Long-term TBI			
Cortical Layers	**Low FBG immunoreactivity**	**High FBG immunoreactivity**	**p**	**d**	**Low FBG immunoreactivity**	**High FBG immunoreactivity**	**p**	**d**
Superficial (Layers 1-2)	3.15% ± 0.26%	2.97% ± 0.69%	*0.82*	*0.17*	2.15% ± 0.12%	2.62% ± 0.18%	*0.78*	*1.64*
Mid layers (3-4)	2.98% ± 0.54%	3.27% ± 0.45%	*0.69*	*0.3*	2.42 ± 0.06%	3.19 ± 0.33%	*0.10*	*1.61*
Deep Layers (5-6)	2.74% ± 0.411	3.15% ± 0.47%	*0.54*	*0.49*	2.32 ± 0.13%	2.72 ± 0.14%	*0.92*	*1.57*

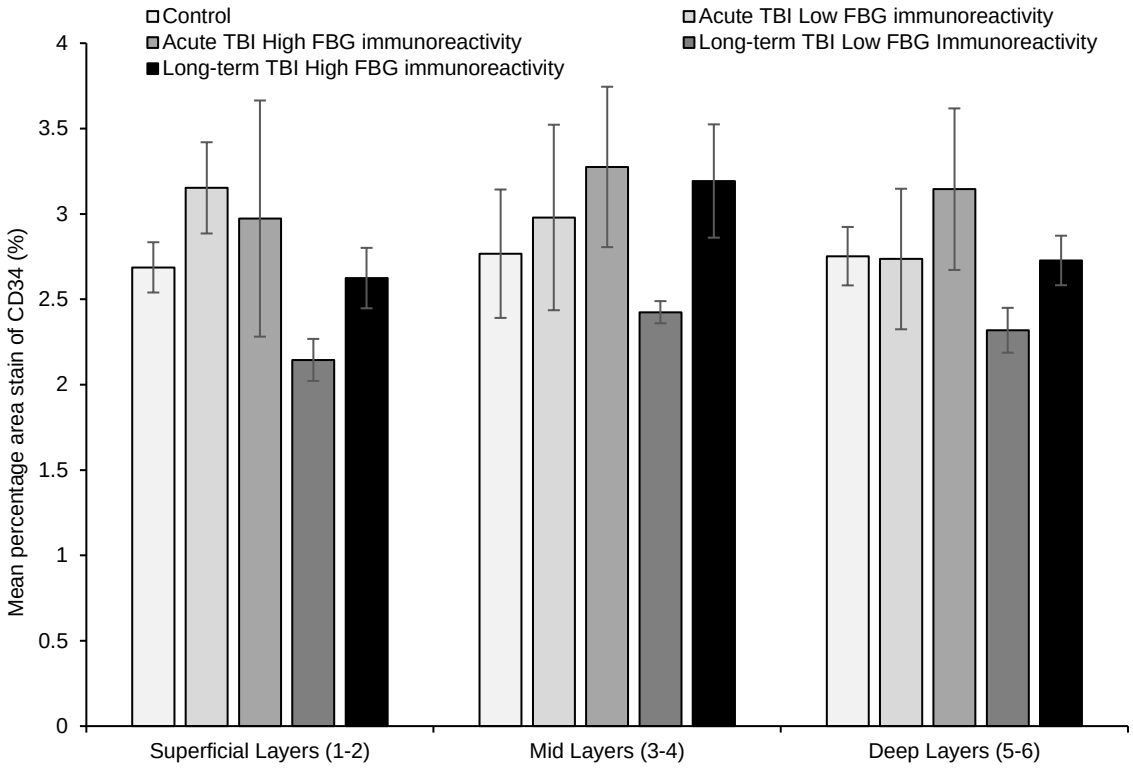

Figure 5-6 Neocortical distribution of CD34 immunoreactivity after TBI in the presence and absence of abnormal FBG immunoreactivity Where the pattern and distribution of CD34 immunoreactivity was observed to be consistent through the varying survivals of TBI compared with controls with no association with abnormal FBG immunoreactivity.

5.3.3 Collagen deposition

Similar to CD34 distribution, the pattern and distribution of collagen IV was evenly spread throughout the cortical layers in both cingulate gyrus and cingulate sulcus and density of vessels in both cortical regions was greater than in the corpus callosum. Collagen IV staining was localised to the blood vessels and predominant in the vascular rich cortical regions compared with the white matter regions, as expected (Figure 5-7). In the cingulate sulcus and corpus callosum, there was no difference in the mean percentage area stain of collagen IV between the groups. However, in the cingulate gyrus, a reduction in the mean percentage

stain of collagen IV was observed in the cingulate gyrus of the TBI groups compared to the uninjured controls (Figure 5-8).

The mean percentage staining of collagen IV in cingulate gyrus of the control group was 3.39% ± 0.25% which reduced to 1.69% ± 0.31% in the acute TBI group ($p = 0.0001$; Student's *t*-test; Cohen's $d = 2$) (Figure 5-8). In the long-term TBI group, the percentage staining of collagen IV was 2.69% ($p = 0.011$; Student's *t*-test, Cohen's $d = 0.85$) (Figure 5-8). The cingulate sulcus did not demonstrate such a reduction in the percentage staining of collagen in the acute TBI cohort. The mean percentage staining of collagen IV in the control group was 1.36% ± 0.08% which was similar to the acute TBI group of 1.34% ± 0.12% ($p = 0.297$; Student's *t*-test; Cohen's $d = 0.04$). The long-term TBI group demonstrated a percentage area stain of collagen IV of 1.50% ± 0.04% compared with controls ($p = 0.246$; Student's *t*-test; Cohen's $d = 0.64$) (Figure 5-8). In the corpus callosum, all groups demonstrated a similar pattern of percentage area stain of collagen IV (Figure 5-8).

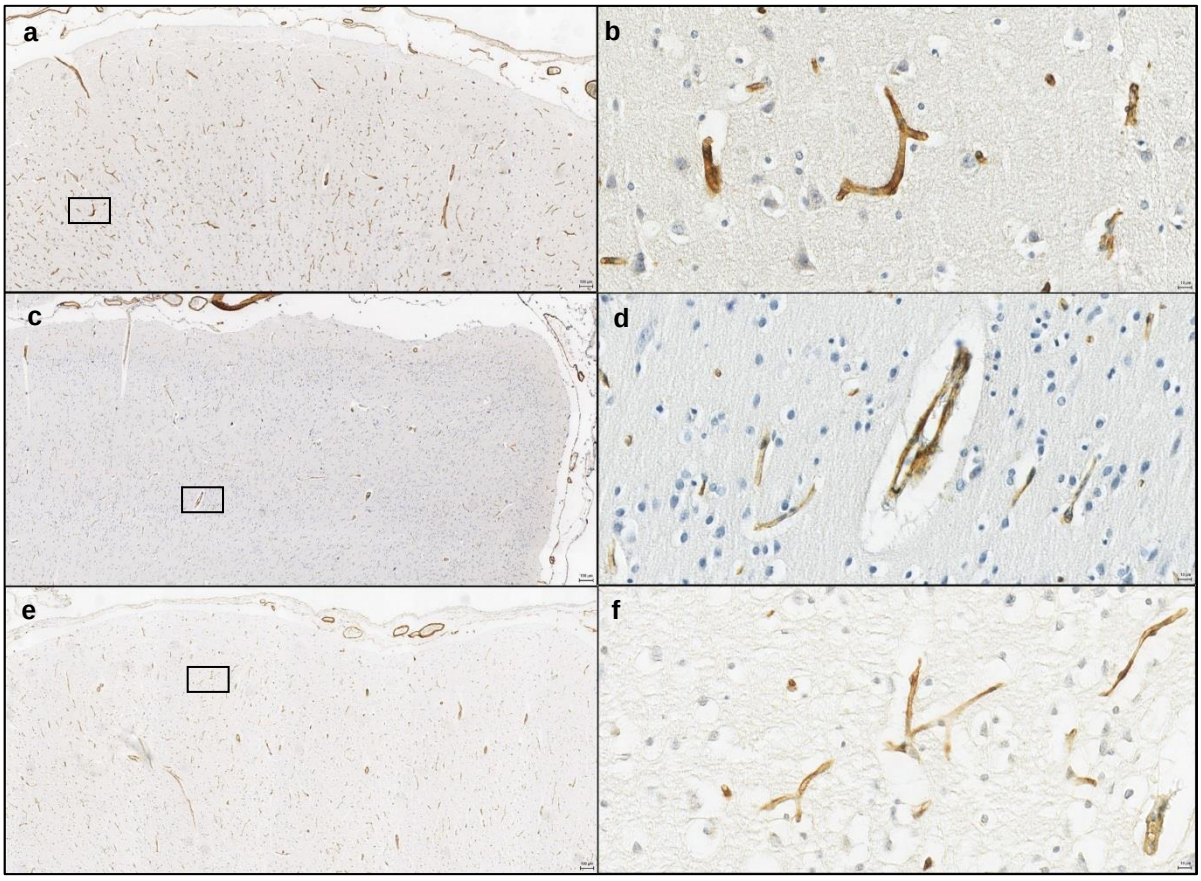

Figure 5-7 Representative images of collagen IV immunoreactivity in the cingulate gyrus after TBI and in uninjured controls Where collagen IV deposition in blood vessels is evidenced by collagen IV immunoreactivity in the neocortical region of the cingulate gyrus. Collagen IV is highlighted around the blood vessels through the cortex and noted in the larger vessels at the subpial plate as expected. (a) Where collagen IV immunoreactivity is expressed in blood vessels in the cingulate gyrus of a 46-year-old male with no history of TBI and corresponding 40x scanned image (b) (c) in a 54-year-old female who survived 54 hours following a TBI sustained by a fall and corresponding 40x scanned image (d) (e) 56-year-old male who survived 3 years following a TBI sustained by a fall and corresponding 40x scanned image (f). Scale Bar = 100µm, scale bar = 10µm (high magnification).

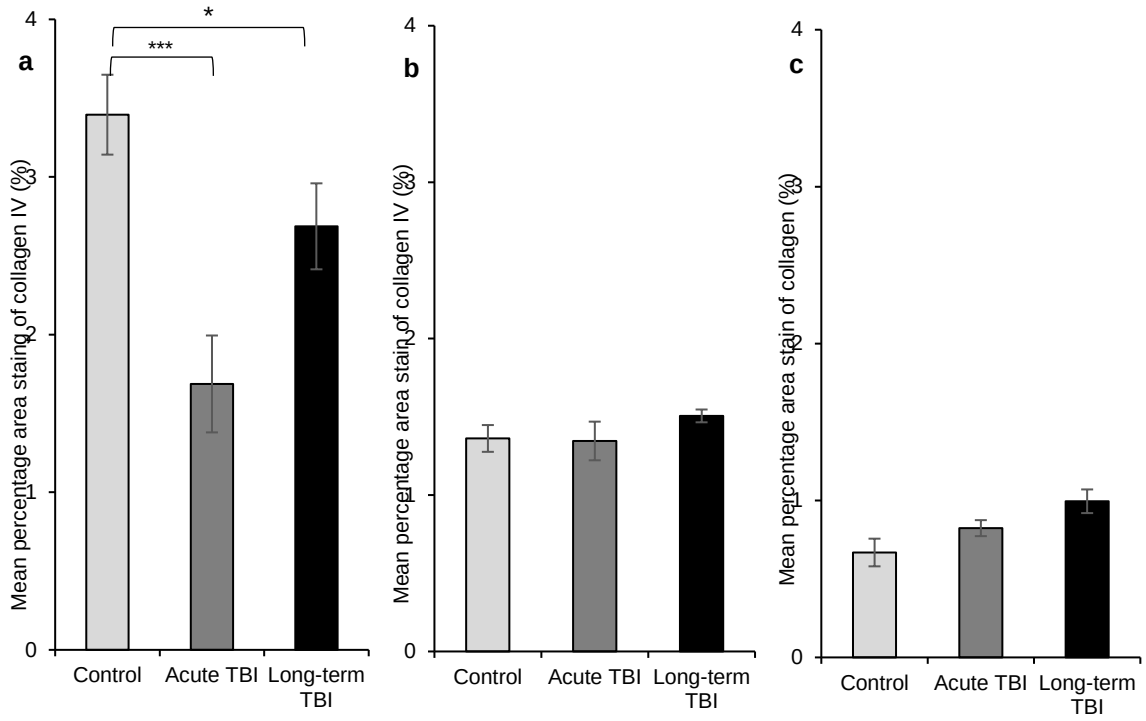

Figure 5-8 Regional distribution of collagen IV immunoreactivity in varying survivals after TBI compared with controls (a) where a decrease in collagen IV immunoreactivity was observed in the cingulate gyrus in the acute TBI group compared with controls and in the long-term TBI cohort compared with uninjured controls (b) No difference in collagen IV immunoreactivity in the cingulate Sulcus after TBI and a similar pattern was observed in the (c) Corpus callosum (* $p < 0.05$; *** $p < 0.0001$; Student's *t*-test; TBI cohort vs control mean)

No association could be demonstrated between collagen IV immunoreactivity and fibrinogen immunoreactivity. In the cingulate gyrus of the acute TBI cohort the mean percentage staining for collagen IV was 2.05% ± 0.11 in cases with minimal fibrinogen immunoreactivity; in cases with high fibrinogen immunoreactivity this was 1.45% ± 0.50 ($p = 0.416$; Student's *t*-test; Cohen's $d = 0.55$) (Figure 5-9). A similar pattern was observed in the long-term TBI cohort where cases with minimal fibrinogen immunoreactivity had a collagen IV percentage staining of 2.39% ± 0.27% and in cases with high fibrinogen immunoreactivity this was 3.22% ± 0.3% ($p = 0.057$; Student's *t*-test; Cohen's $d = 0.96$) (Figure 5-9). The cingulate sulcus demonstrated a similar pattern and distribution as the cingulate gyrus (Figure 5-9).

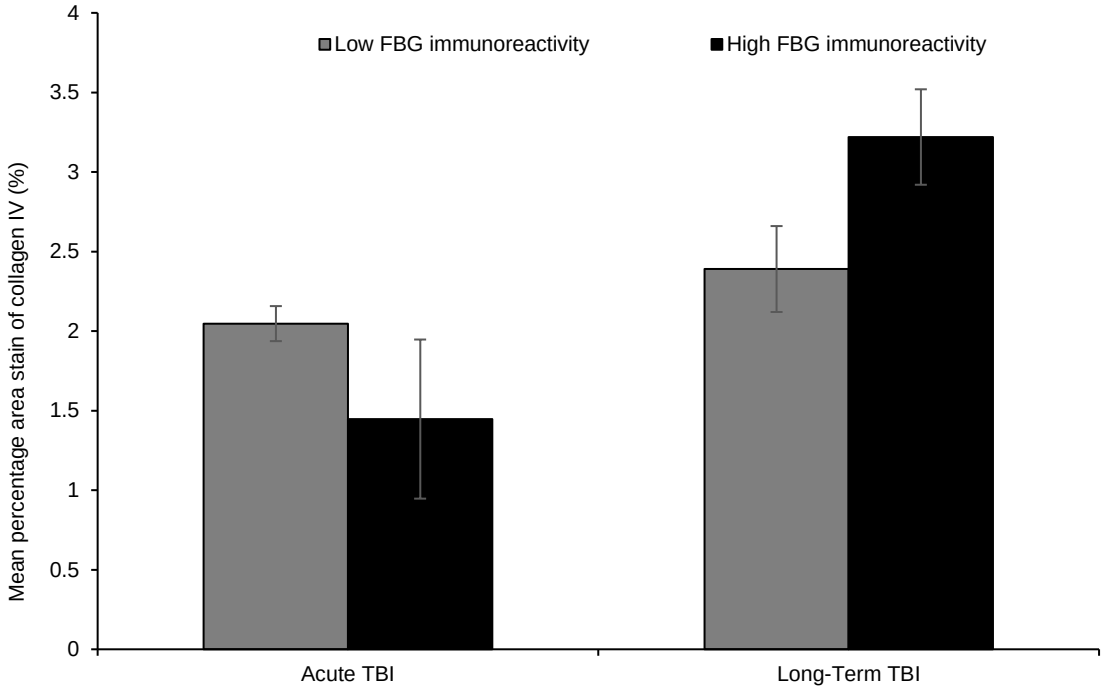

Figure 5-9 Association with collagen IV immunoreactivity and abnormal FBG immunoreactivity following TBI in varying survivals. Where no association could be made between collagen IV immunoreactivity and the presence or absence of abnormal FBG immunoreactivity in varying survivals following TBI (NS).

As described previously, the pattern and distribution of fibrinogen immunoreactivity demonstrated a preference of disruption towards the deeper layers of the cortex. In the cingulate gyrus of acute TBI cases with minimal fibrinogen immunoreactivity the percentage staining of collagen IV in the superficial, mid and deep layers of the cingulate gyrus was 1.94%, 2.06% and 2.14% respectively. Those cases with high fibrinogen immunoreactivity in the acute TBI cohort demonstrated a percentage staining of 0.99%, 1.57% and 1.78% for collagen IV in the superficial, mid and deep layers respectively (Table 7**,** Figure 5-10). Similarly, the long-term TBI group showed no difference between layers. The mean percentage staining of collagen IV in cases with minimal fibrinogen immunoreactivity 1.57%, 2.30% and 2.28% in the superficial, mid and deep layers respectively. In cases with high fibrinogen immunoreactivity the percentage staining of collagen IV was 2.95%, 3.24% and 3.55% in the cortical layers (Table 7**,** Figure 5-10)**.** A similar pattern was observed in the cingulate sulcus with no difference between groups.

Table 7 Mean percentage stain of Collagen IV within cortical layers split by FBG immunoreactivity

	Acute TBI				Long-term TBI			
Cortical Layers	**Low FBG immunoreactivity**	**High FBG immunoreactivity**	**p**	**d**	**Low FBG immunoreactivity**	**High FBG immunoreactivity**	**p**	**d**
Superficial (Layers 1-2)	1.94% ± 0.33%	0.99% ± 0.79%	*0.36*	*0.9*	1.57% ± 0.66%	2.95% ± 0.65%	*0.20*	*1.13*
Mid layers (3-4)	2.06 % ± 0.11%	1.57% ± 0.89%	*0.63*	*0.45*	2.3% ± 0.81%	3.25% ± 0.41%	*0.38*	*0.85*
Deep Layers (5-6)	2.14 % ± 0.18%	1.78% ± 1.2%	*0.79*	*0.24*	2.28% ± 0.58%	3.55% ±0.49%	*0.22*	*1.5*

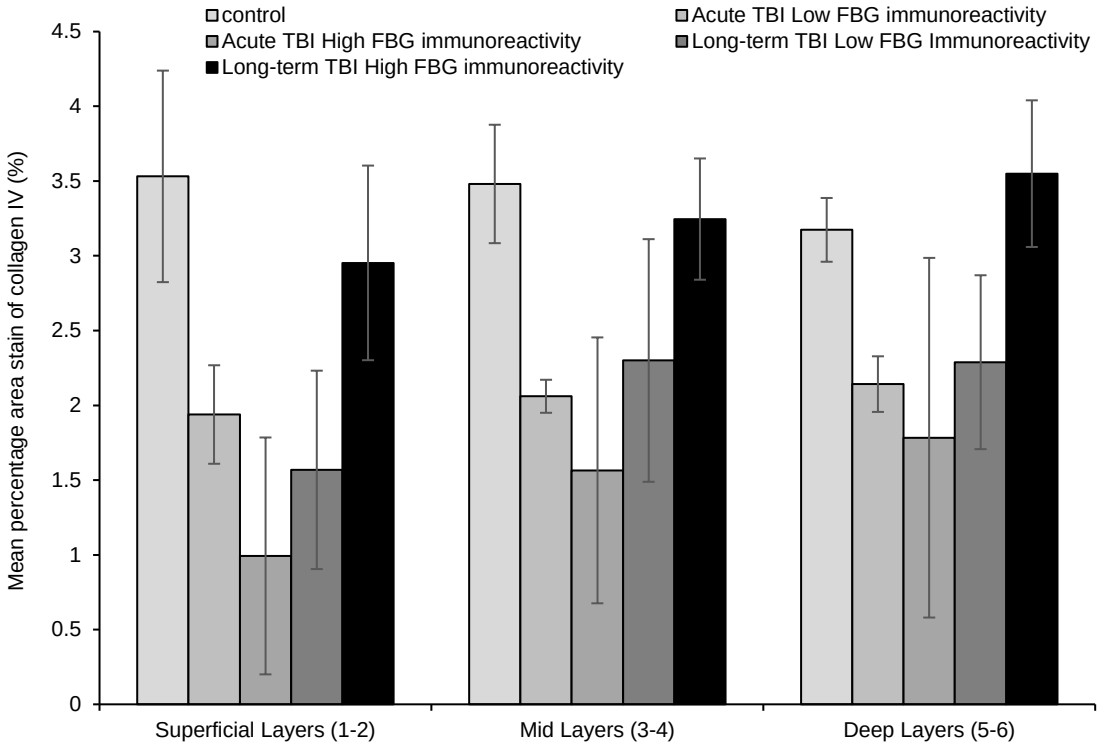

Figure 5-10 Neocortical distribution of collagen immunoreactivity after TBI in the presence and absence of abnormal FBG immunoreactivity. Where the pattern and distribution of collagen IV immunoreactivity is observed to be similar throughout the neocortical layers for all groups with a noted decreased in collagen IV immunoreactivity in the acute TBI with abnormal FBG immunoreactivity in the superficial layer which steadily increases through the cortex to the deep layer (NS).

5.4 Discussion

The aim of this study was to identify changes in cortical thickness and vascularity following a single, moderate to severe to TBI and their association with evidence of BBB disruption. Cortical thickness and vessel density and collagenisation were assessed following TBI. No changes were observed in cortical thickness or in vessel density following TBI in the acute phase or chronic phase when compared with uninjured controls. However, in this small cohort, a change was reported in collagen deposition in the acute phase following TBI. The acute phase TBI cases demonstrated a lower percentage area stain of collagen IV in the cingulate gyrus compared with controls.

Cerebral atrophy has been reported in AD patients where it has been demonstrated using volumetric MRI techniques (Mungas et al., 2002, Im et al., 2008). In AD, this cortical atrophy correlates to cognitive decline (20) and it may also occur prior to onset of dementia (21). From previous literature, varying degrees of cortical thinning are observed across a number of brain regions in AD such as frontal, temporal and medial occipital lobes (Im et al., 2008). Where overall increased rates of whole-brain atrophy following various dementias are similar, analysis of regional atrophy demonstrates differences between dementias such as AD and FTLD (Chan et al., 2001).

Following TBI in humans, cortical atrophy has been previously demonstrated using imaging techniques. One study demonstrated that atrophy after mild to moderate TBI injury was present and it was associated with the severity of injury where a TBI with a loss of consciousness resulted in a greater loss of brain volume (MacKenzie et al., 2002, Wang et al., 2015a, Bergeson et al., 2004). Diffuse white matter atrophy following TBI has previously been reported in both imaging studies (Gale et al., 2005, Levine et al., 2008) and in an autopsy study (Johnson et al., 2013a), however, grey matter atrophy has only been described in imaging studies. Both regional grey matter atrophy affecting the frontotemporal and limbic cortex has been demonstrated following TBI (Gale et al., 2005, Levine et al., 2008) as has significant global cortical atrophy following paediatric TBI (Merkley et al., 2008); all reported by imaging techniques. Conversely, in this current autopsy study, no noted differences between TBI (both in acute phase and chronic phase) and controls were observed. The cohort numbers in this present study were small and from only one region of interest, the cingulate gyrus; therefore, multiple brain regions may need to be assessed in TBI patients identify any regional changes.

To date, there is conflicting data in reporting the changes of vascular density in AD patients. In some autopsy studies a decrease in vessel density in AD is reported (Fischer et al., 1990, Buee et al., 1994); however, others suggest an increase in mean vessel density in AD (Viggars et al., 2011). Cerebral atrophy can often be observed in AD brains, therefore this may distort the vessel density numbers due to a smaller surface area containing similar numbers of vessels; resulting in conflicting data if not analysed to take into account the presence of atrophy (Farkas and Luiten, 2001). Following TBI, reports on changes in vessel density are contradictory. A CCI rodent model reported a decrease in the number of vessel junctions and vessel length (Obenaus et al., 2017). Hayward *et al.* demonstrated alterations in vessel density using a lateral fluid-percussion TBI model where vessel density was assessed by staining of rat endothelial cell antigen-1 (RECA-1) (Hayward et al., 2010, Hayward et al., 2011). Regional changes were reported with an increase in vessel density in the perilesional cortex, and in the ipsilateral thalamus, however no change was reported in the hippocampus (Hayward et al., 2010). In another fluid percussion rodent model, Park *et al.*, reported a global reduction in vessel density where it resolved 2 weeks post-injury in the less severe TBI cohort (Eugene et al., 2008).

A computational model of blast injury investigated the impact on the cerebral vasculature in humans (Hua et al., 2015). It reported that where the maximum strain on the brain model increased, as did the vasculature density (Hua et al., 2015). Using a scanning electron microscope, Rodriguez-Baeza *et al.,* investigated the brain of 10 TBI patients and reported morphological alterations in the microvessels comprising of longitudinal folds, sunken surfaces with craters and a significant flattening with reduction of vessel lumen (Rodriguez-Baeza et al., 2003). This present work is the first autopsy study to investigate vascular density following TBI. Although no noted changes in vascular density were reported between uninjured controls and TBI cases, there was a trend towards an increase in vascular density in the acute TBI cohort compared with age-matched non-demented controls. Both acute and chronic phase TBI cases which demonstrated an increase in BBB disruption where shown to have a slight increase in vessel density compared TBI cases without BBB disruption. Although this was an interesting observation it was not significant.

In AD, a thickening of the basement membrane due to increased collagen deposits has been previously reported (Hardy et al., 1986, Mancardi et al., 1980, Vinters et al., 1994, Kalaria and Pax, 1995, Viggars et al., 2011). Using laser-induced fluorescence spectroscopy on isolated vessels of AD patients and controls, Christov *et al.,* demonstrated significantly higher reflecting levels of collagen (Christov et al., 2008). By carrying out a western blot

analysis they reported elevated levels of type I and type II collagen; however, a reduction in collagen VI subtype was noted. Cheng *et al*, observed an increase in the subtype collagen VI and suggested this increase is a neuroprotective response and may protect neurons against Aβ toxicity by blocking the interactions of $A\beta_{42}$ oligomers and neurons(Cheng et al., 2009).

Following TBI, the evidence of changes in collagen is limited in animal studies. In one study, abnormal visualisation of collagen IV following rodent blast TBI, suggesting a selective increase of collagen which indicates a reorganisation of the vascular extracellular matrix with generation of new vessels (Gama Sosa et al., 2014). In contrast, a fluid percussion rodent TBI model demonstrated a reduction in collagen IV 24 hours after injury; however, no reduction was observed 12 hrs after injury (54). This current study demonstrates a reduction in collagen deposits following a single, moderate to severe TBI, noted in the acute TBI phase that persists into the chronic phase. The distribution of this observation was noted in the cingulate gyrus and was absent in the cingulate sulcus and corpus callosum. However, numbers are small and this observation warrants further investigation. Disruption of the BBB has been previously reported to prevail in the deep layers of the cortex and is notably absent in the depths of the sulci and white matter regions (Chapter 3) (Hay et al., 2015) – indicating that a decrease of collagen IV follows a similar pattern to BBB disruption. Collagen IV is essential for basement membrane stability which is the structural basis of the BBB (Poschl et al., 2004). Therefore, this observation is intriguing and may indicate vessels undergo a change in collagen IV which could lead to vessel vulnerability following TBI; this could predispose vessels to further injury and associated BBB disruption.

Previously, this thesis identified vascular changes following TBI (Chapter 3; 18), where after a single, moderate or severe TBI there is evidence of widespread BBB disruption in a proportion of cases in the acute and chronic phases. However, the structural basis for this acute and persistent BBB disruption following TBI is unknown. It has been suggested that collagen IV is essential for the stability of the basement membrane (Poschl et al., 2004), a key component of the BBB. Following a subarachnoid haemorrhage in rats, Scholler *et al.*, reported both collagen IV degradation and BBB disruption, by albumin extravasation, following SAH (Scholler et al., 2007). Therefore, a marked decrease in collagen IV as seen in this present study may indicate weakening of the BBB early in the pathogenesis of TBI.

It has been suggested that following TBI the brain undergoes neovascularization, the formation of new vessels. Morgan *et al.*, characterised the angiogenic response in an acceleration impact model of TBI and reported a substantial increase in angiogenic growth

factor VEGF and noted the presence of newly formed vessels up to 48-hours post injury (Morgan et al., 2007). Up-regulation of VEGF following TBI has previously been reported and implicated as an important mediator for BBB disruption (Nag et al., 2002, Nag et al., 1997, Chodobski et al., 2003, Thau-Zuchman et al., 2010). Zhang *et al.*, reported that VEGF can markedly enhance angiogenesis in the ischemic brain of rats and that inhibition of VEGF may reduce BBB permeability (Zhang et al., 2000).

5.4.1 Conclusion

Although this study resulted in only one anomaly where a reduction in collagen IV staining was observed in the acute TBI phase persisting into the chronic TBI phase, it suggests that more investigations are warranted to understand the vascular changes following TBI. The reduction in collagen IV staining followed a similar pattern and distribution to BBB disruption with the noted reduction occurring in the deep layers of the gyri. This may suggest a decrease in BM stability in the acute phase following TBI and may contribute towards the persistent BBB disruption following TBI. No changes were observed in the cortical thickness and vessel density; however, numbers were small and focussed on one region; this may present an opportunity to increase numbers and regions to confirm these findings.

6 The glial response following traumatic brain injury

6.1 Introduction

Traumatic brain injury (TBI) is the strongest environmental risk factor for dementia (Molgaard et al., 1990, Mortimer et al., 1985, Mortimer et al., 1991, Graves et al., 1990, O'Meara et al., 1997, Salib and Hillier, 1997, Guo et al., 2000, Schofield et al., 1997, Plassman et al., 2000, Fleminger et al., 2003). Complex neurodegenerative pathologies associated with dementia have been recognised in TBI, such as abnormal accumulations of tau and amyloid β (Aβ), axonal degeneration, neuroinflammation, degradation of white matter and neuronal loss. Reactive glial cells are present in many neurodegenerative diseases, such as Alzheimer's disease, Parkinson's disease, amyotrophic lateral sclerosis (ALS) and Huntington's disease (Miller et al., 2004, Nagele et al., 2004, Hirsch et al., 1998, Lobsiger and Cleveland, 2007, Hirsch et al., 2003); this reactive cellular response has also been identified in TBI tissue in limited studies. In late TBI, a microglial response has been observed (Johnson et al., 2013a), while in CTE tau immunoreactive astrocytes have been identified (McKee et al., 2009, Stein et al., 2014) and in blast TBI, reactive astrocytes have been recognised (Shively et al., 2016). However, the pattern, distribution and temporal dynamics of this cellular response to a single TBI is uncertain.

6.1.1 Astrocytic Response following TBI

Both activated microglia and reactive astrogliosis are heterogeneous in nature with neuroprotective and detrimental effects in the CNS (Laird et al., 2008, Sirko et al., 2015, Bardehle et al., 2013, Myer et al., 2006). Following TBI, astrocytes are important early responders, which precedes the microglial response (Kim and Dustin, 2006), with adenosine triphosphate (ATP) released from injured astrocytic networks guiding the microglial population to site of focal injury (Kim and Dustin, 2006, Davalos et al., 2005, Rouach et al., 2002, Stout et al., 2002, Verderio and Matteoli, 2001). This astrocytic reaction to TBI evokes a number of events including rapid influx of extracellular calcium, sodium release of matrix metalloproteinase-9, secretion of vasoactive molecules and ATP (Hekmatpanah and Hekmatpanah) release (Hoffman et al., 2000, Ostrow et al., 2011, Ahmed et al., 2000). Animal models of TBI have demonstrated that astrocytes exhibit membrane instability and cytoskeleton disassembly (Cullen et al., 2011). Following mild rTBI in transgenic mice, an acute reactive astrogliosis has been reported (Petraglia et al., 2014a, Ojo et al., 2013,

Petraglia et al., 2014b) while in clinical studies investigating head injury in boxers, glial fibrillary acidic protein (GFAP) (an astrocyte structural protein) is used as a biomarker for injury (Neselius et al., 2012, Zetterberg et al., 2006, Zetterberg et al., 2013a).

A limited post-mortem case series examining blast related injuries reported prominent astroglial scarring and reactive astrogliosis in grey–white matter interfaces and subpial glial plate in all chronic blast exposure cases (up to 9 years survival)(Shively et al., 2016). However, they did not find the same pattern in sTBI, although these numbers were limited. In wider studies, astrocytic p-tau pathology in CTE is proposed to be topographically distinct from wider tauopathies, including aging-related tau astrogliopathy (ARTAG) (Lopez-Gonzalez et al., 2013, Lace et al., 2012). Nevertheless, to date, there remains limited work exploring the astrocytic response following TBI, especially sTBI.

6.1.2 Microglial response following TBI

Immediately following injury, TBI induces a complex neuroinflammatory response in both humans and animal models, associated with an acute-phase inflammatory cell reaction featuring polymorphonuclear leukocytes, T lymphocytes, macrophages, and natural killer cells, together with activation of resident microglia (Johnson et al., 2013a, Loane and Byrnes, 2010). Microglia undergo morphological and expressive alterations which contribute to the post-TBI inflammatory pathways (Aihara et al., 1995, Gentleman et al., 2004, Nagamoto-Combs et al., 2007, Wilson et al., 2004, Loane and Byrnes, 2010, Ziebell and Morganti-Kossmann, 2010). Morphological changes can range from ramified, 'resting' state microglia through to activated, amoeboid microglia (Walker et al., 2014). Chronic neuroinflammation has been demonstrated in limited autopsy (Gentleman et al., 2004, Johnson et al., 2013a) and imaging studies, which indicate increased and prolonged microglia activity with long-term survival up to 18 years post-injury (Gentleman et al., 2004, Ramlackhansingh et al., 2011b, Johnson et al., 2013a). Although there is some discordance in autopsy and imaging studies, with persistent microglial activation post-TBI is described as predominantly a white matter pathology in autopsy studies (Johnson et al., 2013a), while imaging studies report a predominantly grey matter pathology, specifically located to the thalamic region (Ramlackhansingh et al., 2011b). In this study, material from the Glasgow TBI Archive will be used to characterise the pattern and distribution of astrogliosis and microgliosis following exposure to single moderate or severe TBI.

Hypothesis: Reactive astrogliosis is present following TBI observed by an increase in GFAP staining at the grey–white matter interfaces and subpial glial plate, with a chronic microglial response localised to white matter.

6.2 Specific Methods and Materials

6.2.1 Case selection and tissue preparation

All brain tissue was obtained from the Glasgow TBI Archive of the Department of Neuropathology, Queen Elizabeth University Hospital, Glasgow, UK. Tissue samples were acquired at routine diagnostic autopsy, with approval for their use in research obtained from the Greater Glasgow and Clyde Biorepository Governance Committee.

Material from patients aged under 60 years at time of death with a history of a single, moderate or severe TBI was selected as acute TBI cases (survival < 14 days from TBI; n = 27) or long-term TBI cases (survival >1 year from TBI; n = 32). Autopsy reports and, where necessary, clinical and forensic records were available for all cases to confirm a history of moderate or severe TBI on presentation as defined by the Glasgow Coma Scale. Uninjured, age-matched controls with no known history of TBI or neurological disease were selected for comparison (n = 21). Demographic and clinical data and detail on neuropathology findings at the original autopsy for each cohort are presented in Table 8.

At the time of the original diagnostic autopsy, whole brains were immersion fixed in 10% formal saline for a minimum of 3 weeks, following which the specimens were examined, sampled using standardized techniques and processed to paraffin tissue blocks. For this study, blocks from a coronal slice of the cerebral hemispheres at mid-thalamic level were selected to include the thalamus, with adjacent internal capsule, and corpus callosum, with adjacent cingulate and superior frontal gyri. From these tissue blocks 8μm sections were prepared for immunohistochemistry procedures.

Table 8 Demographic and clinical information of all groups

		TBI: Acute Survival (n = 27)	TBI: Long-Term Survival (n = 32)	Controls (n = 21)
Mean age (Range)		44.4 years (9-60)	46.3 years (19-60)	39.9 years (14-60)
Males		17 (63%)	31 (96.9%)	13 (62%)
Mean PM Delay (Range)		56.1 hours (3-240)	65.5 hours (9-184.5)	71.6 hours (12-144)
Mean Survival Interval (Range)		69.3 hours (6-216)	7.8 years (1-47)	Not applicable
Cause of TBI	Fall	15 (55.5%)	15 (46.9%)	Not applicable (No history of TBI)
	RTA	7 (25.9%)	5 (15.60%)	
	Assault	4 (14.8%)	8 (25%)	
	Unknown	1 (3.7%)	4 (12.5%)	
Cause of Death	Head injury	25(92.6%)	0	0
	Bronchopneumonia	2(7.4%)	7(21.9%)	1(4.8%)
	ARDS	0	1(3.125%)	0
	Pulmonary thromboembolism	0	0	0
	Heart disease	0	6 (18.8%)	4(16.67%)
	Alcohol related	0	2(6.25%)	0
	Pyelonephritis	0	1(3.125%)	0
	Multi-organ failure	0	1(3.125%)	0
	GIT haemorrhage	0	1(3.125%)	0
	Polytrauma	0	1(3.125%)	0
	Drug overdose	0	0	4(16.67%)
	SUDEP	0	7(21.9%)	8(38.1%)
	Pulmonary oedema	0	1(3.125%)	0
	Septicaemia	0	0	2(8.3%)
	Inhalation of gastric contents	0	0	2(8.3%)
	Unknown	0	4(12.5%)	0

Key: *TBI = traumatic brain injury; SUDEP = sudden unexpected death in epilepsy; GIT = gastrointestinal tract; ARDS= acute respiratory distress syndrome; RTA = road traffic accident*

6.2.2 Routine Histology

Sections from all tissue blocks were stained with haematoxylin and eosin. Following standard dewaxing and rehydration to water, the sections were immersed in haematoxylin for 10 minutes (Mayer, Leica Microsystems, Wetzlar, Germany). Slides were rinsed in water followed by immersion in Scott's tap water substitute (Leica Microsystems, Wetzlar, Germany) and differentiation in 1% acid alcohol. Following rinsing in water the sections were immersed in 25% aqueous eosin Y solution (TCS Biosciences, Buckingham, UK) for 5 minutes and then the sections were rinsed, dehydrated in graded alcohol, cleared and coverslipped.

6.2.3 Immunohistochemistry

Following deparaffinization and rehydration, endogenous peroxidase was quenched via immersion of the sections in 3% aqueous H202 for 15 minutes. Thereafter, heat induced antigen retrieval was performed using microwave pressure cooker for 8 minutes in preheated 0.1M Tris EDTA buffer (pH 8), followed by blocking in 50µl of normal horse serum (Vector Labs, Burlingame, CA, USA) per 5 mL of Optimax buffer (BioGenex, San Ramon, CA, USA) for 30 minutes. The sections were then incubated in primary antibody at 4oC for 20 hours prior to washing and application of biotinylated secondary antibody for 30 minutes, followed by an avidin-biotin complex as per manufacturer's instructions (Vector Labs, Burlingame, CA, USA). Visualisation of the target antigen was achieved by applying the DAB peroxidase substrate kit (Vector Labs, Burlingame, CA, USA), with the sections then counterstained with haematoxylin.

Primary antibodies were selected to reveal: glial fibrillary acidic protein (GFAP) expressed by astrocytes (monoclonal anti-GFAP; clone GA5, 1:250; Leica Biosystems, Milton Keynes, UK), human HLA-DP,DQ,DR (monoclonal anti-CR3/43; 1:800; Dako, Carpinteria, USA) and ionized calcium binding adaptor molecule 1 (Iba-1) expressed in activated microglia (rabbit polyclonal anti-Iba-1; 1:5000; Wako, Japan). Control sections (positive and negative) for each antibody were run in parallel with the test sections to confirm antibody specificity.

Sections were viewed using a Leica DMRB light microscope (Leica Microsystems, Wetzlar, Germany). In addition, for quantitative studies, sections were scanned at 20x using a Hamamatsu Nanozoomer 2.0-HT slide scanner, with the images viewed via the SlidePath Digital Image Hub application (Leica Microsystems, Wetzlar, Germany). The images in this chapter have been digitally captured at 4x (2.3µm per pixel) and 20x (0.46µm per pixel).

6.2.4 Analysis of immunohistochemistry

All sections were reviewed and analysed blind to demographic and clinical data. Analyses were performed in multiple anatomical regions within each block. Specifically, within the callosal block analyses were performed in corpus callosum, crest of cingulate gyrus, depth of cingulate sulcus and subcortical white matter of the cingulate gyrus. In the thalamic block, analyses were performed in the internal capsule and thalamic grey matter.

6.2.4.1 Astrogliosis

In sections stained for GFAP, the extent of the interface astrogliosis was measured, using the measuring tool of the SlidePath Digital Image Hub application, at the superficial glial limitans and the boundary between neocortical grey and immediate subcortical white matter (Figure 6-1a). This was carried out at the crest of the cingulate gyrus and adjacent depth of the cingulate sulcus. The extent of subependymal interface astrogliosis associated with the lateral ventricle was assessed in sections of the thalamus (Figure 6-1b). Multiple measurements were performed for each region in each tissue section, with the largest measure taken as the datapoint for that section.

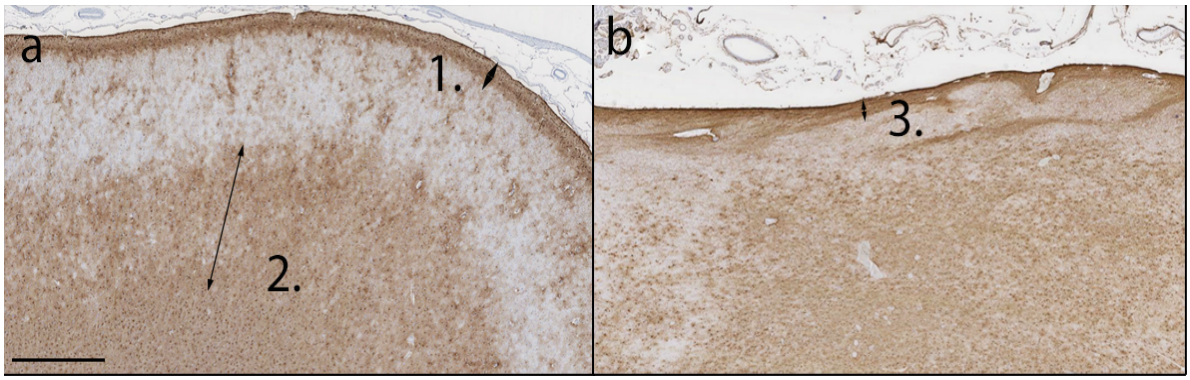

Figure 6-1 Representative measurements of GFAP-immunoreactivity (a) Extent of interface astrogliosis was measured at the superficial glial limitans (SGL) (1) and at the boundary between neocortical grey and immediate subcortical white matter (WMI) (2) in the cingulate gyrus region. (b) Extent of astrogliosis was measured at the subependymal interface associated with the lateral ventricle in the thalamic region (3). Scale bar = 1mm.

Assessment of astroglial extent for each anatomical region was calculated as percentage area of immunostain. Using SlidePath Digital Image Hub software, a 1mm x 1mm square was randomly placed over multiple regions of interest (ROIs) in both grey matter and white matter of the GFAP stained sections. Images of these ROIs were then captured and exported to ImageJ (NIH, Bethesda, MD) where the background was subtracted, and the Colour Deconvolution plugin applied using the installed haematoxylin/ DAB vector (H DAB) to produce separate colour channels for the counterstain (haematoxylin) and specific

immunostaining (DAB). The DAB-specific image was then thresholded and the percentage of positive staining in the ROI calculated using standard algorithms in ImageJ (Figure 6-2).

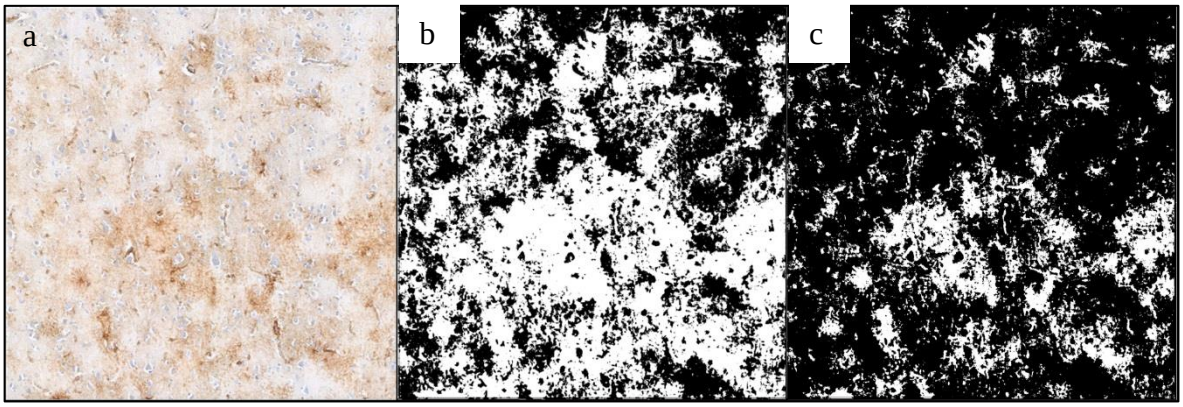

Figure 6-2 Example of Thresholding GFAP using image j (a) original image of GFAP staining in cortex (1mm x 1mm square) (b) raw thresholded image of (a) before adjustment and (c) raw thresholded image of (a) after manual adjustment

6.2.4.2 Microgliosis

Assessments of microglial extent and activation state were performed in sections stained for Iba-1 and CR3/43. Multiple anatomical regions of white matter (corpus callosum, internal capsule and the subcortical region of the cingulate gyrus) and grey matter (cingulate gyrus, cingulate sulcus, superior frontal gyrus and thalamic regions were assessed. For each region, extent of microglial staining was calculated as percentage area of immunostain using the same methodology employed to calculate extent of GFAP immunostaining.

In addition to a quantitative assessment microglial staining, standardized semi-quantitative scores of microglial morphologies were recorded for each region to assess microglial activation state as described previously (Johnson et al., 2013b). Specifically, regions were assessed and reported as either displaying a predominance of cells with amoeboid morphology (A), ramified morphology (R) or mixed amoeboid/ramified morphology (M) (Figure 6-3).

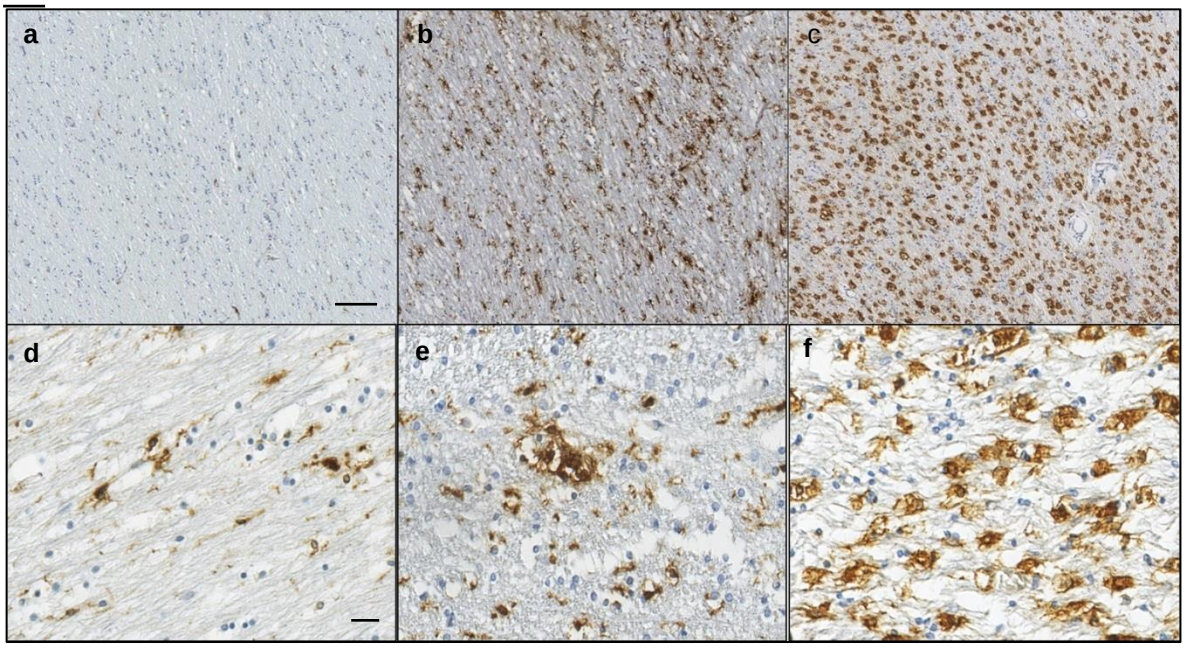

Figure 6-3 Examples of microglia morphology Where (a and d) indicate sparse microglia with fine cell processes (ramified) and (b and e) clusters of activated microglia with shortened processes and (c and f) extensive and densely packed amoeboid microglia displaying minimal or no processes and enlarged cell bodiesFigure 6-3 Scale bar = 100µm (top row) and scale bar = 10µm (bottom row).

6.2.5 Statistical analysis

All data were analysed using SPSS (version 22; IBM, Inc). The $\chi 2$ test and Student's *t*-test were used to assess differences in data between and within cohorts, where appropriate. Cohen's *d* and Cramer's V were used to determine the effect size and to indicate the standardised difference between two means. A Cramer's V value of 0.1 suggested a low practical significance, a value of 0.3 suggested a moderate practical significance and a value of 0.5 suggested a high practical significance. While a Cohen's *d* value of 0.2 suggested a low practical significance, a value of 0.5 suggested a moderate practical significance and a value of 0.8 suggested a high practical significance. All effects were considered statistically significant when $p \leq 0.05$. Measurements results are displayed as means with ± standard error of the mean.

6.3 Results

6.3.1 TBI precipitates an acute, persisting and stereotypical interface astrogliosis

Staining for GFAP in control, uninjured material showed typical pattern staining. Specifically, in the neocortex GFAP-immunoreactive astrocytic profiles with fine and widely ramifying cellular processes were distributed in low density throughout the cortex, with notable concentrations in stereotypical distributions as a thin superficial glial limitans immediately beneath the pia. In addition, astrocytes were localised around occasional penetrating cortical vessels and as a narrow and interrupted border at the interface between neocortical grey matter and underlying subcortical white matter (Figure 6-4a). Within the thalamus, GFAP-immunoreactive astrocytes were again encountered in low density, typically represented by small immunoreactive profiles with fine, ramifying cytoplasmic processes (Figure 6-4b). As in neocortical material, focal concentrations of GFAP-immunoreactive profiles were noted at interface zones around intrathalamic vessels and subependymally. Similarly, sparse astrocytic profiles with fine, widely ramifying cellular processes were typical of the multiple white matter regions assessed.

In contrast to the localised and limited GFAP-immunoreactivity observed in uninjured controls, material from patients dying acutely (survival <14 days) after single, moderate or severe TBI exposure showed increased GFAP-immunoreactivity in a striking and stereotypical pattern and distribution, with immunoreactive astrocytes showing morphological features of astroglial activation within hours of injury (Figure 6-4c and d). Specifically, there was increased percentage area of staining for GFAP in the neocortex of the crests of the cingulate and superficial frontal gyri and in the thalamus when compared to uninjured controls. In contrast, there was no demonstrable change in area of GFAP-immunoreactivity in the neocortex of the depths of the cingulate sulcus or in any white matter region examined (Table 9). Thus, in the deeper cortical layers of the cingulate gyrus, there was a trend of increasing area of GFAP-immunoreactivity in acute TBI cases compared to controls (41% ± 5.2% vs 30% ± 3.8 % respectively; $p = 0.094$; Student's *t*-test; Cohen's $d = 0.61$). While in the equivalent region at the depths of the cingulate sulcus there was no notable increase in immunoreactivity (19% ± 3.6 % vs 26 ± 3.2 % respectively; $p = 0.150$; Student's *t*-test; Cohen's $d = 0.49$).

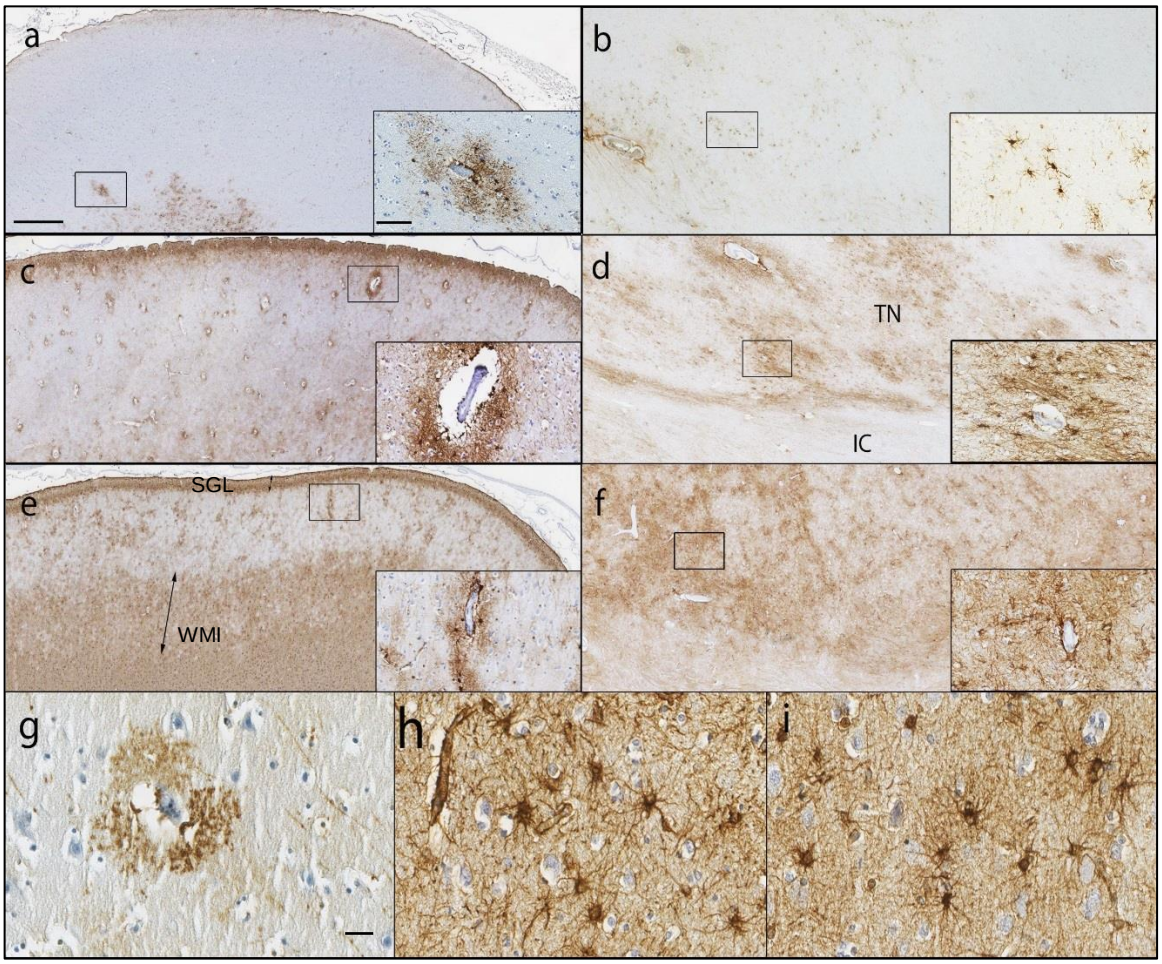

Figure 6-4 Representative images of GFAP-immunoreactivity after TBI and in uninjured controls Punctuated GFAP immunoreactivity observed around blood vessels, along SGL and sparsely populated in the grey matter regions in the cingulate gyrus, as expected (a) in a 33-year-old woman with no history of TBI. In addition, in the thalamic regions GFAP immunoreactivity was limited with a scattering of astrocytes observed throughout in a (b) 34-year-old woman with no history of TBI. However, following TBI, extensive and densely populated astrocytes are demonstrated around blood vessels and at the SGL with an increase of GFAP immunoreactivity observed in the grey matter regions of the cingulate gyrus of a (c) 16-year-old male TBI patient who survived 84 hours after an assault. Furthermore, increased activity of astrocytes are observed in the thalamic nuclei (TN) with limited activity observed in the internal capsule (IC) of a (d) 57-year-old male TBI patient who survived 15 hours after a fall. Extensive GFAP immunoreactivity extending from the WMI into the cortex (as defined by the arrows) and thickening of the SGL (as defined by the arrows), in addition to the densely packed perivascular astrocytes are observed in the cingulate gyrus of a (e) 51-year-old TBI patient who survived 3 years from an assault. Again, densely populated astrocytes are evidenced by an increase of GFAP immunoreactivity in the thalamic nuclei, in contrast to the pale, sparsely populated region of the IC (bottom of the picture) in a (f) 48-year-old male TBI patient who survived 3 years after a fall. (g) GFAP immunoreactivity around blood vessels in the cingulate gyrus of a 33-year-old female with no history of TBI (h) extensive and densely populated astrocytes in the cingulate gyrus of a 60-year-old male TBI patient who died 8 days following a fall of TBI (i) again, increased activity of GFAP immunoreactivity in the cingulate gyrus of a 51-year-old male TBI patient who survived 3 years following an assault. Scale bar = 1mm (low magnification), scale bar = 100µm (high magnification), scale bar = 10µm (g, h and i).

Table 9 Percentage area staining of GFAP immunoreactivity in the cingulate sulcus and white matter regions.

	Cingulate Sulcus	p	d	Subcortical	p	d	Corpus callosum	p	d	Internal Capsule	p	d
Control	25.87% ± 3.19%			7.93% ± 1.25%			6.78% ± 1.35%			8.54% ± 1.21%		
Acute TBI	18.72% ± 3.64%	*0.15*	*0.49*	8.88% ± 0.94%	*0.54*	0.2	7.05% ± 0.78%	*0.86*	*0.06*	9.49% ± 1.08%	*0. 54*	*0.18*
Long-term TBI	24.22% ± 4.71%	*0.78*	*0.09*	9.75% ± 1.08%	*0.28*	0.35	8.08% ± 0.96%	*0.42*	*0.25*	10.04% ± 0.73%	*0. 26*	*0.32*

As in controls, GFAP-immunostain was concentrated at stereotypical structural interface regions: - around parenchymal vessels; at the SGL and grey/white boundary of the neocortex; and in the subependymal zone of the thalamus. Notably, however, there was evidence of expansion of these astroglial interface zones at multiple locations, with expansion of the SGL and WMI at the crests of the cingulate and superficial frontal gyri and extending along penetrating cortical vessels as a widened perivascular astrocytic cuff (Figure 6-5). Further, there was expansion of the subependymal astrocytic zone (SEZ) in acute TBI cases, which almost doubled from 66.6µm ± 15.5µm in controls to 118.7µm ± 17.03µm in acute TBI cases ($p = 0.032$; Student's *t*-test; Cohen's $d = 0.72$) (Figure 6-5).

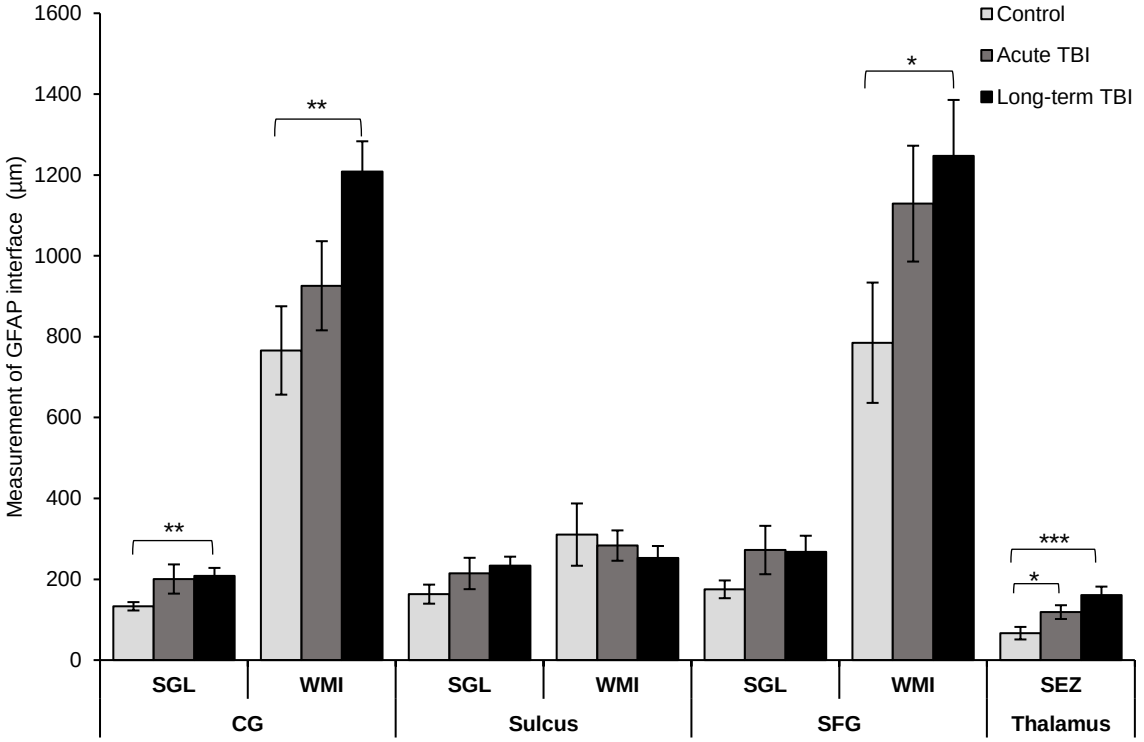

Figure 6-5 Regional distribution of GFAP interface measurements following TBI versus controls In both acute and long-term TBI survivals there was evidence of an increased of astrogliosis in the WMI and SGL as defined by an increase of GFAP immunoreactivity in a higher proportion of TBI survivors than match, uninjured controls in material from the cingulate gyrus (CG), cingulate sulcus, superior frontal gyrus (SFG) and the thalamic subependymal zone (SEZ) (* p<0.01; ** p<0.001; *** p <0.0001; Student's *t*-test TBI vs control GFAP measurement).

This stereotypical grey matter astrogliosis with notable localization to interface zones observed in material from acute TBI survivors persisted and evolved in material from patients dying a year or more after injury (Figure 6-4e and f). Specifically, as in acute survivors there was increased percentage area stain of GFAP-immunoreactivity in the grey matter of the crests of the cingulate and superficial frontal gyri and in the thalamus in material from patients surviving a year or more from a single, moderate or severe TBI than in controls. Again, no notable increase in GFAP-immunoreactivity was demonstrated in the neocortex of the depths of the cingulate sulcus or in any white matter region assessed (Table 9). Thus, in the deeper layers of the cingulate gyrus in patients surviving a year or more from TBI percentage area stain of GFAP was 43% ± 3.4 % compared with 30% ± 3.8 % in controls ($p = 0.012$; Student's *t*-test; Cohen's $d = 0.85$) while in the thalamic region percentage area stain of GFAP increased from 9.4% ± 1.5 % in controls to 14.4% ± 1 % in the late TBI survivors ($p = 0.009$; Student's *t*-test; Cohen's $d = 0.84$). As with acute TBI material, there was localization to the interface regions of the SGL, WMI, SEZ and perivascularly (Figure

6-4e and f). Thus, the SGL of the cingulate gyrus in late survivors of TBI was 208.5μm ± 19.5μm compared to just 133.1μm ± 101μm in controls ($p = 0.002$; Student's *t*-test; Cohen's $d = 0.94$) while the WMI rose from 765.9μm ± 115.99μm in controls to 1208.1μm ± 75.3μm in late TBI survivors ($p = 0.003$; Student's *t*-test; Cohen's $d = 1.01$) (Figure 6-5). Further, there was expansion of the SEZ in late survivors of TBI cases, from 66.6μm ± 15.5μm in controls to 161.1μm ± 20.7μm in long-term TBI cases ($p = 0.001$; Student's *t*-test; Cohen's $d = 1$) (Figure 6-5).

6.3.2 Association of astrogliosis with TBI-associated pathologies

Assessment of haematoxylin and eosin stained sections from both cingulate and thalamic regions confirmed the expected observations of astrogliosis association with a more widespread and diffuse pattern of distribution independent of focal injury. In material from acute TBI survivors, TBI-associated focal haemorrhagic lesions or contusions were observed across 13 of the 27 cases with nearly all (10 out of 13 cases) displaying extensive astrogliosis in the surrounding parenchyma. In 8 of 10 cases (80%), extensive astrogliosis was observed out with the region of focal pathology. Furthermore, diffuse hypoxic and ischemic injury was observed in 93% (25 of 27) of acute TBI cases where no correlation between these pathologies and astrogliosis could be identified. In material from patients surviving 1 year or more after injury there was evidence of old haemorrhages and contusions; demonstrating histologic features consistent with occurring at time of original TBI; in 8 of 32 cases with 12 lesions in total. Focal astrogliosis was observed in only 4 of the 12 lesions with all 8 cases displaying a more widespread diffuse astrogliosis throughout the regions. Of those long-term TBI cases that showed no evidence of focal haemorrhagic or contusional pathology (15 of 32 cases) there was evidence of diffuse astrogliosis in nearly half of cases (7 of 15 cases). Diffuse hypoxic and ischemic injury was observed in 22% (7 of 32 cases) of long-term TBI cases where no correlation between these pathologies and astrogliosis could be identified.

6.3.3 The microglial response is largely localized to white matter after TBI

In keeping with previous observations, in all grey and white matter regions examined staining for CR3/43 or Iba-1 in uninjured, control material revealed microglia showing a predominantly ramified, quiescent morphology, with just occasional cases demonstrating a mixed microglial morphology, and no cases with a predominantly activated, amoeboid

phenotype (

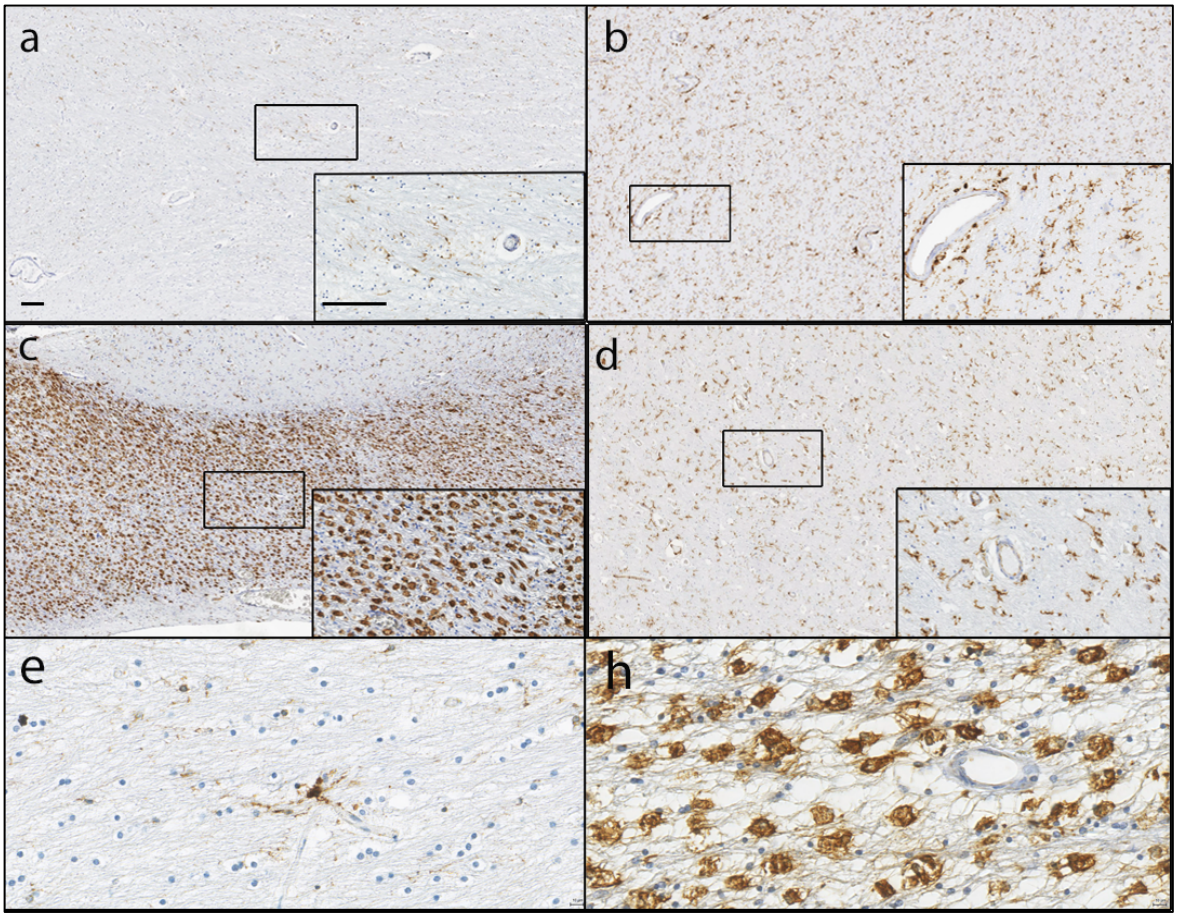

Figure 6-6a and b).

Survival of less than 14 days from a single, moderate or severe TBI resulted in no measurable increase in area staining for either CR3/43 or Iba-1 in any of the multiple white or grey matter regions assessed (Table 10**,** Table 11). However, in isolated white matter regions, namely subcortical white matter and internal capsule, there was evidence of microglial activation, with an increase in cases displaying activated microglial morphologies, predominantly as mixed microglial morphology, rarely as amoeboid (Figure 6-7). Thus, in subcortical white matter where only 2 of 19 controls showed an activated microglial morphology in staining for CR3/43 (mixed phenotype), in acute TBI activated microglia were present in 20 of 26 cases (18 mixed, 2 amoeboid) ($p = 0.0001$; $\chi 2$; Cramer's $V = 0.656$). Similarly, while in the internal capsule only 6 of 20 controls showed an activated microglial morphology (all mixed), this compared to 15 of 26 acute TBI cases with an activated phenotype (13 mixed, 2 amoeboid). In contrast to these findings in the internal capsule and subcortical white matter, no morphological evidence of increased microglial activation over controls was identified in the white matter of the corpus callosum or in multiple grey matter regions assessed. (Figure 6-7).

Table 10 Percentage area staining of Iba-1 and CR3/43 in grey matter regions

Iba-1 **Grey Matter**	**Cingulate Gyrus**	**p**	**d**	**Sulcus**	**p**	**d**	**Thalamus**	**p**	**d**
Control	6.93% ± 0.32%			6.31% ± 0.41%			7.08% ± 0.35%		
Acute	6.22% ± 0.37%	*0.29*	*0.47*	5.88% ± 0.38%	*0.444*	*0.26*	6.09% ± 0.41%	*0.078*	*0.64*
Long-term	6.52% ± 0.31%	*0.56*	*0.27*	5.53% ± 0.40%	*0.183*	*0.45*	6.24% ± 0.57%	*0.221*	*0.44*
CR3/34 Grey Matter	**Cingulate Gyrus**	**p**	**d**	**Sulcus**	**p**	**d**	**Thalamus**	**p**	**d**
Control	1.88% ± 0.54%			2.09% ± 0.47%			2.20% ± 0.48%		
Acute	3.1% ± 0.56%	*0.14*	*0.55*	2.94% ± 0.54%	*0.246*	*0.43*	2.00% ± 0.33%	*0.203*	*0.12*
Long-term	2.41% ± 0.27%	*0.39*	*0.3*	2.61% ± 0.28%	*0.348*	*0.35*	1.93% ± 0.32%	*0.647*	*0.17*

Table 11 Percentage area staining of Iba-1 and CR3/43 in white matter regions

Iba-1 White Matter	**Internal capsule**	**p**	**d**	**Corpus callosum**	**P**	**d**	**Subcortical**	**p**	**d**
Control	6.26% ± 0.36%			6.88% ± 0.47%			6.92% ± 0.46%		
Acute	5.55% ± 0.26%	*0.120*	*0.54*	6.00% ± 0.42%	*0.169*	*0.46*	5.73% ± 0.42%	*0.063*	*0.64*
Long-term	6.02% ± 0.43%	*0.662*	*0.15*	7.54% ± 0.37%	*0.282*	*0.32*	6.70% ± 0.30%	*0.689*	*0.13*
CR3/34 White Matter	**Internal capsule**	**p**	**d**	**Corpus callosum**	**p**	**d**	**Subcortical**	**p**	**d**
Control	6.72% ± 0.66%			3.82% ± 0.50%			4.47% ± 0.41%		
Acute	5.50% ± 0.60%	*0.183*	*0.48*	4.95% ± 0.44%	*0.104*	*0.59*	5.43% ± 0.47%	0.134	0.51
Long-term	6.92% ± 0.63%	*0.824*	*0.08*	5.29% ± 0.59%	*0.063*	*0.56*	5.73% ± 0.53%	0.070	0.58

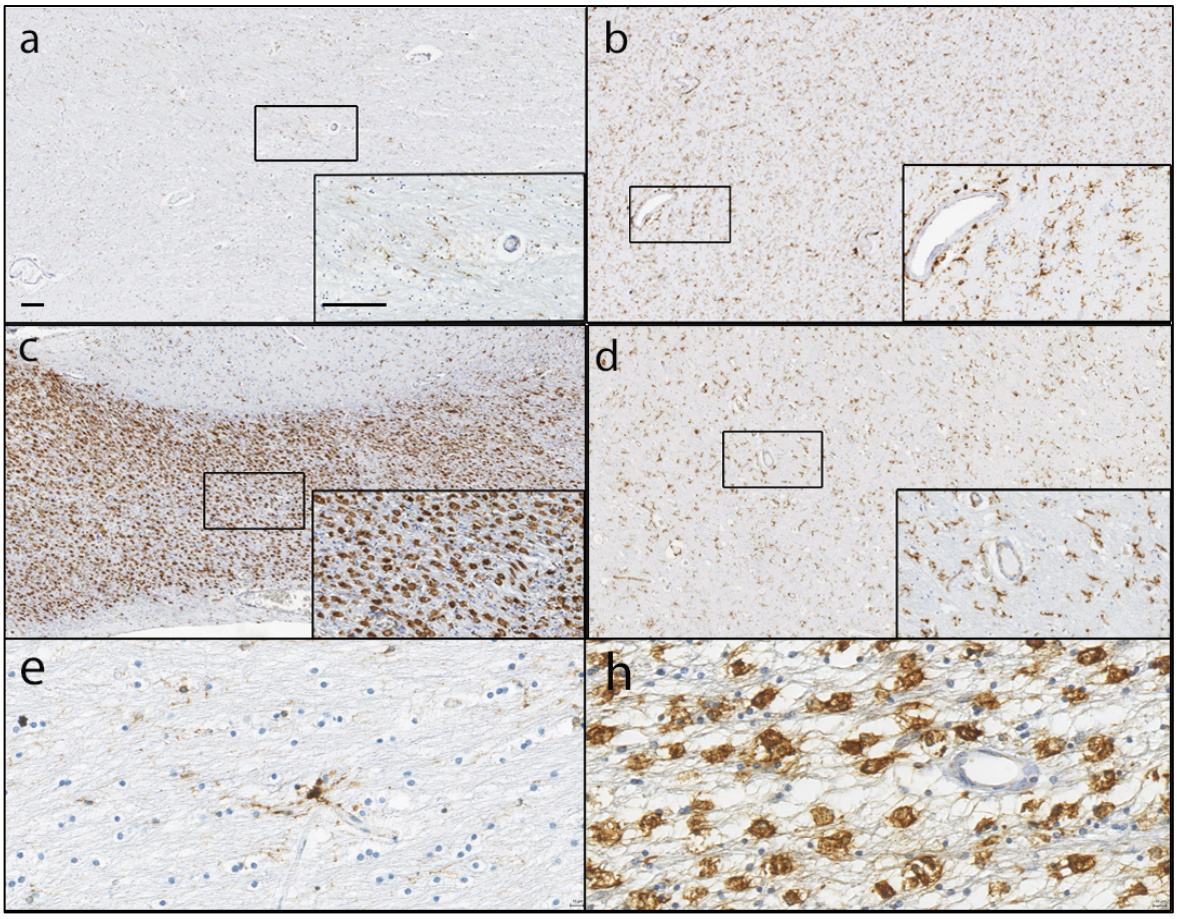

Figure 6-6 Representative images of microglia in controls and following TBI in the corpus callosum and thalamic region Where microglia appear ramified with small cell bodies and fine processed and sparsely populated, as evidenced by CR3/43 immunoreactivity, in the corpus callosum in a (a) 36-year-old woman with no history of TBI. A similar pattern is observed in the thalamic region where microglia are evenly spread throughout, identifying with ramified morphology in (b) 34-year-old woman with no history of TBI (c) demonstrates higher magnification of ramified microglia in the corpus callosum of a 33-year-old female with no history of TBI. However, following TBI a delayed response is observed in the corpus callosum in a proportion of late TBI survivors where microglia adopt an amoeboid morphology with fat, round cell bodies and no processes and densely population in the corpus callosum in a (d) 51-year-old male TBI patient who survived 3 years after an assault. In contrast, in the thalamic region, following TBI, demonstrated a similar pattern as uninjured controls with an even spread of ramified microglia throughout in a 48-year-old male TBI patient who survived 3 years after a fall (e) demonstrates higher magnification of ramified microglia in the corpus callosum of a 36-year-old woman with no history of TBI and (f) demonstrates higher magnification of amoeboid microglia in the corpus callosum of a 37-year-old male TBI patient who died 4 years following a fall. Scale bar = 1mm (low magnification), scale bar = 100µm (high magnification), scale bar = 10µm (higher magnification).

Similar to observations in acute TBI survival, survival of a year or more from a single, moderate or severe TBI resulted in no measurable increase in area staining for either CR3/43 or Iba-1 in any of the multiple white or grey matter regions examined (Table 10**,** Table 11). However, in contrast to localized evidence of early microglial activation in isolated white matter regions of a proportion of acute TBI cases, white matter activation in late survival

was in evidence in all white and grey matter regions assessed, except the thalamus (

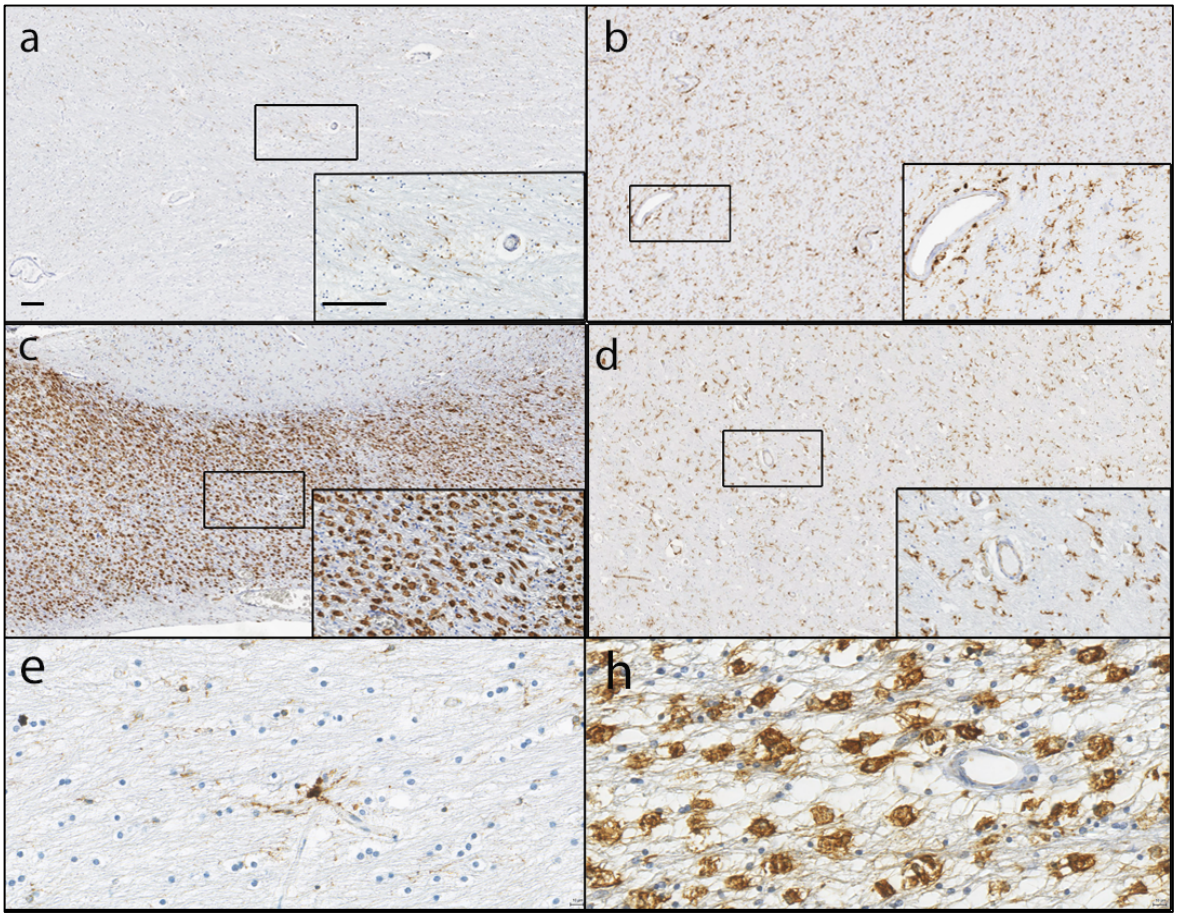

Figure 6-6c and d). Regarding white matter involvement, while similar proportions of cases showed evidence of microglial activation in subcortical white matter and internal capsule as in acute TBI cases, there was notable increased microglial activation in the corpus callosum of late TBI survivors, with microglial activation evident up to 4 years survival in this series. Specifically, in the corpus callosum staining for CR3/43 revealed 24 of 30 cases with activated microglial morphologies (15 mixed, 9 amoeboid) compared to just 3 of 17 controls (all mixed) ($p = 0.0001$; $\chi 2$; Cramer's $V = 0.606$) and 6 of 24 acute TBI cases (all mixed) ($p = 0.0001$; $\chi 2$; Cramer's $V = 0.55$) (Figure 6-7). Further, occasional late TBI survival cases was identified with evidence of early microglial activation in neocortical grey matter of the cingulate gyrus and sulcus and the superior frontal gyrus (Figure 6-7).

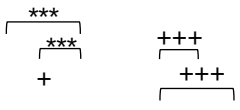

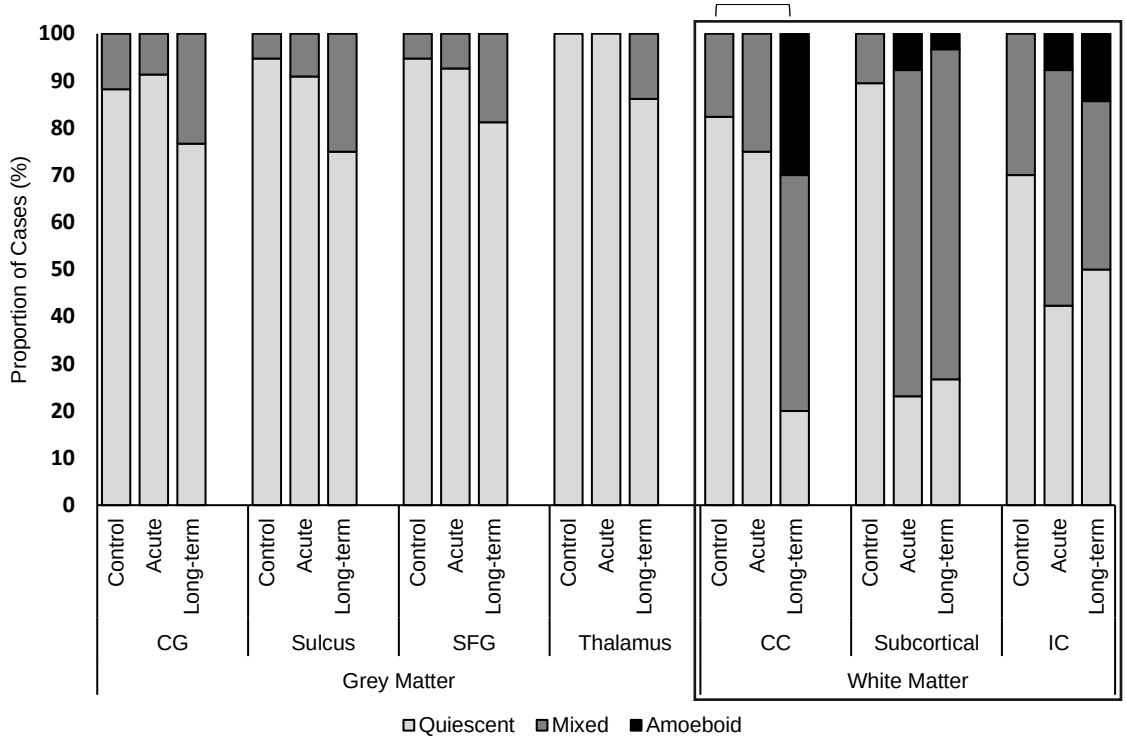

Figure 6-7 Regional distribution of the morphology of microglia as defined by CR3/43 immunoreactivity. No amoeboid activation was observed in any grey matter regions of the Cingulate Gyrus (CG), Cingulate Sulcus (Sulcus), Superior frontal gyrus (SFG) or thalamus. In contrast, in the white matter regions, 30% of long-term TBI cases expressed a population of amoeboid activated microglia in the corpus callosum ($p = 0.0001$; $\chi 2$; TBI versus uninjured controls CR3/43 immunoreactivity), 3% in the subcortical white matter regions and 14% in the internal capsule (NS). A mixed population of microglia was observed in the white matter where 50% of chronic TBI cases demonstrated mixed microglia in the corpus callosum compared with 18% in the controls ($p = 0.0343$; $\chi 2$; TBI versus uninjured controls CR3/43 immunoreactivity). Similarly, in the subcortical region, where 70% of chronic TBI cases and 69% of acute TBI cases demonstrated mixed microglia compared to 11% in the controls ($p = 0.0001$; $\chi 2$; chronic TBI versus uninjured controls CR3/43 immunoreactivity; $p = 0.0002$; $\chi 2$; acute TBI versus uninjured controls CR343 immunoreactivity). Localized evidence of early microglial activation in isolated white matter regions of a proportion of acute TBI cases (8% of cases in the subcortical white matter region and internal capsule) (NS). (+<$p = 0.05$, +++<$p = 0.0005$; mixed microglia; $\chi 2$ TBI cohort v control; ***<$p = 0.0005$; amoeboid microglia; $\chi 2$ TBI cohort v control).

6.4 Discussion

This study has demonstrated histological evidence of a differential glial response following a single, moderate to severe TBI with reactive astrogliosis localised to grey matter regions, while microgliosis appears localised to white matter regions. In turn, reactive astrogliosis is evident in the grey matter immediately after injury and persists into the chronic phase. The microglial response, in contrast, evolves after the acute period following injury and persists in the white matter in the chronic phase.

In humans, evidence of astrogliosis following TBI is limited. A post-mortem study using blast injury suggests a distinct and previously undescribed pattern of interface astroglial scarring at boundaries between brain parenchyma and fluids, and at junctions between grey and white matter (Shively et al., 2016). Staining with GFAP, Shively *et al.* assessed the brains of 5 military cases with chronic blast exposure, 3 military cases with acute blast exposure, 5 cases with chronic survival from single moderate to severe TBI, 5 with a history of opiate use and 3 cases with no neurological disorders. They reported a distinctive pattern of reactive astrogliosis in the blast cases with astroglial scarring at the boundaries between brain parenchyma and fluids, and at junctions between grey and white matter. In contrast to this current study, this pattern of reactive astrogliosis was not reported in the chronic TBI cases examined by that group, however, cohort numbers are very small and information regarding the cases was minimal. The study also reported reactive microgliosis in both white and grey matter, yet the description of assessment used and images of this were not included in the paper. This current study shows that this distinct pattern of interface astroglial scarring at boundaries between brain parenchyma and fluids, and at junctions between grey and white matter is not limited to blast exposure but also noted in a high proportion of cases following a single, moderate to severe TBI.

Much of the evidence surrounding the astrocytic response to TBI has been conducted in animal studies and mainly recounts glial scar formation around focal lesions (Susarla et al., 2014, Villapol et al., 2014, Silver and Miller, 2004, Bardehle et al., 2013). These studies document reactive astrocytosis at the site of injury in the acute phase which persist up to 60 days post injury. Using a mouse CCI, Villapol *et al* observed a robust astrogliosis up to 60 days post-injury with the reactive astrocytes occupying an extended region corresponding to cortical layers II through to layer VI (Villapol et al., 2014). This astrogliosis, however, was only observed around the impact site and around the lesion border. In this current study,

however, the astrogliosis is diffuse in nature and is observed at the interface of the grey and white matter and at boundaries between brain parenchyma and fluids.

Following rTBI in transgenic mice, acute astrogliosis has been identified (Petraglia et al., 2014a, Ojo et al., 2013, Petraglia et al., 2014b, Luo et al., 2014, Ojo et al., 2016). Petraglia *et al*, report a limited acute astrogliosis following a single TBI in mice, with a more persistent, widespread astrogliosis following rTBI associated with tau-immunoreactive astrocytes. A key focus on astrocytes following rTBI, however, remains tau-immunoreactive astrocytes observed in CTE (McKee et al., 2009, Stein et al., 2014). This astrocytic p-tau pathology in CTE is proposed to be topographically distinct from wider tauopathies, including ARTAG; a four-repeat tauopathy featuring thorn shaped astrocytes (Lopez-Gonzalez et al., 2013, Lace et al., 2012).

Where reactive astrogliosis has been reported in a variety of neurodegenerative disease such as ALS, Parkinson's disease and Alzheimer's disease (Colangelo et al., 2014, Glass et al., 2010, Maragakis and Rothstein, 2006) there has been emerging evidence of the physiopathological potential of astrocytes. Reactive astrogliosis has been attributed to both neuroprotective and detrimental effects in the CNS (Laird et al., 2008, Sirko et al., 2015, Bardehle et al., 2013, Myer et al., 2006). By using transgenic mice, there is an indication that reactive astrogliosis is beneficial and neuroprotective, especially in the early stage of AD (Sofroniew and Vinters, 2010), however, this is compromised in chronic neuroinflammation. Various therapeutic approaches have been developed to promote this astrocytic neuroprotection. Cell based studies such as transplantation of human astrocytes, stem cell injections which differentiate into astrocytes at site of lesion and cell grafting strategies have all shown to exert neuroprotection (Giralt et al., 2010, Colangelo et al., 2014). Targeting signalling pathways has also demonstrated therapeutic potential. Toll-like receptors (TLRs) are associated with astrocytic and microglial activation by Aβ; therefore, TLR antagonists may provide new targets for neurodegenerative diseases. These strategies which exert neuroprotection from reactive astrogliosis could potentially be translated in therapeutic targets for TBI, although the therapeutic window may be small, addressing reactive astrogliosis early would be key. More work is needed to obtain a comprehensive understanding of reactive astrogliosis following TBI, the distinct pattern and distribution observed and specific time windows for effective therapeutic interventions.

The striking pattern of reactive astrogliosis following TBI is intriguing and warrants further studies. Astrocytes cover the CNS in an ordered and well-organised manner with

protoplasmic astrocytes lining the grey matter and fibrous astrocytes lining the white matter (Sofroniew and Vinters, 2010). Protoplasmic astrocytes envelop neuronal bodies and synapses and populate individual domains with the distal tips of the astrocytic processes interlocking, forming components of the gap junctions (Sofroniew and Vinters, 2010, Halassa et al., 2007, Bushong et al., 2002). These astrocytes, therefore integrate the neuronal network with the vascular network (Cabezas et al., 2014). The suggestion is made that the pattern and distribution of reactive astrocytes observed here is predominantly a pathology of protoplasmic astrocytes which may indicate a disruption of the neurovascular network.

The pattern of reactive astrogliosis observed in this study occurs in the grey matter, a similar outline as seen in BBB disruption after TBI As determined previously (Chapter 3), there is a leakage of fibrinogen at the site of BBB disruption (Hay et al., 2015). Where fibrinogen has been suggested to induced glial scar formation post injury (Schachtrup et al., 2010), activated glial cells have also been suggested to promote further BBB disruption by releasing TGF, MMPs, VEGF and glutamate (Carpentier et al., 2005, Price et al., 2016, Kim et al., 2005). In addition, astrocytic endfeet fully envelope the cerebral vessels (Mathiisen et al., 2010), which, together with pericytes comprise the BBB (Abbott et al., 2006, Wolburg et al., 2009). Swelling and displacement of these endfeet under pathological conditions can result in a breach of BBB integrity (Watkins et al., 2014, Ito et al., 2011). There is a suggestion from the observations in this study that reactive astrogliosis in the grey matter is associated with BBB disruption. As such, future studies investigating this continuous activation of both astrocytes and BBB disruption may lead to a clearer understanding of the chronic pathologies observed following TBI.

In addition to persistent astrogliosis and interactions with BBB disruption following TBI, this study has also demonstrated that microgliosis observed post-TBI is prominently a white matter pathology; occurring in the white matter tracts of the corpus callosum and internal capsule. This supports the findings by Johnston *et al* (Johnson et al., 2013a) where, in autopsy material from patients surviving a TBI there is evidence of an ongoing neuroinflammatory response years after survival following a single injury. Interestingly, where these observations demonstrate distinct activated microglia in the corpus callosum, in vivo positron emission tomography studies in surviving patients after an sTBI have reported no significant differences in binding in this region, although they have reported a difference in binding in the thalamic region compared with control patients (Ramlackhansingh et al., 2011b).

Where the studies reporting chronic neuroinflammation in the white matter use immunohistochemical techniques (as used here) (Johnson et al., 2013a), imaging studies that report chronic inflammation in the grey matter region of the thalamus used PK11195 PET as a marker. PK-11195 binds selectively to the peripheral benzodiazepine receptor (PBR) (also known as Translocator protein TSPO) which is upregulated in both microglia and reactive astrocytes (Chechneva and Deng, 2016a). This tracer, therefore is relatively non-specific and might mark both reactive microglial and reactive astroglia. This could explain why Ramlackasingh *et al* reported high levels of PK11195 emission in the grey matter; they may have inadvertently been reporting the TSPO emission from astrocytes, shown to be reactive in this current study, rather than microglial activation as interpreted by the authors. Of note, efforts are being made to develop new, more highly specific tracer for PBR binding (Doorduin et al., 2008). In addition, this study used Iba-1 to highlight microglia in the brain, however, it often difficult to distinguish microglia from related cell types such as exogenous monocytes (Ajami et al., 2018, Ajami et al., 2011, Varvel et al., 2016). As such, for future studies, the use of transmembrane protein 119 (Tmem119) may be useful to more accurately demarcate microglia from non-tissue resident monocytes/macrophages (Bennett et al., 2016).

6.4.1 Conclusion

This study has demonstrated histological evidence of a differential glial response following a single, moderate to severe TBI with reactive astrogliosis localised to the grey matter and microgliosis localised to the white matter compared with uninjured controls. The astrogliosis occurs immediately after injury and persists into the chronic phase. In contrast, microglial activation appears after the acute phase post-TBI and persists in the chronic phase. Limitations of the study include challenging numbers to confidently assess the association between reactive astrogliosis and BBB breakdown and suitably distinguish microglial populations.

Where previous studies have reported a distinct and ‘unique’ pattern of astroglial distribution in blast TBI, this study demonstrates that it is not unique to blast injuries but is observed also in survival from a single, moderate to severe TBI. Furthermore, an understanding and appreciation is required when assessing the microglial activation. Using markers for microglia assessment in human imaging studies may pick up astrocytic activation which may lead to conflicting results. Further studies on the differential glial response observed in this study may lead to a clearer understanding of the neurodegeneration pathologies observed

post-TBI and how they interact with one another which may pave way for potential therapeutic targets of TBI.

7 Chronically activated perivascular microglia express M2-like phenotype in white matter tracts following TBI

7.1 Introduction

There is increasing evidence of the association between a history of TBI and late neurodegenerative disorders, with clinical studies reporting increased risk of Alzheimer's disease (AD) in a proportion of TBI survivors (Molgaard et al., 1990, Mortimer et al., 1985, Mortimer et al., 1991, Graves et al., 1990, O'Meara et al., 1997, Salib and Hillier, 1997, Guo et al., 2000, Schofield et al., 1997, Plassman et al., 2000, Fleminger et al., 2003). However, the pathologies driving these late outcomes remain poorly described. Neuroinflammation is increasingly regarded as a key feature of neurodegenerative disorders (Perry et al., 2010, Brettschneider et al., 2012b, Brettschneider et al., 2012a), and as an early event in AD pathogenesis (Town et al., 2008, Wright et al., 2013, Yamamoto et al., 2007, Yoshiyama et al., 2007). More recently, neuroinflammation has been recognised as a key pathology following TBI in autopsy studies (see Chapter 6) (Johnson et al., 2013a) and imaging studies (Ramlackhansingh et al., 2011b), however, it is unclear what drives this persistent inflammation.

7.1.1 Microglia in neurodegeneration

A key feature of neurodegenerative diseases such as AD, Parkinson's disease (PD), Multiple sclerosis (MS) and ALS, is a CNS immune response triggered by microglial activation. Microglia play a fundamental role in maintaining homeostasis in the CNS; and in response to homeostatic changes the microglia become phenotypically active (Perry et al., 2010). Activated microglia are both the consequence and contributors of AD pathology, where immune responses are raised due to a variety of pathologies, such as Aβ plaques, and this continuous activation state becomes neurotoxic. The activation of microglia had both beneficial and detrimental properties, depending on the phenotype being expressed.

Microglia have a diverse spectrum of functionality, which ranges from the neurotoxic and pro-inflammatory M1-like phenotype, through to the neuroprotective and immunosuppressive roles of the M2-like phenotype (Mantovani et al., 2012, Loane and Kumar, 2016, Gordon, 2003). The M2-like phenotype is further categorised into subtypes M2a, M2b and M2c. The M1-like phenotype, when activated, produces high levels of pro-

inflammatory cytokines and chemokines, such as tumour necrosis factor-α (TNF-α), interleukin-6 (IL-6) and interferon-γ (IFN-γ). As such, the M1-like phenotype is suggested to be neurotoxic (Gao et al., 2003, Qin et al., 2004, Loane and Kumar, 2016). Conversely, the M2-like phenotype has a more neuroprotective role. The phenotypic subtype M2a responds to IL-4 and IL-13 stimulation and increases phagocytic activity, the M2b subtype is an intermediate phenotype and has both pro-inflammatory and anti-inflammatory effects and the M2c subtype is a 'de-activated' state which regulates tissue repair and remodelling (Sica and Mantovani, 2012, Simon et al., 2017).

In AD patients, there is an observed shift from the M2-like phenotype to an M1-like phenotypic activation in the temporal course of the disease progression. This has been detected in both humans and mice models (using APP transgenic mice) where an increase of pro-inflammatory cytokines, released by M1-like microglia, has been demonstrated (Heneka and O'Banion, 2007, Rojo et al., 2008, Hoozemans et al., 2006, Wyss-Coray, 2006, Neuroinflammation Working et al., 2000, Varnum and Ikezu, 2012, Solito and Sastre, 2012). In addition, using APP transgenic mice, M1-like activators promote inflammation and inhibit clearance of Aβ from the brain, whereas M2a and M2c-like activators promote Aβ clearance (Yamamoto et al., 2007, Yamamoto et al., 2008, He et al., 2007, Varnum and Ikezu, 2012). This suggests that microglial phenotypes, specifically M1-like, may play a fundamental role of the disease progression, however, further studies are required to support this hypothesis.

7.1.2 Microglia in TBI

Microglia undergo morphological and expressive alterations which contribute to the post-TBI inflammatory pathways (Aihara et al., 1995, Gentleman et al., 2004, Nagamoto-Combs et al., 2007, Wilson et al., 2004, Loane and Byrnes, 2010, Ziebell and Morganti-Kossmann, 2010). These changes can range from ramified, 'resting' state microglia through to activated, amoeboid microglia (Walker et al., 2014). Chronic microglial activation has previously been described in limited autopsy and imaging studies which indicate increased and prolonged microglia activity with long-term survival up to 18 years post-injury (Gentleman et al., 2004, Ramlackhansingh et al., 2011b, Johnson et al., 2013a).

Within the few studies published, there is a consensus of a prolonged and predominant M1-like phenotype following TBI in the controlled cortical impact (CCI) mouse model (Loane et al., 2014, Kumar et al., 2016a). Some studies suggest that both M1 and M2-like

phenotypes are present in the early stages following injury, which is then replaced with a majority of M1-like microglia, detected by an increase of NOX_2 activity (nicotinamide adenine dinucleotide phosphate-oxidase), 7 days following injury (Kumar et al., 2016a, Kumar et al., 2016b). Further studies using the CCI model report a transient peak of M2-like microglia 5 days post-injury, which decreased rapidly thereafter, while M1-like microglia continue to remain elevated up to 14 days post-injury in the cortex, striatum and corpus callosum (Wang et al., 2013). This work suggests that following TBI, there are dynamic microglial changes which vary between grey and white matter. Additionally, Wang *et al*, (2013) report that the M1-like microglial response correlates with the extent of white matter injury observed (Wang et al., 2013). In humans, chronically activated microglia have been reported in the grey matter (Ramlackhansingh et al., 2011b) and white matter (Johnson et al., 2013b) up to 18 years post-TBI, however, the characterisation of the phenotypic profile of these activated microglia is yet to be determined.

7.1.3 Perivascular microglia and BBB

In the animal model of experimental autoimmune encephalomyelitis (EAE) it has been suggested that perivascular clustering of microglia can be induced by fibrinogen leakage, due to BBB disruption (Davalos et al., 2012). The study suggests fibrinogen triggers rapid perivascular microglial response which contributes to axonal damage in EAE, specifically, microglia exhibit cell motility patterns directed specifically toward the vasculature that precede the onset of neurological signs and lesion formation (Davalos et al., 2012). In addition, the M2-like perivascular microglial marker CD163 has been observed to be upregulated in parenchymal microglial in a chronically infected animal with Simian Immunodeficiency Virus Encephalitis (Borda et al., 2008). Borda *et al*, (2008) suggest that this upregulation of parenchymal microglia may be due to BBB disruption.

Following TBI, a study that investigated CD14 (M1-like perivascular microglia marker) expression in human brain lesions also reported a similar pattern (Beschorner et al., 2002a). Where, under normal conditions CD14 would selectively be expressed in perivascular microglia, following TBI, the number of CD14 positive microglia in the parenchyma significantly increased (Beschorner et al., 2002a). Selecting 25 TBI cases from autopsy and 5 control brains, they investigated CD14 expression using immunohistochemical techniques. Beschorner *et al*, (2002) reported that controls expressed CD14 immunoreactive microglia in the perivascular space only, however, following TBI the number of CD14 immunoreactive

microglial increased in the parenchyma. This increase peaked with 4-8 days post-injury and remained elevated weeks post-injury.

Hypothesis: The current study will aim to assess the role of perivascular microglia following TBI, and, by using the M1-like marker CD14 and the M2-like marker CD163, determine the phenotypic profiles associated with post-TBI neuroinflammation.

7.2 Materials and Methods

7.2.1 Case selection and brain tissue Preparation

From the Glasgow TBI archive cases aged under 60 years at time of death with a history of single moderate or severe TBI were selected as acute TBI cases (survival < 14 days from TBI; n = 27) or long-term TBI cases (survival >1 year from TBI; n = 32), together with uninjured, age-matched controls with no known history of TBI or neurological disease (n = 21). Autopsy reports and, where necessary, clinical and forensic records were available for all cases to confirm a history of moderate or severe TBI on presentation as defined by the Glasgow Coma Scale. Demographic and clinical data and detail on neuropathology findings at the original autopsy for each cohort are presented in Table 12.

At the time of the original diagnostic autopsy, whole brains were immersion fixed in 10% formal saline for a minimum of 3 weeks, following which the specimens were examined, sampled using standardized techniques and processed to paraffin tissue blocks. For this study, blocks from a coronal slice of the cerebral hemispheres at mid-thalamic level were selected to include the thalamus, with adjacent internal capsule, and corpus callosum, with adjacent cingulate gyri and sulcus. From these tissue blocks 8μm sections were prepared for immunohistochemistry procedures.

Table 12 Demographics and clinical information of all groups

		TBI: Acute survival (n = 27)	**TBI: Long-term survival (n = 32)**	**Controls (n = 21)**
Mean age (range)		44.4 years (9-60)	46.3 years (19-60)	39.9 years (14-60)
Males		17 (63%)	31 (97%)	13 (62%)
Mean PM delay (range)		56.1 hours (3-240)	65.5 hours (9-184.5)	71.6 hours (12-144)
Mean survival interval (range)		69.3 hours (6-216)	7.8 years (1-47)	Not applicable
Cause of TBI	Fall	15 (55.5%)	15 (46.9%)	Not applicable (No history of TBI)
	RTA	7 (25.9%)	5 (15.60%)	
	Assault	4 (14.8%)	8 (25%)	
	Unknown	1 (3.7%)	4 (12.5%)	
Cause of death	Head injury	25(92.6%)	0	0
	Bronchopneumonia	2(7.4%)	7(21.9%)	1(4.8%)
	ARDS	0	1(3.125%)	0
	Pulmonary thromboembolism	0	0	0
	Heart disease	0	6 (18.8%)	5(23.8%)
	Alcohol related	0	2(6.25%)	0
	Pyelonephritis	0	1(3.125%)	0
	Multi-organ failure	0	1(3.125%)	0
	GIT haemorrhage	0	1(3.125%)	0
	Polytrauma	0	1(3.125%)	0
	Drug overdose	0	0	3(14.3%)
	SUDEP	0	7(21.9%)	8(38.1%)
	Pulmonary oedema	0	1(3.125%)	0
	Septicaemia	0	0	2(8.3%)
	Inhalation of gastric contents	0	0	2(8.3%)
	Unknown	0	4(12.5%)	0

Key: *TBI = traumatic brain injury; SUDEP = sudden unexpected death in epilepsy; GIT = gastrointestinal tract; ARDS= acute respiratory distress syndrome; RTA = road traffic accident*

7.2.2 Immunohistochemistry

Sections were deparaffinised and rehydrated, following which, endogenous peroxidase was quenched via immersion in 3% aqueous H202 for 15 minutes. Thereafter, heat induced antigen retrieval was performed using a microwave pressure cooker for 8 minutes in preheated 0.1M Tris EDTA buffer (pH 8), followed by blocking in 50µl of normal horse serum (Vector Labs, Burlingame, CA, USA) per 5 mL of Optimax buffer (BioGenex, San Ramon, CA, USA) for 30 minutes. Sections were incubated in primary antibody at 4oC for 20 hours prior to washing and biotinylated secondary antibody was applied for 30 minutes, followed by an avidin biotin complex as per manufacturer's instructions (Vectastain Universal Elite Kit, Vector Labs, Burlingame, CA, USA). The target antigen was visualized by applying the DAB peroxidase substrate kit (Vector Labs, Burlingame, CA, USA) then counterstained with haematoxylin.

Primary antibodies were selected to reveal CD163 (monoclonal mouse anit-CD163; 1:1000; Leica Biosystems, Milton Keynes UK), a perivascular microglial marker and marker for M2-like phenotype, and CD14 (monoclonal rabbit anti-CD14; 1:500; Abcam, Cambridge, UK), a perivascular microglial marker and marker for M1-like phenotype. Known positive and negative control sections for each antibody were run in parallel with test sections to confirm antibody specificity.

Sections were viewed using a Leica DMRB light microscope (Leica Microsystems, Wetzlar, Germany). Further, sections were scanned and analysed at 20x using a Hamamatsu Nanozoomer 2.0-HT slide scanner, with the images viewed via the SlidePath Digital Image Hub application (Leica Microsystems, Wetzlar, Germany). The images in this chapter have been digitally captured at 4x (2.3µm per pixel) and 20x (0.46µm per pixel).

7.2.3 Analysis of immunohistochemistry

7.2.3.1 Percentage area stain

Assessment of microglial extent for each anatomical region was calculated as percentage area of immunostain. Using SlidePath Digital Image Hub software, a 1mm x 1mm square was randomly placed over multiple regions of interest (ROI) within grey matter or white matter of CD163 and CD14 stained sections. Images of these ROIs were then captured and exported to ImageJ (NIH, Bethesda, MD) where the background was subtracted, and the Colour Deconvolution plugin applied using the installed Haematoxylin/ DAB vector (H

DAB) to produce separate colour channels for the counterstain (Haematoxylin) and specific immunostaining (DAB). The DAB-specific image was then manually thresholded and the percentage of positive staining in the ROI calculated using standard algorithms in ImageJ.

7.2.3.2 Microglial Morphology Assessment

In addition to a quantitative assessment microglial staining, standardized semi-quantitative scores of microglial morphologies were recorded for each region to assess microglial activation state as described previously (Johnson et al., 2013b). Specifically, regions were assessed and reported as either displaying a predominance of perivascular microglia cells with amoeboid morphology (A), ramified morphology (R) or mixed amoeboid/ramified morphology (M).

7.2.3.3 Perivascular microglia:

In addition to quantitative assessment of microglial staining and of microglial morphologies, standardized semi-quantitative scores of perivascular microglia were assessed in all grey and white matter regions. Semi quantitative scoring was as follows:

Score of 0: Microglia were observed contained in the perivascular space only

Score of 1: In addition to microglia in the perivascular space the is an observed moderate microglia population in the surrounding grey and white matter regions

Score of 2: In addition to microglia in the perivascular space the is an observed extensive, widespread and densely packed population of microglia into the surrounding grey and white matter (Score of 2).

Representative examples of immunohistochemical findings and the corresponding semi-quantitative scores are shown in Figure 7-1.

7.2.4 Statistical analysis

All data were analysed using SPSS (version 22; IBM, Inc.), and applying the $\chi 2$ test or Student's *t*-test to assess data between and within cohorts as appropriate. Cohen's *d* and Cramer's V were used to determine the effect size and to indicate the standardised difference between two means. A Cramer's V value of 0.1 suggested a low practical significance, a value of 0.3 suggested a moderate practical significance and a value of 0.5 suggested a high practical significance. While a Cohen's *d* value of 0.2 suggested a low practical significance, a value of 0.5 suggested a moderate practical significance and a value of 0.8 suggested a high practical significance. All effects were considered statistically significant when $p \leq 0.05$. Quantitative results are expressed as mean ± standard error of the mean.

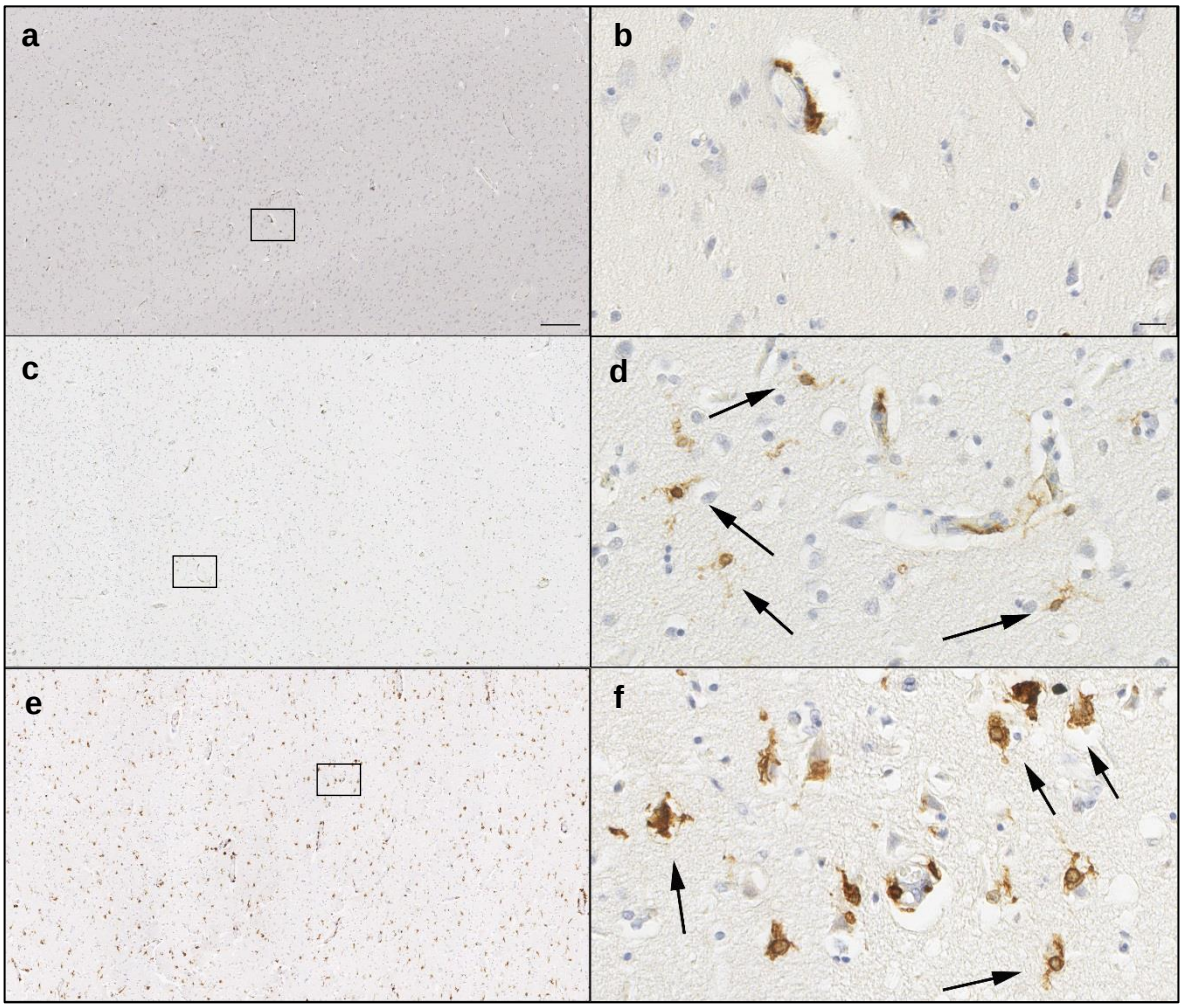

Figure 7-1 Representative images of cortical microglia in cingulate gyrus stained with CD163 Perivascular microglia are contained within the perivascular space only, limited to the blood vessel wall with no microglia in cortex (score of 0) in the cingulate gyrus of (a) a 46-year-old male with no history of traumatic brain injury (TBI) and (b) high magnification of perivascular microglia. In addition to the perivascular microglia, ramified microglia with long processes and fine cell bodies are highlighted in the surrounding cortex (Score of 1) in the cingulate gyrus of (c) a 54-year-old male TBI patient who survived 9 years after a fall and high magnification of microglia beyond perivascular space (d) as demoted by arrows. A more extensive population of perivascular microglia extending beyond the perivascular space into the surrounding cortex (Score of 2) in the cingulate gyrus of (c) a 51-year-old male TBI patient who survived 96 hours following an assault and high magnification of microglia beyond perivascular space as denoted by arrows (f). Scale bar = 100µm, scale bar = 10µm (higher magnification).

7.3 Results

7.3.1 Extent, morphology and distribution of CD14 and CD163 immunoreactive microglia in the white matter

7.3.1.1 Extent of CD14 and CD163 in the white matter tracts

In the control group, microglia were observed as small, fine and feathery cells nestled beside the vessels; sparsely populated in the white matter tracts of corpus callosum and internal capsule (Figure 7-2a). As with the uninjured control group, in material from the acute TBI group, all white matter regions expressed a majority of ramified CD14 and CD163 immunoreactive microglia, localising to similar areas as in the control group; nestle beside vessels (Figure 7-2b). In material from the late survival TBI group, ramified CD14 and CD163 immunoreactive perivascular microglia were again observed throughout all white matter regions, however, in a proportion of late survivors an activated amoeboid microglia population was observed, in the white matter tracts of the corpus callosum and the internal capsule. A higher proportion of CD163 immunoreactive microglia than CD14 immunoreactive microglia is observed (Figure 7-2c). There was no evidence of change in percentage area stain in either CD14 or CD163 in any white matter region between the groups. However, there was a slight increase of percentage stain in both CD14 and CD163 in the corpus callosum of the later survivors of TBI (Figure 7-3).

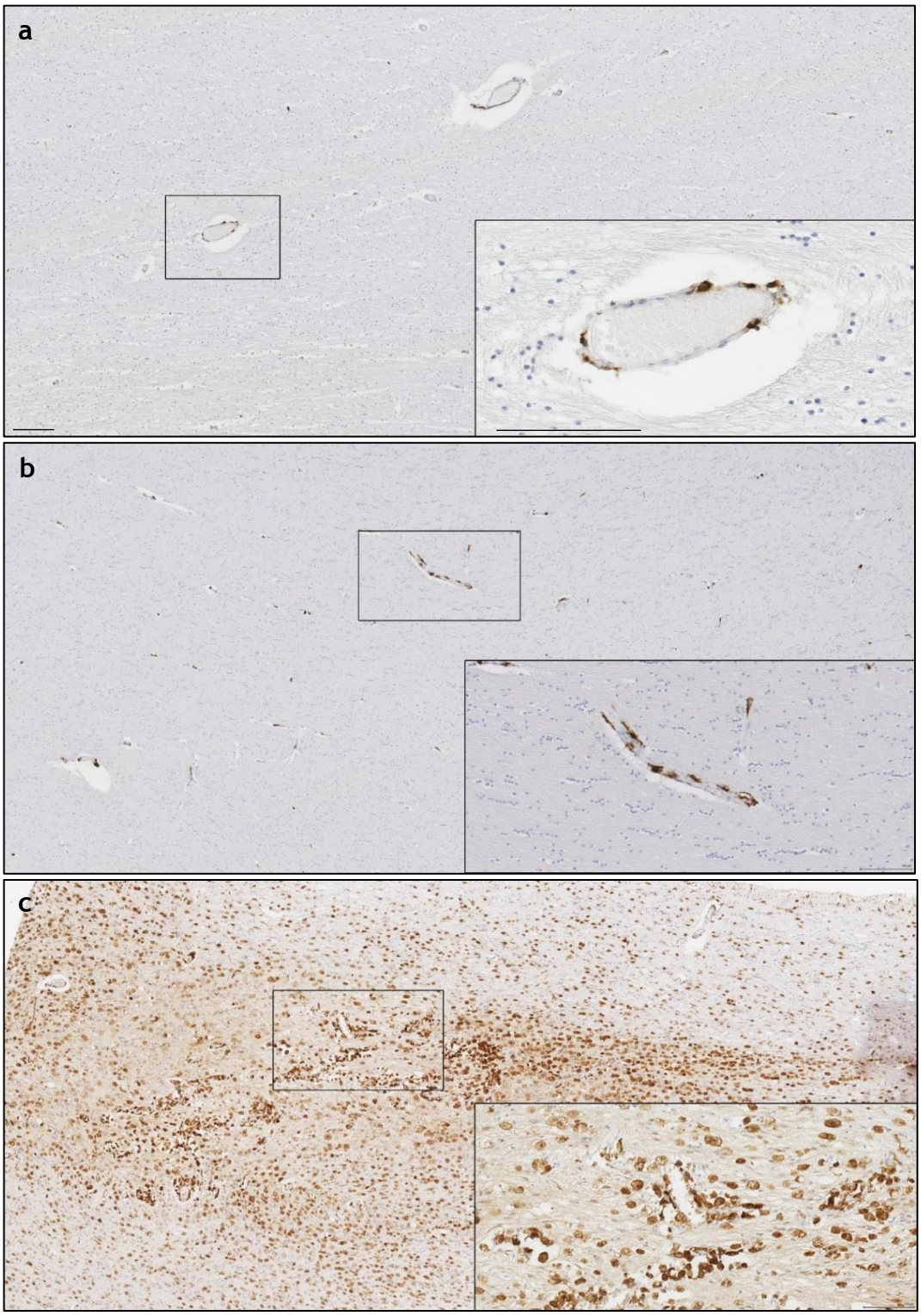

Figure 7-2 Representative images of perivascular microglia in the corpus callosum Where CD163 immunoreactive microglia were confined to the perivascular space and were absence in the surrounding white matter regions, as expected (a) in a 36-year-old female with no history of TBI. A similar pattern is observed in material from acute TBI survival where CD163 immunoreactive cells are limited to around blood vessels in the corpus callosum of a (b) 20-year-old male TBI patient who survived 48 hours following an assault. However, in material from later TBI survivors extensive and densely populated amoeboid CD163 immunoreactive microglia are observed beyond the perivascular space in a (c) 50-year-old male TBI patient who survived 1 year following an assault. Where densely-packed amoeboid CD163 immunoreactive cells are observed to extend beyond the vessels. Scale bar = 1mm (low magnification), scale bar = 100µm (high magnification).

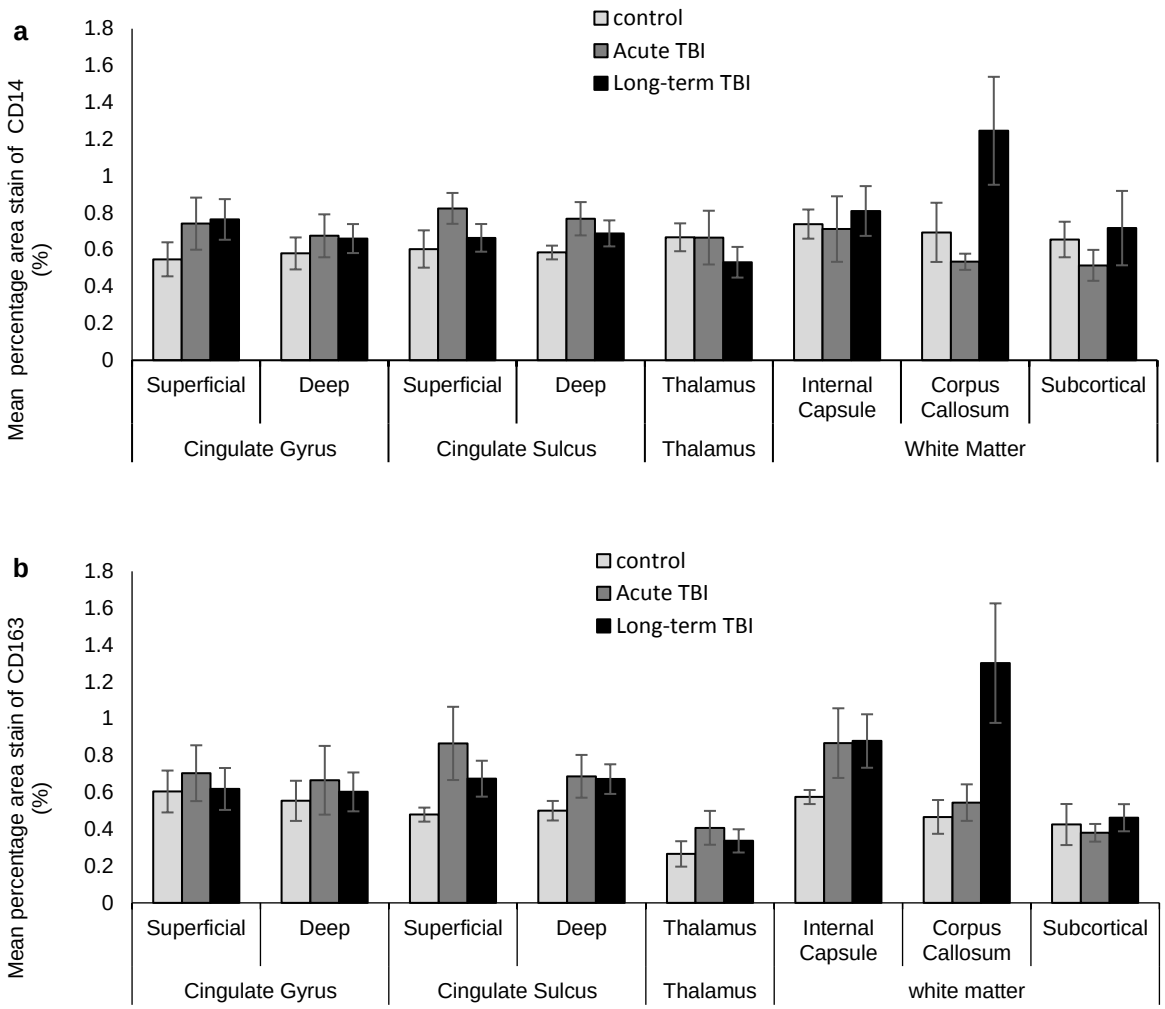

Figure 7-3 Regional distribution of CD14 and CD163 percentage area stain following TBI versus control (a) Percentage area stain of CD14 in all regions assessed. Where no significant increase in area stain in any region was observed, a slight increase was observed in the corpus callosum of later survivors compared with uninured controls ($p = 0.354$; Student's *t*-test; Cohen's $d = 0.45$). (b) Percentage area stain of CD163 in all regions assessed. Where no significant increase in area stain of CD163 was observed in any region, a slight increase was noted in the corpus callosum of later survivors compared with uninured controls ($p = 0.107$; Student's *t*-test; Cohen's $d = 0.67$) and in the internal capsule ($p = 0.051$; Student's *t*-test; Cohen's $d = 0.57$).

7.3.1.2 Morphology of CD14 and CD163 in the white matter tracts

In uninjured, control material a predominately ramified, quiescent morphology of both CD14 and CD163 immunoreactive microglia was demonstrated around blood vessels in all white matter regions examined, with only 1 control demonstrating a mixed morphology of CD163 immunoreactive microglia in the corpus callosum. No controls demonstrated an activated amoeboid morphology in either CD14 or CD163 immunoreactivity (Figure 7-4). In material from the acute TBI group, there was predominantly ramified, quiescent perivascular microglia throughout the white matter regions with 3 cases demonstrating a more mixed morphology in CD14 immunoreactive cells and 2 cases demonstrating mixed CD163 immunoreactive microglia in the corpus callosum, a similar pattern was observed in the internal capsule. In addition, as with the uninjured control group, no cases demonstrated

amoeboid morphology (Figure 7-4). Similar to the acute TBI group, the majority of cases in the long-term TBI group presented with predominantly ramified, quiescent perivascular microglia throughout the white matter regions with limited number of cases demonstrating a mixed morphology of CD14 and CD163 immunoreactive microglia. However, in material from the late survival TBI group, activated amoeboid microglia in the white matter tracts of the corpus callosum and internal capsule in a proportion of cases was observed (Figure 7-2c). In the corpus callosum 7% of cases demonstrated CD14 immunoreactive amoeboid microglia compared with none in the control group ($p = 0.5029$; $\chi 2$; Cramer's $V = 0.184$) and 21% of cases demonstrated CD163 immunoreactive amoeboid microglial compared to uninjured controls ($p = 0.0339$; $\chi 2$; Cramer's $V = 0.333$) (Figure 7-4**,** Figure 7-5)**.** Fewer TBI cases demonstrated activated amoeboid microglia in the internal capsule where only 2 out of 31 cases observed CD14 immunoreactive activated microglia and 1 out of 30 cases observed CD163 immunoreactive activated microglia.

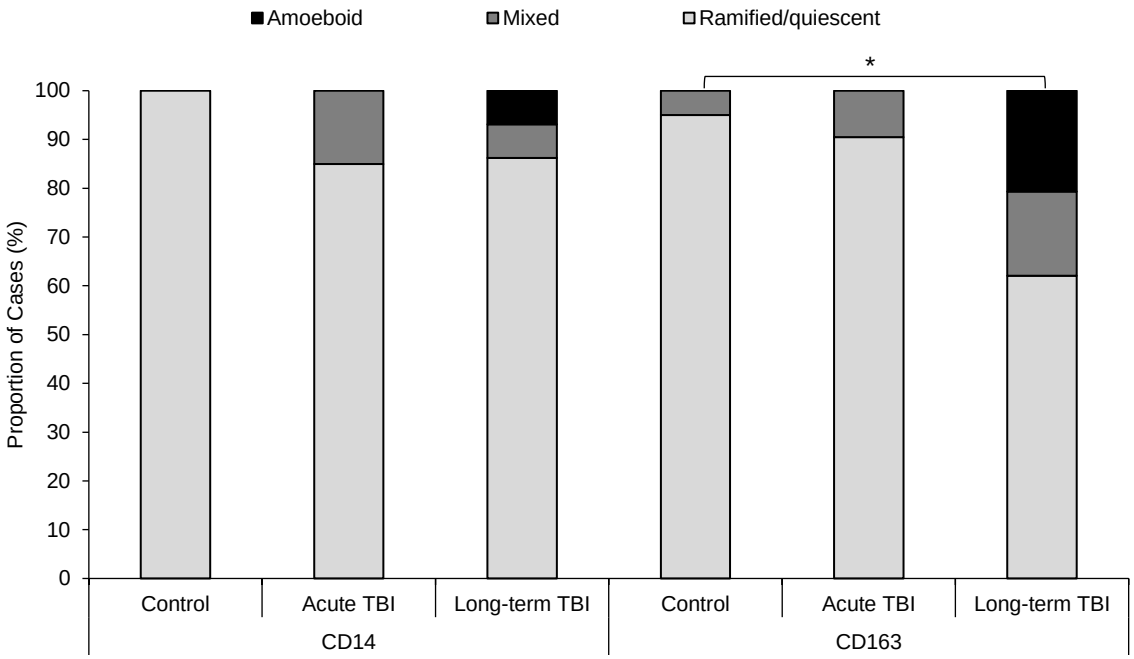

Figure 7-4 Morphology of CD163 and CD14 immunoreactive microglia in the corpus callosum following TBI versus uninjured controls. Where very limited activated perivascular microglia was observed in the uninjured controls and localized evidence of early microglial activation in small proportion of acute TBI cases, in the late survivors of TBI, 21% of cases demonstrated CD163 amoeboid microglia in the corpus callosum and 7% of cases demonstrated CD14 amoeboid microglia ($p = 0.0339$; $\chi 2$; late TBI group vs uninjured controls)

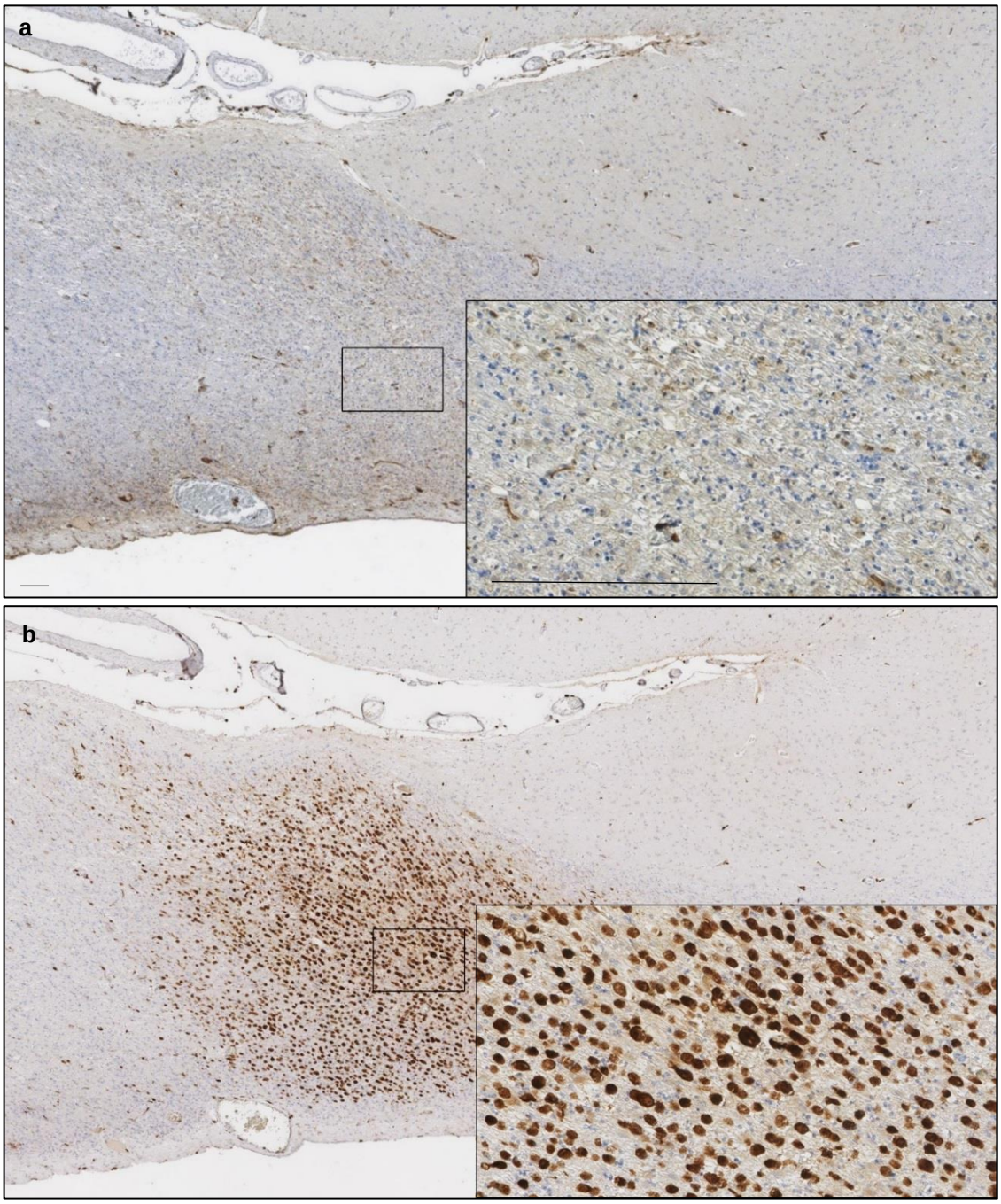

Figure 7-5 Representative images of CD14 and CD163 immunoreactive amoeboid microglia
(a) minimal DAB staining denotes a lack of CD14 immunoreactivity with only sparsely punctuated CD14 positive perivascular microglia, with no amoeboid microglia present, observed in the corpus callosum in the corpus callosum of a 51 year-old male who survived 3 years following a TBI sustained by an assault. However in the same case (b), extensive, densely populated CD163 immunoreactive amoeboid microglia displayed by fat, round cell bodies and no processes in the corpus callosum of the same patient. Scale bar = 1mm (low magnification), scale bar = 100μm (high magnification).

7.3.1.3 Distribution of CD14 and CD163 in the white matter tracts

In material from uninjured control group, both CD14 and CD163 immunoreactive cells were confined to the perivascular space in all controls. In the acute TBI group 3 cases demonstrated CD14 immunoreactive microglia beyond the perivascular space and 5 cases demonstrated CD163 immunoreactive microglia beyond the perivascular space in the corpus

callosum ($p = 0.0693$; $\chi 2$; acute TBI vs uninjured controls). A similar pattern was observed in the subcortical regions and internal capsule. In the material from late survivors of TBI, 5 cases demonstrated CD14 immunoreactive microglia beyond the perivascular space compared with none in the controls ($p = 0.1464$; $\chi 2$; Cramer's $V = 0.261$) and 10 cases demonstrated CD163 immunoreactive microglia beyond the perivascular space compared with uninjured controls ($p = 0.0121$; $\chi 2$; Cramer's $V = 0.391$). Of note, of those late survivor TBI cases which demonstrated CD163 immunoreactive microglia beyond the perivascular space, 90% displayed a mixed or amoeboid morphology (Figure 7-5b).

7.3.2 Extent, morphology and distribution of CD14 and CD163 immunoreactive microglia in the grey matter

7.3.2.1 Extent of CD14 and CD163 in the grey matter regions

In the control group all grey matter regions of the cingulate gyrus, cingulate sulcus and thalamus expressed both perivascular CD14 and CD163 immunoreactive microglia. Microglia were observed as small, fine and feathery cells nestled beside the vessels (Figure 7-6a). In material from the acute TBI group, all regions expressed a majority of quiescent CD14 and CD163 immunoreactive microglia, localising to similar areas as in the control group, however, in a proportion of cases perivascular microglia were observed beside blood vessels as expected but also observed in the surrounding cortex (Figure 7-6b). In material from the late survival TBI group ramified CD14 and CD163 immunoreactive perivascular microglia were observed throughout all grey matter regions with a more mixed morphology observed in a proportion of cases throughout all regions assessed. In addition to the expected perivascular microglia observed around blood vessels, a higher proportion of cases also demonstrated both CD14 and CD163 microglia in the surrounding grey matter regions of cingulate gyrus, cingulate sulcus and thalamus (Figure 7-6c). As with the white matter regions, there was no evidence of change in percentage area stain in either CD14 or CD163 in any grey matter region between the groups (Figure 7-3).

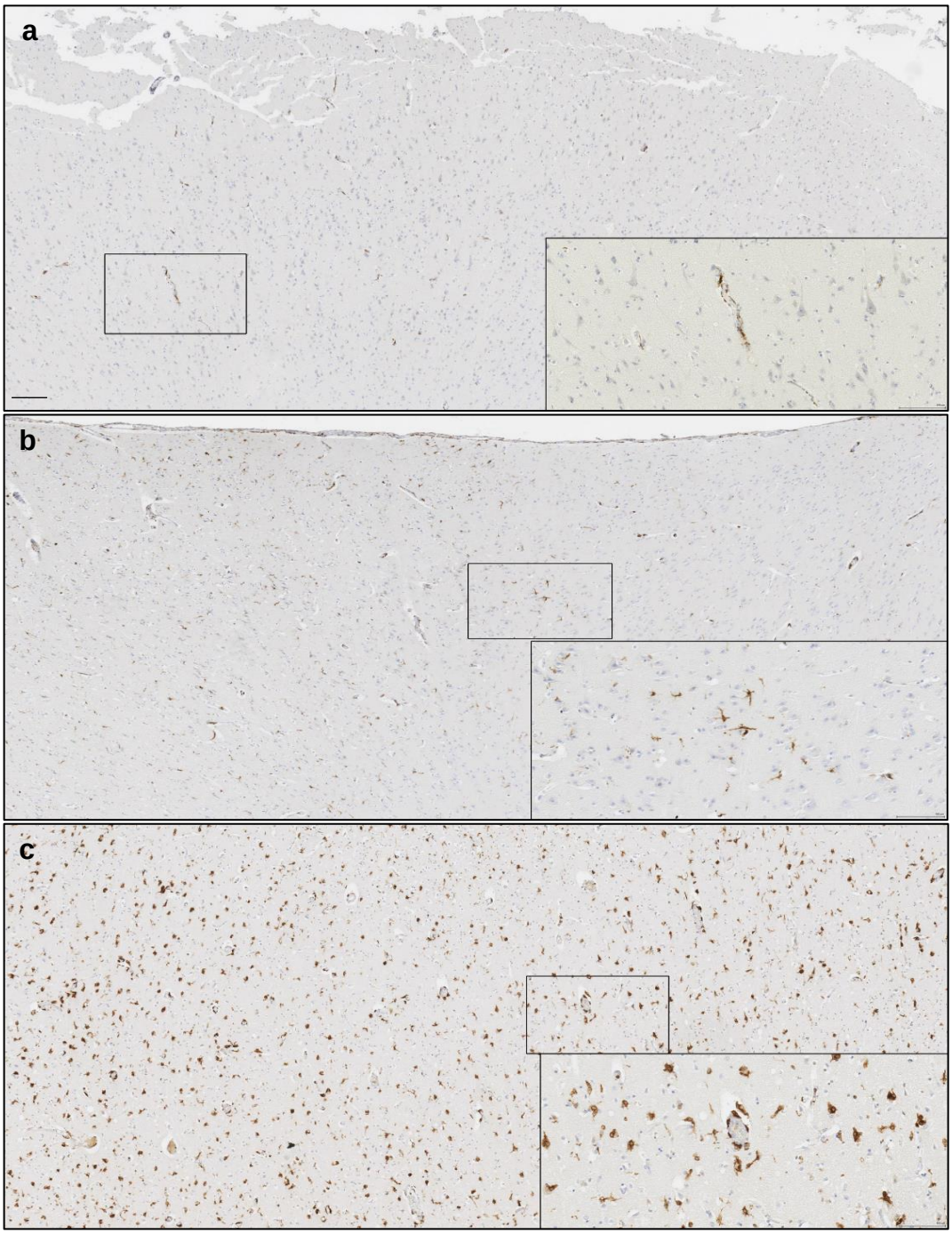

Figure 7-6 Representative images of perivascular microglia in the cingulate gyrus Perivascular CD163 immunoreactive microglia observed sparsely population around blood vessels with an absence of microglia in the surrounding cortex in a (a) 46-year-old male with no history of TBI. In addition to the perivascular microglia observed around the blood vessels, (b) there is a population of ramified CD163 immunoreactive microglia in the surround cortex, in the cingulate gyrus of a 20-year-old male TBI patient who survived 48 hours following an assault. An extensively populated cortical region of the cingulate gyrus (c) with widespread, densely packed CD163 immunoreactive microglia located both around blood vessels and in the surrounding parenchyma in a 19-year-old male TBI patient who survived 5 years following an assault. Scale bar = 1mm, scale bar = 100µm (high magnification)

7.3.2.2 Morphology of CD14 and CD163 in the grey matter regions

In uninjured, control material a predominately ramified, quiescent morphology of both CD14 and CD163 immunoreactive microglia was demonstrated around blood vessels in all grey regions examined. In the cingulate gyrus 1 control demonstrated a mixed population of CD14 immunoreactive microglia. A mixed morphology of CD163 immunoreactive microglia were observed in 2 cases in cingulate gyrus region and 1 case in the cingulate sulcus. No grey matter regions demonstrated an activated amoeboid morphology. Morphologically, the majority of cases in the acute TBI group presented with predominantly ramified, quiescent perivascular microglia throughout grey matter regions with limited number of cases demonstrating a mixed morphology of CD14 and CD163 immunoreactive microglia. In the cingulate gyrus, 21 % of acute TBI cases demonstrated a mixed morphology of CD14 immunoreactive microglia with a similar number (20%) demonstrating a mixed morphology of CD163 immunoreactive cells. No grey matter regions demonstrated an activated amoeboid morphology. In material from the late TBI survivors and similar to the acute TBI material the majority of cases presented with predominantly ramified, quiescent perivascular microglia throughout grey matter regions with limited number of cases demonstrating a mixed morphology of CD14 and CD163 immunoreactive microglia. Only 6% of long-term TBI cases demonstrated a mixed morphology of CD14 immunoreactive cells in the cingulate gyrus and 10% demonstrated with a mixed morphology of CD163 immunoreactive cells in the same region (NS compared with uninjured controls). No grey matter regions demonstrated an activated amoeboid morphology.

7.3.2.3 Distribution of CD14 and CD163 in the grey matter regions

In the control group CD14 and CD163 immunoreactive microglia were predominantly localised to the perivascular space in the grey matter with only 16% of controls demonstrated moderate (score of 1) population of CD14 immunoreactive perivascular microglia in the surrounding cortex whereas only 11% of controls demonstrated moderate (score of 1) population of CD163 immunoreactive microglia to the cortex. No controls displayed an extensive population of microglia in the surrounding cortex (Score of 2). The remaining cases expressed perivascular microglia only (Figure 7-6a**,** Figure 7-7a). A similar pattern was observed in the grey matter of the cingulate sulcus and the thalamus on the control group (Figure 7-7b and c).

From material from the acute TBI survivors, in the cingulate gyrus, 45% of cases demonstrated moderate (score of 1) or extensive (score of 2) population of CD14 immunoreactive microglia in the surrounding cortex (NS). However, 50% of cases demonstrated moderate (score of 1) or extensive (score of 2) population of CD163 immunoreactive microglia in the surrounding cortical region compared with only 11% of cases in the control group ($p = 0.0086$; $\chi 2$; Cramer's $V = 0.413$) (Figure 7-6b, Figure 7-7a). Of those, 7 cases demonstrated an extensive population of CD163 immunoreactive microglia in the cortex. In the cingulate sulcus, 26% and 27% of cases demonstrated a moderate or extensive population of CD14 and CD163 immunoreactive microglia in the surrounding cortex, respectively (Figure 7-7b). A similar pattern was observed in the thalamic region where 35% of cases demonstrated a moderate or extensive population of CD14 immunoreactive microglia beyond the perivascular space and 27% of cases demonstrated a moderate or extensive population of CD163 immunoreactive microglia beyond the perivascular space (NS) (Figure 7-7c).

In the cingulate gyrus from the late TBI group, 47% of cases demonstrated a moderate or extensive population of CD14 immunoreactive microglia in the surrounding cortex compared with 16% in the control group ($p = 0.0347$; $\chi 2$; Cramer's $V = 0.327$). Furthermore, 50% of long-term TBI cases demonstrated a moderate or extensive population of CD163 immunoreactive microglia in the surrounding cortex compared with 11% in the control group ($p = 0.05$; $\chi 2$; Cramer's $V = 0.249$) (Figure 7-6c, Figure 7-7a). Of those, 6 cases demonstrated an extensive population of CD163 immunoreactive microglia in the cortex. In the cingulate sulcus, 31% of cases demonstrated a moderate or extensive population of CD14 immunoreactive microglia in the surrounding cortex (NS compared with uninjured controls) and 38% of cases demonstrated a moderate or extensive population of CD163 immunoreactive microglia in the cortex compared with only 11% in controls ($p = 0.05$; $\chi 2$; Cramer's $V = 0.31$) (Figure 7-7b). In the thalamus 37% of long-term TBI cases demonstrated a moderate or extensive population of CD14 immunoreactive microglia in the surrounding thalamic region ($p = 0.05$; $\chi 2$; Cramer's $V = 0.294$). Furthermore, 36% of cases demonstrated a moderate or extensive population of CD163 immunoreactive microglia in the surrounding thalamic region compared with uninjured controls ($p = 0.05$; $\chi 2$; Cramer's $V = 0.265$) (Figure 7-7c).

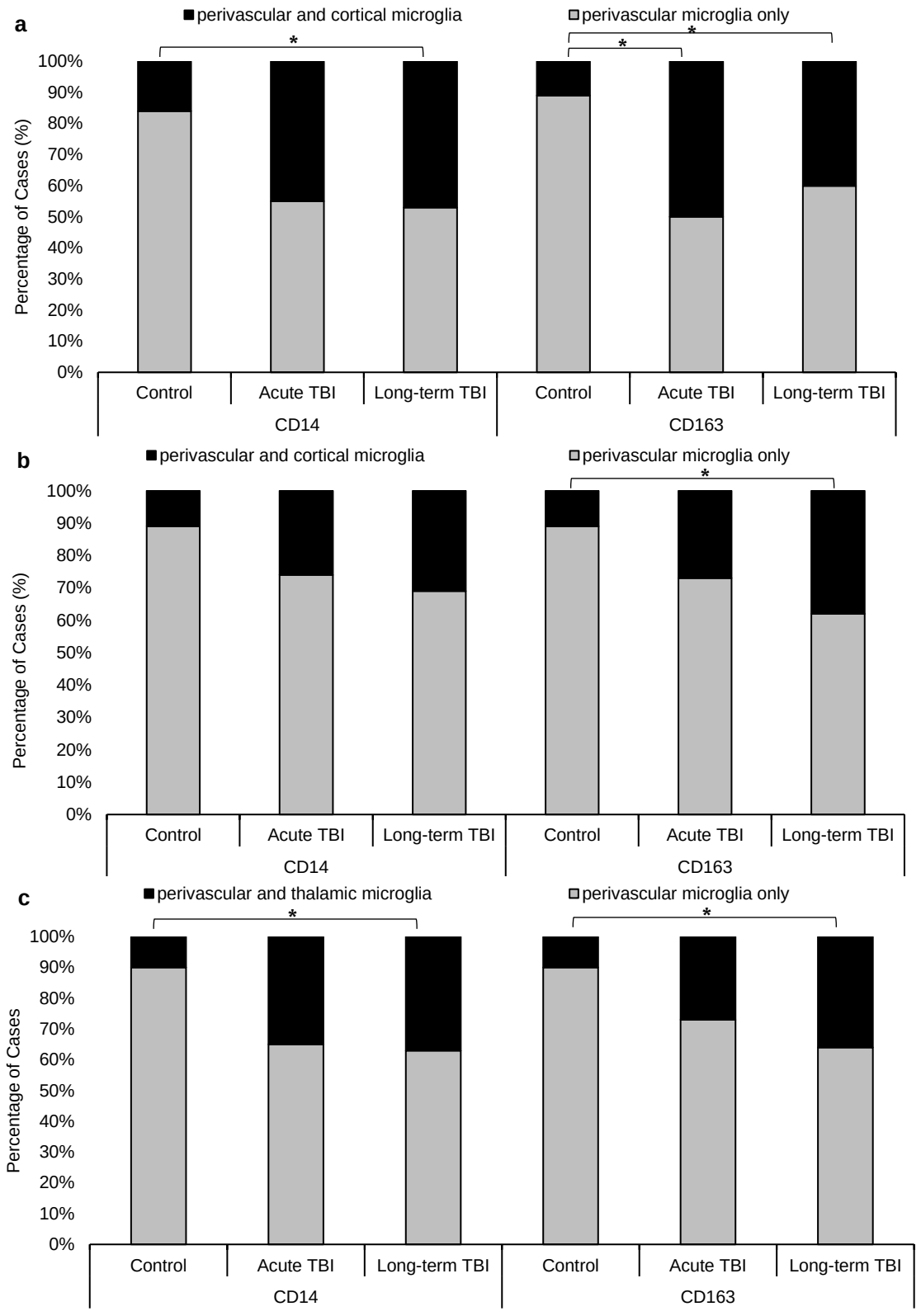

Figure 7-7 Regional distribution of CD14 and CD163 perivascular microglia populated in perivascular space and in surrounding parenchyma. Where uninjured controls expressed predominantly perivascular microglia only, following TBI a proportion of cases in the acute phase and persisting into the late phase (in addition to perivascular microglia) expressed a population of CD14 and CD163 microglia in the surrounding parenchyma in the (a) cingulate gyrus (b) cingulate sulcus and (c) thalamic regions (* $p < 0.01$; $\chi 2$ TBI cohort vs control CD14/CD163 positivity).

7.4 Discussion

This study has demonstrated that activated perivascular microglia in white matter late after exposure to TBI predominantly express an M2-like phenotype. In contrast, and further supporting observations in Chapter 7, there was no notable microglial activation in grey matter in the acute or late phase post-injury in this material. However, following TBI there was a noted extension of perivascular microglia into the surrounding grey matter parenchyma. In contrast to white matter neuroinflammation, was observed in the acute phase and continued into the chronic phase, with both M1-like and M2-like phenotypic profiles being expressed.

In addition to this extensive chronic white matter microglia activation following a single, moderate to severe TBI the activated microglia are observed to predominantly have a M2-like phenotypic profile. Evidence of the microglial phenotypic profiles and temporal course following TBI is limited, with all work to date carried out in animal models of TBI. Where several CCI models report a mixed microglia phenotype 5-7 days post-TBI (Morganti et al., 2016, Turtzo et al., 2014), others report a predominant M1-like phenotype which peaks at 7 days post-TBI (Kumar et al., 2016a, Kumar et al., 2016b) which remains elevated for up to 21-28 days following TBI (Wang et al., 2013, Jin et al., 2012).The lifespan of the mice used in these studies is short; therefore, the temporal course of the microglial phenotypic profiles in humans following TBI is still unknown. This present study has shown that where there is no increase in microglial activation in the acute phase, there is extensive amoeboid microglial activation, up to 4 years post-TBI and the activated microglia present with a predominantly M2-like phenotype.

The characterisation of microglial phenotypes has evolved rapidly from the previous dichotomy (M1 and M2 specific phenotypes) (Ransohoff, 2016) to the current paradigm of a microglial spectrum of functionality. The understanding that microglia become polarized along an activation spectrum, ranging from the classic M1-like phenotype to an alternative M2-like phenotype is now globally accepted (Colton, 2009, Simon et al., 2017)**.** Activated microglia display various phenotypes depending on their responses to different stimuli, sequence of stimuli, and duration of exposure (Perry et al., 2010). The concept that microglia have a range of responses to a number of different stimuli is much more relevant than the limited concept of microglial behaviour as previously thought. In this present study, a late activation of microglia presents on the activation spectrum with an M2-like profile.

In addition to the white matter microglial activation observed in this study, there is also a noted increase of CD14 and CD163 microglia in the grey matter, beyond the perivascular space. While in health, CD14 and CD163 are exclusively expressed in perivascular microglia (Cosenza et al., 2002, Williams et al., 2001a, Ulvestad et al., 1994, Borda et al., 2008, Kim et al., 2006), in this study, these markers are also expressed in microglia in the surrounding cortical regions following TBI. This shift of the "status quo" occurs early after injury and persists into the late phase. Several animal models studying the effects of simian immunodeficiency virus demonstrate this pathology. Borda *et al* (2008) reported CD163 as a selective marker of perivascular macrophages in normal macaques; however, further down the disease progression, CD163 positive microglia are also found in parenchyma (Borda et al., 2008). Borda *et al*, (2008) suggest that this expression of CD163 in parenchymal microglia is due to vascular compromise. This pattern of CD163 expression in the parenchyma is also observed in other animal studies (Kim et al., 2006, Williams et al., 2001a) and in humans investigating human immunodeficiency virus-associated encephalitis (HIVE), AD and Parkinson's disease (Filipowicz et al., 2016, Roberts et al., 2004, Fabriek et al., 2005, Pey et al., 2014). Furthermore, a similar pattern is observed in CD14 expression in HIV infected patients (Fischer-Smith et al., 2001, Cosenza et al., 2002).

Following TBI, these specific perivascular microglial markers have also been observed beyond the perivascular space, in the surrounding parenchyma. Using an open skull weight-drop contusion model, Zhang *et al* (2012) investigated the accumulation of CD163 microglia following TBI. In uninjured control rats CD163 expression was restricted to perivascular and meningeal microglia but not to parenchymal microglia, however, following TBI, they reported significant CD163 immunoreactive microglia with an amoeboid morphology accumulating in the parenchyma (Zhang et al., 2012). This accumulation was observed two days post-TBI and increased in the investigated survival time (up to 96 hours post-TBI). Parenchymal accumulation of CD14 microglia were also observed following TBI in humans (Beschorner et al., 2002a). Similar to CD163 microglia, detection of CD14 in controls was solely by perivascular cells and not in parenchymal microglial cells, however, the number of CD14 microglia in the parenchyma increased within 1 – 2 days post injury; peaked at 4 – 8 days and remained elevated weeks after injury (Beschorner et al., 2002a). This pattern of parenchymal CD14 microglia was also observed in cases of focal cerebral infarctions (Beschorner et al., 2002b).

The present study supports previous observations as it demonstrates parenchymal accumulation of both CD14 and CD163 microglia following TBI. Where the previous human

TBI study investigated brains from 25 patients with an average survival time of 11 days ± 7 days (Beschorner et al., 2002a), this study presents the first evidence of long-term parenchymal accumulation with both CD14 and CD163 observed in the parenchyma of a TBI patient who survived 9 years following a fall. Although, where the previous studies report a focal pathology of parenchymal accumulation around TBI lesions of both CD14 (Beschorner et al., 2002a) and CD163 (Zhang et al., 2012) and in ischemic lesions (Beschorner et al., 2002b) this study displays diffuse accumulation of CD14 and CD163 in cingulate gyrus and thalamic regions. In addition, Zhang *et al* reported CD163 amoeboid activation of the accumulating microglia at the ipsilateral cortex (lesion site); in this study no amoeboid microglia in the grey regions was observed. Whether this accumulation of specific perivascular microglia in the parenchyma is due to migration of the microglia beyond the perivascular space in response to stimuli or that the specific perivascular markers CD14 and CD163 are upregulated in other non-perivascular microglia, it is to be elucidated.

7.4.1 Conclusion

In conclusion, this study demonstrated that in relation to perivascular microglia, the M2-like phenotype is upregulated in activated microglia in the white matter tracts, specifically the corpus callosum, of late survivors following TBI. Furthermore, in the grey matter, there is a widespread, diffuse parenchymal accumulation of perivascular microglia following TBI; however, unlike the white matter pathology, this observation occurs in the acute phase and continues into the chronic phase with both markers being upregulated and no amoeboid activation is observed. These regional differences between the microglial responses following TBI are interesting and warrant further investigations, specifically in regard to their association with BBB disruption.

8 Concluding Remarks

8.1 Summary

The data presented here indicate that following a single, moderate to severe TBI several vascular and cellular pathologies can be induced that may be associated with neurodegenerative diseases. Specifically, BBB disruption is observed in the grey matter regions and occurs in the acute phase in a proportion of survivors which persists into the late phase following injury. Interestingly, where BBB disruption was reported in a cohort of paediatric TBI cases it was preferentially distributed to small vessels unlike adult TBI where BBB disruption was predominantly in larger vessels. In addition to this vascular pathology, these studies elucidate a previously unreported neuroinflammatory response to TBI with specific cellular, anatomical and temporal characteristics. Specifically, in grey matter regions a reactive interface astrogliosis is observed subpially, around cortical vessels, at the boundary between cortical grey and white matter, and subependymally. This interface astrogliosis is evidenced in a proportion of acute and continues into the late phase following TBI and is grey matter centric with no observed white matter change. In contrast, while astrogliosis after TBI is immediate and long-lasting and localised to grey matter, microglial activation is delayed and localised to white matter tracts. In addition, perivascular microglia contribution to this delayed microglial response expressed a predominantly M2-like phenotype. Furthermore, there was extension of microglia into the parenchyma from the perivascular space in grey matter, observed in the acute phase and persisting in a proportion of patients surviving years following injury.

8.2 Vascular Response following TBI

Blood-brain barrier disruption has been demonstrated in the acute phase following TBI using several animal models, however, the evidence of the temporal course is conflicting (Barzo et al., 1996, Habgood et al., 2007, Baldwin et al., 1996, Shapira et al., 1993, Rinder and Olsson, 1968, Shreiber et al., 1999, Smith et al., 1995, Cortez et al., 1989, Ommaya et al., 1964, Hekmatpanah and Hekmatpanah, 1985, Hicks et al., 1993, Povlishock et al., 1978, Baskaya et al., 1997). In addition to animal models of TBI, several clinical studies report elevated levels of serum albumin and S100β in the cerebrospinal fluid (CSF) following a severe TBI, suggesting BBB disruption, (Saw et al., 2014, Stahel et al., 2001, Ho et al., 2014a, Blyth et al., 2009) and one retrospective cohort study observed BBB disruption in nearly half of TBI patients (Ho et al., 2014a). This is the first autopsy study to present BBB

disruption following TBI which appears in the acute phase and persists into the late phase. Furthermore, there is preferential distribution to the crests of the gyri than the depths of the sulci and in the deep layers of the cortex.

A key feature of CTE is abnormal accumulation of hyperphosphorylated tau (Smith et al., 2013) which has also been reported in late survivors of sTBI (Johnson et al., 2012). Interestingly, tau pathology is characterised by the accumulation of abnormal, hyperphosphorylated tau in both neurons and glia, around vessels and with preferential involvement of the depths of the sulci in the neocortical grey matter (Omalu et al., 2011a, McKee et al., 2009). Furthermore, the extravasation of serum proteins such as FBG have been demonstrated to correlate with the presence of AD-type pathology (Viggars et al., 2011). Where similarities in pattern of distribution between tau and BBB disruption are observed (around blood vessels, in neurons and glia) the conflicting distribution in the depths of the sulci and crests of the gyri would be interesting to further investigate. One hypothesis could be that the crests of the gyri are more susceptible to vascular damage than protective location of the depths of the sulci, however, further work would be required to prove this.

Furthermore, it has been well documented that possession of the ε4 allele of the *APOE* gene is also associated with an increased risk of AD (Corder et al., 1993, Saunders et al., 1993) and, to a limited extent, in CTE(Jordan et al., 1997, Kutner et al., 2000, Stein et al., 2015). The APOE protein transports cholesterol to neurons via lipoprotein (LDLR) receptors (Bu, 2009) and supports maintenance and integrity of the BBB (Obermeier et al., 2013). Furthermore, *APOE* knockout mice demonstrated increased vascular permeability, and more specifically, *APOE* ε4 is observed to promote BBB disruption (Hafezi-Moghadam et al., 2007, Nishitsuji et al., 2011, Bell et al., 2012). Unfortunately, cohort numbers were challenging in this work but investigating the relationship between post-TBI BBB disruption and the *APOE* ε4 in association with an increased risk of dementia-like pathologies would be beneficial and may indicate areas of therapeutic intervention.

In addition to a suggested genetic link with post-TBI BBB disruption, investigating the structural deficiencies that occur during the loss of BBB integrity both in the acute phase and late phase would be valuable. Primary damage of the BBB has been described as a result of mechanical forces on the brain that results in acute changes such as shearing injuries, contusions, and haematomas; whereas a secondary BBB damage is due to such events as oedema, inflammation and neurotoxic periphery substances (such as Fibrinogen) entering the CNS (Shlosberg 2010, Price 2016, Petersen et al., 2018). Whether the acute phase post-

TBI BBB breakdown observed in this work was due to primary damage and the late phase post-TBI BBB breakdown was due to secondary damage is unknown but further experiments could confirm this.

Other structural anomalies, such as pericyte loss may also be responsible for the post-TBI breakdown. Pericytes contribute to the stability to microvessels and tight localization of the pericytes with the endothelial cell is crucial for BBB integrity (Armulik et al., 2010, Daneman et al., 2010, Bell et al., 2010, Winkler et al., 2011). Several animal studies have been able to demonstrate that degradation of pericytes can lead to vascular damage by BBB breakdown and subsequence toxic influx and by diminished capillary perfusion (Armulik and Betsholtz, 2010, Bell et al., 2010, Winkler et al., 2011). Furthermore, a reduction of pericytes has been observed in AD patients (Sagare et al., 2013) and in limited animal studies following TBI (Zehendner et al., 2015). This would be an interesting study to undertake and may provide valuable insight to underlying structural deficiencies in post-TBI vessels.

Furthermore, in sharp contrast to adult TBI cases, BBB disruption in paediatric cases appears preferentially distributed to vessels of 10μm or less in diameter, in keeping with capillary sized vessels. This vulnerability of the small vessels was rarely observed in adult material. A notable pathology observed in paediatric TBI is diffuse brain swelling (DBS) where incidence of DBS in clinical series of paediatric severe TBI approximately twice that recorded in adults and is also associated with high mortality (Kazan et al., 1997). DBS can be observed even after mild injury when it is often referred to as second impact syndrome (SIS). Interestingly, where the majority of paediatric TBI cases with reported DBS also presented with BBB disruption, those disrupted vessels showed a propensity to smaller vessels. This suggests there could be a correlation between the capillary pathology and DBS however more work would be required to confirm this. Imaging studies on paediatric TBI patients to record the CBF and CBV and, if any, associated BBB disruption, shortly after injury would be fundamental in understanding the mechanisms behind DBS and may identify key therapeutic targets.

8.3 Cellular response following TBI

In addition to the BBB disruption observed, evidence of a differential glial response following a single, moderate to severe TBI was demonstrated, with reactive astrogliosis localised to the grey matter and activated microglia localised to the white matter. Further, while reactive astrogliosis is evident immediately after injury and persists into the chronic

phase, in contrast, the microglial response evolves after the acute period following injury and persists in white matter in the chronic phase.

This pattern of astrogliosis has been reported in ALS (Nagy et al., 1994), however, only one other post-mortem study has documented this distinct pattern of astrogliosis following TBI, and there following exposure to blast injury (Shively et al., 2016). The study had concluded that the pattern was unique to blast injuries as they did not find the same distribution in their limited series of sTBI cases. Although the sTBI number in that study were small this is an interesting conflict of evidence. Perhaps, this astroglial phenomenon is purely a consequence of TBI, regardless of mechanism of injury or, perhaps, blast injuries sustain a similar closed rotational injury as observed in sTBI (McKee and Robinson, 2014) and therefore may present with the same pathologies. Future studies would be fundamental in supporting these interesting possibilities.

Furthermore, this distinct astroglial pattern is noted to be a grey matter pathology which creates interesting hypotheses around associations with other grey matter pathologies following TBI. This work has demonstrated BBB disruption in the grey matter with preferential distribution in the crests of the gyri than the depths of the sulci and in the deep layers of the neocortical ribbon; the distribution of reactive astrocytes follows a similar pattern. Astrocytes have a key role in maintaining and supporting the BBB (Cabezas et al., 2014) and have previously been reported to be involved in BBB disruption in animal models (Wang et al., 2014) and in AD patients (Zenaro et al., 2017). In addition, studying the relationships to other grey matter pathologies observed following TBI such as abnormal accumulation of tau would be interesting. Tau deposits have been reported following sTBI and CTE around blood vessels, in neurons and glia with preferential involvement of the depths of the sulci in the neocortical grey matter (Smith et al., 2013, Omalu et al., 2011a, McKee et al., 2009, McKee et al., 2010, McKee et al., 2013, Goldstein et al., 2012, Johnson et al., 2012, Stewart et al., 2016), furthermore, tau-immunoreactive thorn-shaped astrocytes are demonstrated in subpial and perivascular locations in the neocortex and subependymally (McKee et al., 2013). This juxtaposition between reactive astrocytes and tau at the subpial plate, around vessels and in the subependymal zone is interesting, however, conflicting patterns in the neocortical layers and in the sulci and gyri could be further investigated. Furthermore, although numbers were challenging in this study, investigating the association between reactive astrocytes and other grey matter pathologies such as BBB disruption and tau may provide a clearer understanding of the chronic pathologies observed following TBI and the mechanisms driving them.

In addition to the grey matter astroglial pathology observed, there is a delayed microglial response arising in the white matter tracts which appears after the acute phase and persists late after TBI. Supporting this study is a previous autopsy study where amoeboid microglia were reported in the corpus callosum of a proportion of chronic TBI cases (Johnson et al., 2013a). In contrast, an *in vivo* positron emission tomography study have reported have reported no significant differences in binding in these regions yet have reported a difference in binding in the grey matter of the thalamic region (Ramlackhansingh et al., 2011b). This imaging study used the marker PK-11195 which binds selectively to the peripheral benzodiazepine receptor (PBR; also known as Translator Protein, TSPO), which is upregulated in both microglia and reactive astrocytes (Chechneva and Deng, 2016a). As such, given the observations reported in this thesis, the possibility that imaging studies in vivo following TBI using such TSPO ligands might be reporting ligand binding to a reactive astrogliosis in grey matter, rather than microgliosis as reported, should be considered.

Interestingly, axonal damage following TBI has been reported in white matter tracts (Johnson et al., 2013c, Browne et al., 2011). Specifically, sites of microglial activation have previously been reported to coincide with neuronal degeneration and axonal abnormality (Maxwell et al., 2010, Giunta et al., 2012). In addition, oligodendrocytes may contribute to post-TBI white matter pathology (Flygt et al., 2016). Oligodendrocytes provide support and insulation for axons therefore, much like the supporting pericytes in the BBB, loss of such fundamental cellular components may render the axons vulnerable to further damage. Further studies to investigate co-localisation of axonal damage and microglial activation, in addition to the impact of oligodendrocytes following TBI would be beneficial and may contribute to sourcing therapeutic targets.

Regarding specific subpopulations of perivascular microglia, these studies show a polarization towards the M2-like phenotype in activated microglia in the white matter tracts. Microglia have diverse spectrums of functionality, which range from the neurotoxic and pro-inflammatory M1-like phenotype, through to the neuroprotective and immunosuppressive roles of the M2-like phenotype (Mantovani et al., 2012, Loane and Kumar, 2016, Gordon, 2003). In animal models of TBI, some studies suggest a predominantly elevated M1-like phenotypic expression (Kumar et al., 2016a, Wang et al., 2013, Jin et al., 2012). However, to-date, this current body of work is the first to explored microglia phenotypes in human TBI, where this study demonstrates that the M2-like phenotype is predominantly expressed in the late phase. Within the polarization spectrum, the M2 phenotype lies towards the anti-inflammatory functionality where M2-like expression is believed to be beneficial and

neuroprotective. Therefore, exploiting favourable properties the microglial states by modulating their phenotypic expression would provide key therapeutic targets.

Interestingly, in addition to the white matter activation of microglia there is a change in the grey matter in a subpopulation of perivascular microglia following TBI. Immediately after injury and persisting into the late phase, perivascular microglia are observed to populate, and increase in density, in the surrounding parenchyma. Similar responses have been reported in animal models of TBI and autopsy studies where the number of perivascular microglia increase in the parenchyma (Beschorner et al., 2002a, Zhang et al., 2012). In addition, in one study of spinal cord injury reports where microglia become enlarged with retracted processes (amoeboid morphology) in the white matter, in contrast, in the grey matter ramified microglia become activated without morphologic transformation (McKay et al., 2007), similar to observations in this study. Whether this accumulation of perivascular microglia in the parenchyma is due to migration of the microglia beyond the perivascular space in response to stimuli, perivascular markers being upregulated in non-perivascular microglia or an infiltration of periphery monocytes is unknown. Further work utilising novel markers such as TMEM could be performed to address if the microglia observed are infiltration monocytes, additionally, further experiments using perivascular markers such as CD45 and CD11b could be performed to confirm the findings in this study.

Future studies investigating the association between the grey matter microglial changes and BBB disruption post-TBI would be valuable in understanding the underlying mechanisms driving post-TBI pathology. Numbers were limited, and any associations could not be determined. Several studies support a relationship between a change in perivascular microglia and BBB disruption (Borda et al., 2008, Davalos et al., 2012). As with astrocytes, microglia form close relationships with the BBB where microglia can influence barrier function (Obermeier et al., 2013). Activation of microglia induces the release of several cytokines such as IL-1β and VEGF which promotes BBB breakdown as seen in AD (Obermeier et al., 2013, da Fonseca et al., 2014, Zenaro et al., 2017). Using markers for VEGF and IL-1β experiments could determine the impact of circulating cytokines on the BBB following TBI. In addition, fibrinogen which is observed in the grey matter regions post-TBI in response to BBB disruption, is reported to activate microglia in AD and induce perivascular clustering (Davalos et al., 2012, Petersen et al., 2018) therefore further understanding on the impact of this neurotoxic substance on the CNS would be beneficial.

This inflammation response post-TBI appears region specific with reactive astrocytes accumulating in the grey matter interfaces, perivascular microglia expressing post-TBI change in the grey matter and activated microglia dominating the white matter tracts. In multiple Sclerosis (MS), white matter lesions are pathologically characterized by the presences of infiltrating immune cells while grey matter lesions have an absence of immune cells (Bo et al., 2006). Furthermore, predominant white matter microglia activation has been observed in the ageing brain and in AD(Raj et al., 2017). Whereas, reactive astrocytes have been reported in the cortical grey matter of ALS (Nagy et al., 1994), however, evidence of this regionally specific inflammation response is limited. Understanding these regional differences in astrocytes and microglia would benefit the wider knowledge of post-TBI pathologies. Whether following TBI, reactive astrocytes are 'switched on' in response to BBB disruption and infiltrating substances in the grey matter while activated microglia target the white matter in response to axonal disruption and subsequence cellular debris is unknown but a possible hypothesis. Exploiting these regional specific responses could create potential therapeutic pathways in post-TBI neurodegeneration.

In summary, this work has demonstrated a distinct vascular response following a single, moderate to severe TBI in humans; furthermore, a persistent cellular response appears in the early phase in distinct regions of the white matter and grey matter. All tissue collected for this work was retrospective, limited clinical data was available and some numbers were challenging. Therefore, associations between pathological findings and clinical outcomes observed are difficult. Prospective studies would be highly advantageous in order to investigate the distinct vascular and cellular responses observed together with the nature of injury, clinical outcomes and possible therapeutic interventions. Another limiting factor was the small study numbers, larger number of cases would allow investigation of associations between the vascular response and cellular pathology observed. Nonetheless, these findings may indicate potential therapeutic interventions by targeting the loss of vascular integrity and may be interesting to examine these findings in context along with associations with known TBI pathologies.

Table 13 Summary of aims, findings and possible future investigations

Hypotheses	Aims	Findings	Future investigations
sTBI results in disruption of BBB function acutely and in long-term survivors.	To characterise the pattern, distribution and temporal evolution of BBB disruption at varying survivals from sTBI.	BBB disruption is observed in the grey matter regions and occurs in the acute phase in a proportion of survivors which persists into the late phase following injury. In addition, in paediatric TBI BBB disruption is preferentially distributed to small vessels	1. Investigate the structural components of the BBB disruption following TBI 2. Investigate the association with Tau, Amyloid and inflammation 3. Investigate the association with *APOE* 4. Investigate the impact on CBF and CBV 5. Investigate the pattern and distribution of BBB disruption
sTBI results in a mixed astroglial and microglial neuroinflammatory response that is geographically and temporally distinct.	To characterise the extent, distribution and temporal evolution of the astroglial and microglial response to sTBI.	In grey matter regions a reactive interface astrogliosis is observed subpially, around cortical vessels, at the boundary between cortical grey and white matter, and subependymally. However, microglial activation is an observed delayed response and localised to the white matter tracts	1. Investigate the associations with astrocytes and BBB 2. Investigate the associations with astrocytes and tau. 3. Investigate microglia activation and axonal damage and oligodendrocytes 4.Investigate relationship between microglia and infiltrating monocytes
The microglial response to sTBI is defined by phenotypically distinct microglial population.	To determine the microglial phenotypes associated with survival from sTBI.	M2-like phenotype is apparent in the delayed activated response in the white matter tracts.	1. Further understanding of Microglial phenotypes post-TBI. 2. Investigate the perivascular microglia with association with BBB 3. Further understanding of the perivascular microglia in the grey matter

Appendix 1 Ethical Approval

WoSRES
West of Scotland Research Ethics Service

NHS
Greater Glasgow and Clyde

West of Scotland REC 4
Ground Floor, Tennent Building
Western Infirmary
38 Church Street
Glasgow
G11 6NT
www.nhsggc.org.uk

Date 10 November 2015
Direct line 0141-211-1722
Fax 0141-211-1847
e-mail Wosrec4@ggc.scot.nhs.uk

Ms Jane Hair
NHS GG&C Biorepository
3rd Floor Laboratory Medicine Building
Southern General Hospital
Glasgow
G51 4TY

Dear Ms Hair

Title of the Research Tissue Bank:	**NHSGGC Biorepository and Pathology Service Tissue Resource**
REC reference:	**10/S0704/60**
Designated Individual:	**Ms Jane Hair**
Amendment number:	**AM04**
Amendment date:	**22 October 2015**
IRAS project ID:	**66111**

The following amendment was reviewed by the Sub-Committee in correspondence:

- The inclusion of the traumatic brain injury tissue collected under study reference 07/S0710/45 and samples from healthy volunteers participating in associated brain injury studies in the Biorepository.

  Also inclusion of samples from the healthy volunteer study, "The Long Term Outcomes of Participation in Elite Level Rugby", in the Biorepository.

  As satellite collections they will be compliant with the Health Improvement Scotland Tissue Banking standards.

Ethical opinion

The Sub-Committee asked for clarification of the types of tissue involved in this substantial amendment and you explained that the tissue from 07/S0710/45 was blood material and the tissue from The Long Term Outcomes of Participation in Elite Level Rugby was blood and brain tissue.

The members of the Committee present gave a favourable ethical opinion of the amendment on the basis described in the notice of amendment form and supporting documentation.

Approved documents

The documents reviewed and approved at the meeting were:

Document	*Version*	*Date*
Notice of Substantial Amendment (RTBs)	AM04	22 October 2015
Other [Letter from Professor Andrew Rankin]	-	22 January 2014

Membership of the Committee

The members of the Ethics Committee who were present at the meeting are listed on the attached sheet.

Statement of compliance

The Committee is constituted in accordance with the Governance Arrangements for Research Ethics Committees and complies fully with the Standard Operating Procedures for Research Ethics Committees in the UK.

We are pleased to welcome researchers and R & D staff at our NRES committee members' training days – see details at http://www.hra.nhs.uk/hra-training/

10/S0704/60	**Please quote this number on all correspondence**

Yours sincerely

For **Dr Brian Neilly**
Chair

Enclosures: *List of names and professions of members who were present at the meeting*

Copy to: *R&D Office, Tennent Building, Western Infirmary*

West of Scotland REC 4

Attendance at Sub-Committee of the REC meeting in November 2015

Committee Members:

Name	*Profession*	*Present*	*Notes*
Miss Fiona Mackelvie	Retired Administrator	Yes	
Dr Brian Neilly (Chair)	Consultant Physician	Yes	
Dr Giles Roditi	Consultant Radiologist	Yes	

Also in attendance:

Name	*Position (or reason for attending)*
Mrs Evelyn Jackson	REC Manager

Appendix 2 Full Cohort and demographics

		TBI: Acute Survival (n = 74)	TBI: Intermediate Survival (n = 11)	TBI: Long-Term Survival (n = 32)	Controls (n = 30)
Mean age (Range)		24 years (4-60)	32 years (17-56)	46.3 years (19-60)	28.3 (7-60)
Males		53 (72%)	11 (100%)	31 (96.9%)	18 (60%)
Mean PM Delay (Range)		46.7 hours (3-240)	74.7 hours (26-192)	65.5 hours (9-184.5)	76.3 hours (12-264 hours)
Mean Survival Interval (Range)		69.1 hours (1-216)	72.8 days (14-279)	7.8 years (1-47)	Not applicable
Cause of TBI	Fall	21 (28.4%)	2 (18%)	15 (46.9%)	Not applicable (No history of TBI)
	RTA	48 (64.9%)	5 (41.6%)	5 (15.60%)	
	Assault	9 (12.2%)	3 (25%)	8 (25%)	
	Unknown	1 (3.7%)	1 (8.3%)	4 (12.5%)	
Cause of Death	Head injury	70(94.6%)	4 (33.3%)	0	0
	Bronchopneumonia	2(2.7%)	4(33.3%)	7(21.9%)	1(3.33%)
	ARDS	2(2.7%)	2(16.7%)	1(3.125%)	0
	Pulmonary thromboembolism	0	1(8.3%)	0	2 (6.67%)
	Heart disease	0	0	6 (18.8%)	6(20%)
	Alcohol related	0	0	2(6.25%)	1 (3.33%)
	Pyelonephritis	0	0	1(3.125%)	1 (3.33%)
	Multi-organ failure	0	0	1(3.125%)	1 (3.33%)
	GIT haemorrhage	0	0	1(3.125%)	1 (3.33%)
	Polytrauma	0	0	1(3.125%)	1 (3.33%)
	Drug overdose	0	0	0	4(13.33%)
	SUDEP			7(21.9%)	8(26.67%)
	Pulmonary oedema	0	0	1(3.125%)	0
	Septicaemia	0	0	0	2(6.67%)
	Inhalation of gastric contents	0	0	0	2(6.67%)
	Unknown	0	0	4(12.5%)	0

Key: *TBI = traumatic brain injury; SUDEP = sudden unexpected death in epilepsy; GIT = gastrointestinal tract; ARDS*
= acute respiratory distress syndrome; RTA = road traffic accident

Appendix 3 List of Antibodies

Antigen	Clone/description	Antibody Source	Method of Antigen Retrieval	concentration
Fibrinogen	Polyclonal rabbit	Dako, USA	Microwave pressure cooker and Tris Buffer (pH8)	1:17,500
IgG	Polyclonal rabbit	Dako, USA	Microwave pressure cooker and Tris Buffer (pH8)	1:10,000
CD34	QBEnd/10	Leica Biosystems, UK	Microwave pressure cooker and Tris Buffer (pH8)	1:100
Collagen IV	CIV 22	Dako ,USA	Microwave pressure cooker and Tris Buffer (pH8)	1:25
GFAP	GA 5	Leica Biosystems, UK	Microwave pressure cooker and Tris Buffer (pH8)	1:250
CR343	Anti-Human HLA-DP,DQ,DR	Dako, USA	Microwave pressure cooker and Tris Buffer (pH8)	1:800
IBA-1	C-terminus of Iba1 Polyclonal rabbit	Wako		1:5000
CD14	goat polyclonal	Abcam, UK	Microwave pressure cooker and Tris Buffer (pH8)	1:500
CD163	10D6	Leica Biosystems, UK	Microwave pressure cooker and Tris Buffer (pH8)	1:1000

Appendix 5 Permissions

Self-Archiving Policy B

Dear Jennifer Hay,

RE Jennifer R. Hay ***et al*** Blood-Brain Barrier Disruption Is an Early Event that May Persist for Many Years After Traumatic Brain Injury in Humans. *Journal of Neuropathology* (2015) 74 (12): 1147-1157

Thank you for your recent email requesting permission to reuse all or part of your article in a thesis/dissertation.

As part of your copyright agreement with Oxford University Press you have retained the right, after publication, to use all or part of the article and abstract, in the preparation of derivative works, extension of the article into a booklength work, in a thesis/dissertation, or in another works collection, provided that a full acknowledgement is made to the original publication in the journal. As a result, you should not require direct permission from Oxford University Press to reuse your article.

However, in line with the journal self-archiving policy, you may only include your **Accepted Manuscript (AM)** in your thesis/dissertation and public availability must be delayed until **12 months** after first online publication in the journal. You should include the following acknowledgment as well as a link to the version of record.

This is a pre-copyedited, author-produced version of an article accepted for publication in [insert journal title] following peer review. The version of record [insert complete citation information here] is available online at: xxxxxxx [insert URL and DOI of the article on the OUP website].

Please Note: Inclusion under a Creative Commons license or any other open-access license allowing onward reuse is prohibited.

For full details of our publication and rights policy please see the attached link to our website:
http://www.oxfordjournals.org/en/access-purchase/rights-and-permissions/self-archiving-policyb.html

If you have any other queries, please feel free to contact us.

Kind regards,

Aaron Edwards | Permissions Assistant|Rights Department
Academic and Journals Divisions|Global Business Development
Oxford University Press | Great Clarendon Street | Oxford | OX2 6DP

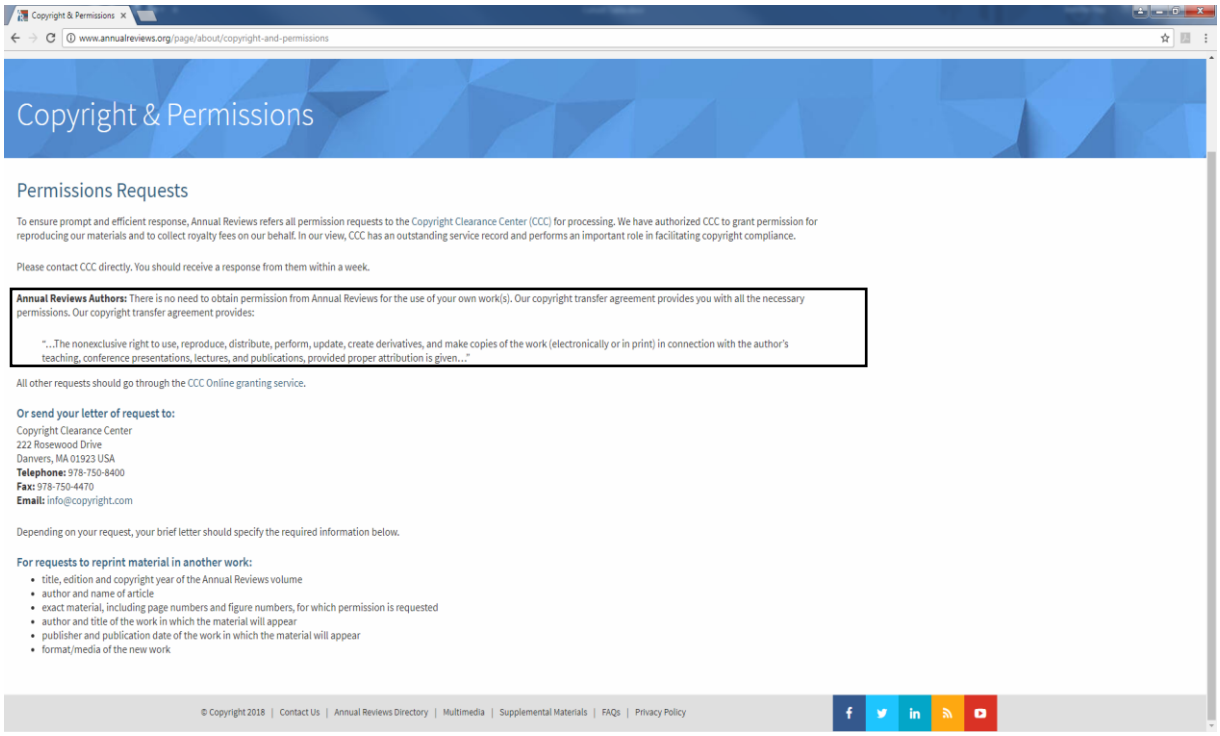

Copyright & Permissions

www.annualreviews.org/page/about/copyright-and-permissions

Copyright & Permissions

Permissions Requests

To ensure prompt and efficient response, Annual Reviews refers all permission requests to the Copyright Clearance Center (CCC) for processing. We have authorized CCC to grant permission for reproducing our materials and to collect royalty fees on our behalf. In our view, CCC has an outstanding service record and performs an important role in facilitating copyright compliance.

Please contact CCC directly. You should receive a response from them within a week.

Annual Reviews Authors: There is no need to obtain permission from Annual Reviews for the use of your own work(s). Our copyright transfer agreement provides you with all the necessary permissions. Our copyright transfer agreement provides:

> "...The nonexclusive right to use, reproduce, distribute, perform, update, create derivatives, and make copies of the work (electronically or in print) in connection with the author's teaching, conference presentations, lectures, and publications, provided proper attribution is given..."

All other requests should go through the CCC Online granting service.

Or send your letter of request to:

Copyright Clearance Center
222 Rosewood Drive
Danvers, MA 01923 USA
Telephone: 978-750-8400
Fax: 978-750-4470
Email: info@copyright.com

Depending on your request, your brief letter should specify the required information below.

For requests to reprint material in another work:

- title, edition and copyright year of the Annual Reviews volume
- author and name of article
- exact material, including page numbers and figure numbers, for which permission is requested
- author and title of the work in which the material will appear
- publisher and publication date of the work in which the material will appear
- format/media of the new work

https://www.elsevier.com/about/our-business/policies/copyright/permissions

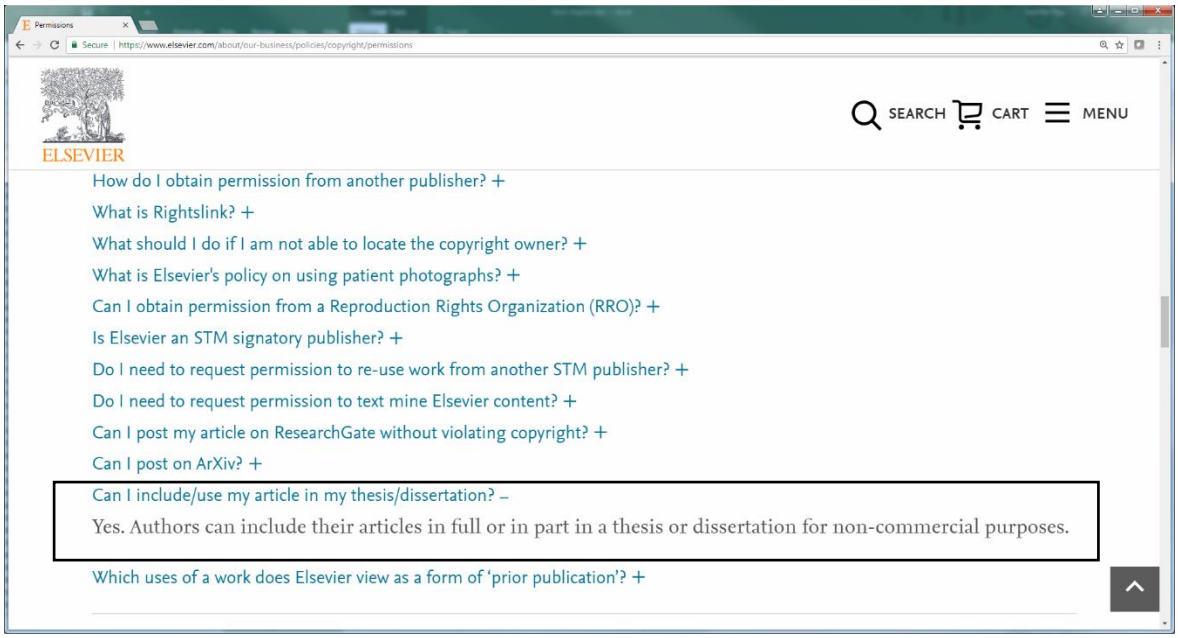

Copyright and authors' rights

(http://authors.bmj.com/policies/copyright-and-authors-rights/)

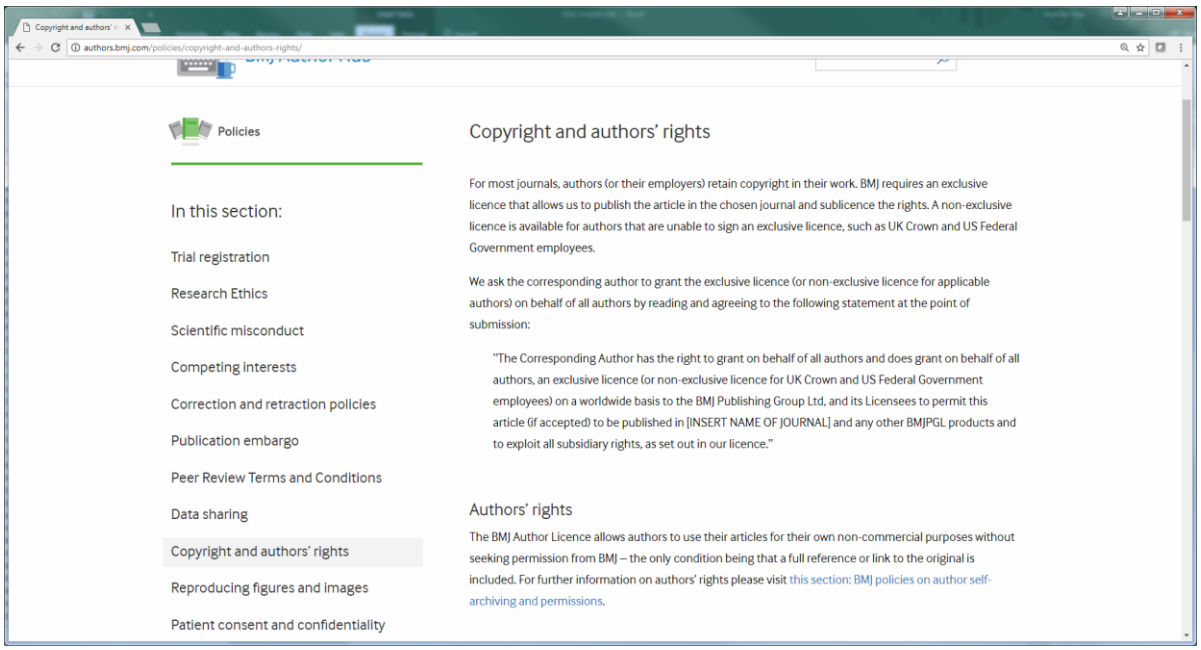

List of References

ABBOTT, N. J., RONNBACK, L. & HANSSON, E. 2006. Astrocyte-endothelial interactions at the blood-brain barrier. *Nat Rev Neurosci,* 7**,** 41-53.

ADAMS, C. W. & BRUTON, C. J. 1989. The cerebral vasculature in dementia pugilistica. *J Neurol Neurosurg Psychiatry,* 52**,** 600-4.

ADAMS, J. H., DOYLE, D., FORD, I., GENNARELLI, T. A., GRAHAM, D. I. & MCLELLAN, D. R. 1989a. Diffuse axonal injury in head injury: definition, diagnosis and grading. *Histopathology,* 15**,** 49-59.

ADAMS, J. H., DOYLE, D., FORD, I., GRAHAM, D. I., MCGEE, M. & MCLELLAN, D. R. 1989b. Brain damage in fatal non-missile head injury in relation to age and type of injury. *Scott Med J,* 34**,** 399-401.

ADAMS, J. H., GRAHAM, D. I., MURRAY, L. S. & SCOTT, G. 1982. Diffuse axonal injury due to nonmissile head injury in humans: an analysis of 45 cases. *Ann Neurol,* 12**,** 557-63.

ADELSON, P. D., SRINIVAS, R., CHANG, Y., BELL, M. & KOCHANEK, P. M. 2011. Cerebrovascular response in children following severe traumatic brain injury. *Childs Nerv Syst,* 27**,** 1465-76.

AHMADZADEH, H., SMITH, D. H. & SHENOY, V. B. 2014. Viscoelasticity of tau proteins leads to strain rate-dependent breaking of microtubules during axonal stretch injury: predictions from a mathematical model. *Biophys J,* 106**,** 1123-33.

AHMED, S. M., RZIGALINSKI, B. A., WILLOUGHBY, K. A., SITTERDING, H. A. & ELLIS, E. F. 2000. Stretch-induced injury alters mitochondrial membrane potential and cellular ATP in cultured astrocytes and neurons. *J Neurochem,* 74**,** 1951-60.

AIHARA, N., HALL, J. J., PITTS, L. H., FUKUDA, K. & NOBLE, L. J. 1995. Altered immunoexpression of microglia and macrophages after mild head injury. *J Neurotrauma,* 12**,** 53-63.

AJAMI, B., BENNETT, J. L., KRIEGER, C., MCNAGNY, K. M. & ROSSI, F. M. 2011. Infiltrating monocytes trigger EAE progression, but do not contribute to the resident microglia pool. *Nat Neurosci,* 14**,** 1142-9.

AJAMI, B., SAMUSIK, N., WIEGHOFER, P., HO, P. P., CROTTI, A., BJORNSON, Z., PRINZ, M., FANTL, W. J., NOLAN, G. P. & STEINMAN, L. 2018. Single-cell mass cytometry reveals distinct populations of brain myeloid cells in mouse neuroinflammation and neurodegeneration models. *Nat Neurosci,* 21**,** 541-551.

ALLSOP, D., HAGA, S., BRUTON, C., ISHII, T. & ROBERTS, G. W. 1990. Neurofibrillary tangles in some cases of dementia pugilistica share antigens with amyloid beta-protein of Alzheimer's disease. *The American Journal of Pathology,* 136**,** 255-260.

AMADUCCI, L. A., FRATIGLIONI, L., ROCCA, W. A., FIESCHI, C., LIVREA, P., PEDONE, D., BRACCO, L., LIPPI, A., GANDOLFO, C., BINO, G. & ET AL. 1986. Risk factors for clinically diagnosed Alzheimer's disease: a case-control study of an Italian population. *Neurology,* 36**,** 922-31.

ANDERSON, V., CATROPPA, C., MORSE, S., HARITOU, F. & ROSENFELD, J. 2000. Recovery of Intellectual Ability following Traumatic Brain Injury in Childhood: Impact of Injury Severity and Age at Injury. *Pediatric Neurosurgery,* 32**,** 282-290.

AREZA-FEGYVERES, R., ROSEMBERG, S., CASTRO, R. M., PORTO, C. S., BAHIA, V. S., CARAMELLI, P. & NITRINI, R. 2007. Dementia pugilistica with clinical features of Alzheimer's disease. *Arq Neuropsiquiatr,* 65**,** 830-3.

ARMULIK, A. & BETSHOLTZ, C. 2010. Role of Pericytes in Vascular Biology. *Experimental Approaches to Diabetic Retinopathy,* 20**,** 194-202.

ARMULIK, A., GENOVE, G., MAE, M., NISANCIOGLU, M. H., WALLGARD, E., NIAUDET, C., HE, L. Q., NORLIN, J., LINDBLOM, P., STRITTMATTER, K., JOHANSSON, B. R. & BETSHOLTZ, C. 2010. Pericytes regulate the blood-brain barrier. *Nature,* 468**,** 557-U231.

BALDWIN, S. A., FUGACCIA, I., BROWN, D. R., BROWN, L. V. & SCHEFF, S. W. 1996. Blood-brain barrier breach following cortical contusion in the rat. *J Neurosurg,* 85**,** 476-81.

BARDEHLE, S., KRUGER, M., BUGGENTHIN, F., SCHWAUSCH, J., NINKOVIC, J., CLEVERS, H., SNIPPERT, H. J., THEIS, F. J., MEYER-LUEHMANN, M., BECHMANN, I., DIMOU, L. & GOTZ, M. 2013. Live imaging of astrocyte responses to acute injury reveals selective juxtavascular proliferation. *Nat Neurosci,* 16**,** 580-6.

BARZO, P., MARMAROU, A., FATOUROS, P., CORWIN, F. & DUNBAR, J. 1996. Magnetic resonance imaging-monitored acute blood-brain barrier changes in experimental traumatic brain injury. *J Neurosurg,* 85**,** 1113-21.

BASKAYA, M. K., RAO, A. M., DOGAN, A., DONALDSON, D. & DEMPSEY, R. J. 1997. The biphasic opening of the blood-brain barrier in the cortex and hippocampus after traumatic brain injury in rats. *Neurosci Lett,* 226**,** 33-6.

BELL, R. D., DEANE, R., CHOW, N., LONG, X., SAGARE, A., SINGH, I., STREB, J. W., GUO, H., RUBIO, A., VAN NOSTRAND, W., MIANO, J. M. & ZLOKOVIC, B. V. 2009. SRF and myocardin regulate LRP-mediated amyloid-beta clearance in brain vascular cells. *Nat Cell Biol,* 11**,** 143-53.

BELL, R. D., WINKLER, E. A., SAGARE, A. P., SINGH, I., LARUE, B., DEANE, R. & ZLOKOVIC, B. V. 2010. Pericytes Control Key Neurovascular Functions and Neuronal Phenotype in the Adult Brain and during Brain Aging. *Neuron,* 68**,** 409-427.

BELL, R. D., WINKLER, E. A., SINGH, I., SAGARE, A. P., DEANE, R., WU, Z., HOLTZMAN, D. M., BETSHOLTZ, C., ARMULIK, A., SALLSTROM, J., BERK, B. C. & ZLOKOVIC, B. V. 2012. Apolipoprotein E controls cerebrovascular integrity via cyclophilin A. *Nature,* 485**,** 512-6.

BELL, R. D. & ZLOKOVIC, B. V. 2009a. Neurovascular mechanisms and blood-brain barrier disorder in Alzheimer's disease. *Acta Neuropathol,* 118**,** 103-13.

BELL, R. D. & ZLOKOVIC, B. V. 2009b. Neurovascular mechanisms and blood-brain barrier disorder in Alzheimer's disease. *Acta Neuropathol,* 118.

BENNETT, M. L., BENNETT, F. C., LIDDELOW, S. A., AJAMI, B., ZAMANIAN, J. L., FERNHOFF, N. B., MULINYAWE, S. B., BOHLEN, C. J., ADIL, A., TUCKER, A., WEISSMAN, I. L., CHANG, E. F., LI, G., GRANT, G. A., HAYDEN GEPHART, M. G. & BARRES, B. A. 2016. New tools for studying microglia in the mouse and human CNS. *Proceedings of the National Academy of Sciences,* 113**,** E1738-E1746.

BERGESON, A. G., LUNDIN, R., PARKINSON, R. B., TATE, D. F., VICTOROFF, J., HOPKINS, R. O. & BIGLER, E. D. 2004. Clinical rating of cortical atrophy and cognitive correlates following traumatic brain injury. *Clin Neuropsychol,* 18**,** 509-20.

BESCHORNER, R., NGUYEN, T. D., GOZALAN, F., PEDAL, I., MATTERN, R., SCHLUESENER, H. J., MEYERMANN, R. & SCHWAB, J. M. 2002a. CD14 expression by activated parenchymal microglia/macrophages and infiltrating monocytes following human traumatic brain injury. *Acta Neuropathol,* 103**,** 541-9.

BESCHORNER, R., SCHLUESENER, H. J., GOZALAN, F., MEYERMANN, R. & SCHWAB, J. M. 2002b. Infiltrating CD14+ monocytes and expression of CD14 by activated

parenchymal microglia/macrophages contribute to the pool of CD14+ cells in ischemic brain lesions. *J Neuroimmunol,* 126**,** 107-15.

BIENIEK, K. F., ROSS, O. A., CORMIER, K. A., WALTON, R. L., SOTO-ORTOLAZA, A., JOHNSTON, A. E., DESARO, P., BOYLAN, K. B., GRAFF-RADFORD, N. R., WSZOLEK, Z. K., RADEMAKERS, R., BOEVE, B. F., MCKEE, A. C. & DICKSON, D. W. 2015. Chronic traumatic encephalopathy pathology in a neurodegenerative disorders brain bank. *Acta Neuropathol,* 130**,** 877-89.

BLANC, F., COLLOBY, S. J., PHILIPPI, N., DE PÉTIGNY, X., JUNG, B., DEMUYNCK, C., PHILLIPPS, C., ANTHONY, P., THOMAS, A., BING, F., LAMY, J., MARTIN-HUNYADI, C., O'BRIEN, J. T., CRETIN, B., MCKEITH, I., ARMSPACH, J.-P. & TAYLOR, J.-P. 2015. Cortical Thickness in Dementia with Lewy Bodies and Alzheimer's Disease: A Comparison of Prodromal and Dementia Stages. *PLOS ONE,* 10**,** e0127396.

BLENNOW, K., JONSSON, M., ANDREASEN, N., ROSENGREN, L., WALLIN, A., HELLSTROM, P. A. & ZETTERBERG, H. 2011. No neurochemical evidence of brain injury after blast overpressure by repeated explosions or firing heavy weapons. *Acta Neurol Scand,* 123**,** 245-51.

BLYTH, B. J., FARHAVAR, A., GEE, C., HAWTHORN, B., HE, H., NAYAK, A., STOCKLEIN, V. & BAZARIAN, J. J. 2009. Validation of serum markers for blood-brain barrier disruption in traumatic brain injury. *J Neurotrauma,* 26**,** 1497-1507.

BO, L., GEURTS, J. J., MORK, S. J. & VAN DER VALK, P. 2006. Grey matter pathology in multiple sclerosis. *Acta Neurol Scand Suppl,* 183**,** 48-50.

BODENSTEINER, J. B. & SCHAEFER, G. B. 1997. Dementia pugilistica and cavum septi pellucidi: born to box? *Sports Med,* 24**,** 361-5.

BOGDANOFF, B. & NATTER, H. M. 1989. Incidence of cavum septum pellucidum in adults: a sign of boxer's encephalopathy. *Neurology,* 39**,** 991-2.

BORDA, J. T., ALVAREZ, X., MOHAN, M., HASEGAWA, A., BERNARDINO, A., JEAN, S., AYE, P. & LACKNER, A. A. 2008. CD163, a marker of perivascular macrophages, is up-regulated by microglia in simian immunodeficiency virus encephalitis after haptoglobin-hemoglobin complex stimulation and is suggestive of breakdown of the blood-brain barrier. *Am J Pathol,* 172**,** 725-37.

BRAAK, H. & BRAAK, E. 1991. Neuropathological stageing of Alzheimer-related changes. *Acta Neuropathol,* 82**,** 239-59.

BRAAK, H., BRAAK, E. & BOHL, J. 1993. Staging of Alzheimer-related cortical destruction. *Eur Neurol,* 33**,** 403-8.

BRANDENBURG, W. & HALLERVORDEN, J. 1954. [Dementia pugilistica with anatomical findings]. *Virchows Arch Pathol Anat Physiol Klin Med,* 325**,** 680-709.

BRETTSCHNEIDER, J., LIBON, D. J., TOLEDO, J. B., XIE, S. X., MCCLUSKEY, L., ELMAN, L., GESER, F., LEE, V. M., GROSSMAN, M. & TROJANOWSKI, J. Q. 2012a. Microglial activation and TDP-43 pathology correlate with executive dysfunction in amyotrophic lateral sclerosis. *Acta Neuropathol,* 123**,** 395-407.

BRETTSCHNEIDER, J., TOLEDO, J. B., VAN DEERLIN, V. M., ELMAN, L., MCCLUSKEY, L., LEE, V. M. & TROJANOWSKI, J. Q. 2012b. Microglial activation correlates with disease progression and upper motor neuron clinical symptoms in amyotrophic lateral sclerosis. *PLoS One,* 7**,** e39216.

BROE, G. A., HENDERSON, A. S., CREASEY, H., MCCUSKER, E., KORTEN, A. E., JORM, A. F., LONGLEY, W. & ANTHONY, J. C. 1990. A case-control study of Alzheimer's disease in Australia. *Neurology,* 40**,** 1698-707.

BROWN, W. R., MOODY, D. M., CHALLA, V. R. & THORE, C. R. 2001. Cerebrovascular pathology in Alzheimer disease. *In:* VELLAS, B., FITTEN, L. J., WINBLAD, B.,

FELDMAN, H., GRUNDMAN, M. & GIACOBINI, E. (eds.) *Research and Practice in Alzheimer's Disease.* Springer, Paris, New York: Serdi Publications.

BROWN, W. R. & THORE, C. R. 2011a. Review: cerebral microvascular pathology in ageing and neurodegeneration. *Neuropathol Appl Neurobiol,* 37**,** 56-74.

BROWN, W. R. & THORE, C. R. 2011b. Review: Cerebral microvascular pathology in aging and neurodegeneration. *Neuropathology and applied neurobiology,* 37**,** 56-74.

BROWNE, K. D., CHEN, X.-H., MEANEY, D. F. & SMITH, D. H. 2011. Mild Traumatic Brain Injury and Diffuse Axonal Injury in Swine. *Journal of Neurotrauma,* 28**,** 1747-1755.

BRUCE, D. A. 1984. Delayed deterioration of consciousness after trivial head injury in childhood. *Br Med J (Clin Res Ed),* 289**,** 715-6.

BRUCE, D. A., ALAVI, A., BILANIUK, L., DOLINSKAS, C., OBRIST, W. & UZZELL, B. 1981. Diffuse cerebral swelling following head injuries in children: the syndrome of "malignant brain edema". *J Neurosurg,* 54**,** 170-8.

BRUCE, D. A., SCHUT, L., BRUNO, L. A., WOOD, J. H. & SUTTON, L. N. 1978. Outcome following severe head injuries in children. *J Neurosurg,* 48**,** 679-88.

BU, G. 2009. Apolipoprotein E and its receptors in Alzheimer's disease: pathways, pathogenesis and therapy. *Nat Rev Neurosci,* 10**,** 333-44.

BUEE, L., HOF, P. R., BOURAS, C., DELACOURTE, A., PERL, D. P., MORRISON, J. H. & FILLIT, H. M. 1994. Pathological alterations of the cerebral microvasculature in Alzheimer's disease and related dementing disorders. *Acta Neuropathol,* 87**,** 469-80.

BUSHONG, E. A., MARTONE, M. E., JONES, Y. Z. & ELLISMAN, M. H. 2002. Protoplasmic astrocytes in CA1 stratum radiatum occupy separate anatomical domains. *J Neurosci,* 22**,** 183-92.

CABEZAS, R., ÁVILA, M., GONZALEZ, J., EL-BACHÁ, R. S., BÁEZ, E., GARCÍA-SEGURA, L. M., JURADO CORONEL, J. C., CAPANI, F., CARDONA-GOMEZ, G. P. & BARRETO, G. E. 2014. Astrocytic modulation of blood brain barrier: perspectives on Parkinson's disease. *Frontiers in Cellular Neuroscience,* 8**,** 211.

CANTU, R. C. 1998. Second-impact syndrome. *Clin Sports Med,* 17**,** 37-44.

CARPENTIER, P. A., BEGOLKA, W. S., OLSON, J. K., ELHOFY, A., KARPUS, W. J. & MILLER, S. D. 2005. Differential activation of astrocytes by innate and adaptive immune stimuli. *Glia,* 49**,** 360-74.

CASSON, I. R., SIEGEL, O., SHAM, R., CAMPBELL, E. A., TARLAU, M. & DIDOMENICO, A. 1984. Brain damage in modern boxers. *Jama,* 251**,** 2663-7.

CDC, N. C. I. P. C. 1999. Taumatic Brain Injury in the United States: A report to congress. Atlanta.

CHAN, D., FOX, N. C., JENKINS, R., SCAHILL, R. I., CRUM, W. R. & ROSSOR, M. N. 2001. Rates of global and regional cerebral atrophy in AD and frontotemporal dementia. *Neurology,* 57**,** 1756-1763.

CHANDRA, V., PHILIPOSE, V., BELL, P. A., LAZAROFF, A. & SCHOENBERG, B. S. 1987. Case-control study of late onset "probable Alzheimer's disease". *Neurology,* 37**,** 1295-300.

CHECHNEVA, O. V. & DENG, W. 2016a. Mitochondrial translocator protein (TSPO), astrocytes and neuroinflammation. *Neural Regen Res,* 11**,** 1056-7.

CHECHNEVA, O. V. & DENG, W. 2016b. Mitochondrial translocator protein (TSPO), astrocytes and neuroinflammation. *Neural Regeneration Research,* 11**,** 1056-1057.

CHEN-PLOTKIN, A. S., LEE, V. M. & TROJANOWSKI, J. Q. 2010. TAR DNA-binding protein 43 in neurodegenerative disease. *Nat Rev Neurol,* 6**,** 211-20.

CHEN, X. H., JOHNSON, V. E., URYU, K., TROJANOWSKI, J. Q. & SMITH, D. H. 2009. A lack of amyloid beta plaques despite persistent accumulation of amyloid beta in axons of long-term survivors of traumatic brain injury. *Brain Pathol,* 19**,** 214-23.

CHEN, X. H., SIMAN, R., IWATA, A., MEANEY, D. F., TROJANOWSKI, J. Q. & SMITH, D. H. 2004. Long-term accumulation of amyloid-beta, beta-secretase, presenilin-1, and caspase-3 in damaged axons following brain trauma. *Am J Pathol,* 165**,** 357-71.

CHENG, J. S., DUBAL, D. B., KIM, D. H., LEGLEITER, J., CHENG, I. H., YU, G.-Q., TESSEUR, I., WYSS-CORAY, T., BONALDO, P. & MUCKE, L. 2009. Collagen VI protects neurons against Aβ toxicity. *Nature neuroscience,* 12**,** 119.

CHERRY, J. D., OLSCHOWKA, J. A. & O'BANION, M. K. 2014. Neuroinflammation and M2 microglia: the good, the bad, and the inflamed. *Journal of Neuroinflammation,* 11**,** 98.

CHODOBSKI, A., CHUNG, I., KOZNIEWSKA, E., IVANENKO, T., CHANG, W., HARRINGTON, J. F., DUNCAN, J. A. & SZMYDYNGER-CHODOBSKA, J. 2003. Early neutrophilic expression of vascular endothelial growth factor after traumatic brain injury. *Neuroscience,* 122**,** 853-67.

CHRISTOV, A., OTTMAN, J., HAMDHEYDARI, L. & GRAMMAS, P. 2008. Structural changes in Alzheimer's disease brain microvessels. *Curr Alzheimer Res,* 5**,** 392-5.

COLANGELO, A. M., ALBERGHINA, L. & PAPA, M. 2014. Astrogliosis as a therapeutic target for neurodegenerative diseases. *Neurosci Lett,* 565**,** 59-64.

COLD, G. E. & JENSEN, F. T. 1980. Cerebral blood flow in the acute phase after head injury. Part 1: Correlation to age of the patients, clinical outcome and localisation of the injured region. *Acta Anaesthesiol Scand,* 24**,** 245-51.

COLE, J. H., JOLLY, A., DE SIMONI, S., BOURKE, N., PATEL, M. C., SCOTT, G. & SHARP, D. J. 2018. Spatial patterns of progressive brain volume loss after moderate-severe traumatic brain injury. *Brain***,** awx354-awx354.

COLE, J. H., LEECH, R., SHARP, D. J. & FOR THE ALZHEIMER'S DISEASE NEUROIMAGING, I. 2015. Prediction of brain age suggests accelerated atrophy after traumatic brain injury. *Annals of Neurology,* 77**,** 571-581.

COLTON, C. A. 2009. Heterogeneity of microglial activation in the innate immune response in the brain. *J Neuroimmune Pharmacol,* 4**,** 399-418.

CONSTANTINIDIS, J. & TISSOT, R. 1967. [Generalized Alzheimer's neurofibrillary lesions without senile plaques. (Presentation of one anatomo-clinical case)]. *Schweiz Arch Neurol Neurochir Psychiatr,* 100**,** 117-30.

CORDER, E. H., SAUNDERS, A. M., STRITTMATTER, W. J., SCHMECHEL, D. E., GASKELL, P. C., SMALL, G. W., ROSES, A. D., HAINES, J. L. & PERICAK-VANCE, M. A. 1993. Gene dose of apolipoprotein E type 4 allele and the risk of Alzheimer's disease in late onset families. *Science,* 261**,** 921-3.

CORONADO VG, M. L., FAUL M, SUGERMAN DE, PEARSONS WS. 2012. *Epidemiology and public health issues,* New York, Demos Med.

CORSELLIS, J. A., BRUTON, C. J. & FREEMAN-BROWNE, D. 1973. The aftermath of boxing. *Psychol Med,* 3**,** 270-303.

CORTEZ, S. C., MCINTOSH, T. K. & NOBLE, L. J. 1989. Experimental fluid percussion brain injury: vascular disruption and neuronal and glial alterations. *Brain Res,* 482**,** 271-82.

COSENZA, M. A., ZHAO, M. L., SI, Q. & LEE, S. C. 2002. Human brain parenchymal microglia express CD14 and CD45 and are productively infected by HIV-1 in HIV-1 encephalitis. *Brain Pathol,* 12**,** 442-55.

CRITCHLEY, M. 1957. Medical aspects of boxing, particularly from a neurological standpoint. *Br Med J,* 1**,** 357-62.

CSUKA, E., MORGANTI-KOSSMANN, M. C., LENZLINGER, P. M., JOLLER, H., TRENTZ, O. & KOSSMANN, T. 1999. IL-10 levels in cerebrospinal fluid and serum of patients with severe traumatic brain injury: relationship to IL-6, TNF-alpha, TGF-beta1 and blood-brain barrier function. *J Neuroimmunol,* 101**,** 211-21.

CULLEN, D. K., VERNEKAR, V. N. & LAPLACA, M. C. 2011. Trauma-induced plasmalemma disruptions in three-dimensional neural cultures are dependent on strain modality and rate. *J Neurotrauma,* 28**,** 2219-33.

DA FONSECA, A. C. C., MATIAS, D., GARCIA, C., AMARAL, R., GERALDO, L. H., FREITAS, C. & LIMA, F. R. S. 2014. The impact of microglial activation on blood-brain barrier in brain diseases. *Frontiers in Cellular Neuroscience,* 8**,** 362.

DAMS-O'CONNOR, K., SPIELMAN, L., HAMMOND, F. M., SAYED, N., CULVER, C. & DIAZ-ARRASTIA, R. 2013. An exploration of clinical dementia phenotypes among individuals with and without traumatic brain injury. *NeuroRehabilitation,* 32**,** 199-209.

DANEMAN, R., ZHOU, L., KEBEDE, A. A. & BARRES, B. A. 2010. Pericytes are required for blood-brain barrier integrity during embryogenesis. *Nature,* 468**,** 562-U238.

DAVALOS, D., GRUTZENDLER, J., YANG, G., KIM, J. V., ZUO, Y., JUNG, S., LITTMAN, D. R., DUSTIN, M. L. & GAN, W. B. 2005. ATP mediates rapid microglial response to local brain injury in vivo. *Nat Neurosci,* 8**,** 752-8.

DAVALOS, D., RYU, J. K., MERLINI, M., BAETEN, K. M., LE MOAN, N., PETERSEN, M. A., DEERINCK, T. J., SMIRNOFF, D. S., BEDARD, C., HAKOZAKI, H., GONIAS MURRAY, S., LING, J. B., LASSMANN, H., DEGEN, J. L., ELLISMAN, M. H. & AKASSOGLOU, K. 2012. Fibrinogen-induced perivascular microglial clustering is required for the development of axonal damage in neuroinflammation. *Nat Commun,* 3**,** 1227.

DEANE, R., SAGARE, A., HAMM, K., PARISI, M., LANE, S., FINN, M. B., HOLTZMAN, D. M. & ZLOKOVIC, B. V. 2008. apoE isoform–specific disruption of amyloid β peptide clearance from mouse brain. *The Journal of Clinical Investigation,* 118**,** 4002-4013.

DEANE, R., WU, Z., SAGARE, A., DAVIS, J., DU YAN, S., HAMM, K., XU, F., PARISI, M., LARUE, B., HU, H. W., SPIJKERS, P., GUO, H., SONG, X., LENTING, P. J., VAN NOSTRAND, W. E. & ZLOKOVIC, B. V. 2004a. LRP/amyloid beta-peptide interaction mediates differential brain efflux of Abeta isoforms. *Neuron,* 43**,** 333-44.

DEANE, R., WU, Z. H., SAGARE, A., DAVIS, J., YAN, S. D., HAMM, K., XU, F., PARISI, M., LARUE, B., HU, H. W., SPIJKERS, P., GUO, H., SONG, X. M., LENTING, P. J., VAN NOSTRAND, W. E. & ZLOKOVIC, B. V. 2004b. LRP/amyloid beta-peptide interaction mediates differential brain efflux of A beta isoforms. *Neuron,* 43**,** 333-344.

DEKOSKY, S. T., BLENNOW, K., IKONOMOVIC, M. D. & GANDY, S. 2013. Acute and chronic traumatic encephalopathies: pathogenesis and biomarkers. *Nat Rev Neurol,* 9**,** 192-200.

DEKOSKY, S. T., IKONOMOVIC, M. D. & GANDY, S. 2010. Traumatic brain injury: football, warfare, and long-term effects. *Minn Med,* 93**,** 46-7.

DESAI, B. S., SCHNEIDER, J. A., LI, J.-L., CARVEY, P. M. & HENDEY, B. 2009. Evidence of angiogenic vessels in Alzheimer's disease. *Journal of neural transmission (Vienna, Austria : 1996),* 116**,** 587-597.

DI BATTISTA, A. P., BUONORA, J. E., RHIND, S. G., HUTCHISON, M. G., BAKER, A. J., RIZOLI, S. B., DIAZ-ARRASTIA, R. & MUELLER, G. P. 2015. Blood Biomarkers in

Moderate-To-Severe Traumatic Brain Injury: Potential Utility of a Multi-Marker Approach in Characterizing Outcome. *Frontiers in Neurology,* 6**,** 110.

DIAZ-ARRASTIA, R., GONG, Y., FAIR, S., SCOTT, K. D., GARCIA, M. C., CARLILE, M. C., AGOSTINI, M. A. & VAN NESS, P. C. 2003. Increased risk of late posttraumatic seizures associated with inheritance of APOE epsilon4 allele. *Arch Neurol,* 60**,** 818-22.

DONAHUE, J. E., FLAHERTY, S. L., JOHANSON, C. E., DUNCAN, J. A., 3RD, SILVERBERG, G. D., MILLER, M. C., TAVARES, R., YANG, W., WU, Q., SABO, E., HOVANESIAN, V. & STOPA, E. G. 2006. RAGE, LRP-1, and amyloid-beta protein in Alzheimer's disease. *Acta Neuropathol,* 112**,** 405-15.

DOORDUIN, J., DE VRIES, E. F., DIERCKX, R. A. & KLEIN, H. C. 2008. PET imaging of the peripheral benzodiazepine receptor: monitoring disease progression and therapy response in neurodegenerative disorders. *Curr Pharm Des,* 14**,** 3297-315.

DRACHMAN , D. A. & NEWELL , K. L. 1999. Case 12-1999. *New England Journal of Medicine,* 340**,** 1269-1277.

DU, A.-T., SCHUFF, N., KRAMER, J. H., ROSEN, H. J., GORNO-TEMPINI, M. L., RANKIN, K., MILLER, B. L. & WEINER, M. W. 2007. Different regional patterns of cortical thinning in Alzheimer's disease and frontotemporal dementia. *Brain : a journal of neurology,* 130**,** 1159-1166.

EISELE, Y. S., OBERMULLER, U., HEILBRONNER, G., BAUMANN, F., KAESER, S. A., WOLBURG, H., WALKER, L. C., STAUFENBIEL, M., HEIKENWALDER, M. & JUCKER, M. 2010. Peripherally applied Abeta-containing inoculates induce cerebral beta-amyloidosis. *Science,* 330**,** 980-2.

EK, C. J., D'ANGELO, B., BABURAMANI, A. A., LEHNER, C., LEVERIN, A. L., SMITH, P. L., NILSSON, H., SVEDIN, P., HAGBERG, H. & MALLARD, C. 2015. Brain barrier properties and cerebral blood flow in neonatal mice exposed to cerebral hypoxia-ischemia. *J Cereb Blood Flow Metab,* 35**,** 818-27.

EUGENE, P., JOSHUA, D. B., ISHITA, P. S. & ANDREW, J. B. 2008. An Analysis of Regional Microvascular Loss and Recovery following Two Grades of Fluid Percussion Trauma: A Role for Hypoxia-Inducible Factors in Traumatic Brain Injury. *Journal of Cerebral Blood Flow & Metabolism,* 29**,** 575-584.

FABRIEK, B. O., VAN HAASTERT, E. S., GALEA, I., POLFLIET, M. M., DOPP, E. D., VAN DEN HEUVEL, M. M., VAN DEN BERG, T. K., DE GROOT, C. J., VAN DER VALK, P. & DIJKSTRA, C. D. 2005. CD163-positive perivascular macrophages in the human CNS express molecules for antigen recognition and presentation. *Glia,* 51**,** 297-305.

FARBOTA, K. D., SODHI, A., BENDLIN, B. B., MCLAREN, D. G., XU, G., ROWLEY, H. A. & JOHNSON, S. C. 2012. Longitudinal volumetric changes following traumatic brain injury: a tensor-based morphometry study. *J Int Neuropsychol Soc,* 18**,** 1006-18.

FARKAS, E. & LUITEN, P. G. 2001. Cerebral microvascular pathology in aging and Alzheimer's disease. *Prog Neurobiol,* 64**,** 575-611.

FARRALL, A. J. & WARDLAW, J. M. 2009. Blood-brain barrier: ageing and microvascular disease--systematic review and meta-analysis. *Neurobiol Aging,* 30**,** 337-52.

FAUL M, X. L., WALD MM, CORONADO VG 2010. Traumatic Brain Injury in the United States: Emergency

Department Visits, Hospitalizations and Deaths 2002–2006. *In:* CDC, N. C. I. P. C. (ed.). Atlanta.

FEKETE, J. F. 1968. Severe brain injury and death following minor hockey accidents: the effectiveness of the "safety helmets" of amateur hockey players. *Can Med Assoc J,* 99**,** 1234-9.

FERGUSON FR, M. C. Chronic encephalopathy in Boxers: 8th international Congress of Neurology. 8th international Congress of Neurology, 1965 Vienna.

FERINI-STRAMBI, L., SMIRNE, S., GARANCINI, P., PINTO, P. & FRANCESCHI, M. 1990. Clinical and epidemiological aspects of Alzheimer's disease with presenile onset: a case control study. *Neuroepidemiology,* 9**,** 39-49.

FILIPOWICZ, A. R., MCGARY, C. M., HOLDER, G. E., LINDGREN, A. A., JOHNSON, E. M., SUGIMOTO, C., KURODA, M. J. & KIM, W.-K. 2016. Proliferation of Perivascular Macrophages Contributes to the Development of Encephalitic Lesions in HIV-Infected Humans and in SIV-Infected Macaques. *Scientific Reports,* 6**,** 32900.

FISCHER-SMITH, T., CROUL, S., SVERSTIUK, A. E., CAPINI, C., L'HEUREUX, D., RÉGULIER, E. G., RICHARDSON, M. W., AMINI, S., MORGELLO, S., KHALILI, K. & RAPPAPORT, J. 2001. CNS invasion by CD14+/CD16+ peripheral blood-derived monocytes in HIV dementia: perivascular accumulation and reservoir of HIV infection. *Journal of NeuroVirology,* 7**,** 528-541.

FISCHER, V. W., SIDDIQI, A. & YUSUFALY, Y. 1990. Altered angioarchitecture in selected areas of brains with Alzheimer's disease. *Acta Neuropathol,* 79**,** 672-9.

FLEMINGER, S., OLIVER, D. L., LOVESTONE, S., RABE-HESKETH, S. & GIORA, A. 2003. Head injury as a risk factor for Alzheimer's disease: the evidence 10 years on; a partial replication. *J Neurol Neurosurg Psychiatry,* 74**,** 857-62.

FLYGT, J., GUMUCIO, A., INGELSSON, M., SKOGLUND, K., HOLM, J., ALAFUZOFF, I. & MARKLUND, N. 2016. Human Traumatic Brain Injury Results in Oligodendrocyte Death and Increases the Number of Oligodendrocyte Progenitor Cells. *J Neuropathol Exp Neurol,* 75**,** 503-15.

FRIEDMAN, G., FROOM, P., SAZBON, L., GRINBLATT, I., SHOCHINA, M., TSENTER, J., BABAEY, S., YEHUDA, B. & GROSWASSER, Z. 1999. Apolipoprotein E-epsilon4 genotype predicts a poor outcome in survivors of traumatic brain injury. *Neurology,* 52**,** 244-8.

GALE, S., BAXTER, L., ROUNDY, N. & JOHNSON, S. 2005. Traumatic brain injury and grey matter concentration: a preliminary voxel based morphometry study. *Journal of Neurology, Neurosurgery, and Psychiatry,* 76**,** 984-988.

GAMA SOSA, M. A., DE GASPERI, R., JANSSEN, P. L., YUK, F. J., ANAZODO, P. C., PRICOP, P. E., PAULINO, A. J., WICINSKI, B., SHAUGHNESS, M. C., MAUDLIN-JERONIMO, E., HALL, A. A., DICKSTEIN, D. L., MCCARRON, R. M., CHAVKO, M., HOF, P. R., AHLERS, S. T. & ELDER, G. A. 2014. Selective vulnerability of the cerebral vasculature to blast injury in a rat model of mild traumatic brain injury. *Acta Neuropathol Commun,* 2**,** 67.

GAO, H. M., LIU, B. & HONG, J. S. 2003. Critical role for microglial NADPH oxidase in rotenone-induced degeneration of dopaminergic neurons. *J Neurosci,* 23**,** 6181-7.

GARDNER, R., HESS, C., POSSIN, K., COHN-SHEEHY, B., KRAMER, J., BERGER, M., MILLER, B., YAFFE, K. & RABINOVICI, G. 2014. Cavum Septum Pellucidum in Symptomatic Retired Pro-football Players (P6.327). *Neurology,* 82.

GARDNER, R. C., HESS, C. P., BRUS-RAMER, M., POSSIN, K. L., COHN-SHEEHY, B. I., KRAMER, J. H., BERGER, M. S., YAFFE, K., MILLER, B. & RABINOVICI, G. D. 2016. Cavum Septum Pellucidum in Retired American Pro-Football Players. *Journal of Neurotrauma,* 33**,** 157-161.

GASPARINI, L., TERNI, B. & SPILLANTINI, M. G. 2007. Frontotemporal dementia with tau pathology. *Neurodegener Dis,* 4**,** 236-53.

GEDDES, J. F., VOWLES, G. H., NICOLL, J. A. & REVESZ, T. 1999. Neuronal cytoskeletal changes are an early consequence of repetitive head injury. *Acta Neuropathol,* 98**,** 171-8.

GEDDES, J. F., VOWLES, G. H., ROBINSON, S. F. & SUTCLIFFE, J. C. 1996. Neurofibrillary tangles, but not Alzheimer-type pathology, in a young boxer. *Neuropathol Appl Neurobiol,* 22**,** 12-6.

GENTLEMAN, S. M., LECLERCQ, P. D., MOYES, L., GRAHAM, D. I., SMITH, C., GRIFFIN, W. S. & NICOLL, J. A. 2004. Long-term intracerebral inflammatory response after traumatic brain injury. *Forensic Sci Int,* 146**,** 97-104.

GENTLEMAN, S. M., NASH, M. J., SWEETING, C. J., GRAHAM, D. I. & ROBERTS, G. W. 1993. Beta-amyloid precursor protein (beta APP) as a marker for axonal injury after head injury. *Neurosci Lett,* 160**,** 139-44.

GESER, F., LEE, V. M. Y. & TROJANOWSKI, J. Q. 2010. Amyotrophic lateral sclerosis and frontotemporal lobar degeneration: A spectrum of TDP-43 proteinopathies. *Neuropathology : official journal of the Japanese Society of Neuropathology,* 30**,** 103-112.

GIRALT, A., FRIEDMAN, H. C., CANEDA-FERRON, B., URBAN, N., MORENO, E., RUBIO, N., BLANCO, J., PETERSON, A., CANALS, J. M. & ALBERCH, J. 2010. BDNF regulation under GFAP promoter provides engineered astrocytes as a new approach for long-term protection in Huntington's disease. *Gene Ther,* 17**,** 1294-308.

GIUNTA, B., OBREGON, D., VELISETTY, R., SANBERG, P. R., BORLONGAN, C. V. & TAN, J. 2012. The immunology of traumatic brain injury: a prime target for Alzheimer's disease prevention. *Journal of Neuroinflammation,* 9**,** 185-185.

GLASS, C. K., SAIJO, K., WINNER, B., MARCHETTO, M. C. & GAGE, F. H. 2010. Mechanisms underlying inflammation in neurodegeneration. *Cell,* 140**,** 918-34.

GLUSHAKOVA, O. Y., JOHNSON, D. & HAYES, R. L. 2014. Delayed increases in microvascular pathology after experimental traumatic brain injury are associated with prolonged inflammation, blood-brain barrier disruption, and progressive white matter damage. *J Neurotrauma,* 31**,** 1180-93.

GOLDSTEIN, L. E., FISHER, A. M., TAGGE, C. A., ZHANG, X. L., VELISEK, L., SULLIVAN, J. A., UPRETI, C., KRACHT, J. M., ERICSSON, M., WOJNAROWICZ, M. W., GOLETIANI, C. J., MAGLAKELIDZE, G. M., CASEY, N., MONCASTER, J. A., MINAEVA, O., MOIR, R. D., NOWINSKI, C. J., STERN, R. A., CANTU, R. C., GEILING, J., BLUSZTAJN, J. K., WOLOZIN, B. L., IKEZU, T., STEIN, T. D., BUDSON, A. E., KOWALL, N. W., CHARGIN, D., SHARON, A., SAMAN, S., HALL, G. F., MOSS, W. C., CLEVELAND, R. O., TANZI, R. E., STANTON, P. K. & MCKEE, A. C. 2012. Chronic traumatic encephalopathy in blast-exposed military veterans and a blast neurotrauma mouse model. *Sci Transl Med,* 4**,** 134ra60.

GORDON, S. 2003. Alternative activation of macrophages. *Nat Rev Immunol,* 3**,** 23-35.

GOVINDARAJAN, K. A., NARAYANA, P. A., HASAN, K. M., WILDE, E. A., LEVIN, H. S., HUNTER, J. V., MILLER, E. R., PATEL, V. K., ROBERTSON, C. S. & MCCARTHY, J. J. 2016. Cortical Thickness in Mild Traumatic Brain Injury. *J Neurotrauma,* 33**,** 1809-1817.

GRAHAM, D. I., FORD, I., ADAMS, J. H., DOYLE, D., LAWRENCE, A. E., MCLELLAN, D. R. & NG, H. K. 1989. Fatal head injury in children. *J Clin Pathol,* 42**,** 18-22.

GRAHMANN, H. & ULE, G. 1957. [Diagnosis of chronic cerebral symptoms in boxers (dementia pugilistica & traumatic encephalopathy of boxers)]. *Psychiatr Neurol (Basel),* 134**,** 261-83.

GRAMMAS, P. 2011. Neurovascular dysfunction, inflammation and endothelial activation: implications for the pathogenesis of Alzheimer's disease. *J Neuroinflammation,* 8**,** 26.

GRAMMAS, P., MOORE, P. & WEIGEL, P. H. 1999. Microvessels from Alzheimer's disease brains kill neurons in vitro. *Am J Pathol,* 154**,** 337-42.

GRAVES, A. B., WHITE, E., KOEPSELL, T. D., REIFLER, B. V., VAN BELLE, G., LARSON, E. B. & RASKIND, M. 1990. The association between head trauma and Alzheimer's disease. *Am J Epidemiol,* 131**,** 491-501.

GUO, Z., CUPPLES, L. A., KURZ, A., AUERBACH, S. H., VOLICER, L., CHUI, H., GREEN, R. C., SADOVNICK, A. D., DUARA, R., DECARLI, C., JOHNSON, K., GO, R. C., GROWDON, J. H., HAINES, J. L., KUKULL, W. A. & FARRER, L. A. 2000. Head injury and the risk of AD in the MIRAGE study. *Neurology,* 54**,** 1316-23.

HABGOOD, M. D., BYE, N., DZIEGIELEWSKA, K. M., EK, C. J., LANE, M. A., POTTER, A., MORGANTI-KOSSMANN, C. & SAUNDERS, N. R. 2007. Changes in blood-brain barrier permeability to large and small molecules following traumatic brain injury in mice. *Eur J Neurosci,* 25**,** 231-8.

HAFEZI-MOGHADAM, A., THOMAS, K. L. & WAGNER, D. D. 2007. ApoE deficiency leads to a progressive age-dependent blood-brain barrier leakage. *Am J Physiol Cell Physiol,* 292**,** C1256-62.

HALASSA, M. M., FELLIN, T., TAKANO, H., DONG, J. H. & HAYDON, P. G. 2007. Synaptic islands defined by the territory of a single astrocyte. *J Neurosci,* 27**,** 6473-7.

HARDY, J. A., MANN, D. M., WESTER, P. & WINBLAD, B. 1986. An integrative hypothesis concerning the pathogenesis and progression of Alzheimer's disease. *Neurobiol Aging,* 7**,** 489-502.

HARTIKAINEN, P., RASANEN, J., JULKUNEN, V., NISKANEN, E., HALLIKAINEN, M., KIVIPELTO, M., VANNINEN, R., REMES, A. M. & SOININEN, H. 2012. Cortical thickness in frontotemporal dementia, mild cognitive impairment, and Alzheimer's disease. *J Alzheimers Dis,* 30**,** 857-74.

HAY, J., JOHNSON, V. E., SMITH, D. H. & STEWART, W. 2016. Chronic Traumatic Encephalopathy: The Neuropathological Legacy of Traumatic Brain Injury. *Annu Rev Pathol,* 11**,** 21-45.

HAY, J. R., JOHNSON, V. E., YOUNG, A. M., SMITH, D. H. & STEWART, W. 2015. Blood-Brain Barrier Disruption Is an Early Event That May Persist for Many Years After Traumatic Brain Injury in Humans. *J Neuropathol Exp Neurol,* 74**,** 1147-57.

HAYES, J. P., LOGUE, M. W., SADEH, N., SPIELBERG, J. M., VERFAELLIE, M., HAYES, S. M., REAGAN, A., SALAT, D. H., WOLF, E. J., MCGLINCHEY, R. E., MILBERG, W. P., STONE, A., SCHICHMAN, S. A. & MILLER, M. W. 2017. Mild traumatic brain injury is associated with reduced cortical thickness in those at risk for Alzheimer's disease. *Brain,* 140**,** 813-825.

HAYWARD, N. M., IMMONEN, R., TUUNANEN, P. I., NDODE-EKANE, X. E., GROHN, O. & PITKANEN, A. 2010. Association of chronic vascular changes with functional outcome after traumatic brain injury in rats. *J Neurotrauma,* 27**,** 2203-19.

HAYWARD, N. M. E. A., TUUNANEN, P. I., IMMONEN, R., NDODE-EKANE, X. E., PITKÄNEN, A. & GRÖHN, O. 2011. Magnetic resonance imaging of regional hemodynamic and cerebrovascular recovery after lateral fluid-percussion brain injury in rats. *Journal of Cerebral Blood Flow & Metabolism,* 31**,** 166-177.

HE, P., ZHONG, Z., LINDHOLM, K., BERNING, L., LEE, W., LEMERE, C., STAUFENBIEL, M., LI, R. & SHEN, Y. 2007. Deletion of tumor necrosis factor death receptor inhibits amyloid β generation and prevents learning and memory deficits in Alzheimer's mice. *The Journal of Cell Biology,* 178**,** 829-841.

HEALTH, I. O. M. C. O. G. W. A. 2009. *Gulf War and Health,*
Volume 7: Long-Term Consequences of Traumatic Brain Injury, Washington, National Academies Press.

HEBERT, O., SCHLUETER, K., HORNSBY, M., VAN GORDER, S., SNODGRASS, S. & COOK, C. 2016. The diagnostic credibility of second impact syndrome: A systematic literature review. *J Sci Med Sport*.

HEKMATPANAH, J. & HEKMATPANAH, C. R. 1985. Microvascular alterations following cerebral contusion in rats. Light, scanning, and electron microscope study. *J Neurosurg,* 62**,** 888-97.

HENEKA, M. T. & O'BANION, M. K. 2007. Inflammatory processes in Alzheimer's disease. *J Neuroimmunol,* 184**,** 69-91.

HICKS, R. R., SMITH, D. H., LOWENSTEIN, D. H., SAINT MARIE, R. & MCINTOSH, T. K. 1993. Mild experimental brain injury in the rat induces cognitive deficits associated with regional neuronal loss in the hippocampus. *J Neurotrauma,* 10**,** 405-14.

HIRAO, K., OHNISHI, T., HIRATA, Y., YAMASHITA, F., MORI, T., MORIGUCHI, Y., MATSUDA, H., NEMOTO, K., IMABAYASHI, E., YAMADA, M., IWAMOTO, T., ARIMA, K. & ASADA, T. 2005. The prediction of rapid conversion to Alzheimer's disease in mild cognitive impairment using regional cerebral blood flow SPECT. *Neuroimage,* 28**,** 1014-21.

HIRSCH, E. C., BREIDERT, T., ROUSSELET, E., HUNOT, S., HARTMANN, A. & MICHEL, P. P. 2003. The role of glial reaction and inflammation in Parkinson's disease. *Ann N Y Acad Sci,* 991**,** 214-28.

HIRSCH, E. C., HUNOT, S., DAMIER, P. & FAUCHEUX, B. 1998. Glial cells and inflammation in Parkinson's disease: a role in neurodegeneration? *Ann Neurol,* 44**,** S115-20.

HO, K. M., HONEYBUL, S., YIP, C. B. & SILBERT, B. I. 2014a. Prognostic significance of blood-brain barrier disruption in patients with severe nonpenetrating traumatic brain injury requiring decompressive craniectomy. *J Neurosurg,* 121**,** 674-9.

HO, K. M., HONEYBUL, S., YIP, C. B. & SILBERT, B. I. 2014b. Prognostic significance of blood-brain barrier disruption in patients with severe nonpenetrating traumatic brain injury requiring decompressive craniectomy. *Journal of Neurosurgery,* 121**,** 674-679.

HOF, P. R., BOURAS, C., BUÉE, L., DELACOURTE, A., PERL, D. P. & MORRISON, J. H. 1992. Differential distribution of neurofibrillary tangles in the cerebral cortex of dementia pugilistica and Alzheimer's disease cases. *Acta Neuropathologica,* 85**,** 23-30.

HOF, P. R., KNABE, R., BOVIER, P. & BOURAS, C. 1991. Neuropathological observations in a case of autism presenting with self-injury behavior. *Acta Neuropathol,* 82**,** 321-6.

HOFFMAN, S. W., RZIGALINSKI, B. A., WILLOUGHBY, K. A. & ELLIS, E. F. 2000. Astrocytes generate isoprostanes in response to trauma or oxygen radicals. *Journal of Neurotrauma,* 17**,** 415-420.

HOOZEMANS, J. J., VEERHUIS, R., ROZEMULLER, J. M. & EIKELENBOOM, P. 2006. Neuroinflammation and regeneration in the early stages of Alzheimer's disease pathology. *Int J Dev Neurosci,* 24**,** 157-65.

HUA, Y., LIN, S. & GU, L. 2015. Relevance of Blood Vessel Networks in Blast-Induced Traumatic Brain Injury. *Computational and Mathematical Methods in Medicine,* 2015**,** 8.

HUH, J. W. & RAGHUPATHI, R. 2009. New Concepts in Treatment of Pediatric Traumatic Brain Injury. *Anesthesiology clinics,* 27**,** 213-240.

HUTTON, M., LENDON, C. L., RIZZU, P., BAKER, M., FROELICH, S., HOULDEN, H., PICKERING-BROWN, S., CHAKRAVERTY, S., ISAACS, A., GROVER, A., HACKETT, J., ADAMSON, J., LINCOLN, S., DICKSON, D., DAVIES, P., PETERSEN, R. C.,

STEVENS, M., DE GRAAFF, E., WAUTERS, E., VAN BAREN, J., HILLEBRAND, M., JOOSSE, M., KWON, J. M., NOWOTNY, P., CHE, L. K., NORTON, J., MORRIS, J. C., REED, L. A., TROJANOWSKI, J., BASUN, H., LANNFELT, L., NEYSTAT, M., FAHN, S., DARK, F., TANNENBERG, T., DODD, P. R., HAYWARD, N., KWOK, J. B., SCHOFIELD, P. R., ANDREADIS, A., SNOWDEN, J., CRAUFURD, D., NEARY, D., OWEN, F., OOSTRA, B. A., HARDY, J., GOATE, A., VAN SWIETEN, J., MANN, D., LYNCH, T. & HEUTINK, P. 1998. Association of missense and 5'-splice-site mutations in tau with the inherited dementia FTDP-17. *Nature,* 393**,** 702-5.

IKONOMOVIC, M. D., URYU, K., ABRAHAMSON, E. E., CIALLELLA, J. R., TROJANOWSKI, J. Q., LEE, V. M., CLARK, R. S., MARION, D. W., WISNIEWSKI, S. R. & DEKOSKY, S. T. 2004. Alzheimer's pathology in human temporal cortex surgically excised after severe brain injury. *Exp Neurol,* 190**,** 192-203.

IM, K., LEE, J.-M., SEO, S. W., YOON, U., KIM, S. T., KIM, Y.-H., KIM, S. I. & NA, D. L. 2008. Variations in cortical thickness with dementia severity in Alzheimer's disease. *Neuroscience Letters,* 436**,** 227-231.

ITO, U., HAKAMATA, Y., KAWAKAMI, E. & OYANAGI, K. 2011. Temporary Focal Cerebral Ischemia Results in Swollen Astrocytic End-Feet That Compress Microvessels and Lead to Focal Cortical Infarction. *Journal of Cerebral Blood Flow & Metabolism,* 31**,** 328-338.

IWATA, N., TSUBUKI, S., TAKAKI, Y., WATANABE, K., SEKIGUCHI, M., HOSOKI, E., KAWASHIMA-MORISHIMA, M., LEE, H. J., HAMA, E., SEKINE-AIZAWA, Y. & SAIDO, T. C. 2000. Identification of the major Abeta1-42-degrading catabolic pathway in brain parenchyma: suppression leads to biochemical and pathological deposition. *Nat Med,* 6**,** 143-50.

J, M. 1937. Dementia Pugilistica. *U.S.Navy Med. Bull***,** 297-303.

JACK, C. R., JR., WISTE, H. J., WEIGAND, S. D., KNOPMAN, D. S., VEMURI, P., MIELKE, M. M., LOWE, V., SENJEM, M. L., GUNTER, J. L., MACHULDA, M. M., GREGG, B. E., PANKRATZ, V. S., ROCCA, W. A. & PETERSEN, R. C. 2015. Age, Sex, and APOE epsilon4 Effects on Memory, Brain Structure, and beta-Amyloid Across the Adult Life Span. *JAMA Neurol,* 72**,** 511-9.

JAEGER, L. B., DOHGU, S., SULTANA, R., LYNCH, J. L., OWEN, J. B., ERICKSON, M. A., SHAH, G. N., PRICE, T. O., FLEEGAL-DEMOTTA, M. A., BUTTERFIELD, D. A. & BANKS, W. A. 2009. Lipopolysaccharide alters the blood-brain barrier transport of amyloid beta protein: a mechanism for inflammation in the progression of Alzheimer's disease. *Brain Behav Immun,* 23**,** 507-17.

JIN, X., ISHII, H., BAI, Z., ITOKAZU, T. & YAMASHITA, T. 2012. Temporal changes in cell marker expression and cellular infiltration in a controlled cortical impact model in adult male C57BL/6 mice. *PLoS One,* 7**,** e41892.

JOHNSON, N. A., JAHNG, G. H., WEINER, M. W., MILLER, B. L., CHUI, H. C., JAGUST, W. J., GORNO-TEMPINI, M. L. & SCHUFF, N. 2005. Pattern of cerebral hypoperfusion in Alzheimer disease and mild cognitive impairment measured with arterial spin-labeling MR imaging: initial experience. *Radiology,* 234**,** 851-9.

JOHNSON, V. E., STEWART, J. E., BEGBIE, F. D., TROJANOWSKI, J. Q., SMITH, D. H. & STEWART, W. 2013a. Inflammation and white matter degeneration persist for years after a single traumatic brain injury. *Brain,* 136**,** 28-42.

JOHNSON, V. E., STEWART, J. E., BEGBIE, F. D., TROJANOWSKI, J. Q., SMITH, D. H. & STEWART, W. 2013b. Inflammation and white matter degeneration persist for years after a single traumatic brain injury. *Brain,* 136**,** 28-42.

JOHNSON, V. E., STEWART, W., GRAHAM, D. I., STEWART, J. E., PRAESTGAARD, A. H. & SMITH, D. H. 2009. A neprilysin polymorphism and amyloid-beta plaques after traumatic brain injury. *J Neurotrauma,* 26**,** 1197-202.

JOHNSON, V. E., STEWART, W. & SMITH, D. H. 2010. Traumatic brain injury and amyloid-beta pathology: a link to Alzheimer's disease? *Nat Rev Neurosci,* 11**,** 361-70.

JOHNSON, V. E., STEWART, W. & SMITH, D. H. 2012. Widespread tau and amyloid-beta pathology many years after a single traumatic brain injury in humans. *Brain Pathol,* 22**,** 142-9.

JOHNSON, V. E., STEWART, W. & SMITH, D. H. 2013c. Axonal pathology in traumatic brain injury. *Exp Neurol,* 246**,** 35-43.

JOHNSON, V. E., STEWART, W. & SMITH, D. H. 2013d. Axonal Pathology in Traumatic Brain Injury. *Experimental neurology,* 246**,** 35-43.

JOHNSON, V. E., STEWART, W., TROJANOWSKI, J. Q. & SMITH, D. H. 2011. Acute and chronically increased immunoreactivity to phosphorylation-independent but not pathological TDP-43 after a single traumatic brain injury in humans. *Acta Neuropathol,* 122**,** 715-26.

JORDAN, B. D., JAHRE, C., HAUSER, W. A., ZIMMERMAN, R. D., ZARRELLI, M., LIPSITZ, E. C., JOHNSON, V., WARREN, R. F., TSAIRIS, P. & FOLK, F. S. 1992. CT of 338 active professional boxers. *Radiology,* 185**,** 509-12.

JORDAN, B. D., KANIK, A. B., HORWICH, M. S., SWEENEY, D., RELKIN, N. R., PETITO, C. K. & GANDY, S. 1995. Apolipoprotein E epsilon 4 and fatal cerebral amyloid angiopathy associated with dementia pugilistica. *Ann Neurol,* 38**,** 698-9.

JORDAN, B. D., RELKIN, N. R., RAVDIN, L. D., JACOBS, A. R., BENNETT, A. & GANDY, S. 1997. Apolipoprotein E epsilon4 associated with chronic traumatic brain injury in boxing. *Jama,* 278**,** 136-40.

JT, S. 1952. *Incidence of cavum septi pellucidi and cavum Vergae in 1,032 human brains*, A.M.A.

JUENGST, S. B., KUMAR, R. G., ARENTH, P. M. & WAGNER, A. K. 2014. Exploratory associations with tumor necrosis factor-alpha, disinhibition and suicidal endorsement after traumatic brain injury. *Brain Behav Immun,* 41**,** 134-43.

KALARIA, R. N. 1996. Cerebral vessels in ageing and Alzheimer's disease. *Pharmacol Ther,* 72**,** 193-214.

KALARIA, R. N. & PAX, A. B. 1995. Increased collagen content of cerebral microvessels in Alzheimer's disease. *Brain Res,* 705**,** 349-52.

KANE, M. J., ANGOA-PEREZ, M., BRIGGS, D. I., VIANO, D. C., KREIPKE, C. W. & KUHN, D. M. 2012. A mouse model of human repetitive mild traumatic brain injury. *J Neurosci Methods,* 203**,** 41-9.

KATZMAN, R., ARONSON, M., FULD, P., KAWAS, C., BROWN, T., MORGENSTERN, H., FRISHMAN, W., GIDEZ, L., EDER, H. & OOI, W. L. 1989. Development of dementing illnesses in an 80-year-old volunteer cohort. *Ann Neurol,* 25**,** 317-24.

KAZAN, S., TUNCER, R., KARASOY, M., RAHAT, O. & SAVEREN, M. 1997. Post-traumatic bilateral diffuse cerebral swelling. *Acta Neurochir (Wien),* 139**,** 295-301; discussion 301-2.

KIM, H. J., FILLMORE, H. L., REEVES, T. M. & PHILLIPS, L. L. 2005. Elevation of hippocampal MMP-3 expression and activity during trauma-induced synaptogenesis. *Exp Neurol,* 192**,** 60-72.

KIM, J. V. & DUSTIN, M. L. 2006. Innate response to focal necrotic injury inside the blood-brain barrier. *J Immunol,* 177**,** 5269-77.

KIM, W.-K., ALVAREZ, X., FISHER, J., BRONFIN, B., WESTMORELAND, S., MCLAURIN, J. & WILLIAMS, K. 2006. CD163 Identifies Perivascular Macrophages in Normal and Viral Encephalitic Brains and Potential Precursors to Perivascular Macrophages in Blood. *The American Journal of Pathology,* 168**,** 822-834.

KING, A., SWEENEY, F., BODI, I., TROAKES, C., MAEKAWA, S. & AL-SARRAJ, S. 2010. Abnormal TDP-43 expression is identified in the neocortex in cases of dementia pugilistica, but is mainly confined to the limbic system when identified in high and moderate stages of Alzheimer's disease. *Neuropathology,* 30**,** 408-19.

KIRK, J., PLUMB, J., MIRAKHUR, M. & MCQUAID, S. 2003. Tight junctional abnormality in multiple sclerosis white matter affects all calibres of vessel and is associated with blood-brain barrier leakage and active demyelination. *J Pathol,* 201**,** 319-27.

KOKOSKA, E. R., SMITH, G. S., PITTMAN, T. & WEBER, T. R. 1998. Early hypotension worsens neurological outcome in pediatric patients with moderately severe head trauma. *J Pediatr Surg,* 33**,** 333-8.

KOSSMANN, T., HANS, V. H., IMHOF, H. G., STOCKER, R., GROB, P., TRENTZ, O. & MORGANTI-KOSSMANN, C. 1995. Intrathecal and serum interleukin-6 and the acute-phase response in patients with severe traumatic brain injuries. *Shock,* 4**,** 311-7.

KRISTMAN, V. L., TATOR, C. H., KREIGER, N., RICHARDS, D., MAINWARING, L., JAGLAL, S., TOMLINSON, G. & COMPER, P. 2008. Does the apolipoprotein epsilon 4 allele predispose varsity athletes to concussion? A prospective cohort study. *Clin J Sport Med,* 18**,** 322-8.

KUMAR, A., ALVAREZ-CRODA, D. M., STOICA, B. A., FADEN, A. I. & LOANE, D. J. 2016a. Microglial/Macrophage Polarization Dynamics following Traumatic Brain Injury. *J Neurotrauma,* 33**,** 1732-1750.

KUMAR, A., BARRETT, J. P., ALVAREZ-CRODA, D.-M., STOICA, B. A., FADEN, A. I. & LOANE, D. J. 2016b. NOX2 drives M1-like microglial/macrophage activation and neurodegeneration following experimental traumatic brain injury. *Brain, Behavior, and Immunity,* 58**,** 291-309.

KUMAR, A., STOICA, B. A., SABIRZHANOV, B., BURNS, M. P., FADEN, A. I. & LOANE, D. J. 2013. Traumatic brain injury in aged animals increases lesion size and chronically alters microglial/macrophage classical and alternative activation states. *Neurobiol Aging,* 34**,** 1397-411.

KUMAR, R. G., BOLES, J. A. & WAGNER, A. K. 2015. Chronic Inflammation After Severe Traumatic Brain Injury: Characterization and Associations With Outcome at 6 and 12 Months Postinjury. *J Head Trauma Rehabil,* 30**,** 369-81.

KUTNER, K. C., ERLANGER, D. M., TSAI, J., JORDAN, B. & RELKIN, N. R. 2000. Lower cognitive performance of older football players possessing apolipoprotein E epsilon4. *Neurosurgery,* 47**,** 651-7; discussion 657-8.

LACE, G., INCE, P. G., BRAYNE, C., SAVVA, G. M., MATTHEWS, F. E., DE SILVA, R., SIMPSON, J. E. & WHARTON, S. B. 2012. Mesial Temporal Astrocyte Tau Pathology in the MRC-CFAS Ageing Brain Cohort. *Dementia and Geriatric Cognitive Disorders,* 34**,** 15-24.

LAHOZ, C., SCHAEFER, E. J., CUPPLES, L. A., WILSON, P. W., LEVY, D., OSGOOD, D., PARPOS, S., PEDRO-BOTET, J., DALY, J. A. & ORDOVAS, J. M. 2001. Apolipoprotein E genotype and cardiovascular disease in the Framingham Heart Study. *Atherosclerosis,* 154**,** 529-37.

LAIRD, M. D., VENDER, J. R. & DHANDAPANI, K. M. 2008. Opposing roles for reactive astrocytes following traumatic brain injury. *Neurosignals,* 16**,** 154-64.

LAUNER, L. J., ANDERSEN, K., DEWEY, M. E., LETENNEUR, L., OTT, A., AMADUCCI, L. A., BRAYNE, C., COPELAND, J. R., DARTIGUES, J. F., KRAGH-SORENSEN, P., LOBO, A., MARTINEZ-LAGE, J. M., STIJNEN, T. & HOFMAN, A. 1999. Rates and risk factors for dementia and Alzheimer's disease: results from EURODEM

pooled analyses. EURODEM Incidence Research Group and Work Groups. European Studies of Dementia. *Neurology,* 52**,** 78-84.
LERCH, J. P. & EVANS, A. C. 2005. Cortical thickness analysis examined through power analysis and a population simulation. *Neuroimage,* 24**,** 163-73.
LERCH, J. P., PRUESSNER, J. C., ZIJDENBOS, A., HAMPEL, H., TEIPEL, S. J. & EVANS, A. C. 2005. Focal Decline of Cortical Thickness in Alzheimer's Disease Identified by Computational Neuroanatomy. *Cerebral Cortex,* 15**,** 995-1001.
LEVINE, B., KOVACEVIC, N., NICA, E. I., CHEUNG, G., GAO, F., SCHWARTZ, M. L. & BLACK, S. E. 2008. The Toronto traumatic brain injury study: injury severity and quantified MRI. *Neurology,* 70**,** 771-8.
LI, Y., LI, Y., LI, X., ZHANG, S., ZHAO, J., ZHU, X. & TIAN, G. 2017. Head Injury as a Risk Factor for Dementia and Alzheimer's Disease: A Systematic Review and Meta-Analysis of 32 Observational Studies. *PLOS ONE,* 12**,** e0169650.
LI, Z., LIANG, G., MA, T., LI, J., WANG, P., LIU, L., YU, B., LIU, Y. & XUE, Y. 2015. Blood-brain barrier permeability change and regulation mechanism after subarachnoid hemorrhage. *Metab Brain Dis,* 30**,** 597-603.
LIAQUAT, I., DUNN, L. T., NICOLL, J. A. R., TEASDALE, G. M. & NORRIE, J. D. 2002. Effect of apolipoprotein E genotype on hematoma volume after trauma. *Journal of Neurosurgery,* 96**,** 90-96.
LIBERMAN, J. N., STEWART, W. F., WESNES, K. & TRONCOSO, J. 2002. Apolipoprotein E epsilon 4 and short-term recovery from predominantly mild brain injury. *Neurology,* 58**,** 1038-44.
LICHTMAN, S. W., SELIGER, G., TYCKO, B. & MARDER, K. 2000. Apolipoprotein E and functional recovery from brain injury following postacute rehabilitation. *Neurology,* 55**,** 1536-9.
LINDQVIST, D., WOLKOWITZ, O. M., MELLON, S., YEHUDA, R., FLORY, J. D., HENN-HAASE, C., BIERER, L. M., ABU-AMARA, D., COY, M., NEYLAN, T. C., MAKOTKINE, I., REUS, V. I., YAN, X., TAYLOR, N. M., MARMAR, C. R. & DHABHAR, F. S. 2014. Proinflammatory milieu in combat-related PTSD is independent of depression and early life stress. *Brain Behav Immun,* 42**,** 81-8.
LINDSLEY, C. W. 2017. Chronic Traumatic Encephalopathy (CTE): A Brief Historical Overview and Recent Focus on NFL Players. *ACS Chemical Neuroscience,* 8**,** 1629-1631.
LOANE, D. J. & BYRNES, K. R. 2010. Role of microglia in neurotrauma. *Neurotherapeutics,* 7**,** 366-77.
LOANE, D. J. & KUMAR, A. 2016. Microglia in the TBI Brain: The Good, The Bad, And The Dysregulated. *Experimental neurology,* 275**,** 316-327.
LOANE, D. J., KUMAR, A., STOICA, B. A., CABATBAT, R. & FADEN, A. I. 2014. Progressive neurodegeneration after experimental brain trauma: association with chronic microglial activation. *J Neuropathol Exp Neurol,* 73**,** 14-29.
LOBSIGER, C. S. & CLEVELAND, D. W. 2007. Glial cells as intrinsic components of non-cell-autonomous neurodegenerative disease. *Nat Neurosci,* 10**,** 1355-60.
LOPEZ-GONZALEZ, I., CARMONA, M., BLANCO, R., LUNA-MUNOZ, J., MARTINEZ-MANDONADO, A., MENA, R. & FERRER, I. 2013. Characterization of thorn-shaped astrocytes in white matter of temporal lobe in Alzheimer's disease brains. *Brain Pathol,* 23**,** 144-53.
LUO, J., NGUYEN, A., VILLEDA, S., ZHANG, H., DING, Z., LINDSEY, D., BIERI, G., CASTELLANO, J. M., BEAUPRE, G. S. & WYSS-CORAY, T. 2014. Long-term cognitive impairments and pathological alterations in a mouse model of repetitive mild traumatic brain injury. *Front Neurol,* 5**,** 12.
LYE, T. C. & SHORES, E. A. 2000. Traumatic brain injury as a risk factor for Alzheimer's disease: a review. *Neuropsychol Rev,* 10**,** 115-29.

MACKENZIE, J. D., SIDDIQI, F., BABB, J. S., BAGLEY, L. J., MANNON, L. J., SINSON, G. P. & GROSSMAN, R. I. 2002. Brain atrophy in mild or moderate traumatic brain injury: a longitudinal quantitative analysis. *AJNR Am J Neuroradiol,* 23**,** 1509-15.

MACMICKING, J., XIE, Q. W. & NATHAN, C. 1997. Nitric oxide and macrophage function. *Annu Rev Immunol,* 15.

MACPHERSON, P. & TEASDALE, E. 1988. CT demonstration of a 5th ventricle—a finding to KO boxers? *Neuroradiology,* 30**,** 506-510.

MAHLEY, R. W. & RALL, S. C., JR. 2000. Apolipoprotein E: far more than a lipid transport protein. *Annu Rev Genomics Hum Genet,* 1**,** 507-37.

MANCARDI, G. L., PERDELLI, F., RIVANO, C., LEONARDI, A. & BUGIANI, O. 1980. Thickening of the basement membrane of cortical capillaries in Alzheimer's disease. *Acta Neuropathol,* 49**,** 79-83.

MANN, D. M., YATES, P. O. & HAWKES, J. 1983. The pathology of the human locus ceruleus. *Clin Neuropathol,* 2**,** 1-7.

MANTOVANI, A., BISWAS, S. K., GALDIERO, M. R., SICA, A. & LOCATI, M. 2012. Macrophage plasticity and polarization in tissue repair and remodelling. *J Pathol,* 229.

MARAGAKIS, N. J. & ROTHSTEIN, J. D. 2006. Mechanisms of Disease: astrocytes in neurodegenerative disease. *Nat Clin Pract Neurol,* 2**,** 679-89.

MARCHI, N., BAZARIAN, J. J., PUVENNA, V., JANIGRO, M., GHOSH, C., ZHONG, J., ZHU, T., BLACKMAN, E., STEWART, D., ELLIS, J., BUTLER, R. & JANIGRO, D. 2013. Consequences of repeated blood-brain barrier disruption in football players. *PLoS One,* 8**,** e56805.

MARMAROU, A., SIGNORETTI, S., AYGOK, G., FATOUROS, P. & PORTELLA, G. 2006a. Traumatic brain edema in diffuse and focal injury: cellular or vasogenic? *Acta Neurochir Suppl,* 96**,** 24-9.

MARMAROU, A., SIGNORETTI, S., FATOUROS, P. P., PORTELLA, G., AYGOK, G. A. & BULLOCK, M. R. 2006b. Predominance of cellular edema in traumatic brain swelling in patients with severe head injuries. *J Neurosurg,* 104**,** 720-30.

MARTLAND, H. S. 1928. Punch drunk. *Journal of the American Medical Association,* 91**,** 1103-1107.

MATHIISEN, T. M., LEHRE, K. P., DANBOLT, N. C. & OTTERSEN, O. P. 2010. The perivascular astroglial sheath provides a complete covering of the brain microvessels: an electron microscopic 3D reconstruction. *Glia,* 58**,** 1094-103.

MAUGANS, T. A., FARLEY, C., ALTAYE, M., LEACH, J. & CECIL, K. M. 2012. Pediatric sports-related concussion produces cerebral blood flow alterations. *Pediatrics,* 129**,** 28-37.

MAURI, M., SINFORIANI, E., BONO, G., CITTADELLA, R., QUATTRONE, A., BOLLER, F. & NAPPI, G. 2006. Interaction between Apolipoprotein epsilon 4 and traumatic brain injury in patients with Alzheimer's disease and Mild Cognitive Impairment. *Funct Neurol,* 21**,** 223-8.

MAWDSLEY, C. & FERGUSON, F. R. 1963. Neurological Disease in Boxers. *Lancet,* 2**,** 795-801.

MAWUENYEGA, K. G., SIGURDSON, W., OVOD, V., MUNSELL, L., KASTEN, T., MORRIS, J. C., YARASHESKI, K. E. & BATEMAN, R. J. 2010. Decreased clearance of CNS beta-amyloid in Alzheimer's disease. *Science,* 330**,** 1774.

MAXWELL, W. L., DHILLON, K., HARPER, L., ESPIN, J., MACINTOSH, T. K., SMITH, D. H. & GRAHAM, D. I. 2003. There is differential loss of pyramidal cells from the human hippocampus with survival after blunt head injury. *J Neuropathol Exp Neurol,* 62**,** 272-9.

MAXWELL, W. L., IRVINE, A., ADAMS, J. H., GRAHAM, D. I. & GENNARELLI, T. A. 1988. Response of cerebral microvasculature to brain injury. *J Pathol,* 155**,** 327-35.

MAXWELL, W. L., MACKINNON, M. A., SMITH, D. H., MCINTOSH, T. K. & GRAHAM, D. I. 2006. Thalamic nuclei after human blunt head injury. *J Neuropathol Exp Neurol,* 65**,** 478-88.

MAXWELL, W. L., MACKINNON, M. A., STEWART, J. E. & GRAHAM, D. I. 2010. Stereology of cerebral cortex after traumatic brain injury matched to the Glasgow outcome score. *Brain,* 133**,** 139-60.

MAXWELL, W. L., WHITFIELD, P. C., SUZEN, B., GRAHAM, D. I., ADAMS, J. H., WATT, C. & GENNARELLI, T. A. 1992. The cerebrovascular response to experimental lateral head acceleration. *Acta Neuropathol,* 84**,** 289-96.

MAYEUX, R., OTTMAN, R., MAESTRE, G., NGAI, C., TANG, M. X., GINSBERG, H., CHUN, M., TYCKO, B. & SHELANSKI, M. 1995. Synergistic effects of traumatic head injury and apolipoprotein-epsilon 4 in patients with Alzheimer's disease. *Neurology,* 45**,** 555-7.

MCKAY, S. M., BROOKS, D. J., HU, P. & MCLACHLAN, E. M. 2007. Distinct types of microglial activation in white and grey matter of rat lumbosacral cord after mid-thoracic spinal transection. *J Neuropathol Exp Neurol,* 66**,** 698-710.

MCKEE, A. C., CANTU, R. C., NOWINSKI, C. J., HEDLEY-WHYTE, E. T., GAVETT, B. E., BUDSON, A. E., SANTINI, V. E., LEE, H. S., KUBILUS, C. A. & STERN, R. A. 2009. Chronic traumatic encephalopathy in athletes: progressive tauopathy after repetitive head injury. *J Neuropathol Exp Neurol,* 68**,** 709-35.

MCKEE, A. C. & DANESHVAR, D. H. 2015. The neuropathology of traumatic brain injury. *Handbook of clinical neurology,* 127**,** 45-66.

MCKEE, A. C., DANESHVAR, D. H., ALVAREZ, V. E. & STEIN, T. D. 2014. The neuropathology of sport. *Acta Neuropathol,* 127**,** 29-51.

MCKEE, A. C., GAVETT, B. E., STERN, R. A., NOWINSKI, C. J., CANTU, R. C., KOWALL, N. W., PERL, D. P., HEDLEY-WHYTE, E. T., PRICE, B., SULLIVAN, C., MORIN, P., LEE, H. S., KUBILUS, C. A., DANESHVAR, D. H., WULFF, M. & BUDSON, A. E. 2010. TDP-43 proteinopathy and motor neuron disease in chronic traumatic encephalopathy. *J Neuropathol Exp Neurol,* 69**,** 918-29.

MCKEE, A. C. & ROBINSON, M. E. 2014. Military-related traumatic brain injury and neurodegeneration. *Alzheimer's & Dementia,* 10**,** S242-S253.

MCKEE, A. C., STERN, R. A., NOWINSKI, C. J., STEIN, T. D., ALVAREZ, V. E., DANESHVAR, D. H., LEE, H. S., WOJTOWICZ, S. M., HALL, G., BAUGH, C. M., RILEY, D. O., KUBILUS, C. A., CORMIER, K. A., JACOBS, M. A., MARTIN, B. R., ABRAHAM, C. R., IKEZU, T., REICHARD, R. R., WOLOZIN, B. L., BUDSON, A. E., GOLDSTEIN, L. E., KOWALL, N. W. & CANTU, R. C. 2013. The spectrum of disease in chronic traumatic encephalopathy. *Brain,* 136**,** 43-64.

MEHTA, K. M., OTT, A., KALMIJN, S., SLOOTER, A. J., VAN DUIJN, C. M., HOFMAN, A. & BRETELER, M. M. 1999. Head trauma and risk of dementia and Alzheimer's disease: The Rotterdam Study. *Neurology,* 53**,** 1959-62.

MERKLEY, T. L., BIGLER, E. D., WILDE, E. A., MCCAULEY, S. R., HUNTER, J. V. & LEVIN, H. S. 2008. Diffuse changes in cortical thickness in pediatric moderate-to-severe traumatic brain injury. *J Neurotrauma,* 25**,** 1343-5.

MEZ, J., DANESHVAR, D. H., KIERNAN, P. T., ABDOLMOHAMMADI, B., ALVAREZ, V. E., HUBER, B. R., ALOSCO, M. L., SOLOMON, T. M., NOWINSKI, C. J., MCHALE, L., CORMIER, K. A., KUBILUS, C. A., MARTIN, B. M., MURPHY, L., BAUGH, C. M., MONTENIGRO, P. H., CHAISSON, C. E., TRIPODIS, Y., KOWALL, N. W., WEUVE, J., MCCLEAN, M. D., CANTU, R. C., GOLDSTEIN, L. E., KATZ, D. I., STERN, R. A., STEIN, T. D. & MCKEE, A. C. 2017. Clinicopathological Evaluation of Chronic

Traumatic Encephalopathy in Players of American Football. *Jama,* 318**,** 360-370.

MICHAEL, A. P., STOUT, J., ROSKOS, P. T., BOLZENIUS, J., GFELLER, J., MOGUL, D. & BUCHOLZ, R. 2015. Evaluation of Cortical Thickness after Traumatic Brain Injury in Military Veterans. *J Neurotrauma,* 32**,** 1751-8.

MICHALAK, Z., OBARI, D., ELLIS, M., THOM, M. & SISODIYA, S. M. 2017. Neuropathology of SUDEP: Role of inflammation, blood-brain barrier impairment, and hypoxia. *Neurology,* 88**,** 551-561.

MILLER, A. H. & RAISON, C. L. 2016. The role of inflammation in depression: from evolutionary imperative to modern treatment target. *Nat Rev Immunol,* 16**,** 22-34.

MILLER, D. W., COOKSON, M. R. & DICKSON, D. W. 2004. Glial cell inclusions and the pathogenesis of neurodegenerative diseases. *Neuron glia biology,* 1**,** 13-21.

MOISSE, K., MEPHAM, J., VOLKENING, K., WELCH, I., HILL, T. & STRONG, M. J. 2009a. Cytosolic TDP-43 expression following axotomy is associated with caspase 3 activation in NFL-/- mice: support for a role for TDP-43 in the physiological response to neuronal injury. *Brain Res,* 1296**,** 176-86.

MOISSE, K., VOLKENING, K., LEYSTRA-LANTZ, C., WELCH, I., HILL, T. & STRONG, M. J. 2009b. Divergent patterns of cytosolic TDP-43 and neuronal progranulin expression following axotomy: implications for TDP-43 in the physiological response to neuronal injury. *Brain Res,* 1249**,** 202-11.

MOLGAARD, C. A., STANFORD, E. P., MORTON, D. J., RYDEN, L. A., SCHUBERT, K. R. & GOLBECK, A. L. 1990. Epidemiology of head trauma and neurocognitive impairment in a multi-ethnic population. *Neuroepidemiology,* 9**,** 233-42.

MORGAN, R., KREIPKE, C. W., ROBERTS, G., BAGCHI, M. & RAFOLS, J. A. 2007. Neovascularization following traumatic brain injury: possible evidence for both angiogenesis and vasculogenesis. *Neurol Res,* 29**,** 375-81.

MORGANTI, J. M., RIPARIP, L.-K. & ROSI, S. 2016. Call Off the Dog(ma): M1/M2 Polarization Is Concurrent following Traumatic Brain Injury. *PLOS ONE,* 11**,** e0148001.

MORTIMER, J. A., FRENCH, L. R., HUTTON, J. T. & SCHUMAN, L. M. 1985. Head injury as a risk factor for Alzheimer's disease. *Neurology,* 35**,** 264-7.

MORTIMER, J. A., VAN DUIJN, C. M., CHANDRA, V., FRATIGLIONI, L., GRAVES, A. B., HEYMAN, A., JORM, A. F., KOKMEN, E., KONDO, K., ROCCA, W. A. & ET AL. 1991. Head trauma as a risk factor for Alzheimer's disease: a collaborative re-analysis of case-control studies. EURODEM Risk Factors Research Group. *Int J Epidemiol,* 20 Suppl 2**,** S28-35.

MOUZON, B. C., BACHMEIER, C., FERRO, A., OJO, J. O., CRYNEN, G., ACKER, C. M., DAVIES, P., MULLAN, M., STEWART, W. & CRAWFORD, F. 2014. Chronic neuropathological and neurobehavioral changes in a repetitive mild traumatic brain injury model. *Ann Neurol,* 75**,** 241-54.

MUIZELAAR, J. P., WARD, J. D., MARMAROU, A., NEWLON, P. G. & WACHI, A. 1989. Cerebral blood flow and metabolism in severely head-injured children. Part 2: Autoregulation. *J Neurosurg,* 71**,** 72-6.

MUNGAS, D., REED, B. R., JAGUST, W. J., DECARLI, C., MACK, W. J., KRAMER, J. H., WEINER, M. W., SCHUFF, N. & CHUI, H. C. 2002. Volumetric MRI predicts rate of cognitive decline related to AD and cerebrovascular disease. *Neurology,* 59**,** 867-73.

MYER, D. J., GURKOFF, G. G., LEE, S. M., HOVDA, D. A. & SOFRONIEW, M. V. 2006. Essential protective roles of reactive astrocytes in traumatic brain injury. *Brain,* 129**,** 2761-72.

NAG, S., ESKANDARIAN, M. R., DAVIS, J. & EUBANKS, J. H. 2002. Differential expression of vascular endothelial growth factor-A (VEGF-A) and VEGF-B after brain injury. *J Neuropathol Exp Neurol,* 61**,** 778-88.

NAG, S., TAKAHASHI, J. L. & KILTY, D. W. 1997. Role of vascular endothelial growth factor in blood-brain barrier breakdown and angiogenesis in brain trauma. *J Neuropathol Exp Neurol,* 56**,** 912-21.

NAGAMOTO-COMBS, K., MCNEAL, D. W., MORECRAFT, R. J. & COMBS, C. K. 2007. Prolonged microgliosis in the rhesus monkey central nervous system after traumatic brain injury. *J Neurotrauma,* 24**,** 1719-42.

NAGELE, R. G., WEGIEL, J., VENKATARAMAN, V., IMAKI, H., WANG, K. C. & WEGIEL, J. 2004. Contribution of glial cells to the development of amyloid plaques in Alzheimer's disease. *Neurobiol Aging,* 25**,** 663-74.

NAGY, D., KATO, T. & KUSHNER, P. D. 1994. Reactive astrocytes are widespread in the cortical gray matter of amyotrophic lateral sclerosis. *J Neurosci Res,* 38**,** 336-47.

NESELIUS, S., BRISBY, H., THEODORSSON, A., BLENNOW, K., ZETTERBERG, H. & MARCUSSON, J. 2012. CSF-biomarkers in Olympic boxing: diagnosis and effects of repetitive head trauma. *PLoS One,* 7**,** e33606.

NEUBUERGER, K. T., SINTON, D. W. & DENST, J. 1959. Cerebral atrophy associated with boxing. *AMA Arch Neurol Psychiatry,* 81**,** 403-8.

NEUMANN, M., KWONG, L. K., SAMPATHU, D. M., TROJANOWSKI, J. Q. & LEE, V. M. 2007. TDP-43 proteinopathy in frontotemporal lobar degeneration and amyotrophic lateral sclerosis: protein misfolding diseases without amyloidosis. *Arch Neurol,* 64**,** 1388-94.

NEUMANN, M., SAMPATHU, D. M., KWONG, L. K., TRUAX, A. C., MICSENYI, M. C., CHOU, T. T., BRUCE, J., SCHUCK, T., GROSSMAN, M., CLARK, C. M., MCCLUSKEY, L. F., MILLER, B. L., MASLIAH, E., MACKENZIE, I. R., FELDMAN, H., FEIDEN, W., KRETZSCHMAR, H. A., TROJANOWSKI, J. Q. & LEE, V. M. 2006. Ubiquitinated TDP-43 in frontotemporal lobar degeneration and amyotrophic lateral sclerosis. *Science,* 314**,** 130-3.

NEUROINFLAMMATION WORKING, G., AKIYAMA, H., BARGER, S., BARNUM, S., BRADT, B., BAUER, J., COLE, G. M., COOPER, N. R., EIKELENBOOM, P., EMMERLING, M., FIEBICH, B. L., FINCH, C. E., FRAUTSCHY, S., GRIFFIN, W. S. T., HAMPEL, H., HULL, M., LANDRETH, G., LUE, L. F., MRAK, R., MACKENZIE, I. R., MCGEER, P. L., O'BANION, M. K., PACHTER, J., PASINETTI, G., PLATA–SALAMAN, C., ROGERS, J., RYDEL, R., SHEN, Y., STREIT, W., STROHMEYER, R., TOOYOMA, I., VAN MUISWINKEL, F. L., VEERHUIS, R., WALKER, D., WEBSTER, S., WEGRZYNIAK, B., WENK, G. & WYSS–CORAY, T. 2000. Inflammation and Alzheimer's disease. *Neurobiology of aging,* 21**,** 383-421.

NICOLL, J. A., ROBERTS, G. W. & GRAHAM, D. I. 1995. Apolipoprotein E epsilon 4 allele is associated with deposition of amyloid beta-protein following head injury. *Nat Med,* 1**,** 135-7.

NISHITSUJI, K., HOSONO, T., NAKAMURA, T., BU, G. & MICHIKAWA, M. 2011. Apolipoprotein E regulates the integrity of tight junctions in an isoform-dependent manner in an in vitro blood-brain barrier model. *J Biol Chem,* 286**,** 17536-42.

NOWAK, L. A., SMITH, G. G. & REYES, P. F. 2009. Dementia in a retired world boxing champion: case report and literature review. *Clin Neuropathol,* 28**,** 275-80.

O'BRIEN, J. T., BLAMIRE, A. J., WATSON, R. & COLLOBY, S. J. ASSESSMENT OF REGIONAL CORTICAL THICKNESS ON MRI IN DEMENTIA WITH LEWY BODIES AND ALZHEIMER'S DISEASE. *Alzheimer's & Dementia: The Journal of the Alzheimer's Association,* 10**,** P242.

O'MEARA, E. S., KUKULL, W. A., SHEPPARD, L., BOWEN, J. D., MCCORMICK, W. C., TERI, L., PFANSCHMIDT, M., THOMPSON, J. D., SCHELLENBERG, G. D. & LARSON, E. B. 1997. Head injury and risk of Alzheimer's disease by apolipoprotein E genotype. *Am J Epidemiol,* 146**,** 373-84.

OBENAUS, A., NG, M., ORANTES, A. M., KINNEY-LANG, E., RASHID, F., HAMER, M., DEFAZIO, R. A., TANG, J., ZHANG, J. H. & PEARCE, W. J. 2017. Traumatic brain injury results in acute rarefication of the vascular network. *Scientific Reports,* 7**,** 239.

OBERMEIER, B., DANEMAN, R. & RANSOHOFF, R. M. 2013. Development, maintenance and disruption of the blood-brain barrier. *Nature medicine,* 19**,** 1584-1596.

OJO, J.-O., MOUZON, B., GREENBERG, M. B., BACHMEIER, C., MULLAN, M. & CRAWFORD, F. 2013. Repetitive Mild Traumatic Brain Injury Augments Tau Pathology and Glial Activation in Aged hTau Mice. *Journal of Neuropathology & Experimental Neurology,* 72**,** 137-151.

OJO, J. O., MOUZON, B., ALGAMAL, M., LEARY, P., LYNCH, C., ABDULLAH, L., EVANS, J., MULLAN, M., BACHMEIER, C., STEWART, W. & CRAWFORD, F. 2016. Chronic Repetitive Mild Traumatic Brain Injury Results in Reduced Cerebral Blood Flow, Axonal Injury, Gliosis, and Increased T-Tau and Tau Oligomers. *J Neuropathol Exp Neurol,* 75**,** 636-55.

OMALU, B., BAILES, J., HAMILTON, R. L., KAMBOH, M. I., HAMMERS, J., CASE, M. & FITZSIMMONS, R. 2011a. Emerging histomorphologic phenotypes of chronic traumatic encephalopathy in American athletes. *Neurosurgery,* 69**,** 173-83; discussion 183.

OMALU, B., HAMMERS, J. L., BAILES, J., HAMILTON, R. L., KAMBOH, M. I., WEBSTER, G. & FITZSIMMONS, R. P. 2011b. Chronic traumatic encephalopathy in an Iraqi war veteran with posttraumatic stress disorder who committed suicide. *Neurosurg Focus,* 31**,** E3.

OMALU, B. I., DEKOSKY, S. T., HAMILTON, R. L., MINSTER, R. L., KAMBOH, M. I., SHAKIR, A. M. & WECHT, C. H. 2006a. Chronic traumatic encephalopathy in a national football league player: part II. *Neurosurgery,* 59**,** 1086-92; discussion 1092-3.

OMALU, B. I., DEKOSKY, S. T., MINSTER, R. L., KAMBOH, M. I., HAMILTON, R. L. & WECHT, C. H. 2005. Chronic traumatic encephalopathy in a National Football League player. *Neurosurgery,* 57**,** 128-34; discussion 128-34.

OMALU, B. I., DEKOSKY, S. T., MINSTER, R. L., KAMBOH, M. I., HAMILTON, R. L. & WECHT, C. H. 2006b. Chronic Traumatic Encephalopathy in a National Football League Player. *Neurosurgery,* 58**,** E1003.

OMALU, B. I., FITZSIMMONS, R. P., HAMMERS, J. & BAILES, J. 2010a. Chronic traumatic encephalopathy in a professional American wrestler. *J Forensic Nurs,* 6**,** 130-6.

OMALU, B. I., HAMILTON, R. L., KAMBOH, M. I., DEKOSKY, S. T. & BAILES, J. 2010b. Chronic traumatic encephalopathy (CTE) in a National Football League Player: Case report and emerging medicolegal practice questions. *J Forensic Nurs,* 6**,** 40-6.

OMMAYA, A. K., ROCKOFF, S. D. & BALDWIN, M. 1964. Experimental Concussion; a First Report. *J Neurosurg,* 21**,** 249-65.

OSTROW, L. W., SUCHYNA, T. M. & SACHS, F. 2011. Stretch induced endothelin-1 secretion by adult rat astrocytes involves calcium influx via stretch-activated ion channels (SACs). *Biochemical and Biophysical Research Communications,* 410**,** 81-86.

PARSONAGE, M. 2016. Traumatic brain injury and offending. Centre for Mental health.

PAUL, J., STRICKLAND, S. & MELCHOR, J. P. 2007. Fibrin deposition accelerates neurovascular damage and neuroinflammation in mouse models of Alzheimer's disease. *J Exp Med,* 204**,** 1999-2008.

PAYNE, E. E. 1968. Brains of boxers. *Neurochirurgia (Stuttg),* 11**,** 173-88.

PERRY, V. H., NICOLL, J. A. & HOLMES, C. 2010. Microglia in neurodegenerative disease. *Nat Rev Neurol,* 6**,** 193-201.

PETERSEN, M. A., RYU, J. K. & AKASSOGLOU, K. 2018. Fibrinogen in neurological diseases: mechanisms, imaging and therapeutics. *Nat Rev Neurosci,* 19**,** 283-301.

PETRAGLIA, A. L., PLOG, B. A., DAYAWANSA, S., DASHNAW, M. L., CZERNIECKA, K., WALKER, C. T., CHEN, M., HYRIEN, O., ILIFF, J. J., DEANE, R., HUANG, J. H. & NEDERGAARD, M. 2014a. The pathophysiology underlying repetitive mild traumatic brain injury in a novel mouse model of chronic traumatic encephalopathy. *Surg Neurol Int,* 5**,** 184.

PETRAGLIA, A. L., PLOG, B. A., DAYAWANSA, S., DASHNAW, M. L., CZERNIECKA, K., WALKER, C. T., CHEN, M., HYRIEN, O., ILIFF, J. J., DEANE, R., HUANG, J. H. & NEDERGAARD, M. 2014b. The pathophysiology underlying repetitive mild traumatic brain injury in a novel mouse model of chronic traumatic encephalopathy. *Surgical Neurology International,* 5**,** 184.

PEY, P., PEARCE, R. K. B., KALAITZAKIS, M. E., GRIFFIN, W. S. T. & GENTLEMAN, S. M. 2014. Phenotypic profile of alternative activation marker CD163 is different in Alzheimer's and Parkinson's disease. *Acta Neuropathologica Communications,* 2**,** 21-21.

PICKLES, W. 1950. Acute general edema of the brain in children with head injuries. *N Engl J Med,* 242**,** 607-11.

PIGULA, F. A., WALD, S. L., SHACKFORD, S. R. & VANE, D. W. 1993. The effect of hypotension and hypoxia on children with severe head injuries. *J Pediatr Surg,* 28**,** 310-4; discussion 315-6.

PITTMAN, A. M., MYERS, A. J., DUCKWORTH, J., BRYDEN, L., HANSON, M., ABOU-SLEIMAN, P., WOOD, N. W., HARDY, J., LEES, A. & DE SILVA, R. 2004. The structure of the tau haplotype in controls and in progressive supranuclear palsy. *Hum Mol Genet,* 13**,** 1267-74.

PLASSMAN, B. L. & GRAFMAN, J. 2015. Traumatic brain injury and late-life dementia. *Handb Clin Neurol,* 128**,** 711-22.

PLASSMAN, B. L., HAVLIK, R. J., STEFFENS, D. C., HELMS, M. J., NEWMAN, T. N., DROSDICK, D., PHILLIPS, C., GAU, B. A., WELSH-BOHMER, K. A., BURKE, J. R., GURALNIK, J. M. & BREITNER, J. C. 2000. Documented head injury in early adulthood and risk of Alzheimer's disease and other dementias. *Neurology,* 55**,** 1158-66.

POSCHL, E., SCHLOTZER-SCHREHARDT, U., BRACHVOGEL, B., SAITO, K., NINOMIYA, Y. & MAYER, U. 2004. Collagen IV is essential for basement membrane stability but dispensable for initiation of its assembly during early development. *Development,* 131**,** 1619-28.

POVLISHOCK, J. T., BECKER, D. P., SULLIVAN, H. G. & MILLER, J. D. 1978. Vascular permeability alterations to horseradish peroxidase in experimental brain injury. *Brain Res,* 153**,** 223-39.

POVLISHOCK, J. T., KONTOS, H. A., WEI, E. P., ROSENBLUM, W. I. & BECKER, D. P. 1980. Changes in the cerebral vasculature after hypertension and trauma: a combined scanning and transmission electron microscopic analysis. *Adv Exp Med Biol,* 131**,** 227-41.

PRICE, L., WILSON, C. & GRANT, G. 2016. Blood-Brain Barrier Pathophysiology following Traumatic Brain Injury. *In:* LASKOWITZ, D. & GRANT, G. (eds.) *Translational Research in Traumatic Brain Injury.* Boca Raton (FL).

PRINCE, P. M. K. A. P. M. 2007. Dementia UK. London: Alzheimer's society.

QIN, L., LIU, Y., WANG, T., WEI, S. J., BLOCK, M. L., WILSON, B., LIU, B. & HONG, J. S. 2004. NADPH oxidase mediates lipopolysaccharide-induced neurotoxicity and proinflammatory gene expression in activated microglia. *J Biol Chem,* 279**,** 1415-21.

RAJ, D., YIN, Z., BREUR, M., DOORDUIN, J., HOLTMAN, I. R., OLAH, M., MANTINGH-OTTER, I. J., VAN DAM, D., DE DEYN, P. P., DEN DUNNEN, W., EGGEN, B. J. L., AMOR, S. & BODDEKE, E. 2017. Increased White Matter Inflammation in Aging- and Alzheimer's Disease Brain. *Frontiers in Molecular Neuroscience,* 10**,** 206.

RAMLACKHANSINGH, A. F., BROOKS, D. J., GREENWOOD, R. J., BOSE, S. K., TURKHEIMER, F. E., KINNUNEN, K. M., GENTLEMAN, S., HECKEMANN, R. A., GUNANAYAGAM, K., GELOSA, G. & SHARP, D. J. 2011a. Inflammation after trauma: microglial activation and traumatic brain injury. *Ann Neurol,* 70**,** 374-83.

RAMLACKHANSINGH, A. F., BROOKS, D. J., GREENWOOD, R. J., BOSE, S. K., TURKHEIMER, F. E., KINNUNEN, K. M., GENTLEMAN, S., HECKEMANN, R. A., GUNANAYAGAM, K., GELOSA, G. & SHARP, D. J. 2011b. Inflammation after trauma: Microglial activation and traumatic brain injury. *Annals of Neurology,* 70**,** 374-383.

RANSOHOFF, R. M. 2016. A polarizing question: do M1 and M2 microglia exist? *Nat Neurosci,* 19**,** 987-91.

RINDER, L. & OLSSON, Y. 1968. Studies on vascular permeability changes in experimental brain concussion. I. Distribution of circulating fluorescent indicators in brain and cervical cord after sudden mechanical loading of the brain. *Acta Neuropathol,* 11**,** 183-200.

ROBERTS, A. H. 1969. *Brain damage in boxers : a study of the prevalence of traumatic encephalopathy among ex-professional boxers* London, Pitman Medical & Scientific Publishing.

ROBERTS, E. S., MASLIAH, E. & FOX, H. S. 2004. CD163 identifies a unique population of ramified microglia in HIV encephalitis (HIVE). *J Neuropathol Exp Neurol,* 63**,** 1255-64.

ROBERTS, G. W., ALLSOP, D. & BRUTON, C. 1990a. The occult aftermath of boxing. *J Neurol Neurosurg Psychiatry,* 53**,** 373-8.

ROBERTS, G. W., GENTLEMAN, S. M., LYNCH, A. & GRAHAM, D. I. 1991. beta A4 amyloid protein deposition in brain after head trauma. *Lancet,* 338**,** 1422-3.

ROBERTS, G. W., GENTLEMAN, S. M., LYNCH, A., MURRAY, L., LANDON, M. & GRAHAM, D. I. 1994. Beta amyloid protein deposition in the brain after severe head injury: implications for the pathogenesis of Alzheimer's disease. *J Neurol Neurosurg Psychiatry,* 57**,** 419-25.

ROBERTS, G. W., WHITWELL, H. L., ACLAND, P. R. & BRUTON, C. J. 1990b. Dementia in a punch-drunk wife. *Lancet,* 335**,** 918-9.

RODRIGUEZ-BAEZA, A., REINA-DE LA TORRE, F., POCA, A., MARTI, M. & GARNACHO, A. 2003. Morphological features in human cortical brain microvessels after head injury: a three-dimensional and immunocytochemical study. *Anat Rec A Discov Mol Cell Evol Biol,* 273**,** 583-93.

ROJO, L. E., FERNANDEZ, J. A., MACCIONI, A. A., JIMENEZ, J. M. & MACCIONI, R. B. 2008. Neuroinflammation: implications for the pathogenesis and molecular diagnosis of Alzheimer's disease. *Arch Med Res,* 39**,** 1-16.

ROSS, D. E. 2011. Review of longitudinal studies of MRI brain volumetry in patients with traumatic brain injury. *Brain Inj,* 25**,** 1271-8.

ROSS, D. E., OCHS, A. L., SEABAUGH, J. M., DEMARK, M. F., SHRADER, C. R., MARWITZ, J. H. & HAVRANEK, M. D. 2012. Progressive brain atrophy in patients with chronic neuropsychiatric symptoms after mild traumatic brain injury: a preliminary study. *Brain Inj,* 26**,** 1500-9.

ROUACH, N., AVIGNONE, E., MEME, W., KOULAKOFF, A., VENANCE, L., BLOMSTRAND, F. & GIAUME, C. 2002. Gap junctions and connexin expression in the normal and pathological central nervous system. *Biol Cell,* 94**,** 457-75.

SAGARE, A. P., BELL, R. D., ZHAO, Z., MA, Q., WINKLER, E. A., RAMANATHAN, A. & ZLOKOVIC, B. V. 2013. Pericyte loss influences Alzheimer-like neurodegeneration in mice. *Nat Commun,* 4**,** 2932.

SAING, T., DICK, M., NELSON, P. T., KIM, R. C., CRIBBS, D. H. & HEAD, E. 2012. Frontal cortex neuropathology in dementia pugilistica. *J Neurotrauma,* 29**,** 1054-70.

SALIB, E. & HILLIER, V. 1997. Head injury and the risk of Alzheimer's disease: a case control study. *Int J Geriatr Psychiatry,* 12**,** 363-8.

SANDOVAL, K. E. & WITT, K. A. 2008. Blood-brain barrier tight junction permeability and ischemic stroke. *Neurobiol Dis,* 32**,** 200-19.

SATO, T., TAKEUCHI, S., SAITO, A., DING, W., BAMBA, H., MATSUURA, H., HISA, Y., TOOYAMA, I. & URUSHITANI, M. 2009. Axonal ligation induces transient redistribution of TDP-43 in brainstem motor neurons. *Neuroscience,* 164**,** 1565-78.

SAUNDERS, A. M., STRITTMATTER, W. J., SCHMECHEL, D., GEORGE-HYSLOP, P. H., PERICAK-VANCE, M. A., JOO, S. H., ROSI, B. L., GUSELLA, J. F., CRAPPER-MACLACHLAN, D. R., ALBERTS, M. J. & ET AL. 1993. Association of apolipoprotein E allele epsilon 4 with late-onset familial and sporadic Alzheimer's disease. *Neurology,* 43**,** 1467-72.

SAUNDERS, N. R., LIDDELOW, S. A. & DZIEGIELEWSKA, K. M. 2012. Barrier Mechanisms in the Developing Brain. *Frontiers in Pharmacology,* 3**,** 46.

SAUNDERS, R. L. & HARBAUGH, R. E. 1984. The second impact in catastrophic contact-sports head trauma. *JAMA,* 252**,** 538-9.

SAVJANI, R. R., TAYLOR, B. A., ACION, L., WILDE, E. A. & JORGE, R. E. 2017. Accelerated Changes in Cortical Thickness Measurements with Age in Military Service Members with Traumatic Brain Injury. *J Neurotrauma*.

SAW, M. M., CHAMBERLAIN, J., BARR, M., MORGAN, M. P., BURNETT, J. R. & HO, K. M. 2014. Differential disruption of blood-brain barrier in severe traumatic brain injury. *Neurocrit Care,* 20**,** 209-16.

SAYED, N., CULVER, C., DAMS-O'CONNOR, K., HAMMOND, F. & DIAZ-ARRASTIA, R. 2013. Clinical phenotype of dementia after traumatic brain injury. *J Neurotrauma,* 30**,** 1117-22.

SCHACHTRUP, C., RYU, J. K., HELMRICK, M., VAGENA, E., GALANAKIS, D. K., DEGEN, J. L., MARGOLIS, R. U. & AKASSOGLOU, K. 2010. Fibrinogen triggers astrocyte scar formation by promoting the availability of active TGF-β after vascular damage. *The Journal of neuroscience : the official journal of the Society for Neuroscience,* 30**,** 5843-5854.

SCHMIDT, M. L., ZHUKAREVA, V., NEWELL, K. L., LEE, V. M. & TROJANOWSKI, J. Q. 2001. Tau isoform profile and phosphorylation state in dementia pugilistica recapitulate Alzheimer's disease. *Acta Neuropathol,* 101**,** 518-24.

SCHOFIELD, P. W., TANG, M., MARDER, K., BELL, K., DOONEIEF, G., CHUN, M., SANO, M., STERN, Y. & MAYEUX, R. 1997. Alzheimer's disease after remote head injury: an incidence study. *J Neurol Neurosurg Psychiatry,* 62**,** 119-24.

SCHOLLER, K., TRINKL, A., KLOPOTOWSKI, M., THAL, S. C., PLESNILA, N., TRABOLD, R., HAMANN, G. F., SCHMID-ELSAESSER, R. & ZAUSINGER, S. 2007. Characterization of microvascular basal lamina damage and blood-brain barrier dysfunction following subarachnoid hemorrhage in rats. *Brain Res,* 1142**,** 237-46.

SEMPLE, B. D., BLOMGREN, K., GIMLIN, K., FERRIERO, D. M. & NOBLE-HAEUSSLEIN, L. J. 2013. Brain development in rodents and humans: Identifying benchmarks of maturation and vulnerability to injury across species. *Prog Neurobiol,* 106-107**,** 1-16.

SHAPIRA, Y., SETTON, D., ARTRU, A. A. & SHOHAMI, E. 1993. Blood-brain barrier permeability, cerebral edema, and neurologic function after closed head injury in rats. *Anesth Analg,* 77**,** 141-8.

SHARPLES, P. M., MATTHEWS, D. S. & EYRE, J. A. 1995. Cerebral blood flow and metabolism in children with severe head injuries. Part 2: Cerebrovascular resistance and its determinants. *J Neurol Neurosurg Psychiatry,* 58**,** 153-9.

SHAW, K., MACKINNON, M. A., RAGHUPATHI, R., SAATMAN, K. E., MCLNTOSH, T. K. & GRAHAM, D. I. 2001. TUNEL-positive staining in white and grey matter after fatal head injury in man. *Clin Neuropathol,* 20**,** 106-12.

SHERRIFF, F. E., BRIDGES, L. R. & SIVALOGANATHAN, S. 1994. Early detection of axonal injury after human head trauma using immunocytochemistry for beta-amyloid precursor protein. *Acta Neuropathol,* 87**,** 55-62.

SHIBATA, M., YAMADA, S., KUMAR, S. R., CALERO, M., BADING, J., FRANGIONE, B., HOLTZMAN, D. M., MILLER, C. A., STRICKLAND, D. K., GHISO, J. & ZLOKOVIC, B. V. 2000a. Clearance of Alzheimer's amyloid-beta(1-40) peptide from brain by LDL receptor-related protein-1 at the blood-brain barrier. *Journal of Clinical Investigation,* 106**,** 1489-1499.

SHIBATA, M., YAMADA, S., KUMAR, S. R., CALERO, M., BADING, J., FRANGIONE, B., HOLTZMAN, D. M., MILLER, C. A., STRICKLAND, D. K., GHISO, J. & ZLOKOVIC, B. V. 2000b. Clearance of Alzheimer's amyloid-ss(1-40) peptide from brain by LDL receptor-related protein-1 at the blood-brain barrier. *J Clin Invest,* 106**,** 1489-99.

SHIVELY, S., SCHER, A. I., PERL, D. P. & DIAZ-ARRASTIA, R. 2012. Dementia resulting from traumatic brain injury: What is the pathology? *Archives of Neurology,* 69**,** 1245-1251.

SHIVELY, S. B., HORKAYNE-SZAKALY, I., JONES, R. V., KELLY, J. P., ARMSTRONG, R. C. & PERL, D. P. Characterisation of interface astroglial scarring in the human brain after blast exposure: a post-mortem case series. *The Lancet Neurology,* 15**,** 944-953.

SHIVELY, S. B., HORKAYNE-SZAKALY, I., JONES, R. V., KELLY, J. P., ARMSTRONG, R. C. & PERL, D. P. 2016. Characterisation of interface astroglial scarring in the human brain after blast exposure: a post-mortem case series. *Lancet Neurol,* 15**,** 944-953.

SHREIBER, D. I., SMITH, D. H. & MEANEY, D. F. 1999. Immediate in vivo response of the cortex and the blood-brain barrier following dynamic cortical deformation in the rat. *Neurosci Lett,* 259**,** 5-8.

SICA, A. & MANTOVANI, A. 2012. Macrophage plasticity and polarization: in vivo veritas. *J Clin Invest,* 122**,** 787-95.

SILVER, J. & MILLER, J. H. 2004. Regeneration beyond the glial scar. *Nat Rev Neurosci,* 5**,** 146-56.

SIMON, D. W., MCGEACHY, M. J., BAYIR, H., CLARK, R. S., LOANE, D. J. & KOCHANEK, P. M. 2017. The far-reaching scope of neuroinflammation after traumatic brain injury. *Nat Rev Neurol,* 13**,** 171-191.

SIRKO, S., IRMLER, M., GASCÓN, S., BEK, S., SCHNEIDER, S., DIMOU, L., OBERMANN, J., DE SOUZA PAIVA, D., POIRIER, F., BECKERS, J., HAUCK, S. M., BARDE, Y.-A. & GÖTZ, M. 2015. Astrocyte reactivity after brain injury—: The role of galectins 1 and 3. *Glia,* 63**,** 2340-2361.

SMITH, C., GRAHAM, D. I., MURRAY, L. S. & NICOLL, J. A. 2003a. Tau immunohistochemistry in acute brain injury. *Neuropathol Appl Neurobiol,* 29**,** 496-502.

SMITH, C., GRAHAM, D. I., MURRAY, L. S., STEWART, J. & NICOLL, J. A. 2006. Association of APOE e4 and cerebrovascular pathology in traumatic brain injury. *J Neurol Neurosurg Psychiatry,* 77**,** 363-6.

SMITH, D. H., CHEN, X. H., IWATA, A. & GRAHAM, D. I. 2003b. Amyloid beta accumulation in axons after traumatic brain injury in humans. *J Neurosurg,* 98**,** 1072-7.

SMITH, D. H., CHEN, X. H., NONAKA, M., TROJANOWSKI, J. Q., LEE, V. M., SAATMAN, K. E., LEONI, M. J., XU, B. N., WOLF, J. A. & MEANEY, D. F. 1999. Accumulation of amyloid beta and tau and the formation of neurofilament inclusions following diffuse brain injury in the pig. *J Neuropathol Exp Neurol,* 58**,** 982-92.

SMITH, D. H., JOHNSON, V. E. & STEWART, W. 2013. Chronic neuropathologies of single and repetitive TBI: substrates of dementia? *Nat Rev Neurol,* 9**,** 211-21.

SMITH, D. H., SOARES, H. D., PIERCE, J. S., PERLMAN, K. G., SAATMAN, K. E., MEANEY, D. F., DIXON, C. E. & MCINTOSH, T. K. 1995. A model of parasagittal controlled cortical impact in the mouse: cognitive and histopathologic effects. *J Neurotrauma,* 12**,** 169-78.

SMITH, D. H., URYU, K., SAATMAN, K. E., TROJANOWSKI, J. Q. & MCINTOSH, T. K. 2003c. Protein accumulation in traumatic brain injury. *Neuromolecular Med,* 4**,** 59-72.

SOFRONIEW, M. V. & VINTERS, H. V. 2010. Astrocytes: biology and pathology. *Acta Neuropathologica,* 119**,** 7-35.

SOLITO, E. & SASTRE, M. 2012. Microglia Function in Alzheimer's Disease. *Frontiers in Pharmacology,* 3**,** 14.

SORBI S, N. B., PIACENTINI S, REPICE A, LATORRACA S, ET AL. 1995. ApoE as a prognostic factor for post-traumatic coma. *Nat.Med***,** 1.

SPILLANE, J. D. 1962. Five boxers. *Br Med J,* 2**,** 1205-10.

SPILLANTINI, M. G. & GOEDERT, M. 1998. Tau protein pathology in neurodegenerative diseases. *Trends Neurosci,* 21**,** 428-33.

STAHEL, P. F., MORGANTI-KOSSMANN, M. C., PEREZ, D., REDAELLI, C., GLOOR, B., TRENTZ, O. & KOSSMANN, T. 2001. Intrathecal levels of complement-derived soluble membrane attack complex (sC5b-9) correlate with blood-brain barrier dysfunction in patients with traumatic brain injury. *J Neurotrauma,* 18**,** 773-81.

STARR, J. M., FARRALL, A. J., ARMITAGE, P., MCGURN, B. & WARDLAW, J. 2009. Blood-brain barrier permeability in Alzheimer's disease: a case-control MRI study. *Psychiatry Res,* 171**,** 232-41.

STEFANSSON, H., HELGASON, A., THORLEIFSSON, G., STEINTHORSDOTTIR, V., MASSON, G., BARNARD, J., BAKER, A., JONASDOTTIR, A., INGASON, A., GUDNADOTTIR, V. G., DESNICA, N., HICKS, A., GYLFASON, A., GUDBJARTSSON, D. F., JONSDOTTIR, G. M., SAINZ, J., AGNARSSON, K., BIRGISDOTTIR, B., GHOSH, S., OLAFSDOTTIR, A., CAZIER, J. B., KRISTJANSSON, K., FRIGGE, M. L., THORGEIRSSON, T. E., GULCHER, J. R., KONG, A. & STEFANSSON, K. 2005. A common inversion under selection in Europeans. *Nat Genet,* 37**,** 129-37.

STEIN, T. D., ALVAREZ, V. E. & MCKEE, A. C. 2014. Chronic traumatic encephalopathy: a spectrum of neuropathological changes following repetitive brain trauma in athletes and military personnel. *Alzheimer's Research & Therapy,* 6**,** 4-4.

STEIN, T. D., MONTENIGRO, P. H., ALVAREZ, V. E., XIA, W., CRARY, J. F., TRIPODIS, Y., DANESHVAR, D. H., MEZ, J., SOLOMON, T., MENG, G., KUBILUS, C. A., CORMIER, K. A., MENG, S., BABCOCK, K., KIERNAN, P., MURPHY, L., NOWINSKI, C. J., MARTIN, B., DIXON, D., STERN, R. A., CANTU, R. C., KOWALL, N. W. & MCKEE, A. C. 2015. Beta-amyloid deposition in chronic traumatic encephalopathy. *Acta Neuropathol,* 130**,** 21-34.

STEWART, W., MCNAMARA, P. H., LAWLOR, B., HUTCHINSON, S. & FARRELL, M. 2016. Chronic traumatic encephalopathy: a potential late and under recognized consequence of rugby union? *QJM,* 109**,** 11-5.

STILES, J. & JERNIGAN, T. L. 2010. The basics of brain development. *Neuropsychol Rev,* 20**,** 327-48.

STOUT, C. E., COSTANTIN, J. L., NAUS, C. C. & CHARLES, A. C. 2002. Intercellular calcium signaling in astrocytes via ATP release through connexin hemichannels. *J Biol Chem,* 277**,** 10482-8.

STRICH, S. J. 1956. Diffuse degeneration of the cerebral white matter in severe dementia following head injury. *J Neurol Neurosurg Psychiatry,* 19**,** 163-85.

SUNDSTROM A, M. P., NILSSON LG, CRUTS M, ADOLFSSON R, ET AL. 2004. APOE influences on neuropsychological function after mild head injury: within-person comparisons. *Neurology***,** 1963-66.

SUSARLA, B. T., VILLAPOL, S., YI, J. H., GELLER, H. M. & SYMES, A. J. 2014. Temporal patterns of cortical proliferation of glial cell populations after traumatic brain injury in mice. *ASN Neuro,* 6**,** 159-70.

SUTCLIFFE, J. G., HEDLUND, P. B., THOMAS, E. A., BLOOM, F. E. & HILBUSH, B. S. 2011. Peripheral reduction of beta-amyloid is sufficient to reduce brain beta-amyloid: implications for Alzheimer's disease. *J Neurosci Res,* 89**,** 808-14.

SUZUKI, T., ISHII, I., INOUE, S., MATSUDA, H., KURODA, M., ABE, K., AMINO, S., ARAI, H., HANYU, H. & KATSUNUMA, H. 1990. [Reproducibility of a non-invasive quantitative assessment of cerebral blood flow using 123I-IMP SPECT]. *Kaku Igaku,* 27**,** 1331-6.

SWEENEY, M. D., SAGARE, A. P. & ZLOKOVIC, B. V. 2018. Blood-brain barrier breakdown in Alzheimer disease and other neurodegenerative disorders. *Nat Rev Neurol*.

TAMAKI, K., SADOSHIMA, S. & HEISTAD, D. D. 1984. Increased susceptibility to osmotic disruption of the blood-brain barrier in chronic hypertension. *Hypertension,* 6**,** 633-8.

TANG-SCHOMER, M. D., JOHNSON, V. E., BAAS, P. W., STEWART, W. & SMITH, D. H. 2012. Partial interruption of axonal transport due to microtubule breakage accounts for the formation of periodic varicosities after traumatic axonal injury. *Exp Neurol,* 233**,** 364-72.

TANG-SCHOMER, M. D., PATEL, A. R., BAAS, P. W. & SMITH, D. H. 2010. Mechanical breaking of microtubules in axons during dynamic stretch injury underlies delayed elasticity, microtubule disassembly, and axon degeneration. *Faseb j,* 24**,** 1401-10.

TEASDALE, G. M., MURRAY, G. D. & NICOLL, J. A. 2005. The association between APOE epsilon4, age and outcome after head injury: a prospective cohort study. *Brain,* 128**,** 2556-61.

TEASDALE, G. M., NICOLL, J. A., MURRAY, G. & FIDDES, M. 1997. Association of apolipoprotein E polymorphism with outcome after head injury. *Lancet,* 350**,** 1069-71.

THAU-ZUCHMAN, O., SHOHAMI, E., ALEXANDROVICH, A. G. & LEKER, R. R. 2010. Vascular endothelial growth factor increases neurogenesis after traumatic brain injury. *J Cereb Blood Flow Metab,* 30**,** 1008-16.

THOMAS, M., HAAS, T. S., DOERER, J. J., HODGES, J. S., AICHER, B. O., GARBERICH, R. F., MUELLER, F. O., CANTU, R. C. & MARON, B. J. 2011. Epidemiology of sudden death in young, competitive athletes due to blunt trauma. *Pediatrics,* 128**,** e1-8.

TIERNEY, R. T., MANSELL, J. L., HIGGINS, M., MCDEVITT, J. K., TOONE, N., GAUGHAN, J. P., MISHRA, A. & KRYNETSKIY, E. 2010. Apolipoprotein E genotype and concussion in college athletes. *Clin J Sport Med,* 20**,** 464-8.

TOMAIUOLO, F., CARLESIMO, G. A., DI PAOLA, M., PETRIDES, M., FERA, F., BONANNI, R., FORMISANO, R., PASQUALETTI, P. & CALTAGIRONE, C. 2004. Gross morphology and morphometric sequelae in the hippocampus, fornix, and corpus callosum of patients with severe non-missile traumatic brain injury without macroscopically detectable lesions: a T1 weighted MRI study. *J Neurol Neurosurg Psychiatry,* 75**,** 1314-22.

TOMKINS, O., FEINTUCH, A., BENIFLA, M., COHEN, A., FRIEDMAN, A. & SHELEF, I. 2011. Blood-brain barrier breakdown following traumatic brain injury: a possible role in posttraumatic epilepsy. *Cardiovasc Psychiatry Neurol,* 2011**,** 765923.

TONTISIRIN, N., ARMSTEAD, W., WAITAYAWINYU, P., MOORE, A., UDOMPHORN, Y., ZIMMERMAN, J. J., CHESNUT, R. & VAVILALA, M. S. 2007. Change in cerebral autoregulation as a function of time in children after severe traumatic brain injury: a case series. *Childs Nerv Syst,* 23**,** 1163-9.

TOWN, T., LAOUAR, Y., PITTENGER, C., MORI, T., SZEKELY, C. A., TAN, J., DUMAN, R. S. & FLAVELL, R. A. 2008. Blocking TGF-beta-Smad2/3 innate immune signaling mitigates Alzheimer-like pathology. *Nat Med,* 14**,** 681-7.

TURNER, A. J., ISAAC, R. E. & COATES, D. 2001. The neprilysin (NEP) family of zinc metalloendopeptidases: genomics and function. *Bioessays,* 23**,** 261-9.

TURTZO, L. C., LESCHER, J., JANES, L., DEAN, D. D., BUDDE, M. D. & FRANK, J. A. 2014. Macrophagic and microglial responses after focal traumatic brain injury in the female rat. *J Neuroinflammation,* 11**,** 82.

UJIIE, M., DICKSTEIN, D. L., CARLOW, D. A. & JEFFERIES, W. A. 2003. Blood-brain barrier permeability precedes senile plaque formation in an Alzheimer disease model. *Microcirculation,* 10**,** 463-70.

ULVESTAD, E., WILLIAMS, K., MORK, S., ANTEL, J. & NYLAND, H. 1994. Phenotypic differences between human monocytes/macrophages and microglial cells studied in situ and in vitro. *J Neuropathol Exp Neurol,* 53**,** 492-501.

UNTERBERG, A. W., STOVER, J., KRESS, B. & KIENING, K. L. 2004. Edema and brain trauma. *Neuroscience,* 129**,** 1021-9.

VAN DUIJN, C. M., TANJA, T. A., HAAXMA, R., SCHULTE, W., SAAN, R. J., LAMERIS, A. J., ANTONIDES-HENDRIKS, G. & HOFMAN, A. 1992. Head trauma and the risk of Alzheimer's disease. *Am J Epidemiol,* 135**,** 775-82.

VAN OIJEN, M., WITTEMAN, J. C., HOFMAN, A., KOUDSTAAL, P. J. & BRETELER, M. M. 2005. Fibrinogen is associated with an increased risk of Alzheimer disease and vascular dementia. *Stroke,* 36**,** 2637-41.

VAN VULPEN, M., KAL, H. B., TAPHOORN, M. J. & EL-SHAROUNI, S. Y. 2002. Changes in blood-brain barrier permeability induced by radiotherapy: implications for timing of chemotherapy? (Review). *Oncol Rep,* 9**,** 683-8.

VARNUM, M. M. & IKEZU, T. 2012. The classification of microglial activation phenotypes on neurodegeneration and regeneration in Alzheimer's disease brain. *Arch Immunol Ther Exp (Warsz),* 60**,** 251-66.

VARVEL, N. H., NEHER, J. J., BOSCH, A., WANG, W., RANSOHOFF, R. M., MILLER, R. J. & DINGLEDINE, R. 2016. Infiltrating monocytes promote brain inflammation and exacerbate neuronal damage after status epilepticus. *Proceedings of the*

National Academy of Sciences of the United States of America, 113**,** E5665-E5674.

VAVILALA, M. S., BOWEN, A., LAM, A. M., UFFMAN, J. C., POWELL, J., WINN, H. R. & RIVARA, F. P. 2003. Blood pressure and outcome after severe pediatric traumatic brain injury. *J Trauma,* 55**,** 1039-44.

VAVILALA, M. S., LEE, L. A., BODDU, K., VISCO, E., NEWELL, D. W., ZIMMERMAN, J. J. & LAM, A. M. 2004. Cerebral autoregulation in pediatric traumatic brain injury. *Pediatr Crit Care Med,* 5**,** 257-63.

VAVILALA, M. S., MUANGMAN, S., TONTISIRIN, N., FISK, D., ROSCIGNO, C., MITCHELL, P., KIRKNESS, C., ZIMMERMAN, J. J., CHESNUT, R. & LAM, A. M. 2006. Impaired cerebral autoregulation and 6-month outcome in children with severe traumatic brain injury: preliminary findings. *Dev Neurosci,* 28**,** 348-53.

VAZ, R., SARMENTO, A., BORGES, N., CRUZ, C. & AZEVEDO, I. 1997. Ultrastructural study of brain microvessels in patients with traumatic cerebral contusions. *Acta Neurochir (Wien),* 139**,** 215-20.

VAZ, R., SARMENTO, A., BORGES, N., CRUZ, C. & AZEVEDO, T. 1998. Experimental traumatic cerebral contusion: morphological study of brain microvessels and characterization of the oedema. *Acta Neurochir (Wien),* 140**,** 76-81.

VERDERIO, C. & MATTEOLI, M. 2001. ATP mediates calcium signaling between astrocytes and microglial cells: modulation by IFN-gamma. *J Immunol,* 166**,** 6383-91.

VIGGARS, A. P., WHARTON, S. B., SIMPSON, J. E., MATTHEWS, F. E., BRAYNE, C., SAVVA, G. M., GARWOOD, C., DREW, D., SHAW, P. J. & INCE, P. G. 2011. Alterations in the blood brain barrier in ageing cerebral cortex in relationship to Alzheimer-type pathology: a study in the MRC-CFAS population neuropathology cohort. *Neurosci Lett,* 505**,** 25-30.

VILLAPOL, S., BYRNES, K. R. & SYMES, A. J. 2014. Temporal dynamics of cerebral blood flow, cortical damage, apoptosis, astrocyte-vasculature interaction and astrogliosis in the pericontusional region after traumatic brain injury. *Front Neurol,* 5**,** 82.

VINTERS, H. V., SECOR, D. L., READ, S. L., FRAZEE, J. G., TOMIYASU, U., STANLEY, T. M., FERREIRO, J. A. & AKERS, M. A. 1994. Microvasculature in brain biopsy specimens from patients with Alzheimer's disease: an immunohistochemical and ultrastructural study. *Ultrastruct Pathol,* 18**,** 333-48.

WALKER, F. R., BEYNON, S. B., JONES, K. A., ZHAO, Z., KONGSUI, R., CAIRNS, M. & NILSSON, M. 2014. Dynamic structural remodelling of microglia in health and disease: A review of the models, the signals and the mechanisms. *Brain, Behavior, and Immunity,* 37**,** 1-14.

WANG, G., ZHANG, J., HU, X., ZHANG, L., MAO, L., JIANG, X., LIOU, A. K., LEAK, R. K., GAO, Y. & CHEN, J. 2013. Microglia/macrophage polarization dynamics in white matter after traumatic brain injury. *J Cereb Blood Flow Metab,* 33**,** 1864-74.

WANG, X., XIE, H., COTTON, A. S., TAMBURRINO, M. B., BRICKMAN, K. R., LEWIS, T. J., MCLEAN, S. A. & LIBERZON, I. 2015a. Early cortical thickness change after mild traumatic brain injury following motor vehicle collision. *J Neurotrauma,* 32**,** 455-63.

WANG, Y., JIN, S., SONOBE, Y., CHENG, Y., HORIUCHI, H., PARAJULI, B., KAWANOKUCHI, J., MIZUNO, T., TAKEUCHI, H. & SUZUMURA, A. 2014. Interleukin-1β Induces Blood–Brain Barrier Disruption by Downregulating Sonic Hedgehog in Astrocytes. *PLOS ONE,* 9**,** e110024.

WANG, Y., WEST, J. D., BAILEY, J. N., WESTFALL, D. R., XIAO, H., ARNOLD, T. W., KERSEY, P. A., SAYKIN, A. J. & MCDONALD, B. C. 2015b. Decreased cerebral

blood flow in chronic pediatric mild TBI: an MRI perfusion study. *Dev Neuropsychol,* 40**,** 40-4.

WARNER, M. A., MARQUEZ DE LA PLATA, C., SPENCE, J., WANG, J. Y., HARPER, C., MOORE, C., DEVOUS, M. & DIAZ-ARRASTIA, R. 2010. Assessing spatial relationships between axonal integrity, regional brain volumes, and neuropsychological outcomes after traumatic axonal injury. *J Neurotrauma,* 27**,** 2121-30.

WATKINS, S., ROBEL, S., KIMBROUGH, I. F., ROBERT, S. M., ELLIS-DAVIES, G. & SONTHEIMER, H. 2014. Disruption of astrocyte-vascular coupling and the blood-brain barrier by invading glioma cells. *Nat Commun,* 5**,** 4196.

WEI, E. P., DIETRICH, W. D., POVLISHOCK, J. T., NAVARI, R. M. & KONTOS, H. A. 1980. Functional, morphological, and metabolic abnormalities of the cerebral microcirculation after concussive brain injury in cats. *Circ Res,* 46**,** 37-47.

WEINSTEIN, E., TURNER, M., KUZMA, B. B. & FEUER, H. 2013. Second impact syndrome in football: new imaging and insights into a rare and devastating condition. *Journal of Neurosurgery: Pediatrics,* 11**,** 331-334.

WEISSBERG, I., VEKSLER, R., KAMINTSKY, L., SAAR-ASHKENAZY, R., MILIKOVSKY, D. Z., SHELEF, I. & FRIEDMAN, A. 2014. Imaging blood-brain barrier dysfunction in football players. *JAMA Neurol,* 71**,** 1453-5.

WETJEN, N. M., PICHELMANN, M. A. & ATKINSON, J. L. 2010. Second impact syndrome: concussion and second injury brain complications. *J Am Coll Surg,* 211**,** 553-7.

WILLIAMS, D. B., ANNEGERS, J. F., KOKMEN, E., O'BRIEN, P. C. & KURLAND, L. T. 1991. Brain injury and neurologic sequelae: a cohort study of dementia, parkinsonism, and amyotrophic lateral sclerosis. *Neurology,* 41**,** 1554-7.

WILLIAMS, D. J. & TANNENBERG, A. E. 1996. Dementia pugilistica in an alcoholic achondroplastic dwarf. *Pathology,* 28**,** 102-4.

WILLIAMS, K. C., COREY, S., WESTMORELAND, S. V., PAULEY, D., KNIGHT, H., DEBAKKER, C., ALVAREZ, X. & LACKNER, A. A. 2001a. Perivascular macrophages are the primary cell type productively infected by simian immunodeficiency virus in the brains of macaques: implications for the neuropathogenesis of AIDS. *J Exp Med,* 193**,** 905-15.

WILLIAMS, S., RAGHUPATHI, R., MACKINNON, M. A., MCINTOSH, T. K., SAATMAN, K. E. & GRAHAM, D. I. 2001b. In situ DNA fragmentation occurs in white matter up to 12 months after head injury in man. *Acta Neuropathol,* 102**,** 581-90.

WILSON, S., RAGHUPATHI, R., SAATMAN, K. E., MACKINNON, M. A., MCINTOSH, T. K. & GRAHAM, D. I. 2004. Continued in situ DNA fragmentation of microglia/macrophages in white matter weeks and months after traumatic brain injury. *J Neurotrauma,* 21**,** 239-50.

WINKLER, E. A., BELL, R. D. & ZLOKOVIC, B. V. 2011. Central nervous system pericytes in health and disease. *Nature Neuroscience,* 14**,** 1398-1405.

WOLBURG, H., NOELL, S., MACK, A., WOLBURG-BUCHHOLZ, K. & FALLIER-BECKER, P. 2009. Brain endothelial cells and the glio-vascular complex. *Cell Tissue Res,* 335**,** 75-96.

WRIGHT, A. L., ZINN, R., HOHENSINN, B., KONEN, L. M., BEYNON, S. B., TAN, R. P., CLARK, I. A., ABDIPRANOTO, A. & VISSEL, B. 2013. Neuroinflammation and Neuronal Loss Precede Aβ Plaque Deposition in the hAPP-J20 Mouse Model of Alzheimer's Disease. *PLOS ONE,* 8**,** e59586.

WYSS-CORAY, T. 2006. Inflammation in Alzheimer disease: driving force, bystander or beneficial response? *Nat Med,* 12**,** 1005-15.

XU, G., ZHANG, H., ZHANG, S., FAN, X. & LIU, X. 2008. Plasma fibrinogen is associated with cognitive decline and risk for dementia in patients with mild cognitive impairment. *Int J Clin Pract,* 62**,** 1070-5.

YAMAMOTO, M., KIYOTA, T., HORIBA, M., BUESCHER, J. L., WALSH, S. M., GENDELMAN, H. E. & IKEZU, T. 2007. Interferon-gamma and tumor necrosis factor-alpha regulate amyloid-beta plaque deposition and beta-secretase expression in Swedish mutant APP transgenic mice. *Am J Pathol,* 170**,** 680-92.

YAMAMOTO, M., KIYOTA, T., WALSH, S. M., LIU, J., KIPNIS, J. & IKEZU, T. 2008. Cytokine-mediated inhibition of fibrillar amyloid-β peptide degradation by human mononuclear phagocytes. *Journal of immunology (Baltimore, Md. : 1950),* 181**,** 3877-3886.

YAN, S. D., CHEN, X., FU, J., CHEN, M., ZHU, H., ROHER, A., SLATTERY, T., ZHAO, L., NAGASHIMA, M., MORSER, J., MIGHELI, A., NAWROTH, P., STERN, D. & SCHMIDT, A. M. 1996. RAGE and amyloid-beta peptide neurotoxicity in Alzheimer's disease. *Nature,* 382**,** 685-91.

YAN, S. F., RAMASAMY, R. & SCHMIDT, A. M. 2010. The RAGE axis: a fundamental mechanism signaling danger to the vulnerable vasculature. *Circ Res,* 106**,** 842-53.

YANG, G. Y., BETZ, A. L., CHENEVERT, T. L., BRUNBERG, J. A. & HOFF, J. T. 1994. Experimental intracerebral hemorrhage: relationship between brain edema, blood flow, and blood-brain barrier permeability in rats. *J Neurosurg,* 81**,** 93-102.

YASOJIMA, K., AKIYAMA, H., MCGEER, E. G. & MCGEER, P. L. 2001. Reduced neprilysin in high plaque areas of Alzheimer brain: a possible relationship to deficient degradation of beta-amyloid peptide. *Neurosci Lett,* 297**,** 97-100.

YOSHIYAMA, Y., HIGUCHI, M., ZHANG, B., HUANG, S. M., IWATA, N., SAIDO, T. C., MAEDA, J., SUHARA, T., TROJANOWSKI, J. Q. & LEE, V. M. 2007. Synapse loss and microglial activation precede tangles in a P301S tauopathy mouse model. *Neuron,* 53**,** 337-51.

ZEHENDNER, C. M., SEBASTIANI, A., HUGONNET, A., BISCHOFF, F., LUHMANN, H. J. & THAL, S. C. 2015. Traumatic brain injury results in rapid pericyte loss followed by reactive pericytosis in the cerebral cortex. *Sci Rep,* 5**,** 13497.

ZENARO, E., PIACENTINO, G. & CONSTANTIN, G. 2017. The blood-brain barrier in Alzheimer's disease. *Neurobiology of Disease,* 107**,** 41-56.

ZETTERBERG, H., HIETALA, M. A., JONSSON, M., ANDREASEN, N., STYRUD, E., KARLSSON, I., EDMAN, A., POPA, C., RASULZADA, A., WAHLUND, L. O., MEHTA, P. D., ROSENGREN, L., BLENNOW, K. & WALLIN, A. 2006. Neurochemical aftermath of amateur boxing. *Arch Neurol,* 63**,** 1277-80.

ZETTERBERG, H., SMITH, D. H. & BLENNOW, K. 2013a. Biomarkers of mild traumatic brain injury in cerebrospinal fluid and blood. *Nat Rev Neurol,* 9**,** 201-210.

ZETTERBERG, H., SMITH, D. H. & BLENNOW, K. 2013b. Biomarkers of mild traumatic brain injury in cerebrospinal fluid and blood. *Nature reviews. Neurology,* 9**,** 201-210.

ZHANG, Y. & PARDRIDGE, W. M. 2001. Mediated efflux of IgG molecules from brain to blood across the blood-brain barrier. *J Neuroimmunol,* 114**,** 168-72.

ZHANG, Z., ZHANG, Z. Y., WU, Y. & SCHLUESENER, H. J. 2012. Lesional accumulation of CD163+ macrophages/microglia in rat traumatic brain injury. *Brain Res,* 1461**,** 102-10.

ZHANG, Z. G., ZHANG, L., JIANG, Q., ZHANG, R., DAVIES, K., POWERS, C., BRUGGEN, N. & CHOPP, M. 2000. VEGF enhances angiogenesis and promotes blood-brain barrier leakage in the ischemic brain. *J Clin Invest,* 106**,** 829-38.

ZIEBELL, J. M. & MORGANTI-KOSSMANN, M. C. 2010. Involvement of pro- and anti-inflammatory cytokines and chemokines in the pathophysiology of traumatic brain injury. *Neurotherapeutics,* 7**,** 22-30.

ZIPSER, B. D., JOHANSON, C. E., GONZALEZ, L., BERZIN, T. M., TAVARES, R., HULETTE, C. M., VITEK, M. P., HOVANESIAN, V. & STOPA, E. G. 2007a. Microvascular injury and blood-brain barrier leakage in Alzheimer's disease. *Neurobiol Aging,* 28**,** 977-86.

ZIPSER, B. D., JOHANSON, C. E., GONZALEZ, L., BERZIN, T. M., TAVARES, R., HULETTE, C. M., VITEK, M. P., HOVANESIAN, V. & STOPA, E. G. 2007b. Microvascular injury and blood-brain barrier leakage in Alzheimer's disease. *Neurobiol Aging,* 28.

ZLOKOVIC, B. V. 2011. Neurovascular pathways to neurodegeneration in Alzheimer's disease and other disorders. *Nat Rev Neurosci,* 12**,** 723-38.

ZLOKOVIC, B. V., DEANE, R., SAGARE, A. P., BELL, R. D. & WINKLER, E. A. 2010. Low-density lipoprotein receptor-related protein-1: a serial clearance homeostatic mechanism controlling Alzheimer's amyloid beta-peptide elimination from the brain. *J Neurochem,* 115**,** 1077-89.

ZWIENENBERG, M. & MUIZELAAR, J. P. 1999. Severe pediatric head injury: the role of hyperemia revisited. *J Neurotrauma,* 16**,** 937-43.